CLOCK GENES
AND
FEMALE REPRODUCTION

Cynthia Chen
BSc (Hons) Genetics: University of Wales College Cardiff
MSc Neuroscience: Institute of Psychiatry, King's College London

MRC Human Reproductive Science Unit
Centre for Reproductive Biology
The University of Edinburgh
The Queen's Medical Research Institute
47 Little France Crescent
Edinburgh EH16 4TJ

Thesis submitted to the University of Edinburgh
for the degree of Doctor of Philosophy

2009

DECLARATION

The studies in this thesis were the unaided work of the author, except where acknowledgment is made by reference. The work described in this thesis has not been previously accepted for, or is currently being submitted for another degree or qualification.

Cynthia Chen
2009

ACKNOWLEDGEMENTS

I would, of course, firstly like to thank my supervisors: Professor Gerald Lincoln and Dr W. Colin Duncan for their support and supervision. I would like to acknowledge the contribution of Julie Bell, for performing PCRs of the human CL, the results of which are included in Chapter 4. I would also like to acknowledge the contribution of Arantza Asnal, who performed some of the IHC of the clock proteins in the human CL. I would like to thank Edwin Carter for performing the RIAs of P_4 and melatonin, which are included in Chapters 5 and 6. I am also very grateful to Professor Alan McNeilly for his invaluable support and help in raising the ovine PER1 antibodies in-house. I would also like to thank the staff at the Marshall Building, particularly Marjorie Thomson, Joan Docherty and the late Norah Anderson. I would also like to thank Dr Pamela Brown for her help with Western blots and Dr Kevin Morgan for his help with all things bioinformatic. I would also like to thank the staff at the CRB for their help and advice. Finally, I would like to thank my friends and family for their patience, friendship and support.

PRESENTATIONS PERTAINING TO THIS THESIS

Localisation and expression of clock genes in the human corpus luteum

Cynthia Chen, Gerald Lincoln, W. Colin Duncan
Oral presentation at Fertility 2007 conference of Joint UK Fertility Societies.

Abstract:
Introduction: The molecular regulation of the lifespan of the human corpus luteum remains unelucidated. Clock genes have been reported to be involved in reproduction, as regulators of temporal processes in central and peripheral tissues. Recent observations of clock gene expression in mammalian ovarian tissue have led us to hypothesise that the human corpus luteum expresses clock genes and that this expression is involved in regulation of the luteal lifespan. We aimed to investigate whether clock gene expression was down-regulated during luteolysis.
Methods: Human corpora lutea (*n*=18) were obtained at time of benign surgery. They were dated, based on the time of LH surge, as Early (*n*=6), Mid (*n*=6) and Late (*n*=6) luteal phase. Expression of the canonical clock genes: *Per1*, *Per2*, *Cry1*, *Bmal1* and *Clock* was analysed using qRT-PCR and localised using immunohistochemistry.
Results & Discussion: Several cell types, most notably the steriodogenic cells, within the human corpus luteum express all of the canonical clock genes. This suggests that a peripheral clock functions within the luteal cells. There was no significant change in the expression or localisation of any of the clock genes across the luteal phases. Therefore, any role for the clock genes in the regulation of luteolytic timing is not related to changes in their levels of expression or localisation. Further work is required to investigate whether changes in phase-relationships between the expression of these genes is involved.

Clock genes and the regulation of reproduction

Cynthia Chen

LIST OF ABBREVIATIONS

% Max	percentage of the maximum value
% v/v	volume in volume percentage
®	registered tradmark
20α-HSD	20-alpha hydroxysteroid dehydrogenase
3βHSD	3-beta hydroxysteroid dehydrogenase
3V	third ventricle
ABC-HRP	avidin-biotin conjugated horseradish peroxidase
ANOVA	analysis of variance
arntl	*aryl hydrocarbon receptor nuclear translocator-like protein 1* gene
bHLH	basic helix-loop-helix
BLAST	Basic Local Alignment Search Tool
bmal1	*brain and muscle aryl hydrocarbon receptor nuclear translocator-like protein 1* gene
bp	base pair(s)
BSA	bovine serum albumin
CAD	caspase-activated DNase
CD31	cluster of differentiation 31
CD68	cluster of differentiation 68
CK1ε	casein kinase 1 epsilon
CK1δ	casein kinase 1 delta
CL	corpus luteum
clk	*circadian locomotor output cycles kaput* or *clock* gene
CNS	central nervous system
COREC	Common Research Ethics Committee
cry	*cryptochrome* gene
cry1	*cryptochrome1* gene
cry2	*cryptochrome2* gene
CT	clock time
C_T	crossing threshold
CTGF	connective tissue growth factor
CWS	cell wall skeleton
d	day(s)
D1	day 1 of culture (one day spent in culture)
D8	day 8 of culture (eight days spent in culture)
D8 hCG	day 8 of culture with hCG treatment (hCG treated after eight days spent in culture)
DAB	3,3'-diaminobenzidine tetrahydrochloride
DAPI	4'-6-diamidino-2-phenylindole
DD	dark:dark schedule of 12 hours dark and 12 hours dark (constant dark)
DNA	deoxyribonucleic acid
DNase	deoxyribonuclease
dNTP	deoxynucleotide triphosphate
E_2	œstradiol
E20	embryonic day 20
EFREC	Edinburgh Fertility and Reproductive Endocrine Centre

EL	early luteal
ELISA	enzyme-linked immunosorbent assay
ERα	œstrogen receptor alpha
ERβ	œstrogen receptor beta
GABA	gamma-aminobutyric acid
GARB	goat anti-rabbit biotinylated
GC	guanine-cytosine
GHT	geniculohypothalamic tract
GnRH	gonadotrophin-releasing hormone
h	hour(s)
H_2O_2	hydrogen peroxide
hCG	human choronic gonadotrophin
HPG	hypothalamopituitary gonadal
ICAD	inhibitor of CAD
IFNτ	interferon gamma
IGF	insulin-like growth factors
IGFBP	insulin-like growth factor binding proteins
IgG	immunoglobulin G
IHC	immunohistochemistry
IVF	*in vitro* fertilisation
KCl	potassium chloride
KLH	keyhole limpet haemocyanin
LCA	leucocyte common antigen
LD	light:dark
LD 12:12	light:dark schedule of 12 hours light and 12 hours dark
LDL	low-density lipoprotein (cholesterol)
LGC	luteinised granulosa cell
LGN	lateral geniculate nuclei
LH	luteinising hormone
LHR	luteinising hormone receptor
LL	late luteal
LLC	large lutein cell
MBS	m-maleimidobenzoyl-N-hydroxysuccinimide ester
ME	median eminence
Mg^{2+}	magnesium ion
MGB	major groove binder
$MgCl_2$	magnesium chloride
min	minute(s)
ML	mid-luteal
MMP-2	matrix metalloproteinase 2
MMP-9	matrix metalloproteinase 9
MPL	monophosphoryl lipid A
mRNA	messenger ribonucleic acid
MT_1	type 1 melatonin receptor
MT_2	type 2 melatonin receptor
MuLV	Moloney murine leukaemia virus
n	*n*-number (number of data items)
NAD^+	oxidised nicotinamide adenine dinucleotide
NADH	nicotinamide adenine dinucleotide
$NADP^+$	oxidised nicotinamide adenine dinucleotide phosphate

NADPH	nicotinamide adenine dinucleotide phosphate
NCBI	National Center for Biotechnology Information
NFQ	non-fluorescent quencher
NGS	normal goat serum
OC	optic chiasm
oCRY1	ovine CRYPTOCHROME1 protein
oligo(dT)	oligodeoxythymidylate
oPER1	ovine PERIOD1 protein
Ovx	ovariectomised
P	*P*-value (the probability of observing the test statistic, if the test statistic were distributed as it would be under the null hypothesis)
P10	postnatal day 10
P2	postnatal day 2
P20	postnatal day 20
P30	postnatal day 30
P_4	progesterone
PACAP	pituitary adenylate cyclase-activating peptide
PAI-1	plasminogen activator inhibitor-1
PAS	Period-ARNT-Singleminded
PBS	phosphate-buffered saline
PBST	phosphate-buffered saline-Tween
PCR	polymerase chain reaction
per	*period* gene
per1	*period1* gene
per2	*period2* gene
per3	*period3* gene
PeVN	periventricular nucleus
$PGF_{2\alpha}$	prostaglandin F 2-alpha
POA	pre-optic area
poly(A^+)	polyadenylate
PR	progesterone receptor
PT	*pars tuberalis*
PVN	paraventricular nucleus
qRT-PCR	quantitative reverse-transcribed polymerase chain reaction
REV-ERBα	REV-ERB alpha
RHT	retinohypothalamic tract
RIA	radiolabelled immuno-assay or radio-immuno-assay
RIN	RNA Integrity Number
RNA	ribonucleic acid
RNase	ribonuclease
ROR	retinoic acid receptor-related orphan receptor
RORE	retinoic acid receptor-related orphan receptor promoter elements
RORα	retinoic acid receptor-related orphan receptor alpha
RORβ	retinoic acid receptor-related orphan receptor beta
RORγ	retinoic acid receptor-related orphan receptor gamma
RPM	revolutions per minute
RT-PCR	reverse-transcribed polymerase chain reaction
s	second(s)
SARB	swine anti-rabbit biotinylated
SCN	suprachiasmatic nucleus

SDS-PAGE	sodium dodecyl sulphate polyacrylamide gel electrophoresis
SLC	small lutein cell
SON	supraoptic nucleus
SRC-1	steroid hormone receptor co-activator-1
SS	serum shock
StAR	the steroidogenic acute regulatory protein
TAE	Tris-acetate-EDTA
Taq	*Thermus aquaticus* DNA polymerase
TDM	trehalose dicorynomycolate
TGFα	tumour growth factor alpha
tim	*timeless* gene
TIM	TIMELESS protein
TIMP1	Tissue inhibitor of metalloproteinases-1
TIMP2	Tissue inhibitor of metalloproteinases-2
T_m	melting temperature
TSA	Tyramide Signal Amplification
™	trademark
UV	ultraviolet
V	volts
VEGF	vascular endothelial growth factor
VIP	vasoactive intestinal peptide
vipr2	vasoactive intestinal peptide receptor 2
VP	vasopressin
VPAC2	vasoactive intestinal peptide receptor 2
ZT	zeitgeber time
α-SMA	alpha-smooth muscle actin

NB. Nouns in lowercase italics are genes e.g. *per1* and uppercase are proteins, e.g. PER1.

CONTENTS

LIST OF FIGURES

LIST OF TABLES

1 ABSTRACT

The involvement of clock genes in the temporal regulation of the function and lifespan of the corpus luteum (CL) has not been investigated in detail. Immunohistochemistry and real-time quantitative PCR techniques were used to examine the expression of the canonical clock genes: *period1, period2, period3, cryptochrome1, cryptochrome2, clock* and *bmal1*, at protein and mRNA levels respectively. The expression of the clock genes was examined in the human CL, cultured luteinised granulosa cells, cultured luteal fibroblast-like cells and the ovine CL.

The main findings were that clock genes are expressed in the human and ovine CL; that this expression is manifest at mRNA and protein level in all discernible cell types within the human and ovine CL, and that the pattern of mRNA expression differs between the early luteal phase compared to the late luteal phase. The circadian expression of the clock genes was established in the ovine CL during the late luteal phase and could not be determined in the human CL, although indications from cultured luteinised granulosa cells and luteal fibroblast-like cells suggest that this may also be the case in humans. With the exception of *per2*, the circadian pattern of clock gene expression emerged in the late luteal phase CL when the early luteal phase CL did not demonstrate circadian clock gene expression. This emergence later in the lifespan of the CL was akin to that observed in embryonic development, where the clock genes are initially non-rhythmic but then acquire circadian rhythmicity with age. In this case, the clock genes have been proposed to perform a non-classical circadian timing role in the timing of embryonic development.

The *per2* gene was also found to be special, in its loss rather than gain of rhythmic gene expression across the luteal lifespan and in its protein localisation in the cytoplasm of some granulosa-lutein cells. The exceptional behaviour of *per2* is consistent with a growing body of evidence supporting its role as a unique clock gene in many respects, able to maintain circadian protein levels in the absence of circadian

gene expression, integrating peripheral clock inputs and outputs and acting as a tumour suppressor gene.

The CL was also found to be a potential target of melatonin regulation, based on its possession of melatonin MT_1 receptors and the timing of circadian *cry1* gene expression in the late luteal phase. The expression of *cry1* is known to be directly melatonin-induced in the PT and appeared to be similarly activated, downstream of a melatonin signal, in the CL. This supports the evolving view of a hierarchical organisation of the central and peripheral clocks, which are integrated in order to establish information feedback loops that maintain circadian homeostasis, and which can regulate seasonal physiology.

2 INTRODUCTION

2.1 HISTORY OF CHRONOBIOLOGY

Chronobiology is defined as the study of periodic or cyclic phenomena in living organisms (Vitaterna et al., 2001). Periodic phenomena in natural history have been observed and recorded as early as 10 000 BC in Palaeolithic art and described in writing as early as the 4th century BC by Androsthenes, Alexander the Great's scribe (McClung, 2006, Sturiale, 1997). Androsthenes recorded the daily diurnal opening and nocturnal closing of tamarind tree leaves in Tylos (modern day Bahrain) (McClung, 2006, Sturiale, 1997, Chandrashekaran, 1998). Many centuries later, in 1729, the French astronomer, Jean-Jacques d'Ortous de Mairan made a departure from astronomy, to perform experiments on heliotrope plants, that exhibited the same periodic phenomena as the tamarind trees. He placed the plants in constant darkness and observed that their leaves continued to open during the day and close during the night, despite the absence of daylight time cues (McClung, 2006, Sturiale, 1997, Chandrashekaran, 1998).

Around 20 years later, the eminent Swedish botanist, Carolus Linnaeus, famously designed his flower clock, which consisted of flowers that, predictably and regularly, opened and closed at different times of day (Sturiale, 1997, Chandrashekaran, 1998). After almost a century, another botanist, Augustin Pyrame de Candolle, determined that the free-running period of the heliotrope plant was 22 to 23 hours. This was discernibly shorter than 24 hours and implied that this circadian rhythm was generated, not simply as a response to the day-night environment but rather, as an endogenous rhythm (McClung, 2006). Plant leaf movements continued to be used as the only model of circadian biology for the next century (Figure 2.1).

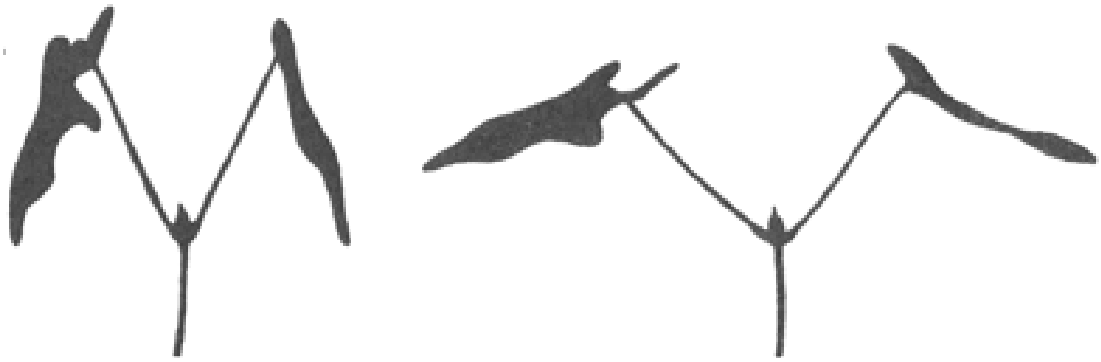

Figure 2.1 Opening and closing leaf movements of runner bean plants, *Phaseolus coccineus* (McClung, 2006).

It was not until the 1930s, that these repeated observations began to lead towards more sophisticated conclusions that still apply today. It was around this time that German chronobiologist, Erwin Bünning, first established that the endogenous circadian rhythm of runner bean leaf movements was heritable (Bunning, 1964). He also hypothesised that these plants, by dint of possessing a circadian rhythm in light sensitivity, were able to track the daylength by measuring how far the day 'encroached' into the night (Bunning and Moser, 1969). He went on to study the circadian rhythms of *Drosophila* eclosion (the emergence of adult fruit flies from their pupa) (Saunders, 2005). This model became one that was also used by Jürgen Aschoff and Colin Pittendrigh, two other pioneers of modern chronobiology (Daan, 1998). It was also around the 1930s that Karl von Frisch and Ingeborg Beling performed their classic experiments with honeybees which, they deduced, were able to navigate using the sun's position in the sky because they could intrinsically tell the time of day (Sturiale, 1997). These experiments were corroborated around 1950 by another German ethologist, Gustav Kramer, who similarly concluded that European starlings also navigated using the sun's azimuth, again by virtue of possessing internal clocks (Schmidt-Koenig et al., 1991).

In the following two decades, Jürgen Aschoff in Germany and Colin Pittendrigh in the United States would go on to play key roles in laying the foundations of the biological rhythms field as it now stands. Aschoff worked predominantly with humans and was

able to prove that humans, like many other species, possessed and were subject to circadian behaviour and physiology (Aschoff, 1998). He derived several protocols for plotting phase response curves that describe the circadian responses to environmental cues, particularly to light and its parametric properties, such as intensity and wave frequency (Aschoff, 1999). He thus demonstrated, along with Pittendrigh, that although the internal circadian clocks of many species were endogenous, they were entrainable by various environmental time cues that he dubbed zeitgebers (from the German *zeit* meaning 'time and *geber* meaning 'giver') (Aschoff and Pohl, 1978). Pittendrigh also established that internal clocks were temperature-compensated and went on to delineate the phase response curve of circadian entrainment by zeitgebers, particularly by the non-parametric properties of light (Bruce and Pittendrigh, 1956). These properties refer to parameters such as the timing and duration of light exposure (Pittendrigh and Takamura, 1987). Bünning, Aschoff and Pittendrigh together established the fundamental principles and the central lines of enquiry of biological rhythms research in an early culmination of information and discussion with other scientists, in a seminal symposium, convened by Pittendrigh in 1960 and chaired by Bünning, held in Cold Spring Harbor, USA (Pittendrigh, 1960, Halberg et al., 2003).

The Proceedings from this symposium are still relevant today, despite pre-dating many of the key advances in molecular biology that followed Crick and Watson's elucidation of the structure of DNA in 1953 (Watson and Crick, 1953). They include a list of "Empirical Generalizations" on biological clocks, many of which still hold true (Pittendrigh, 1960, Evans, 1961). Amongst these "Generalizations" was the definition of circadian rhythms as rhythms that maintain a period that cycled, independently of external time cues, in approximately the same period as the earth's rotation of 24 hours. The term, circadian, is derived from the Latin *circa* meaning 'about' and *diel* meaning 'day' and was first proposed by Franz Halberg in 1959 (Halberg et al., 2003). The "Generalizations" further stated that these rhythms were endogenous, self-sustained oscillations that were innate and ubiquitous in all living systems. It is now evident that this is true in virtually all species and at all levels of biological organisation, from the

subcellular to the entire organism. It was also generally recognised that the period and phase of these rhythms could be shifted or entrained in a variety of specific ways (Lobban, 1960, Pittendrigh, 1960, Cloudsley-Thompson, 1960).

It was at this landmark symposium that *biological rhythms* were more clearly defined and distinguished from *physiological rhythms*. Biological rhythms belong to a specific class of principally temporal biology that is distinct from that of physiological rhythms, in both evolutionary and physiological origin. Biological rhythms are highly conserved and are thought to have arisen early in evolutionary time as a result of adaptation to cyclical environmental phenomena (Paranjpe and Sharma, 2005). The genotoxic stress imposed by the ultraviolet rays of the sun is hypothesised to be a key motivator for the circadian adaptation to the day-night cycle. Some argue that an internal clock was actually essential to all life originating on our cyclically driven planet. In any case, the possession of an endogenous clock was also a highly selected trait as it allowed the organism to anticipate environmental changes, thus enabling it to better optimise its energy uptake and expenditure (Paranjpe and Sharma, 2005). This anticipation can clearly be seen when the periodicities of these biological rhythms are maintained at an almost constant frequency in the absence of environmental time cues, as was observed in de Mairan's heliotrope plant experiments (Moore-Ede et al., 1984).

Biological rhythms are thus seen to be specifically clock-driven and are not considered, like physiological rhythms, to be the incidental temporal results of physiology or metabolic processes. This is further supported by the lack of variation seen in the periodicities of biological rhythms between species and organisms of different size and metabolic status. This is in contrast to physiological rhythms, such as heartbeat, which vary in periodicity or frequency according to the species and the organism's activity level and temperature. Biological rhythms generally follow periodicities that reflect well-recognised environmental cycles, principally those of the solar day, lunar day, lunar month and seasons. Physiological rhythms tend to comprise a wide continuum of infradian and ultradian periodicities. Infradian rhythms have periods of over 24 hours;

such as the œstrous cycle of most vertebrates and ultradian rhythms have periods of less than 24 hours, such as the heartbeat of all animals. The final criterion that biological rhythms fulfil, and physiological ones do not, is that they are directly responsive to entrainment by environmental phenomena (Pittendrigh, 1960, Lobban, 1960, Aschoff, 1960).

The main outcome of this historic symposium was the consolidation of the myriad strands of research into a single academic discipline that revolved around, effectively, just one basic biological phenomenon: chronobiology. Two central avenues of investigation emerged. One addressed questions regarding the overall properties of circadian clocks, classifying their more corporeal aspects such as anatomical localisation and gross responses to altered light-dark schedules. The other focused on the essential mathematic characterisation of the rhythms and elucidation of the underlying clockwork machinery that generated them. It emerged, after the discovery of *Drosophila* mutants with aberrant circadian rhythms in 1971 that this machinery occurs at a fundamental molecular level (Konopka and Benzer, 1971). The study of circadian clocks continued apace and gathered momentum with the advent of new experimental techniques such as the polymerase chain reaction (PCR), developed by Kary Mullis in 1981 (Stetler et al., 1982). Nowadays, these two threads of research, effectively the study of the *clocks* versus that of the *clockwork*, have become less divergent. The field has in general become more integrated as a discipline, looking now at *clock systems* at various levels of organisation, incorporating other biological disciplines. These other disciplines in turn address the issue of clocks and clockwork within their studies. The integral role that biological clocks play in virtually all physiology and behaviour reflect their ancient and highly conserved nature and despite their primitive origins, they are complex and highly evolved and continue to provide serious propositions for modern scientific interrogation.

2.2 BEHAVIOURAL PROPERTIES OF CLOCKS

Circadian behaviour in both plants and animals continue to be observed and measured in present-day experiments. One such measurement involves the production of actograms (Acebo and LeBourgeois, 2006, Brown et al., 1990a, Brown et al., 1990b). Sensors are placed on the subject animal that measure physiological and behavioural parameters like body temperature, heart rate and locomotor activity. These parameters are recorded continuously over time. The data is then analysed using software that correlate the various parameters measured and incorporate timing intervals such as light-dark schedules. This information is then often presented in circadian research as an actogram graph, which plots locomotor activity against time (Figure 2.2).

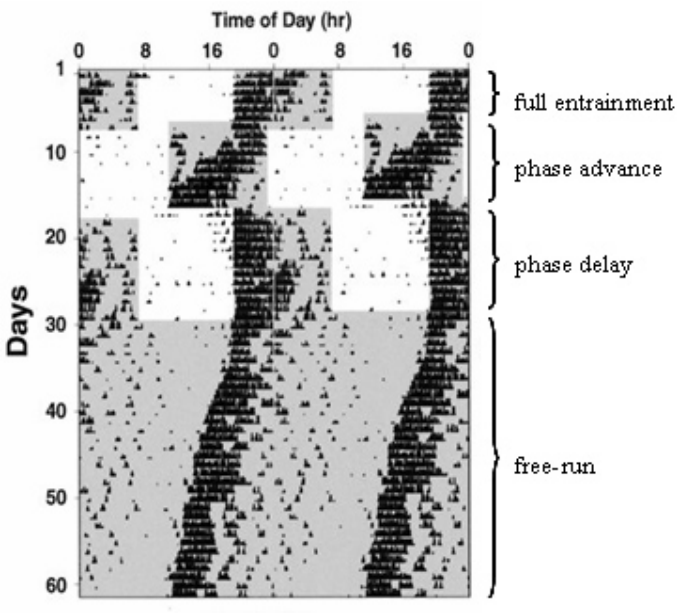

Figure 2.2 This is a classic example of an actogram. It was plotted by Harmar *et al*. and is of a wild-type mouse (Shen et al., 2000). The shaded regions refer to night time and the unshaded regions refer to daytime. As the actogram travels across the *x*-axis, it logs any locomotor activity with a black spike. Lack of activity can be seen as an absence of episodes (blocks of activity). The subject's activity and inactivity is thus continuously recorded. Each day of recording is then charted down the *y*-axis. The *x*-axis is double-plotted to more clearly display any temporal patterns of activity.

This actogram (Figure 2.2) clearly shows the delineation of circadian locomotor activity, gated in this instance, with a nocturnal species, to the night time, as represented by the prevalence of episodes falling within the shaded areas. The change in the position of the shaded areas refers to a change in the light-dark schedule, where the timing of light and dark have been shifted; in a way not unlike that elicited by a jetlag-inducing transmeridian flight. This shift in the environmental phase results in the subject responding by similarly phase shifting its physiology and behaviour, in keeping with the new light-dark schedule. It phase shifts its locomotor activity so that it can continue to be active in the subjective night, in order to preserve the selective advantage that this confers (Paranjpe and Sharma, 2005). The subject however can only phase shift overt circadian behaviour such as locomotor activity by a finite amount each day and so, it can take several days for entrainment and re-synchrony to the light-dark schedule to be fully achieved (Yamazaki et al., 2000). Once achieved though, the maintenance of locomotor activity within the night time becomes stably maintained as before.

The animal can phase shift in one of two directions; it can either *phase advance* or *phase delay* (Illnerova et al., 1989). In this example, the lighting schedules have been manipulated to challenge the animal to phase shift its circadian biology, measured using its locomotor activity. The animal is first entrained to a light-dark schedule where there are 12 hours light and 12 hours darkness. This LD 12:12 division in time is one that is maintained throughout all of the experiments. This maintenance in the phase relationship between the light phase and dark phase is one that is reflected by the responses of the animal (Shen et al., 2000). The animal divides its time in the same proportions to its active and inactive phases, thus also maintaining a constant phase relationship. The actogram shows that the mouse is a nocturnal animal, most active in the early half of the night and most inactive throughout the day. This strategy could be reasoned to have evolved in order to avoid predation and reduce interspecies competition for food sources during the daytime (Paranjpe and Sharma, 2005).

Once stably entrained to the first lighting schedule, the animal is tested by drastically advancing the onset of darkness, so shortening the daytime on that day. This mimics the change in timing of the environmental day-night cycle that is experienced in eastward transmeridian flight (Vokac et al., 1984, Gundel and Wegmann, 1989). The animal is then forced to re-entrain to the new cycle by similarly phase advancing its circadian rhythms. The actogram shows this as the animal's activity gradually shifts from the later half of the night time back to the early half. Once fully re-entrained, the animal is tested again. This time, daytime is extended on one day by delaying the onset of darkness. This would be equivalent to the time difference experience with westward transmeridian flight. The animal again re-synchronises its biology to its new environmental time, by phase delaying its own circadian clock (Roenneberg and Merrow, 2007, Kennaway, 2004, Johnson et al., 2003). This can be seen as it delays starting activity until the onset of darkness, though there remains a little residual activity in what used to be the early portion of the night. The residual activity eventually comes to a halt and the entrainment to the new time-zone is complete.

Placing the animal in complete darkness (DD) abolishes the phase relationship of the environmental cycle as well as removing the most potent entrainment stimulus: light (Hastings et al., 1998). The animal continues to maintain its circadian rhythms and phase relationship between different rhythms in the absence of light. This implies that these rhythms are endogenously driven by an autonomous clock rather than by an environment-reactive mechanism (Rosbash, 1995). The autonomous circadian rhythm is not orchestrated exactly to 24 hours. In this rodent, it can be seen to run at a little less than 24 hours. This less-than-24 hour *free-running* period results in a slight phase advance every day. This phase advance does not have much impact on the animal in lighting schedules that are unaltered, where there is no entrainment or no apparent requirement for entrainment. However, return to a lighting schedule corresponding to the previous light-dark cycle would mean that the animal would be incrementally more out-of-synch with the environmental time with each passing day of free-running (Treherne et al., 1977). Therefore, in order to stay synchronised with the environmental

clock, the organism needs to slightly phase delay its own endogenous clock every day. This delay is provided by daily entrainment to light (Foster and Helfrich-Forster, 2001, Rea, 1998). The requirement for daily entrainment enables the stabilisation of the clock and its rhythms in accordance with the geophysical environment. The daily calibration also permits the detection of any temporal environmental changes and enables the clock to fine-tune or adapt accordingly (Rea, 1998).

2.3 ENTRAINMENT PHYSIOLOGY

The clock functions autonomously as an oscillator. An oscillator transforms input information into a recurring periodic output signal. The input in the mammalian system is the photic information directed from the retina in the entrainment pathway. The oscillator is the master pacemaker, the suprachiasmatic nucleus (SCN). The output is the rhythmic signal that is directed to the rest of the organism. These three components govern the relay of environmental temporal information to the entire organism (Ikonomov and Stoynev, 1994). They are illustrated in Figure 2.3.

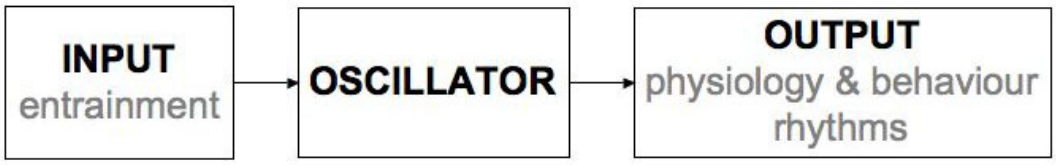

Figure 2.3 Schematic of the components of a circadian system in an organism.

The most potent zeitgeber for the circadian system in mammals is bright light (Gooley et al., 2001). Light is detected by photoreceptors in the inner and outer retinal cell layers of the eye. There are three types of retinal photoreceptor: rods, cones and melanopsin

ganglion cells. Rods are rhodopsin-containing photoreceptors that reside in the outer cell layer of the retina. They detect green (middle wavelength) and blue (short wavelength) light only and are therefore more useful for scotopic vision in dim light conditions. Cones are the main photoreceptors used to detect polychromatic bright light during the day. They possess many photopigments or opsins and cover a wide range of green, blue and red (long wavelength) light. They too are located in the outer cell layer. Together, the rods and cones detect light for visual processing. The photic information is transduced to the intergeniculate leaflet of the lateral geniculate nuclei (LGN) in the thalamus where it is then relayed to the primary visual cortex in the posterior occipital lobe of the brain. Here, the information is collated to form images that represent the visible environment with great resolution (Dacey et al., 2005).

The principal photoreceptors of the circadian system are a small subset of ganglion cells that reside in the inner cell layer of the retina. They contain the photopigment, melanopsin; an opsin, like rhodopsin, that employs a vitamin A-derived chromophore. It is sensitive to blue light with a maximum absorbance in humans at a wavelength of 480 nm (Qiu et al., 2005). These photoreceptors do not detect the various wavelengths of light with great acuity; rather they function to detect the general light intensity or irradiance. This information is transmitted via the retinohypothalamic tract (RHT) to the hypothalamic SCN, where it is used to entrain the circadian clocks of the master circadian pacemaker (Hannibal et al., 2000, Dacey et al., 2005).

Although the rods and cones function principally to detect photic information for image-formation, they also have some effect on the circadian entrainment system. Rods attenuate and cones enhance the circadian effects of melanopsin receptor activation. The visual system also directs information to the non-visual system from the intergeniculate leaflet via the geniculohypothalamic tract (GHT) (Gonzalez and Dyball, 2006). Conversely, melanopsin receptors, which function mainly for circadian entrainment, are speculated to also provide irradiance information directly to the image-formation system. This slight overlap in function between the photoreceptors, in their otherwise

essentially distinct roles, enables the integrated provision of stereoscopic environmental information regarding space and time (Foster, 2005, Hattar et al., 2003).

The SCN also integrates neurotransmitter inputs from other brain areas, such as serotonin from the midbrain Raphe nuclei and histamine from the tuberomammillary nuclei, as well as humoral signals such as melatonin from the pineal gland and œstrogen-directed signals from the ovary (Gonzalez and Dyball, 2006, De La Iglesia et al., 1999, Perreau-Lenz et al., 2004b, Nakamura et al., 2001, Nakamura et al., 2005, Kow and Pfaff, 1984).

2.4 THE SUPRACHIASMATIC NUCLEUS

The SCN is a bilaterally paired nucleus in the ventral hypothalamus, comprising a heterogeneous mix of approximately 20 000 neurones and associated glia (Moga and Moore, 1997). The localisation of the master pacemaker was first isolated, in rats, to the hypothalamus by Carl Richter in the United States in the 1960s (Richter, 1978). He ablated the hypothalamus of rats and observed the loss of rhythmicity in their drinking, feeding and locomotor behaviour. Sousa-Pinto and Castro-Correia in Portugal in 1970 used retrograde staining of degenerating neurones to identify that retinal projections pass to the SCN (Sousa-Pinto and Castro-Correia, 1970). Around two years later, Robert Moore and Nicholas Lenn in Chicago used radiolabelled tracers to trace the projections of retinal ganglion cells to the LGN and SCN (Moore and Lenn, 1972). Moore also performed SCN-lesion studies that resulted in the loss of rhythmicity in circadian adrenal corticosterone secretion in rats (Moore and Eichler, 1972). He concluded that the SCN was a likely participant in the production of rhythmic events such as those controlling the hypothalamo-pituitary regulation of adrenal function (Moore and Eichler, 1972).

Further evidence supporting the SCN as the master clock or oscillator can be provided by the elucidation of neurotransmitter connections involved in the circadian input pathway. The RHT is composed of the retinal ganglion cell axons, a subset of which is involved in mediating photic information to the circadian oscillator (Gooley et al., 2001). These cells secrete glutamate and pituitary adenylate cyclase-activating peptide (PACAP), and project to the SCN, which possesses glutamate and PACAP receptors (Hannibal et al., 2000, Hannibal et al., 2004). The GHT also projects to the SCN, which again possesses the relevant receptors for the neuropeptide Y, encephalin and GABA secreted by the GHT neurones (Abrahamson and Moore, 2001, Lall and Biello, 2003).

Functional studies have now proved conclusively that the SCN is the seat of the mammalian master pacemaker. Irving Zucker and Freidrich Stephan in Berkeley performed lesion studies that showed the selective loss of circadian drinking behaviour in rats with bilateral SCN lesions (Stephan and Zucker, 1972). Lesions elsewhere in the brain did not have any effect on circadian drinking. Inouye and Kawamura in Tokyo isolated the SCN *in situ* by cutting around it to form a hypothalamic 'island' using an L-shaped Halász knife (Inouye and Kawamura, 1979). Cells within the island were found to retain their multi-unit electrical rhythmicity while those outside of the island were found to have lost theirs. The SCN cells were thus shown to be autonomously rhythmic in the absence of neural and humoral input from outside the hypothalamus.

The loss of circadian rhythmicity was found to be reinstated by SCN transplant (Lehman et al., 1987). In 1987, Michael Lehman, Rae Silver and Eric Bittman's research teams in New York and Amherst found that fœtal SCN grafts reinstated free-running locomotor activity rhythms in SCN-lesioned arrhythmic adult golden hamsters. The fœtal grafts developed and were observed receiving neural input from the host retina as well as output projections to the host brain. The SCN was also able to reinstate some of the circadian rhythms of SCN-lesioned animals apparently using diffusible factors, emanating from encapsulated SCN tissue deposited into the third ventricle (Silver et al., 1996). Martin Ralph and Michael Menaker further showed in 1988 that the SCN

transplant-rescued rhythms of SCN-lesioned hamsters corresponded to the SCN donor rather than the host (Ralph and Menaker, 1988). They were able to do this by transplanting a *tau* mutant SCN into a wild-type hamster. The *tau* mutation is a point mutation in the semi-dominant autosomal gene for the serine-threonine phosphorylation-catalysing enzyme, casein kinase 1 epsilon (CK1ε) gene. The *tau* behavioural phenotype is a shortened free-running period of the hamster's circadian rhythms, which can be measured using locomotor activity monitoring, of either 20 hours in homozygotes or 22 hours in heterozygotes. The circadian rhythms of the host animal after transplantation corresponded to that of the transplanted *tau* mutant SCN. It was clear by 1991 that the SCN contained the dominant pacemaker cells responsible for generating overt circadian rhythms in mammals (Ralph and Lehman, 1991).

SCN organotypic slice cultures were found to maintain free-running rhythmicity in neuronal firing and secretion (Yamaguchi et al., 2003, Shinohara et al., 1994, Herzog et al., 1997). Dissociated SCN cells also maintained rhythmic output and were found to entrain fibroblasts when co-cultured (Welsh et al., 1995, Allen et al., 2001). Only SCN cells have been found to be able to entrain other cells (Pando et al., 2002, Allen et al., 2001). However, it is now evident that the SCN is not the only mammalian pacemaker. Circadian physiology has so far initially used a relatively restricted range of physiological parameters, such as locomotor activity or adrenal corticosterone secretion. Developing other ways of measuring circadian physiology, using different circadianly-driven processes, has lead to the discovery of new clocks or pacemakers; some that can free-run sustainably, independent of the SCN and be entrained by zeitgebers other than SCN outputs.

One such putative pacemaker is the elusive food-entrainable clock. There is a growing wealth of evidence to support the existence of such a clock in mammals (Saper and Fuller, 2007). Studies in non-mammalian vertebrates, such as birds, reptiles, amphibians and fish, have also demonstrated the existence of non-SCN pacemakers (LeSauter et al., 1996, Guilding and Piggins, 2007). The pineal gland, for instance, replaces the SCN as

the master pacemaker in house sparrows, whereas it works co-operatively with the SCN (Zimmerman and Menaker, 1979, Abraham et al., 2003) and the retina as a system of pacemakers in the European starling (King and Follett, 1997, Tosini et al., 2008). As such, it is plausible to suppose that there may be a hierarchy of pacemakers, in the brain or other organs, which form part of an entire mammalian circadian system and which govern other circadian parameters that have yet to be measured and fully described.

Thus far, the SCN remains the only pacemaker that can be defined as a tissue composed of cells that are intrinsically and synchronously rhythmic *in vivo* and *in vitro*, that are absolutely necessary for driving the overt circadian biology of an organism and that are able to stably confer rhythmicity, according to its own phase and period, to a new host organism when transplanted.

2.5 MAMMALIAN CLOCKWORK MACHINERY

The SCN contains many thousands of cells, each expressing a circadian rhythm. This rhythm is generated by a small number of highly conserved genes – called clock genes – that interact through their proteins to produce a circadian oscillation. It is the *co-ordination* of the rhythmic cells that generates the unique pacemaker properties of the SCN. Cells in most tissues and organs also express clock genes but they are less robustly rhythmic than the SCN.

The molecular machinery of the cell-autonomous clock is summarised in Figure 2.4.

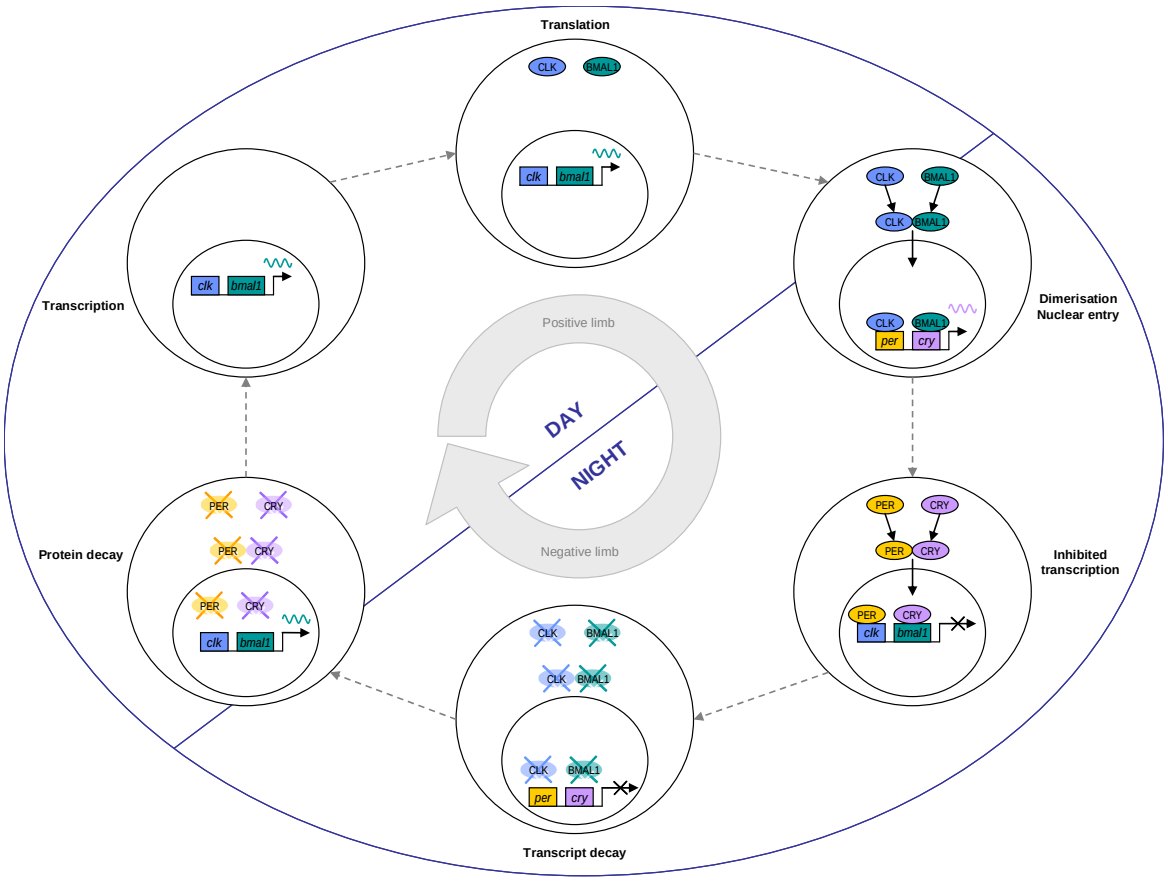

Figure 2.4 The transcription-translation feedback loops of the canonical clock genes that constitute the circadian clock. CLOCK (CLK) and BMAL1 proteins form the positive limb of the feedback loop, driving transcription of *period* (*per*) and *cryptochrome* (*cry*). PERIOD (PER) and CRYPTOCHROME (CRY) proteins feedback to inhibit the *clk* and *bmal1* negative limb of the clock; thus producing a 24-h oscillation.

The key mammalian clock genes are *clock*, *bmal1*, p*eriod* and *cryptochrome*. The name: *clock* (*clk*) stands for c*ircadian locomotor output cycles kaput*. The clock gene: *bmal1* stands for *Brain and muscle aryl hydrocarbon receptor nuclear translocator-like protein 1* and is also known as *ARNTL*, *mop3* or *tic*. There are three homologs of the *period* (*per*) gene, *period1* (*per1*), *period2* (*per2*) and *period3* (*per3*). There are two homologs of the *cryptochrome* (*cry*) gene, *cryptochrome1* (*cry1*) and *cryptochrome2* (*cry2*). All the clock genes share some sequence homology with each other, possessing E-box and E'-box elements in their promoter regions. Their proteins consequently possess common domains, typified by Period-ARNT-Singleminded (PAS) domains that allow

clock proteins to bind to each other. Clock proteins all also possess basic helix-loop-helix (bHLH) domains that enable them to bind to DNA (Kume et al., 1999, Reppert, 2000, Reppert and Weaver, 2001, Lee et al., 2001, Jin et al., 1999).

These genes are transcribed and translated, in the daytime, into proteins, CLK and BMAL1, which dimerise with each other along their PAS domains in the cytoplasm. These CLK:BMAL1 heterodimers translocate to the nucleus and act as transcription factors, binding to the promoter E-box elements of the *per* and *cry* genes, thus activating their transcription. The genes: *per1*, *per2*, *per3* are expressed first once the CLK:BMAL1 have activated transcription, followed by *cry1* and *cry2*. PER1, PER2 and PER3 proteins are obligate heterodimers with CRY1 and CRY2 proteins (Figure 2.4).

The CRY proteins stabilise the PER proteins, preventing them from being ubiquitinylated and degraded by the proteosome. PER:CRY dimers accumulate in discrete foci in the cytoplasm of the cell during the daytime. After 4-6 hours, the dimers abruptly dissociate and the single proteins move rapidly into the nucleus. Once in the nucleus, the PER and CRY proteins inactivate daytime *bmal1* transcription. The CRY proteins, in particular, may bind directly to the CLK:BMAL1 dimer to form a complex, to alter its phosphorylation status and ability to activate transcription (Dardente et al., 2007, Ishikawa et al., 2002, Glossop and Hardin, 2002). The prevention of *bmal1* transcription results in a decrease in BMAL1 that subsequently stops activation of *per1*, *per2*, *per3*, *cry1* and *cry2* transcription. The nuclear PER and CRY proteins also bind to undimerised CLK and BMAL1 respectively, thus again preventing CLK:BMAL1 from activating transcription, at night time.

The lack of *per* and *cry* transcription results in a decrease in PERs and CRYs, as degraded transcripts are not replaced. Over time, the amount of PER and CRY is no longer sufficient to significantly repress activation of the *bmal1* promoters. Thus, *clk* and *bmal1* transcription and translation re-initiates the next circadian cycle. Therefore *clk* and *bmal1* genes and proteins act as the positive limb of the feedback loop while the

per and *cry* genes and proteins act as the negative limb. Together, they constitute the self-sustained, autoregulated transcriptional-translational feedback loop that is effectively the clockwork or machinery of the cellular circadian clock.

The circadian clock incorporates a further feedback loop, involving genes that modulate the period of the circadian machinery (Figure 2.5). This second loop, interlocks with the primary circadian feedback loop and imposes post-translation mechanisms of regulation on the canonical clock genes. These mechanisms involve the action of the retinoic acid receptor-related orphan receptors (RORs), particularly ROR alpha (RORα or RORA). Also involved are receptors from the orphan receptor family: REV-ERBs, particularly REV-ERB alpha (REV-ERBα). The action of phosphorylation enzymes is also crucial, particularly that of the casein kinases: 1 epsilon (CK1ε) and 1 delta (CK1δ). Both RORs and REV-ERBs are circadianly expressed, orphan nuclear receptors that possess E-boxes in their gene promoters. They can thus, be activated by CLK and BMAL1.

Receptor-related orphan receptors alpha (RORα or RORA), beta (RORβ or RORB) and gamma (RORγ or RORC) are transcriptional modulators which are able to bind onto the ROR promoter element (RORE) on the *bmal1* gene, to up-regulate *bmal1* transcription (Guillaumond et al., 2005, Emery and Reppert, 2004). The *rev-erbα* gene is a constitutive repressor of gene transcription and when activated by CLK:BMAL1 binding, represses *bmal1* transcription (Preitner et al., 2002). The RORs and REV-ERBs are thought to work in competition to modulate the circadian clockwork machinery (Guillaumond et al., 2005).

CK1ε and CK1δ are enzymes that catalyse the phosphorylation, at serine or threonine residues, of proteins, such as PER and CRY. Phosphorylation of undimerised PER results in its degradation in the ubiquitin-proteosome proteolysis pathway. Phosphorylation of the PER and CRY dimers can inhibit nuclear transport as well as promote proteolysis. PER and CRY are thus prevented from inactivating *clock* and

bmal1 transcription (Vielhaber et al., 2000, Lowrey and Takahashi, 2000, Gallego et al., 2006, Dey et al., 2005, Allada et al., 2001).

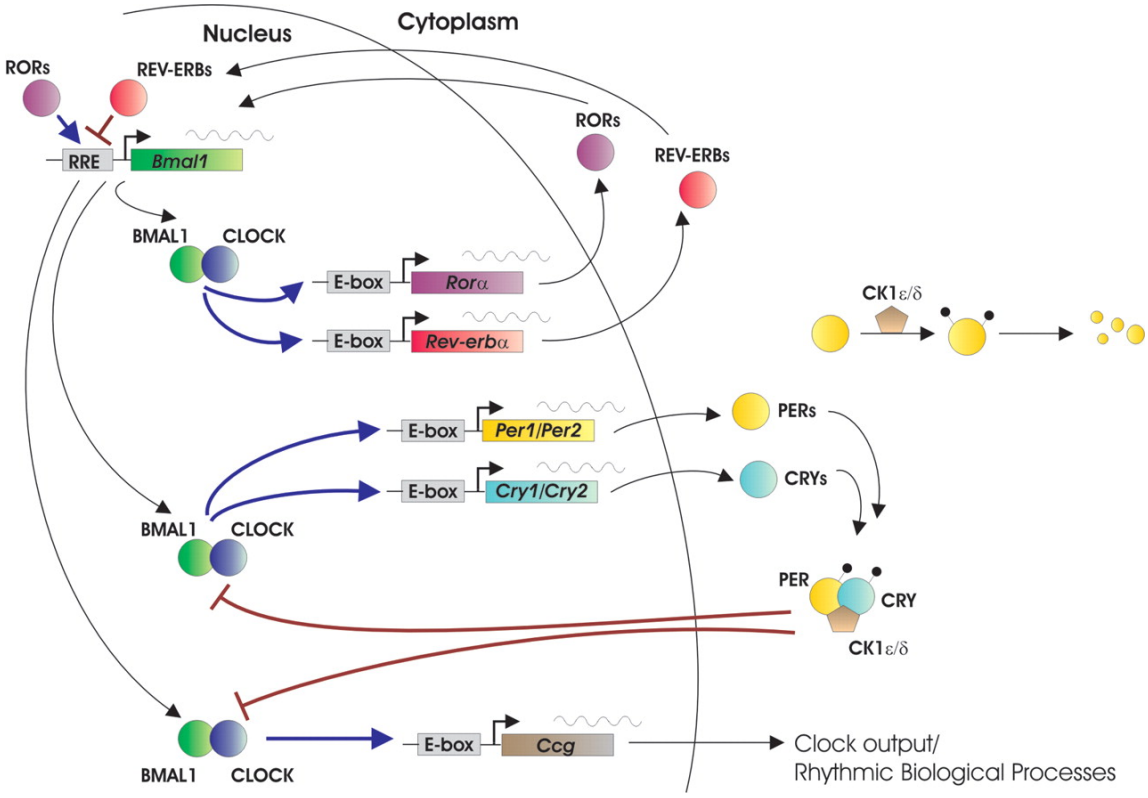

Figure 2.5 The complex, interlocked autoregulatory transcription-translation feedback loops that produce a circadian period (Boden and Kennaway, 2006).

Further post-translational mechanisms, along with epigenetic interactions have also been implicated in playing a mechanistic role in the circadian oscillator (Stratmann and Schibler, 2006, Dardente and Cermakian, 2007).

Circadian rhythms have been observed in histone acetylation (Etchegaray et al., 2003). Many of the core clock components have been identified as potential targets of histone acetyltranferases and deacetyltransferases (Nakahata et al., 2007). The *per1* and *per2* promoters also show circadian histone H3 acetylation, which along with the associated

polymerase activity, peaks concurrently with mRNA levels (Etchegaray et al., 2003). CLK itself can act as a histone acetlytransferase, a property that proved essential for the rescue of clock gene rhythmicity in *clk* mutant mice (Doi et al., 2006). Histone deacetyltransferases are also used, for example by mammalian CRY in transcriptional repression (Naruse et al., 2004). It is clear that chromatin remodelling has an important part to play in clock gene transcription and so, the timing of clock (Naruse et al., 2004). The process of chromatin remodelling often involves other co-activator proteins that are recruited and assembled into complexes for transcriptional activity (Etchegaray et al., 2003). This implicates that other proteins, apart from the canonical core clock components, are subtly involved in the regulation of the circadian clock.

The metabolic status of the cell is also a key influence on the regulation of the circadian clock (Rutter et al., 2001, Rutter et al., 2002). The binding of CLK to E-box elements *in vitro* is strictly regulated by the redox state of the cell. The redox state is generated by the energy metabolism ongoing in the cell and refers specifically to the ratio of reduced nicotinamide adenine dinucleotides (NADH or NADPH) to oxidised nicotinamide adenine dinucleotides (NAD^+ or $NADP^+$). Glucose uptake by the cell can thus also influence the running of the clock (Schibler and Sassone-Corsi, 2002).

It has been proposed that these multiple transcription-translation loops, interwoven with post-translational and epigenetic interactions, exist to confer a specific degree of flexibility, required by the clock in order for it to adapt to the normal physiological and environmental fluctuations encountered daily, without producing overly noisy fluctuations in its own system. The system is thus able to simultaneously co-ordinate key properties such as robust entrainment and temperature-compensation (Rand et al., 2006). Understanding more about the circadian machinery continues to be a major goal of the circadian rhythms field, as new clock components are likely to be discovered along with new perspectives offered by structural biology of the clock proteins and systems biology applying computational modelling to the feedback loop mechanisms (Takahashi, 2004). This computational approach deals much with the actual mechanics

of the clockwork machinery and aims to accurately model the clockwork, such that the model can be used to explain and predict phenomena observed in field experiments (De Haro and Panda, 2006, Forger et al., 2003, Forger et al., 2007).

Some have argued that this 'general oscillator' mechanism is common to all clocks and that, despite the high level of conservation of the core molecular components between species and cell types, there are a variety of specialisations, that can distinguish the properties of clocks such as those in the SCN and the peripheral tissues in mammals (Glossop and Hardin, 2002). Mutations in clock genes have been demonstrated to affect central clocks differently to peripheral clocks. Although the molecular events occurring in central and peripheral clocks are fundamentally the same, there are some key differences. Understanding how central and peripheral clocks work, in themselves and together, should provide a better dissection of underlying clockwork machinery.

2.6 CENTRAL AND PERIPHERAL CLOCKS

The subordinate clocks in cells in peripheral tissues have many of the same properties as the cells of the SCN. They are relatively robust in their rhythmic clock gene expression, with the transcriptional activators expressed in antiphase to the transcriptional repressors, in interlocked feedback loops that are sustained in the absence of the SCN and humoral signals (Balsalobre, 2002). They are also resistant to biochemical and structural changes imposed by the cell division cycle, in fact, interacting with the cell cycle. The circadian clock can gate the entry of dividing cells into the S phase of the cell cycle as well as confer an initial entrainment of sorts to the subsequent daughter cells. Peripheral clocks are also able to withstand varying transcription rates (Stratmann and Schibler, 2006, Nagoshi et al., 2004).

Peripheral clocks however differ from central clocks in some of their properties and modes of function, related to specialised function in the periphery. Peripheral clocks still function to provide circadian information that allows the various cells and tissues to temporally co-ordinate their biochemical, physiological and behavioural processes. Whilst SCN neurones are able to sustain synchronised circadian rhythms in clock gene expression and electrical firing for days and even years in culture, peripheral cells, such as fibroblasts from cell lines or from adult or embryonic tissues, apparently lose rhythmicity.

This dampening of the rhythm can be reversed however, by exposure to serum-shock or other chemical or physical treatments. Closer observation has elucidated that although the clock in individual peripheral cells can be persistently self-sustained, it is the synchrony between the cell oscillators that is lost over time. Thus, an overall population effect is seen as a dampening of circadian rhythm behaviour. The serum-shock is thought to work as an entrainment signal, resetting the various de-synchronised cell clocks back to the same time and phase. The lack of stringent coupling in peripheral clocks is considered more useful as they are required to also respond and incorporate temporal information from multiple sources. Looser coupling enables these clocks to adapt more quickly and efficiently than the central clocks.

Peripheral clocks often show a delayed phase compared to the SCN. The peripheral clock gene mRNA and protein peaks and troughs may be four hours behind those of the SCN (Balsalobre, 2002). This time lag is likely to be accounted for, in part, by the delay that is incurred in the SCN relay and in part, by the intrinsic timing of the peripheral organs and tissues. These differences may occur due to differential responses to SCN signalling and/or the effect of other timing information. The degree of influence exerted on peripheral clocks by non-SCN signalling appears to vary between cells and tissues, and may explain why peripheral clocks respond differently from the central clocks, to circadian perturbations like changes in environmental temperatures or feeding times (Brown et al., 2002).

Furthermore, the peripheral clocks can be uncoupled from the master clock *in vivo* by a variety of other zeitgebers. Feeding schedules have dramatic effects on the phase of peripheral clocks in the liver, kidney and heart. The daytime feeding of nocturnal animals has been shown to completely invert the phase of the circadian gene expression in food-metabolising tissues such as the liver, kidneys and pancreas. The phase of the circadian gene expression the SCN however remains unchanged (Schibler and Sassone-Corsi, 2002). The uncoupling of the peripheral clocks from the central clocks seems to be inhibited by the glucocorticoid hormones, which have also been implicated in the maintenance of circadian S phases in cell division (Schibler and Sassone-Corsi, 2002, Pitts et al., 2003). The *VPAC2 receptor* (also known as *vipr2*) knock-out mouse, that has a weak SCN system due to poor signalling in the SCN, shows very robust food entrainment rhythms, as measured by locomotor activity, corticosterone secretion and clock gene expression in the liver (Sheward et al., 2007). The timing information from the feeding regimen is seemingly transduced by a putative food-entrainable oscillator, which can function as a pacemaker. Food-entrained circadian rhythms can even be sustained in the absence of feeding time cues in $clk^{-/-}$ mutant mice that are arrhythmic in their locomotor activity (Pitts et al., 2003). Thus, a regular feeding schedule allows the organism an alternative way of sampling the geophysical environmental time, apart from the light of the sun (Mistlberger, 2006).

Another secondary time cue can be provided by core body temperature of an organism. This is cyclical and is influenced by the animal's sleep-arousal status, locomotor activity, food intake and metabolism (Schibler and Sassone-Corsi, 2002). Although central pacemakers like the SCN are temperature-compensated, peripheral clocks can be altered by temperature. Rat cellular clocks *in vitro* that would have rapidly dampened *en masse* were synchronised by circadian oscillations in temperature that reflected the core body temperature of mice. *In vivo*, inversion of the circadian environmental temperature cycles caused mice to similarly invert the phases of their liver clocks. Their SCN however was able to maintain its original phase (Brown et al., 2002).

Evidence is mounting that there is still much to discover about the similarities and differences in the functions of central and peripheral clocks. The signalling from the central to the peripheral clocks has been relatively well observed. The signalling which must occur in the opposite direction, from the peripheral to the central clocks, have however been less well delineated. Many peripheral clocks interact with each other in order to maintain some synchrony and co-ordinate of their circadian rhythms. They are also likely to provide feedback signalling to the central pacemaker, regarding physiological and metabolic status.

It is therefore important to elucidate more about how peripheral clocks impact the central clock. One system that offers avenues of investigation is that regulating the reproductive axis. Reproduction, particularly in females, is governed by temporal processes. The female reproductive or menstrual cycle lasts an average of 28 days in humans. The corpus luteum in women has a very precise 14-day lifespan, when fertilisation of the ovum does not occur. The timing of the LH surge which initiates ovulation is, certainly in rodents, gated by a circadian clock mechanism (de la Iglesia and Schwartz, 2006). The female reproductive tract is well known to receive and deliver signals, both humorally and nervously, from and to the central nervous system (CNS), particularly the hypothalamus and pituitary gland (Everett and Sawyer, 1950, de la Iglesia and Schwartz, 2006). The SCN is part of the hypothalamus. The female reproductive axis thus provides a focus for investigating circadian rhythm function, propagation and communication.

2.7 SCN OUTPUTS AND CO-ORDINATION

Once the environmental time cues have been inputed, the SCN outputs provide time cues that allow the peripheral clocks to entrain their timing to match the environment. The SCN uses both neuronal and humoral signalling to co-ordinate the peripheral clocks. This has been shown using SCN transplantation and parabiosis experiments. Only some of the overt circadian rhythms lost in SCN-lesioned animals have been rescued by diffusible signals in specially encapsulated SCN transplants and parabiosis experiments (Guo et al., 2005). This suggests that neuronal connections are also necessary. The main brain cells directly targeted by the SCN are the endocrine neurones in the adjacent hypothalamus, the autonomic neurones of the paraventricular nucleus (PVN), as well as neurones on other regions of the hypothalamus and rest of the brain (Buijs and Kalsbeek, 2001). These targets, in turn, signal environmental time to other cells in the rest of the brain and body and co-ordinate processes such as sleep, locomotor activity, food intake and hormone secretion.

One key output of the SCN in mammals is a multi-synaptic pathway projecting via the PVN to the pineal gland. The pineal gland produces melatonin during the night and the nocturnal increase in melatonin concentrations signals to the rest of the body that it is night time. Melatonin is a sleep-promoting signal, mediating changes such as the drop in core body temperature via the sympathetic nervous system (Krauchi et al., 2006). The SCN is known to inhibit melatonin secretion during the daytime via gamma-aminobutyric acid-releasing neuronal (GABAergic) efferents to the PVN, which inhibit melatonin synthesis in the pineal gland (Kalsbeek et al., 1999, Perreau-Lenz et al., 2004a). The SCN also plays a role in activating the nocturnal peak in melatonin secretion, using glutaminergic innervation of the PVN, which signals to the pineal gland (Perreau-Lenz et al., 2004a, Perreau-Lenz et al., 2004b). Melatonin acts by binding to specific melatonin receptors, like type one melatonin receptors (MT_1) and type two melatonin receptors (MT_2). Melatonin receptors are abundant in the PT of the pituitary gland as well as the SCN and other brain areas such as the hippocampus (Williams et al.,

1995, de Reviers et al., 1991). They can also be found in other organ systems, including the testes and the ovary (Pang et al., 1998).

Other humoral outputs from the SCN include vasopressin (VP), which is released in a circadian fashion into the cerebrospinal fluid; and prokineticin 2 and transforming growth factor alpha (TGFα), which are strong candidates for signalling time from the SCN (Schibler and Sassone-Corsi, 2002).

2.8 THE SCN AND THE HYPOTHALAMO-PITUITARY-GONADAL AXIS

The hypothalamic-pituitary-gonadal (HPG) axis is involved in the control of reproduction via the hypothalamus, pituitary gland and gonads. The hypothalamus, which serves as a relay station, transduces information neurally to the pituitary. The pituitary gland responds to the hypothalamic signals and produces humoral factors, such as hormones, which then signal to the gonads: the ovaries or testes. The gonads then effect the key mechanisms of reproduction: ovulation and spermatogenesis.

Circadian timing and clock genes are known to provide time control for the HPG axis (de la Iglesia and Schwartz, 2006, Miller et al., 2004). There are many levels in the HPG heirarchy at which circadian timing may work (Figure 2.6).

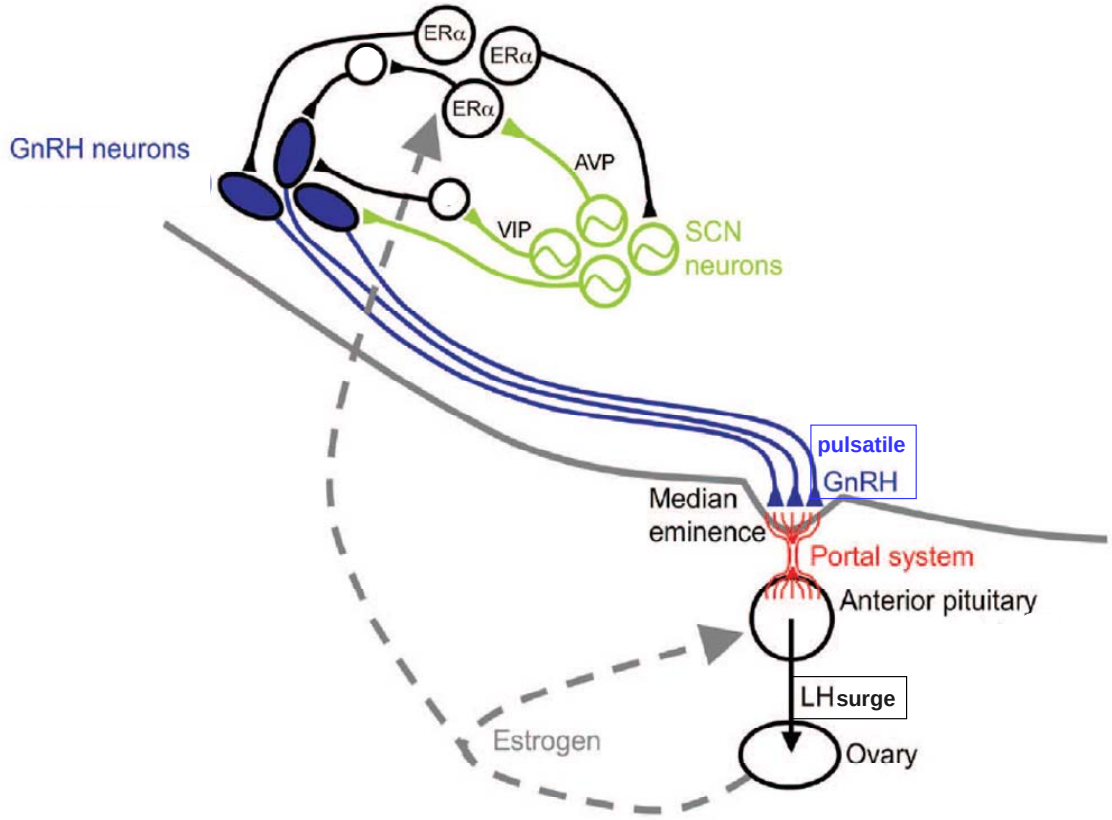

Figure 2.6Timing in the hypothalamic-pituitary-gonadal axis (de la Iglesia and Schwartz, 2006).

At the level of the brain, the SCN affects the reproductive axis through the control of gonadotrophin releasing hormone (GnRH). GnRH is released in a pulsatile fashion from nerve terminals in the median eminence of the basal hypothalamus into the hypothalamo-pituitary portal blood system to control the synthesis and secretion of the gonadotrophins. LH and FSH from the gonadotrophs in the anterior pituitary gland act on the gonads to stimulate gamete development and hormone synthesis. In order to regulate the reproductive axis, the GnRH neurones are subject to input directly from the SCN as well as indirectly via œstrogen-responsive neurones in the pre-optic area (POA) (Mahoney and Smale, 2005, Van der Beek et al., 1997). In addition, GnRH neurones have been seen to express clock genes, which may be involved in the timing of GnRH release (de la Iglesia and Schwartz, 2006).

In female rodents, the SCN acts to gate the LH surge to the afternoon to control the timing of ovulation (Everett and Sawyer, 1950, Kalra, 1993, Palm et al., 2001). Nocturnal rodents thus use the circadian clock to synchronise their ovulation with the night time, when they are most active and most likely to encounter males. This synchrony optimises the chances of conception.

The circadian control of the pre-ovulatory LH surge was first described in rats and published in a seminal paper by Everett and Sawyer in 1950 (Everett and Sawyer, 1950). Rats have a four or five day œstrous cycle. They ovulate on day one, up to 12 hours after the pre-ovulatory LH surge on the day of proœstrous. If the pre-ovulatory LH surge is inhibited for a few hours, as with the administration of a short-term barbiturate sedative, ovulation does not then occur a few hours later. Rather it is delayed until the afternoon of the following day. This is because there is a time window in which ovulation can occur. It can only be triggered the following day, when the LH surge falls again within the afternoon time window. If the rat is ovariectomised and permissive amounts of oeatradiol administered, the LH surge is seen to occur daily, gated every day to the afternoon (Figure 2.7). This gating of the LH surge and subsequently, of ovulation, is dictated by the circadian clock. The SCN, when ablated by hypothalamic knife cuts, is no longer able to communicate neurally. This results in the loss of œstrous cyclicity and disturbance of LH periodicity (Nunez and Stephan, 1977). Mutation of the clock genes have also resulted in perturbed œstrous cycles and abnormal LH surges (Miller et al., 2004). The clock genes and the SCN have therefore been shown to be essential for the maintenance of œstrous cyclicity and reproductive timing (Ball, 2007).

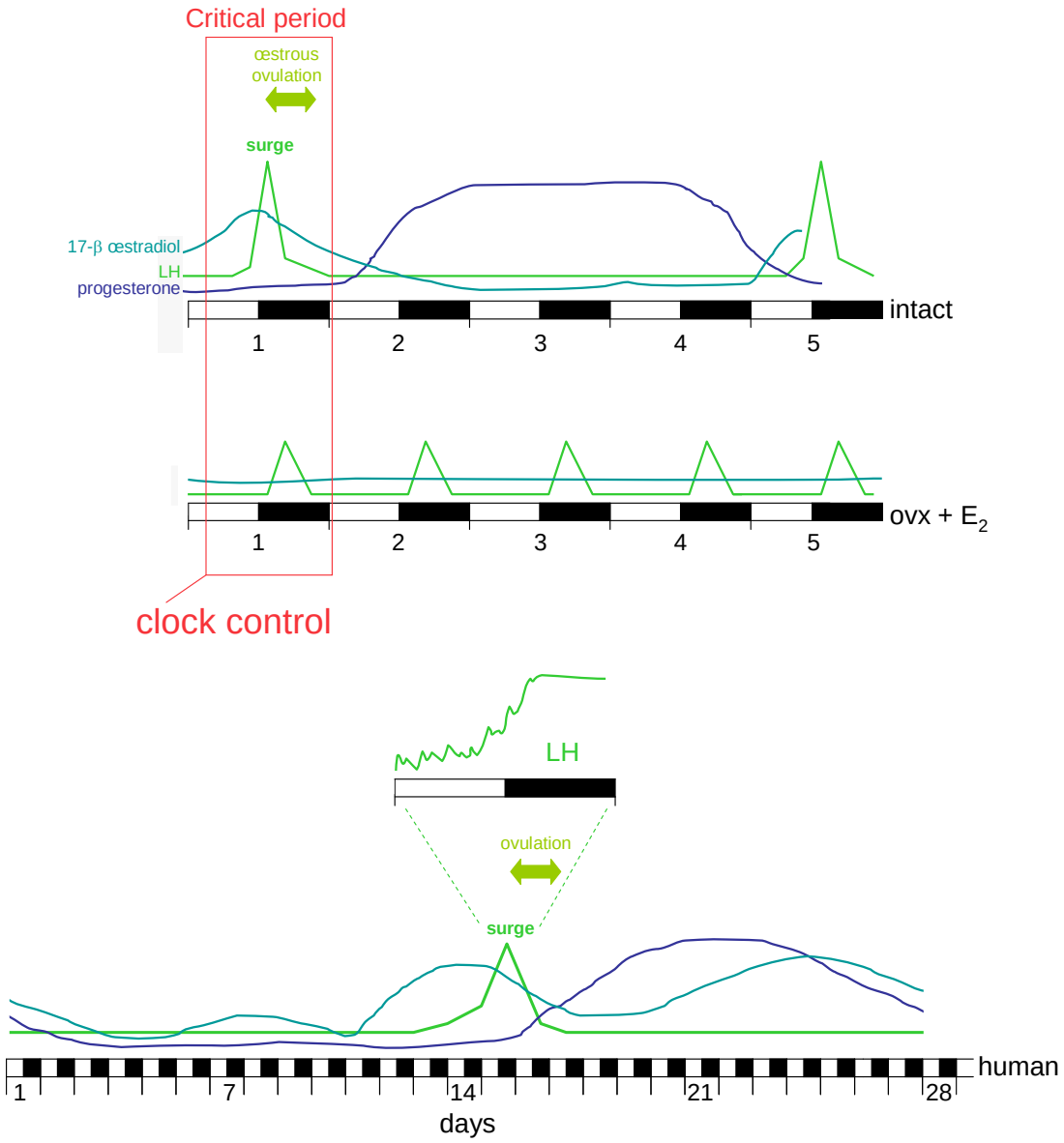

Figure 2.7 The circadian clock-controlled LH surge occurs in a critical period in rat œstrous cycle. This occurs in intact animals (intact) where the daily or circadian LH peak is masked by overriding hormone physiology, but is revealed to be truly circadian when the hormonal signals are removed by ovariectomy of the animal (ovx + E_2), which is then supplemented with œstradiol, as œstradiol is permissive for the LH surge. This circadian gating of the LH surge and thus, ovulation, is comparable to that of the human menstrual cycle (adapted from Lincoln, G. A.).

It is not just in the œstrous cycles of rodents that the circadian clock functions. It is also likely to function to regulate the menstrual cycles of higher primates, including women. Shift work and frequent transmeridian flights have been correlated with irregular

menstrual cycles and an increased incidence of reproductive cancers in humans (Lauria et al., 2006, Megdal et al., 2005, Baker and Driver, 2007).

Many other pituitary hormones involved in reproduction are regulated in a circadian manner in the hypothalamus. *VP* is expressed in a circadian rhythm in the SCN, PeVN, PVN and SON (Moore et al., 2002, Moga and Moore, 1997). Oxytocin is potentially circadianly regulated and has been proposed to gate the circadian timing of birth (Roizen et al., 2007, Goldstein, 2004). Neurophysin has also been observed to be expressed in the hypothalamus, particularly in the SCN (Okamura et al., 1995). GH, ACTH and TSH levels have all been found to fluctuate in circadian rhythms and all these hormones are involved in reproduction (Szafarczyk et al., 1983, Luboshitzky, 2000, Thorner et al., 1995, Cano et al., 2008). As they all are regulated by or closely associated with circadian rhythms, one might infer that circadian rhythms, emanating from the hypothalamus, regulating pituitary hormones, are in fact (to some degree) regulating reproduction (Luboshitzky, 2000).

Furthermore, the clock genes are expressed in both male and female gonads as well as in other reproductive tissues. The gene *per* is constitutively expressed in the fruit fly (*Drosophila melanogaster*) ovary, as is another fruit fly clock gene, *timeless* (*tim*). Female flies lacking either *per* or *tim* produce almost fifty per cent fewer progeny and mature oocytes than wild-type females (Beaver et al., 2003). The clock genes: *clk*, *bmal1*, *per1*, *per2*, *per3*, *cry1*, *cry2* and *tim* were all detected in the unfertilised oocytes, uteri and fallopian tubes of pregnant mice (Johnson et al., 2002). The function of these genes in either the fruit fly or mammalian ovary however has yet to be elucidated. Expression of *clk*, *bmal1*, *per1*, *per2* and *cry1* has also been detected in the mouse testes. In addition, PER1 and CLK could be localised in the mouse testis (Alvarez et al., 2003, Morse et al., 2003). Again, the function of these clock genes and proteins has yet to be discovered.

Reproductive events in the brain, ovary, fallopian tube and uterus also all occur with close temporal synchrony to each other. Timing of mating in many non-primate species corresponds with the timing of the LH surge and subsequently, the timing of ovulation (Boden and Kennaway, 2006). Nocturnal rodent females exhibit behaviour that prompts males to copulate at a time which coincides with ovulation during the middle of the night. The synchronisation of the timing of mating to coincide with that of ovulation also appears to be much the same in diurnal rodents, like the African grass rat (*Arvicanthis niloticus*), as well as in humans. African grass rats ovulate in the latter half of the dark phase and mate during the early morning. Humans also tend to ovulate in the late night, following an LH surge some time between midnight and 0800 h (Kennaway, 2005). There has also been observed a major peak in sexual activity in the late night as well as a minor peak in the early morning. The co-ordination and synchrony of these various temporally orchestrated processes must be performed in tandem: both within the organism and with its external environment.

Clock gene knockout and mutant animals also frequently display aberrant and subfertile reproductive capacity. Female *clk*$^{-/-}$ mutant mice have irregular and extended œstrous cycles, increased fœtal resorption and a high rate of full-term pregnancy failure (Miller et al., 2004). They also lack the co-ordinated LH surge that is required on the day of proœstrous. This LH surge fails even with œstradiol and GnRH priming of the gonadotrophs. Although most mutant animals did not produce an LH surge, a few individuals were able to produce a small increase in LH levels that was sufficient to induce ovulation. This increase was significantly smaller than that of the wild-type. Furthermore, male reproductive function was also affected in clock gene mutants. Clock gene mutant fruit flies display a low-fertility phenotype (Beaver et al., 2002). They produce around forty per cent fewer progeny after mating with wild-type females. These females lay fewer eggs and of these eggs, there is a greater rate of unfertilised eggs. The *per* or *tim* null mutant males, both released significantly less sperm from their testes into the seminal vesicles. Although the actual mechanism remains undefined, it is clear that the clock genes are involved in regulating both female and male gonadal

function. All this evidence clearly implies that there is a function for the clock genes in the regulation of the reproductive axis and therefore, reproduction. The clock genes appear to affect various hierarchical stages of reproductive regulation. The reproductive axis can therefore be viewed as a mirror of whole body systems with a pacemaker that is integrated by feedback signals from slave clocks, such as those in the gonads.

2.9 SPECIAL FOCUS ON THE HUMAN FEMALE REPRODUCTIVE CYCLE

Female reproductive cycles begin in adults, once sexual maturity is reached. The fundamental reproductive units of these cycles are the gametes or ova, which begin developing *in utero*. Primordial or precursor germ cells, also known as gonocytes, are visible in embryos as early as the third week after conception (Pereda et al., 2006). Conception occurs when the ovulated oocyte is fertilised by a spermatazoan, usually in the fallopian tubes, also known as the oviduct. After fertilisation, the resulting zygote proceeds through a series of cleavages, producing first two cells, then four cells, then eight and so forth, doubling the number of cells each time (Figure 2.8). The mass of cells, around the 128-cell stage, then assume a structure, arranging into a spherical layer that surround a fluid-filled cavity called the blastocoel.

These surrounding blastomere cells then differentiate into two cell types, which characterise the structure as a blastocyst. One cell type comprises an outer layer of cells called the trophoblast layer or outer cell mass. The other cell type forms a mass within the trophoblast layer, called the inner cell mass or embryoblast. The trophoblast goes on to become the placenta, as the blastocyst cells invade and implant in the endometrial lining of the uterus. Implantation occurs about six to seven days after fertilisation, when

the blastocyst exits the fallopian tube and so, enters the uterus (Figure 2.8). The embryoblast differentiates into many cell types as development progresses *in utero*, producing both extra-embryonic and embryonic tissues. One of these embryonic tissues is the embryonic mesoderm, which eventually gives rise to the gonads and germ cells.

Around 14 days after fertilisation, the blastocyst invaginates and cells migrate in the process of gastrulation. The resulting gastrula continues restructuring and differentiating into the embryonic disc, with cells forming the primitive streak within a couple of days of gastrulation. By the third week of gestation, the early embryo is recognisable and the primordial germ cells visible (Pereda et al., 2006).

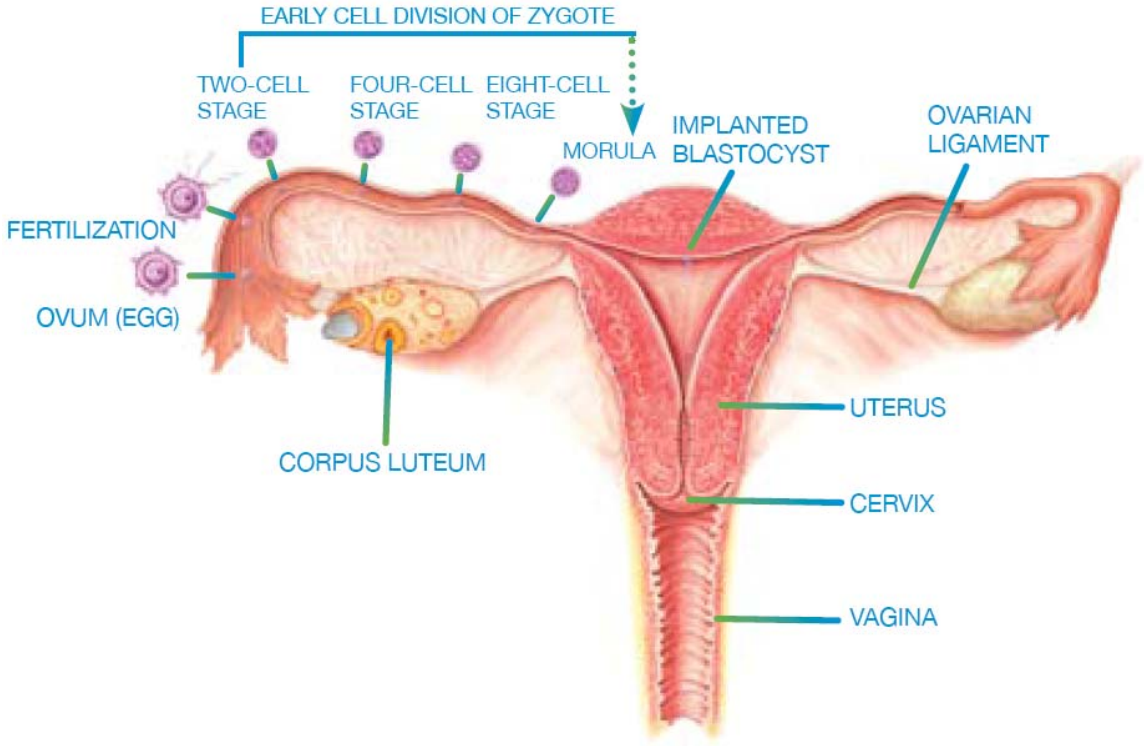

Figure 2.8The reproductive process from ovulation to implantation (adapted from the Common Gynecological Disorders Anatomical Chart, Anatomical Chart Company: http://www.anatomical.com/).

In the early embryo, the primodial germ cells of male and female embryos appear alike. The determination of sex has however already been made; during fertilisation, based on the haploid sex chromosome present in the fertilising spermatozoan. If the spermatozoan contained a Y chromosome; this combined with the X of the oocyte would produce an embryo with XY chromosomes: therefore, a male. If the spermatozoan contained an X chromosome; this combined with the X of the oocyte would produce an embryo with two X chromosomes: therefore, a female. The haploid germ cells of males are correspondingly able to possess either an X or a Y chromosome, while the haploid germ cells of females are able to possess only X chromosomes. As the embryo develops, the germs cells acquire more characteristic sex-specific morphology.

The primordial germ cells, like the cells that form somatic tissues, are diploid, possessing 23 paired chromosomes. These primordial germ cells will eventually become haploid germ cells, possessing only half the chromosomal complement: 23 unpaired chromosomes, by the process of meiosis. The premeiotic diploid primordial germ cells originate from the ventral wall of the hindgut, near the allantois. They divide mitotically and continue proliferating as they migrate through the hindgut and into the genital ridge, where somatic mesenchyme cells, also derived from embryonic mesoderm, are differentiating to form the matrix of the gonads. This migration is largely complete by about five to seven weeks of gestation.

The primordial germ cells then undergo two further processes: meiosis and atresia, while continuing to proliferate. Meiosis is the division of cells that produces haploid daughter cells, known as the gametes. Meiosis occurs with two rounds of cell division: the initial round, meiosis I, occurring much like mitosis except with independent assortment and recombination of the chromosomes, giving rise to novel diploid cells, which then undergo a second round of cell division, meiosis II, to produce four novel haploid cells. Each round of meiosis is divided into four stages: prophase, metaphase, anaphase and telophase. The prophase of the first meiotic division: prophase I can be further subdivided into leptotene, zygotene, pachytene, diplotene and diakinesis stages.

In females, some of the primordial germ cells at the genital ridge undergo meiosis until they are arrested at the diplotene stage of prophase I, thus becoming primary oocytes that are dictyate. Some of the oocytes acquire a layer of squamous pre-granulosa cells around them, thus becoming primordial follicles. The formation of primordial follicles begins around the 16th week of gestation. Simultaneously, some of these follicles as well as primary oocytes are lost by a process of apoptotic cell death called atresia. Thus, the opposing effects of continual mitosis and atresia result in a peak number of germ cells of approximately six to seven million around 20 weeks of gestation, a number that then falls sharply to approximately two million by the time of birth (Macklon and Fauser, 1999, Johnson and Everitt, 2000).

At birth, the pool of primordial follicles becomes finite, as mitotic proliferation of the germ cells has stopped. The primordial follicles become quiescent and stop developing until puberty *i.e.* sexual maturity is reached, at which time the follicles can resume growing and maturing. Although a few primordial follicles do sporadically and incompletely resume development, becoming primary and even pre-antral secondary follicles, prior to puberty, it is not until sexual maturity is reached that follicles are regularly recruited into resuming development. Throughout the time leading up to puberty, atresia continues to occur and only approximately 400 000 follicles survive at puberty (Johnson and Everitt, 2000, McLaughlin and McIver, 2009).

The onset of puberty in the early teens, is influenced by many factors, including nutrition and body fat content (Johnson and Everitt, 2000). The hypothalamus initiates the process by up-regulating the activity of the pulsatile GnRH-secreting neurones, which drive the anterior pituitary gland to secrete FSH and LH. These hormones, in turn, cause the gonads to grow to adult size and stimulate both gametogenesis and steroidogenesis. The sex steroids promote the development of secondary sexual characteristics such as body and pubic hair growth, widening of the pelvis, increased weight and redistribution of fat deposition in women (Johnson and Everitt, 2000).

After puberty, the gonadotrophins continue to be secreted, in a cyclical fashion that drives the menstrual or ovarian reproductive cycle. The gonadotrophins play a particularly crucial role in the later stages of follicle development. Around a thousand follicles are recruited into a pool of developing follicles in each reproductive cycle. These follicles can be primordial or primary follicles. Primordial follicles resume development into primary follicles, characterised by increased follicular size and altered squamous pre-granulosa cells, which have become cuboidal and are arranged in a single cell layer around the primary oocyte. The granulosa cells also acquire proliferative potential and as the single layer of cells multiply, they become arranged in several cell layers around the oocyte, thus denoting the transition of the primary follicle into a secondary pre-antral follicle.

Although the oocyte of the secondary pre-antral follicle continues to be arrested in meiosis I, it is able to grow and produce ribosomal and messenger RNA, the latter of which is used to generate proteins that are stored for later use in oocyte maturation and early post-fertilisation oocyte development (Johnson and Everitt, 2000). The oocyte also secretes a glycoprotein-rich matrix, which forms a thick membrane around the oocyte called the *zona pellucida* (Flechon et al., 1984). Ovarian stromal cells condense around the follicle and differentiate into follicular theca cells. The theca cells possess LH receptors and upon LH stimulation, they proliferate and facilitate vascularisation, secreting steroids such as androgens (Figure 2.11). They then develop into two layers: a *theca interna* that is glandular and highly vascularised and a *theca externa* that acts as fibrous outer capsule enclosing the follicle (Figure 2.9) (Johnson and Everitt, 2000).

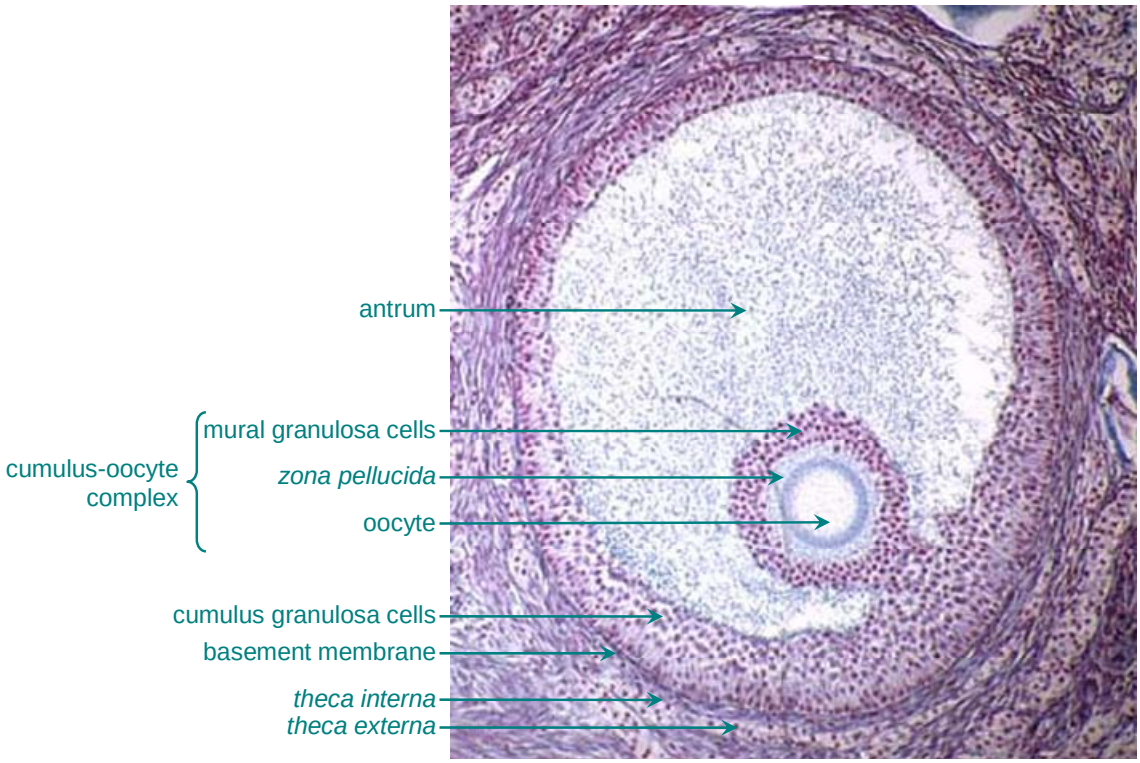

Figure 2.9 Photomicrograph cross-section of a rat antral follicle, stained with heamotoxylin and eosin (adapted from Alex Imholtz's Biology webpage, Prince George's Community College, MD, USA: http://academic.pgcc.edu/~aimholtz/AandP/PracPrac/Repro/secondaryandgraafian.jpg).

The granulosa cells secrete a viscous fluid that combines with serum transudate in-between the cells to create a fluid-filled cavity in the middle of the follicle called the antrum (Figure 2.10). The antrum denotes the maturation of the pre-antral follicle into an antral or secondary or secondary vesicular follicle. The size of the antrum grows, as does that of the follicle. As the antral cavity increases, the oocyte becomes suspended in the fluid. It is closely surrounded by a dense layer of granulosa cells and is tethered to the antrum wall by a thin stalk of cumulus granulosa cells (Figure 2.10). The cells surrounding the oocyte are now referred to as cumulus granulosa cells, while the granulosa cells comprising the main granulosa cell layer are referred to as the mural granulosa cells. The cumulus granulosa cells are likely to provide oocyte maintenance, while being regulated by the oocyte in turn (Gilchrist et al., 2008, Eppig et al., 2002). The mural granulosa cells are involved in steroidogenesis and the regulation of follicular

rupture. The oocytes of antral follicles are also able to now progress through meiosis I *in vitro* and are thus referred to as being meiotically competent, though they continue to remain arrested in meiosis I *in vivo*.

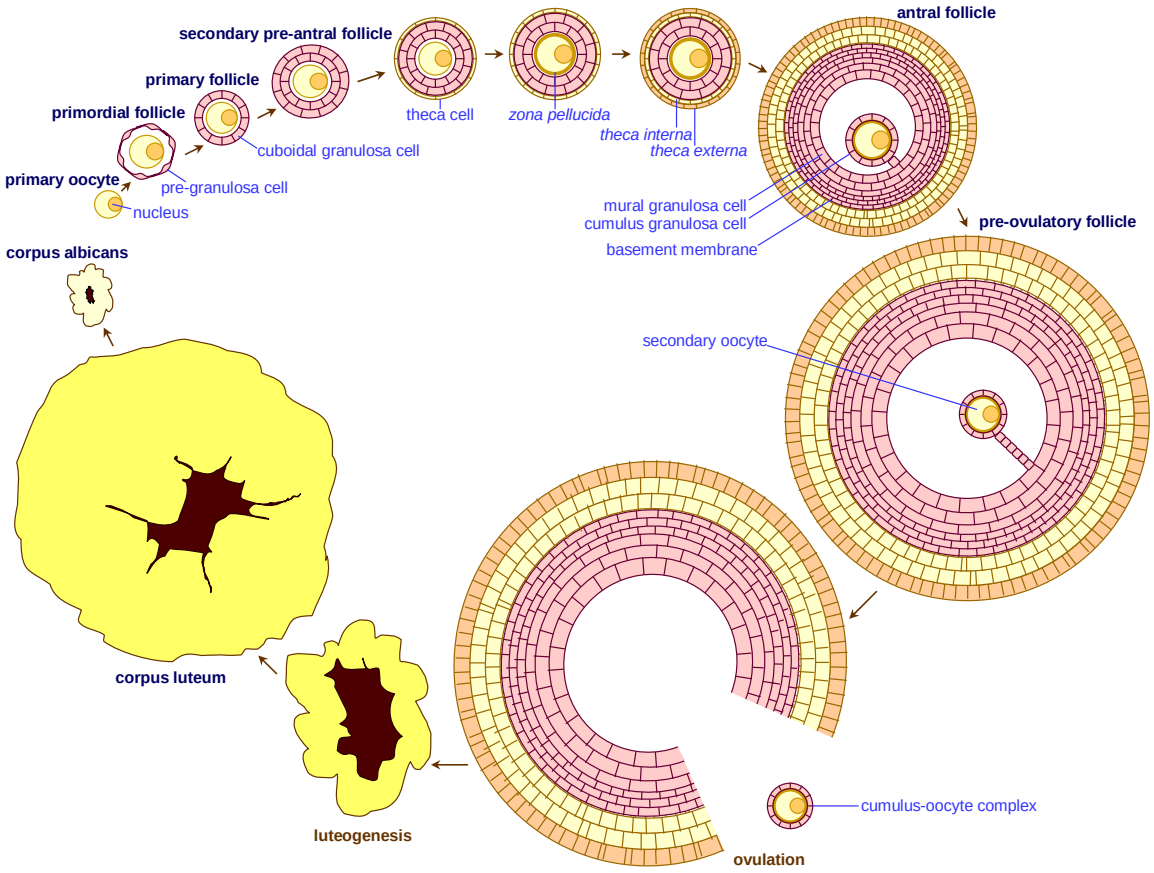

Figure 2.10 The ovarian cycle.

As the antral follicles continue to grow with increasing cell numbers and antral size, they become gonadotrophin-dependent, requiring FSH and LH receptors in order to avoid atresia. Meanwhile, primary, secondary pre-antral follicles and early antral follicles up to 2 mm in diameter, while gonadotrophin-responsive, by dint of possessing granulosa cell FSH receptors, are not gonadotrophin-dependent (Johnson and Everitt, 2000). FSH

stimulates the growth of follicles and increases in concentration during the follicular phase of the menstrual cycle.

The development of the primordial follicle into an antral follicle takes an average of 85 days, the equivalent of three menstrual cycles. The recruitment of primordial follicles occurs in waves, once every menstrual cycle (McLaughlin and McIver, 2009, Baerwald, 2009). By the time the antral stage is reached, only about six to ten follicles remain out of the thousand or so recruited in the same wave; the rest having been lost by atresia (Johnson and Everitt, 2000). The surviving antral follicles are now ready to be recruited into the reproductive or menstrual cycle where one of them will become the dominant follicle of the cycle that will be ovulated. The timing of the attainment of the antral stage must coincide with the ovarian hormonal milieu, which fluctuates with the reproductive cycle and must be optimal for successful recruitment and maturation of the antral follicles. If the timing does not coincide, the follicle does not mature any further and becomes atretic.

When successfully recruited into the reproductive cycle, the follicles continue to grow and the the antral space continues to enlarge. The follicles begin to produce œstradiol, which is largely synthesised from the androgens produced by the *theca interna* cells. The androgens pass from the theca cells, through the basement membrane and into the granulosa cells, where the stimulation by FSH enables the activation of aromatase, which catalyses the conversion of the androgens into œstrogens, particularly œstradiol. The androgens also stimulate aromatase activity in the granulosa cells, resulting in increased œstrogen synthesis. Œstrogens also have an intrafollicular effect, increasing granulosa cell proliferation and oestrogen receptor synthesis, thus increasing its own production in a positive feedback loop. The antral follicles therefore grow rapidly as does the amount of œstrogen secreted. These large amounts of œstradiol also feed back to the hypothalamus and anterior pituitary gland, where they repress FSH secretion from the anterior pituitary (Figure 2.11). The subsequent drop in FSH levels causes the atresia of smaller, competing follicles, leaving a sole survivor: the largest follicle, which

is able to survive as it is the most FSH-sensitive. Thus, the dominant follicle is selected for further maturation (Johnson and Everitt, 2000).

It acquires LH receptors on its granulosa cells, under the influence of FSH and œstrogens. It must time this acquisition in order that both the theca and granulosa cells can respond to the pre-ovulatory LH surge. The LH surge occurs as a result of increasing œstrogen levels from the antral follicles that signal to the hypothalamus, which directs the tonic release of LH from the pituitary gland. The rising œstradiol now reverses the œstradiol repression of FSH secretion, creating a positive feedback loop with FSH and LH (Figure 2.11). The rising LH levels reach a threshold value, after which the release of LH surges to a sudden maximum. It is this pre-ovulatory LH surge, gated by the circadian clock to the afternoon, that allows the adequately responsive dominant follicle to enter the pre-ovulatory stage of growth and that triggers ovulation 36 hours after the surge (Figure 2.11).

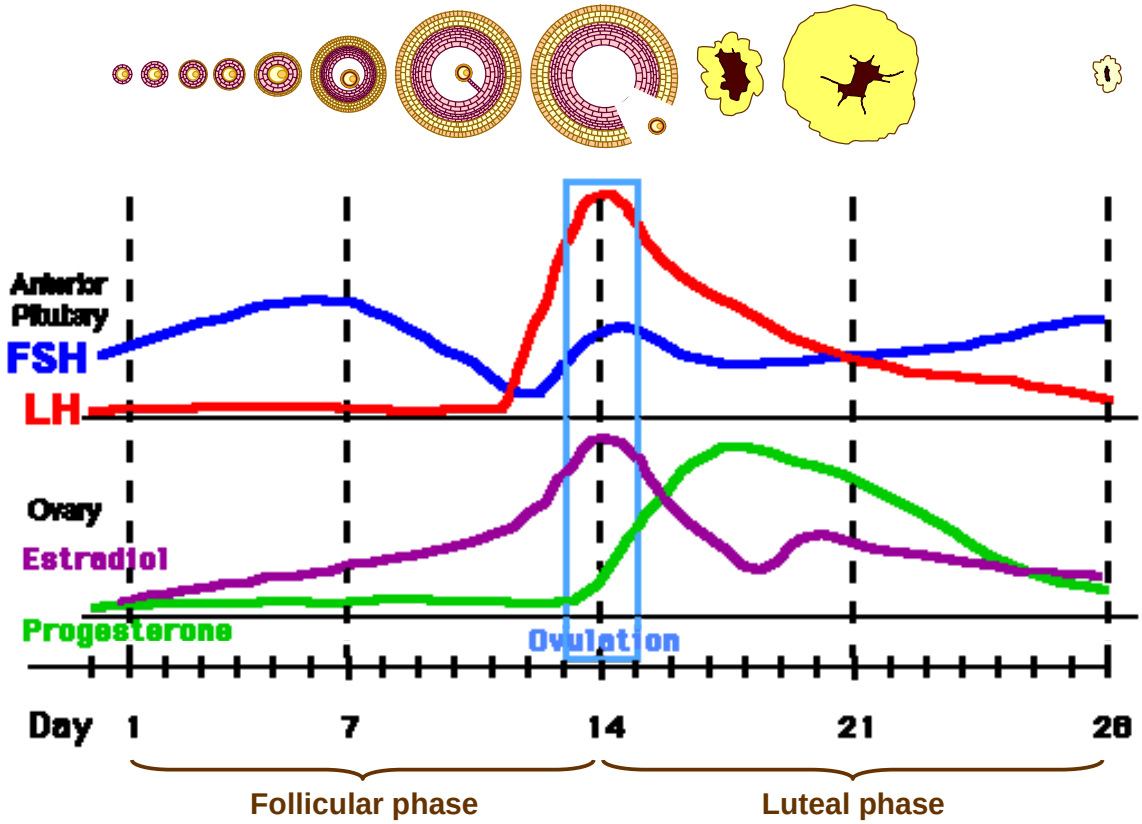

Figure 2.11 Hormone levels across the ovarian cycle. The follicle makes œstrogen that increases exponentially as it develops. High concentrations of œstrogen promote a surge of gonadotrophins. This causes follicular rupture, oocyte release and transformation of the remaining cells into the corpus luteum that secretes large amounts of progesterone as well as some œstrogen (adapted from The University of New South Wales (UNSW) Embryology program Version 5.7 September 2006: http://embryology.med.unsw.edu.au/wwwhuman/MCycle/images/Mcycle.GIF).

After the LH surge, the final follicular growth phase is rapid with changes in the follicular cells as well as the oocyte. The pattern of follicular steroid secretion is altered, with a transient rise in œstrogen and androgen levels within 2 hours after the LH surge, followed by a decline. The rise in these steroid levels coincide with changes in the theca cell layer, which become hyperaemic. The outer layer of granulosa cells also change, with œstrogen synthesis being halted and progesterone synthesis being initiated. The synthesis of progesterone is further stimulated by LH acting on the recently acquired receptors of the granulosa cells. At the same time, the follicular cells lose or become largely unable to bind FSH and œstrogen.

The LH surge also drives the oocyte into exiting meiotic arrest and completing its first meiotic division (Motlik and Kubelka, 1990). The two diploid cells thus produced are not identical, as virtually all the cytoplasm segregates with one of the daughter cells, known as the secondary oocyte, while the other receives very little apart from its diploid chromosomes. The latter cell is referred to as the first polar body, which subsequently dies. The secondary oocyte continues to mature. The unequal division of the cytoplasm between the daughter cells means that the protein stores are conserved in the secondary oocyte. The secondary oocyte undergoes meiosis II but arrests at the second metaphase spindle (metaphase II). By the end of the pre-ovulatory phase, the follicle and follicular fluid have rapidly expanded, so that the peripheral layers of thecal and mural granulosa cells with the intervening basement membrane have become relatively thin. The diploid secondary oocyte with its cumulus granulosa cells, collectively known as the cumulus-oocyte mass is now tenuously tethered by a thinning stalk to the peripheral follicular cell layers. The increasing size of the follicle and its position in the ovary causes it to bulge out of the ovarian wall. The bulge becomes thinner due to protease activity and less vascularised, and eventually ruptures, releasing the cumulus-oocyte mass into the peritoneal cavity (Figure 2.10) (Johnson and Everitt, 2000).

The ovulated cumulus-oocyte complex is captured by the fimbriae of the fallopian tube, where cilia beat it towards the uterus. The oocyte now has a six-hour window in which it can be fertilised. If a spermatozoan does penetrate the *zona pellucida* that then acts to prevent polyspermic fertilisation, the male and female gametes then fuse. The oocyte-spermatazoan fusion activates an influx of calcium from oocyte stores, which alters the calcium concentration in the oocyte such that it exits meiotic II arrest and proceeds to the completion of meiosis II. The completion of meiotic division results in the production of two haploid daughter cells: a daughter cell which is fused with the spermatozoan to create a zygote and a second polar body which is expelled. Gamete fusion initiates a developmental programme as the zygote travels along the oviduct and into the uterus, where it implants in the endometrium and develops into an embryo, then

into a fœtus which is then born. If the oocyte is not fertilised, it dies and is lost with menstrual discharge (Johnson and Everitt, 2000).

Implantation of the blastocyst is dependent on progesterone support, provided by the corpus luteum. The corpus luteum is formed from the follicular cells of the ruptured pre-ovulatory follicle that were not expelled from the ovary during ovulation. The luteinised mural granulosa cells enlarge, stop proliferating and differentiate into LH-responsive, progesterone-secreting granulosa-lutein cells. The theca cells, now known as theca-lutein cells, are maintained and continue to produce the androgen substrate for luteal œstradiol synthesis. The basement membrane between the theca and granulosa cells breaks down and the previously avascular granulosa cells develop a marked blood supply (Figure 2.10). These cells are remodelled into a vascular yellow structure that gives this glandular tissue its name: the "yellow body" or *corpus luteum* (CL).

The CL rapidly increases in size and secretes increasing amounts of progesterone, 17-hydroxyprogesterone, œstradiol and inhibin, under the influence of LH. Progesterone is a necessary requirement of the conceptus, which in turn is able to maintain the CL using the secretion of human chorionic gonadotrophin (hCG) that acts through the LH receptor. Luteal steroids and other peptides, such as inhibin, are able to suppress gonadotrophin secretion from the anterior pituitary gland. The CL serves to promote implantation and support the survival of the conceptus, which comprises the placenta, its membranes and the implanted embryo. The CL is also able to block further ovulation.

In women, the *CL of pregnancy* persists until some time between the 9^{th} and 14^{th} week of pregnancy, after which time, its luteal function begins to fade, as the conceptus or feto-placental unit becomes increasingly able to independently produce sufficient quantities of progesterone and other hormones (Johnson and Everitt, 2000). By 20 weeks, both luteal function and plasma hCG levels have declined dramatically. The feto-placental unit is now able to sustain itself with its own hormone production.

The failure to conceive does not however impact on the formation of the CL in women. The lifespan of this CL, now called the *CL of the reproductive cycle*, is however curtailed by the lack of pregnancy. The CL of pregnancy persists for only about 14 days, before it regress into a white structure, called the corpus albicans. During its relatively short lifespan, its fully functional status declines steadily until it degenerates completely. The corpus albicans becomes scar tissue, which is eventually resorbed by the ovary. Overt menstruation then occurs with the discharge of the uterine endometrium, unfertilised oocyte and blood. Thus, a new ovarian reproductive cycle begins.

The ovarian reproductive cycle lasts approximately 28 days and accounts for the time required for antral follicle recruitment and maturation, ovulation, CL formation and regression. The time taken for antral follicle recruitment and maturation lasts approximately 14 days and can vary greatly between individual women as well as between cycles in the same individual. This time, from the onset of menstruation to the time of ovulation is referred to as the follicular phase or stage of the reproductive cycle (Figure 2.11). Ovulation is virtually instantaneous and occurs on average 36 hours after the LH surge. It is immediately followed by the non-conception luteal phase, which lasts a relatively invariate 14 days, during which time the CL is formed, functions briefly then regresses. The timing of the luteal lifespan is relatively fixed and constant between individual women and between ovarian cycles in the same individual. If conception and successful implantation occurs, the CL persists. The ovarian cycle is subsequently suspended for the duration of pregnancy. It resumes fully at the end of the lactation period, once the baby is fully weaned (Johnson and Everitt, 2000).

2.10 LUTEOGENESIS

The relatively precise timing of the luteal lifespan in the absence of conception suggests there may be a function for clock genes and circadian clockwork. Therefore, some timing machinery is likely to reside within the corpus luteum. The corpus luteum undergoes many rapid changes as soon as it is formed. Its whole endocrinology becomes vastly different from that of a follicle. Massive tissue and vascular remodelling occurs within a scant few days (Johnson and Everitt, 2000). These processes are likely to require temporal as well as spatial co-ordination and synchronisation.

The *luteinisation* of the post-ovulatory 'follicle' proceeds as the ruptured follicle collapses in on itself. The granulosa cell layer is thrown into folds around the breached antrum. The antrum, made up of elements of blood and follicular fluid contains a core of fibrin, a clotting factor, which now undergoes fibrosis. The basement membrane between the theca and granulosa cell layers also breaks down. The *theca interna* cells are then borne into the incipient CL by the invasion of connective and vascular tissue at the folds of the granulosa cell layer (Figure 2.12). The vascular tissue continues invading until the cavity of the collapsed follicle is reached. The connective tissue also continues to invade, in radially orientated strands which can form divisions or septa within the CL. This also allows the penetration of large blood vessels deeper into the CL. Extensive capillary branching completes the angiogenesis of the CL. The mature CL now receives the highest blood supply per unit mass of any organ in the body (Johnson and Everitt, 2000, Murphy, 2000).

The theca cells form small lutein cells, referred to as the *theca-lutein* cells. They produce progesterone and androgens and remain rich in LH receptors. The follicular granulosa cells stop dividing and undergo rapid hypertrophy. They grow into large lutein cells, referred to as *granulosa-lutein* cells (Figure 2.12). They are heavily stocked with mitochondria, smooth endoplasmic reticula, lipid droplets, Golgi bodies and in many species, a carotenoid pigment called lutein. It is lutein that confers the

characteristic pale yellow or orange colouring to corpora lutea. The granulosa-lutein cells, importantly, also develop LH/hCG receptors (Murphy, 2000, Johnson and Everitt, 2000).

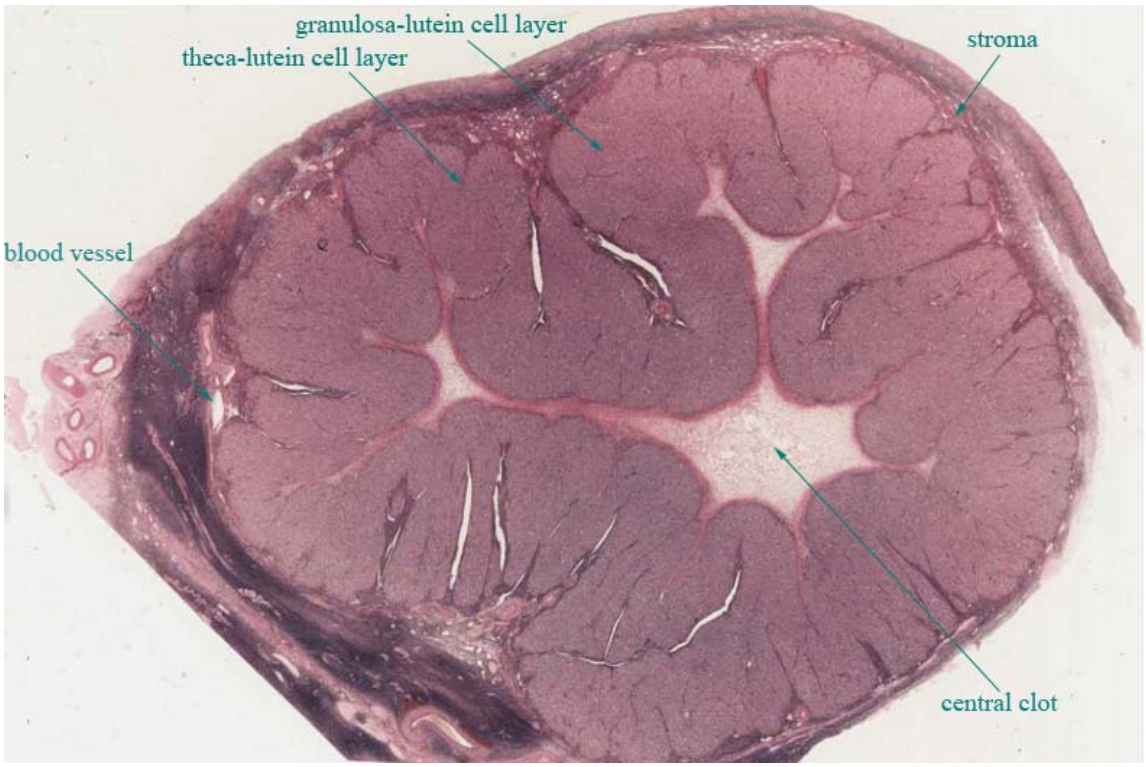

Figure 2.12 Cross-section of a human CL showing the infoldings of the vascular steroidogenic cell layers around a central clot (adapted from SBPMD Histology Laboratory Manual, Columbia University, NY, USA: http://www.columbia.edu/itc/hs/medical/sbpm_histology/slides/slide_064.jpg).

The granulosa-lutein cells are the main source of progestogen hormones in the CL. In most species, the principal progestogen is progesterone. Progesterone, as its name implies, is a key requirement for implantation and early pregnancy. Although the granulosa-lutein cells produce the bulk of the progesterone released by the CL, the theca-lutein cells are also able to synthesise progesterone. Progesterone is synthesised from cholesterol in a series of chemical reactions, catalysed by enzymes, most notably 3β-hydroxysteroid dehydrogenase (3β-HSD) (Figure 2.13).

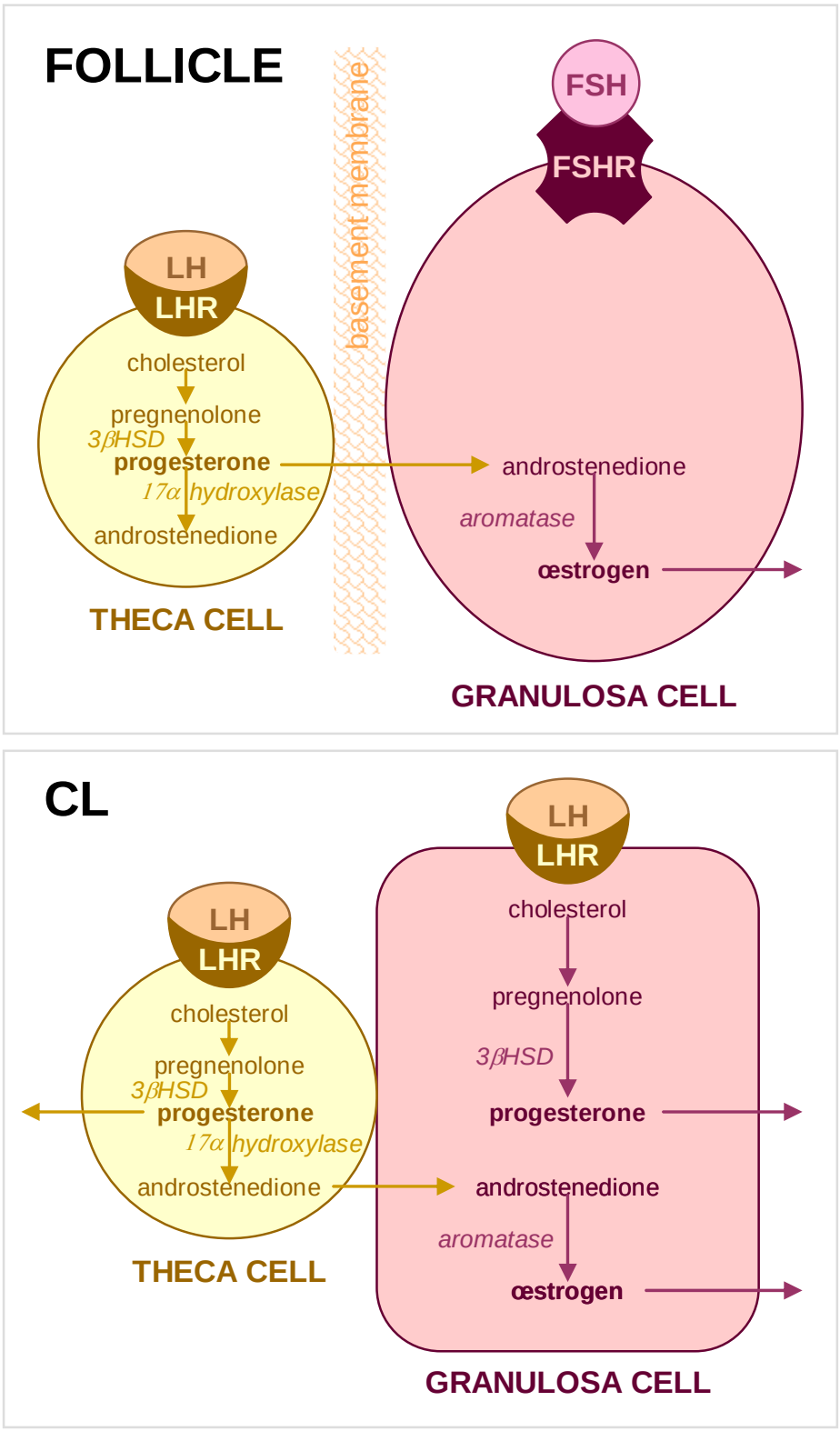

Figure 2.13 Two-cell-two-gonadotrophin theory of œstradiol synthesis in the follicle and in the CL.

Primate granulosa-lutein cells also secrete significant amounts of 17α-hydroxyprogesterone. In a few species, like humans, they also secrete notable amounts of œstrogens, particularly 17β-œstradiol (Murphy, 2000). The œstradiol is derived from an androgen precursor obtained from the theca-lutein cells, just as it occurs in the follicle (Figure 2.13). The theca-lutein cells produce the androgen precursor: androstenedione, from cholesterol using a series of enzymes (Figure 2.13). The androstenedione is then converted into œstrogen, via another series of enzyme-catalysed reactions, in the granulosa-lutein cells. The key enzyme involved in this is the cytochrome P450 aromatase. Granulosa-lutein cells do not possess the necessary enzyme to produce an androgen precursor for œstradiol. They therefore, most likely, have obtained androstenedione from the theca-lutein cells, to produce œstrogen. This involvement of the two cell types in steroidogenesis is referred to as the *two-cell-two-gonadotrophin* or *cell co-operative hypothesis* (Johnson and Everitt, 2000) (Figure 2.1).

The granulosa-lutein cells also secrete other hormones, including inhibin, oxytocin and relaxin. The role of luteal oxytocin and relaxin in women is not entirely clear. Inhibin is able to suppress FSH synthesis and secretion and is likely to be involved in preventing follicular development. However, FSH inhibition during the luteal phase is largely driven by negative feedback from œstradiol in women and sheep (Welt et al., 2003, McKinnon and Voss, 1995).

2.11 CORPUS LUTEUM MAINTENANCE

A luteotrophic complex of chemicals is required to maintain a viable CL. Human chorionic gonadotrophin is considered to be the key ingredient in this complex. In humans, it is produced by the conceptus, in increasing amounts with time. It functions as a maternal-recognition-of-pregnancy signal. It is able to act on the LH receptors of

the luteal steroidogenic cells in order to regulate them. Other species have markedly different mechanisms for maintaining the CL. For example, rats and hamsters require the provision of prolactin in their luteotrophic complex. In these species, the granulosa-lutein cells possess prolactin receptors, which are often already present in the pre-ovulatory follicle. The prolactin is released from the pituitary gland after ovulation as a response to mating stimulus. It thus functions a signal indicating that mating has occurred and provokes the CL into differentiating into a CL of pregnancy. Once this signal has been received, the CL persists until parturition. There is no requirement in this case for a maternal recognition of pregnancy (Johnson and Everitt, 2000, Murphy, 2000).

The maintenance of the CL can vary considerably between species. Some species, such as the sheep, do not require a trophic signal from the pregnancy or recognition of mating stimulus. Here, the CL is maintained in the absence of a luteolytic signal (Johnson and Everitt, 2000). Normally, two weeks after ovulation, the uterus will produce prostaglandin $F_{2\alpha}$ ($PGF_{2\alpha}$) by default. This is now able to act on the CL which in turn feeds forward to further augment $PGF_{2\alpha}$. $PGF_{2\alpha}$ is luteolytic in nature and causes the CL to degenerate. Pregnancy is able to stop this prostaglandin signalling and so prevent luteolysis. $PGF_{2\alpha}$ is a hormone-like substance that is episodically secreted by uterine endometrial cells, to act on dedicated membrane-associated receptors, to induce apoptosis of luteal cells (Diaz et al., 2002, Niswender et al., 2007). This luteolytic signal occurs due to P_4 signalling from the CL throughout the oestrous cycle. During the early phase, the luteal P_4 secretion inhibits uterine $PGF_{2\alpha}$ release. As time passes, the continued secretion of the P_4 becomes less and less effective at inhibiting the release of $PGF_{2\alpha}$ from the uterus. By the mid-luteal phase, P_4 is no longer able to block $PGF_{2\alpha}$ release. The endometrial tissue has begun to lose its sensitivity to P_4 and so, $PGF_{2\alpha}$ is increasingly secreted. Thus, by virtue of its initial and continued secretion, P_4 is considered the key regulator of luteal lifespan in sheep (Schams and Berisha, 2004). It is not just the uterine endometrial cells that secrete $PGF_{2\alpha}$; the CL itself secretes $PGF_{2\alpha}$.

The effect of the luteal $PGF_{2\alpha}$ however is unlike that derived from the endometrium. The luteal $PGF_{2\alpha}$ is luteotrophic during the early and mid-luteal phases. P_4 is again involved in regulating the $PGF_{2\alpha}$ secretion, this time from the CL. It has been observed that the inhibition of P_4 has produced opposite effects on $PGF_{2\alpha}$ release, depending on the luteal phase. Antagonism of P_4 during the EL phase results in a reduction of luteal $PGF_{2\alpha}$ secretion. Antagonism of P_4 during the mid-luteal phase however results in an increase in luteal $PGF_{2\alpha}$ secretion (Dupre et al., 2008). The conceptus uses interferon tau (IFNτ) to signal to the uterus to prevent it issuing the luteolytic $PGF_{2\alpha}$ signal. The sheep thus employs an anti-luteolytic strategy as opposed to the human luteotrophic strategy.

Other species, such as dogs, do not employ any maternal recognition at all. They produce and maintain corpora lutea, irrespective of their pregnancy status. Thus, even in the absence of pregnancy, they are able to maintain a *pseudopregnancy*. Horses, on the other hand, use maternal recognition of pregnancy but do so in a slightly different way to humans. Horses produce accessory corpora lutea throughout pregnancy. There is often a primary and a secondary corpus luteum present in the ovary at any one time. They use their equine gonadotrophin signal to maintain a steady turnover of these corpora lutea (Murphy, 2000, Johnson and Everitt, 2000). These various ways of maintaining corpora lutea extend inevitably into a correspondingly wide array of molecular mechanism regulating luteal function in different species.

2.12 LUTEOLYSIS

Luteolysis is the functional and structural degradation of the corpus luteum that occurs at the end of the luteal phase in the absence of pregnancy. It is necessary that the CL, in

the absence of pregnancy, be eliminated from the body rapidly in order to allow the recovery of normal reproductive function as steroids and inhibin from the CL inhibit ovulation. The luteolytic processes involved in the degeneration of the CL of pregnancy are less well understood and are probably not identical to those of the degeneration of the CL of the reproductive cycle. It is the luteolysis of the CL of the reproductive cycle which will be focussed on here.

Luteolysis progresses firstly, with a loss of function, then with a loss of structural integrity, although these processes are intimately linked and run in parallel. Progesterone production and secretion decline drastically and eventually cease. This is associated with an initiation of programmed cell death within the CL. The luteal cells die mainly by apoptosis, although necrosis and autophagy have also been implicated (Stocco et al., 2007). Tissue remodelling causes involution of the whole structure with the loss of vascularisation (Stocco et al., 2007). This results in a gland formed principally by connective scar tissue. It is then called the corpus albicans, due to its white colour. The corpus albicans has no known function. It is resorbed by the ovary and replaced by ovarian stroma (Stocco et al., 2007).

The processes that trigger luteal regression remain poorly understood. Many processes have been implicated, involving the action of prostaglandins, prolactin and luteinising hormone for example. Unravelling the roles of these complex processes is further complicated by the fact that they seem to vary greatly between species. In some species, luteolysis, like luteal maintenance, can be an active process, whereas in others, it can be a passive process. Active processes involve the triggering of CL destruction by luteocidal signals. Passive processes may involve the withdrawal of luteotrophic signals which then, more indirectly initiate the destruction of the CL.

In rats, the trigger for luteolysis is the pre-ovulatory LH surge of the next ovarian cycle. In ruminants, like cattle and sheep, the trigger appears to be a luteocidal $PGF_{2\alpha}$ signal. In humans, it is the lack of a luteotrophic gonadotrophin signal that appears to trigger

luteolysis (Sugino and Okuda, 2007). All these signals cause the cessation of progesterone biosynthesis. The catabolism of progesterone may also occur and this is particularly well described in rodents (Stocco et al., 2007). Progesterone secretion declines when it is catabolised into 20α-dihydroprogesterone. This catabolism is catalysed by 20α-hydroxysteroid dehydrogenase (20α-HSD). $PGF_{2\alpha}$ has been shown to increase 20α-HSD levels, which in turn increase the depletion of the protective progesterone from the luteal cells. Prolactin has also been reported to alter 20α-HSD levels in the CL.

There are many ways in which the loss of progesterone can adversely affect the CL (Sugino and Okuda, 2007, Stocco et al., 2007). The depletion of progesterone can relieve the inhibition of apoptotic receptors on the surface of the luteal cells; receptors such as Fas. These Fas receptors are then no longer prevented from binding to Fas-ligands. Once this interaction takes place, the Fas and Fas-ligand complexes are able to directly activate protease enzymes that orchestrate apoptosis. These calcium-dependent proteases are called *caspases*. They catalyse the cleavage of cellular structural proteins, such as myosin in the cytoskeleton and lamins in the nuclear scaffold. They also work to cleave other caspases, thus initiating them in a caspase cascade. Fas and Fas-ligand complexes upregulate caspase-8, an initiator caspase. It, in turn, activates the executioner caspase, caspase-3. Caspase-3 catalyses the cleavage of the endonuclease, caspase-activated DNase (CAD) from its inhibitor: inhibitor of CAD (ICAD). The released CAD then enters the nucleus, where it proceeds to fragment the DNA. DNA repair mechanisms are also compromised and the nuclear scaffold impaired. The apoptotic demise of the cell is then inevitable (Sugino and Okuda, 2007, Stocco et al., 2007). Other forms of programmed cell death apart from apoptosis are also thought to be involved in the luteolytic process. The degree to which apoptosis contributes towards the programmed cell death mechanisms involved in luteolysis appears vary over the course of the entire luteolytic process and may vary between species (Morales et al., 2000). The contribution of the various programmed cell death mechanisms towards the demise of the CL is also likely to be observed in the duration of the luteolytic process

itself, which has been reported to be shorter in some primates than in species such as the sheep (Fraser et al., 1999).

The reduction in progesterone is also associated with an invasion of immune cells. Some of these cells are able to produce Fas-ligand. Some also possess prolactin receptors and are therefore, likely to be directed by prolactin, in prolactin-mediated luteolytic processes. Many second messenger systems appear to be involved in the transduction of extracellular luteolytic apoptosis signals (Sugino and Okuda, 2007, Stocco et al., 2007).

Luteal cells have also been observed undergoing autophagy. This is another form of programmed cell death, where the cell breaks down its own cellular components using lysosomal vesicles or vacuoles and effectively digests itself. This process is often initiated by changes in mitochondrial permeability. These changes would be triggered by a luteolytic signal (Stocco et al., 2007).

Necrosis also accounts for some of the luteolytic cell death, in both rodents and primates. The apoptosis of rodent luteal endothelial cells is followed by the necrosis of steroidogenic cells. It has been proposed that the loss of vascular endothelial cells in corpora lutea can lead to secondary ischaemia, which in turn leads to necrosis of the steroidogenic luteal cells (Stocco et al., 2007).

Luteolysis is a very special example of the body's routine use of programmed cell death. It appears to be triggered by various extrinsic humoral factors, some of which derive from the uterine endometrium. It is mediated by an array of processes, which are regulated in complex, intersecting pathways. Triggering mechanisms and how they effect the luteolytic process remain, as yet, not fully characterised. The various specific luteolytic processes themselves are also not yet fully delineated. Separating the processes that are common from those that are not, between species, may also unveil some of underlying principles that govern luteolysis.

2.13 TIMING IN THE CORPUS LUTEUM

The processes of luteinisation, luteal maintenance and luteolysis are varied and complex. Some of these processes may are likely to involve some sort of temporal aspect in its regulation. The human CL, for example, has a uniquely well-timed luteal phase. In the absence of pregnancy, it lasts 14 days before the initiation of luteolysis (Heffner and Schust, 2006).

Timing is clearly important in many aspects of reproductive physiology. It is important in the timing of pulsatile release of many hormones, such as GnRH from the brain. It is crucial for the temporal co-ordination of many processes, such as in the timing of mating or oestrus with the timing of ovulation. Timing also appears to be important in the regulation of fallopian tube function (Boden and Kennaway, 2006). It is also likely to be important in regulating the lifespan of the CL of the reproductive cycle and hence, also of luteal function. There is a dearth of information regarding the temporal regulation of luteal lifespan and function. Hence, the focus of the current thesis is to provide a better understanding of the temporal workings of the corpus luteum, particularly to elucidating a possible role played by clock genes and circadian clocks.

2.14 SUMMARY

To summarise, circadian clocks exist in virtually all organisms. They are found at various levels of organisation, from individual cells to whole, multicellular organisms.

They are driven by interconnecting, autoregulated transcription-translation negative-feedback loops. The principal genes being transcribed and translated in these loops are the canonical clock genes: *clk*, *bmal1*, *per1*, *per2*, *per3*, *cry1* and *cry2*. These genes are rhythmically expressed and translated with a circadian period.

The various circadian clocks of an organism are organised hierarchically. Circadian clocks can be designated as central or peripheral. Central clocks are pacemakers. They are directly entrained by the circadian geophysical environment via sunlight. Only one central master clock has been identified in mammals. It is the SCN that resides in the hypothalamus. It works as a master clock, directing the timing of slave clocks. These slave clocks are peripheral clocks, residing in peripheral tissue outside of the SCN. They are entrained principally by the central clock. They are however, also able to integrate other timing information from elsewhere in the tissue or body and from the geophysical environment. The precise way that circadian clocks function in the SCN and the periphery is not yet understood. There are many similarities and many key differences.

The hypothalamus (in which the SCN resides) is vital to the regulation of the pituitary gland. It is able to regulate the secretion of pituitary hormones in a timely manner. The pituitary hormones are involved in many numerous physiological processes. One of these processes, in which virtually all the pituitary hormones are involved, is reproduction. Many timing phenomena affect reproductive function. There appears to be significant windows of time during which several key female reproductive processes are performed. Ovulation, mating, luteolysis and parturition all occur predominantly at certain times. Clock genes have been found expressed in brain regions involved in reproductive function as well as in the reproductive organs of both sexes. Moreover, clock gene knockouts and mutations often demonstrate impaired reproductive and subfertile phenotypes.

The, human and ovine, CL appear to be regulated in a timely fashion. The human CL of

the reproductive cycle undergoes luteolysis after 14 days without luteotrophic support from a conceptus. The ovine CL of the reproductive cycle undergoes luteolysis after 14 days without inactivation by a conceptus of a default luteotrophic signal issued by the uterus. This apparently specific gating of the timing luteolysis suggests that there is a timing mechanism akin to a clock at work in the female reproductive tract. Whether this clock resides in the CL, the ovary, the uterus or elsewhere has yet to be elucidated. Whether clock genes and circadian timing are involved in this luteal clock also remains a mystery. How this luteal clock functions is also unknown. It is proposed that putative timing mechanisms be examined in the human and ovine CL. Special attention should also be paid to the hypothalamus and the pituitary gland, as these are also crucial regulators of reproductive timing.

3 CLOCK PROTEIN LOCALISATION IN THE HUMAN CORPUS LUTEUM THROUGHOUT THE LUTEAL LIFESPAN

3.1 INTRODUCTION

3.1.1 HUMAN CORPUS LUTEUM

The human CL is special in that it possesses a relatively fixed lifespan, that is endogenously regulated. This is unique amongst mammals and contrasts greatly to the relatively unfixed duration of the follicular phase of the ovarian cycle (Lenton and Woodward, 1988, Atkinson et al., 1975, Neill, 2005, Behrman, 1993). Once generated, the human CL persists for 14 days before spontaneously degenerating and disappearing; that is, unless it is maintained by luteotrophic factors signalling from a conceptus.

It is not known what governs the timing of the luteal lifespan or what triggers its spontaneous demise in the absence of pregnancy (Duncan, 2000). Other programmes of luteal regression follow a luteolytic process, where a luteocidal signal is automatically sent unless it is forestalled by pregnancy (Auletta and Flint, 1988). This is the case for ruminants such as sheep, where, without pregnancy, pulsatile $PGF_{2\alpha}$ is released from the uterus and causes luteolysis after 12 days. This predictable luteal lifespan however, is different from that of the human, because it is determined by exogeneous rather than endogenous factors (Neill, 2005, Niswender et al., 2007, Niswender et al., 2000). Therefore, if the luteal lifespan was governed by a clock, it may lie at the level of the uterus and/or the hypothalamus and/or the pituitary gland in ruminants, because the hypothalamus and pituitary govern the pulsatile release of oxytocin that closes the positive feedback loop of uterine $PGF_{2\alpha}$ secretion (Silvia et al., 1991).

The human CL also seems to have a clock of its own. This has been supported by three bodies of evidence. Firstly, the restoration of ovarian cyclic function, by pulsatile GnRH treatment, of hypogonadal infertile women and hypothalamus-lesioned primates, does not account for the determination of the luteal lifespan (Loucopoulos and Ferin, 1984, Johnson and Everitt, 2000, Pohl et al., 1983). Secondly, manipulation of the GnRH or LH pulse frequency or LH concentrations do not alter the lifespan of the CL, suggesting that although the pulsatile LH permits the luteal lifespan, it does not time it (Neill, 2005). Thirdly, cultured luteinised granulosa cells (LGCs), that have been obtained from pre-ovulatory follicles under an assisted conception protocol, appear to possess some inherent timing (Myers et al., 2007a, van den Driesche et al., 2008). These cells are able to persist in culture for approximately 14 days before disappearing, unless they are rescued by hCG treatment. This implies that the timing of the non-conception style luteal lifespan is intrinsic to the cells of the CL itself and is not dependent on exogenous factors, such as gonadotrophins, which are permissive.

Gonadotrophins do however play an important role in the maintenance of the CL and the absence of sufficient LH/hCG activity has been correlated with the demise of the CL. It is known that *in vivo*, the normal lifespan of the human CL is supported by LH from the pituitary gland (Stouffer, 2003). It is also known that although the manipulation of LH does not directly alter the timing of the luteal lifespan, its total removal does however cause luteolysis, which can then indirectly shorten the lifespan of that CL (Duncan et al., 1996, Fraser et al., 1995). Human chorionic gonadotrophin also augments the human CL during pregnancy. It is secreted by the conceptus and acts to signal maternal recognition of pregnancy that facilitates the luteal support of early gestation (Stouffer et al., 1989). It is so potent a luteotrophic factor that hCG treatment of non-pregnant women and luteal cells *in vitro* results in the forestalling of luteolysis and thus, the extension of the luteal lifespan (Duncan et al., 1996, Illingworth et al., 1990). Therefore, it could be argued that although the intrinsic timing system that controls the luteal lifespan does not necessarily require gonadotrophins, gonadotrophins do however interact with that system in order to affect its timing and so, prolong or shorten the

lifespan of the CL. This is further supported by the fact that the longer the CL persists, the greater the amount of hCG it needs to maintain its fully functional status, indicating that the CL actually *ages,* but that it also requires exogenous factors to extend its lifespan beyond the 14-day norm.

From the studies already described, it is evident that the human CL provides a unique opportunity for investigating the temporal regulation of a key reproductive process, which is intrinsic to the reproductive tissue. The whole process of reproduction is largely reliant on co-ordinated timing. As such, the elucidation of how this is provided would be an important contribution to existing knowledge, which may also have clinical application in procedures such as those conducted in assisted reproduction. Furthermore, the mechanism by which hCG affects the luteal lifespan and luteolysis may be revealed; a mechanism that has long evaded detailed explanation (Duncan, 2000).

It is therefore proposed, that as the CL has a cell-based clock, regulated by the most well-described cellular clock components in biology: the circadian clock genes. These genes have already been observed in areas of the mammalian female reproductive tract, in structures such as the fallopian tubes, ovary and uterus. They have not however been investigated in the CL in general and in the human CL in particular (Kennaway et al., 2003, Boden and Kennaway, 2006). The putative luteal clock genes are proposed to comprise a circadian clock functioning, as it does in other peripheral tissues, independently but open to exogenous signalling of temporal information from co-ordinating pacemaker clocks. This information may be provided by the ovarian hormonal milieu which is regulated by the hypothalamus, the part of the brain that also incidentally contains the master pacemaker. It is proposed that the putative circadian clock in the CL works as a timer, accruing time which counts down towards luteolysis, thus determining the length of the luteal lifespan. This timer can be overridden or reset by hCG signalling, which facilitates the extension of the luteal lifespan during pregnancy. In order to first address the validity of this hypothesis, it is necessary to demonstrate *bona fide* clock gene expression, by looking at the clock proteins, in the

human CL. This expression must also persist across the luteal lifespan if the clock genes were to behave as a timer for the orchestration of the luteal lifespan. The luteal cell types expressing the clock genes may also be important in the provision of temporal regulation, as various luteal cell types perform various specific luteal functions, such as steroidogenesis, vascularisation, tissue support and modelling.

Therefore this chapter aims:

1. to localise the expression of the canonical clock proteins: CLK, BMAL1, PER1, PER2, CRY1 and CRY2 in the human CL using immunohistochemistry;

2. to determine which cell types in the human CL express the clock genes over the luteal lifespan in a normal, non-conception, reproductive cycle.

3.2 MATERIALS AND METHODS

3.2.1 ETHICAL APPROVAL

Ethical approval for the use of human corpora lutea was obtained from the Reproductive Medicine Subcommittee of the Lothian Medical Ethics Committee, as well as being re-approved by the Common Research Ethics Committee (COREC) on two further occasions. Informed consent was then obtained from all the patients and their consultant gynaecologists. The recruitment of patients and the collection of corpora lutea was initiated and performed by Dr W. Colin Duncan, under the supervision of Dr Peter J. Illingworth and continued in collaboration with Prof Hamish M. Fraser.

3.2.2 SAMPLING HUMAN CORPORA LUTEA

Human corpora lutea were enucleated, at the time of surgery, from women undergoing hysterectomy for benign reasons as described previously (Duncan et al., 1998a). All the women had regular menstrual cycles and had not received any hormonal treatment for three months prior to engaging in the study. Prior to surgery, the women collected urine samples every morning and these were analysed for LH concentrations. The date of the urinary LH surge was determined and the stage of the luteal phase was classified accordingly.

There were 8 corpora lutea in the early luteal phase, dated to within 1 to 5 days after the LH surge; 12 corpora lutea in the mid-luteal phase of 6 to10 days after LH surge and 6 corpora lutea in the late luteal phase, 10 to 14 days after LH surge. This dating of the corpora lutea was corroborated by endometrial biopsy (Maybin and Duncan, 2004). The timing of the CL collection however could not be standardised but all corpora lutea were sampled between 10:00 and 15:00 hours clock time. At operation, the whole CL was

enucleated from the ovary by blunt dissection and the ovary oversewn. The tissue was immediately divided into radial blocks in order to ensure that the whole thickness of the gland was represented in any piece. The tissues were collected over a period of 12 years to provide a tissue bank and stored as paraffin wax-embedded blocks in dedicated containers at room temperature.

3.2.3 CONVENTIONAL IMMUNOHISTOCHEMISTRY

The pieces of human luteal tissue were immediately immersion-fixed in 4% paraformaldehyde and processed into paraffin wax blocks. The blocks were sectioned at 5 μm thick on a Leica Jung RM 2035 microtome (Leica Microsystems, Milton Keynes, UK) and mounted on Menzel-Gläser Superfrost® Plus slides (BDH via VWR International Ltd, Leicester, UK), then left to dry and adhere at 40°C overnight. The dried sections were then stored at room temperature.

The sections were dewaxed in 100% xylene and rehydrated in a series of graduated alcohols then water. They were then antigen retrieved by pressure cooking in 0.01 M citrate buffer (pH 6) for 5 min at full pressure, then left to stand for 20 min and finally cooled under running tap water. Any endogenous peroxidase activity in the tissues was blocked by washing the sections in 3% (v/v) hydrogen peroxide (H_2O_2) in 40% methanol for 30 min at room temperature. The sections were then washed three times for 5 min in phosphate-buffered saline (PBS) (0.01 M phosphate, pH 7.4, and 0.85% NaCl). Any nonspecific antibody-binding sites were blocked by incubating sections in blocking serum composed of normal goat serum (NGS) (Autogen Bioclear UK Ltd, Wiltshire, UK) diluted 1:4 in PBS containing 5% bovine serum albumin (BSA) (Sigma, Dorset, UK). The sections were then incubated in humidity chambers, overnight at 4°C with the primary antibody diluted in blocking serum.

The primary antibodies against clock proteins (Autogen Bioclear UK Ltd, Wiltshire, UK) were used at various dilutions, in blocking solution, determined during pilot studies (Table 3.1). Control sections were incubated with antibody and control peptide in blocking serum to confirm the specific action of the primary antibody. Clock protein control peptides (Autogen Bioclear UK Ltd, Wiltshire, UK) were added, ten times in excess of the antibody concentration, to the antibody diluted in blocking serum and mixed well by brief vortexing and incubating overnight at 4^{o}C before adding to the sections. The luteal steriodogenic cell marker antibody against 3-beta hydroxysteroid dehydrogenase (3βHSD) (kindly supplied by Prof J. Ian Mason, Department of Clinical Biochemistry, The University of Edinburgh, Edinburgh, UK) was used at a 1:1000 dilution, diluted in blocking serum, without antigen retrieval.

ANTIBODY	IHC CONC.	SECONDARY ANTIBODY
Rabbit anti-human PER1 IgG	1:200	GARB
Rabbit anti-mouse PER2 IgG	1:100	GARB
Rabbit anti-mouse CRY1 IgG	1:20	GARB
Rabbit anti-mouse CRY2 IgG	1:100	GARB
Rabbit anti-drosophila BMAL1 IgG	1:80	GARB
Rabbit anti-human CLOCK IgG	1:80	GARB
Rabbit anti-porcine 3βHSD	1:1000	GARB

Table 3.1 Primary antibodies used in this study, indicating the species that the antibody was raised in and against, the dilution used and the appropriate secondary antibody.

Excess primary antibody was washed off in three 10-min PBS washes. The sections were then incubated with goat anti-rabbit biotinylated (GARB) (Vector Labs, California, USA), diluted 1:500 in blocking serum, for 1 h at room temperature. Unbound antibody was washed off in three 10-min PBS washes. Avidin-biotin conjugated with horseradish

peroxidase (ABC-HRP) (Dako, Cambridge, UK), diluted in 0.05 M Tris-HCl (pH 7.4) according to the manufacturer's instructions, was added to the sections. They were incubated at room temperature for 30 min then the excess ABC-HRP was washed off in three 5-min PBS washes. The ABC-HRP was then detected using the peroxidase substrate, 3,3'-diaminobenzidine tetrahydrochloride (DAB) (Dako, Cambridge, UK). When the DAB staining was optimal (neither too weak nor too strong), as detected under a Zeiss ICS KF2 light microscope (Carl Zeiss Ltd, Welwyn Garden City, Hertfordshire, UK), the peroxide reaction was stopped, by immersing the sections in distilled water. The DAB stain was effectively that of the immunoreactive-protein.

The sections were then counterstained with a nuclear stain: Harris' haematoxylin (BDH via VWR International Ltd, Leicester, UK) and dehydrated in graduated alcohols and xylene. They were then mounted (Cover Glass; VWR International Ltd, Leicester, UK) with Pertex© mounting medium (Cell Path, Hertfordshire, UK). The cellular localisation of the immunoreactive protein was examined and any staining photographed, using a Provis AX70 microscope (Olympus Optical, London, UK) fitted with a Canon DS6031 digital camera (Canon Europe, Amsterdam, The Netherlands).

One of the clock protein primary antibodies however failed to work using conventional IHC. The polyclonal anti-CLK IgG failed to work in any of the human, ovine and murine tissues tested. The tissues used were ovine and murine brain and testes, and human CL. The antibody was supposed to work in human and murine tissues (Alpha Diagnostic International Clock Antibody Catalogue Number: CLO12-P Product Specification Sheet). Various fixatives and fixation methods were tested, combined with a variety of antigen-retrieval methods, including no antigen retrieval at all. A range of concentrations and incubation and wash times were also employed for both the primary and the secondary antibodies. The signal was also amplified using Tyramide. Alternative IHC methods using frozen tissue were also employed. Thin (5 μm) cryosectioned murine and ovine brain sections were mounted onto slides, fixed in a variety of fixatives for various durations and then processed as per the conventional

IHC. Thick (50 μm) sections of cryoprotected and non-cryoprotected murine and ovine brain tissues were also used, in a free-floating system, for IHC with anti-CLK. Finally, dot blots and Western blots of ovine proteins were performed using anti-CLK. The proteins were obtained from various ovine brain and somatic tissues, including the mediobasal hypothalamus that contains the SCN, the pituitary gland, the liver, the testis and 16 other tissues. Despite all these attempts to successfully use the anti-CLK antibody to detect CLK, it was not possible to evince any meaningful localisation of the CLK protein in any of the tissues used, in any of the methods employed. It was finally decided that the successful localisation of BMAL1 would suffice for the initial localisation of a clock protein that belonged to the positive limb of the circadian clock mechanism.

3.2.4 IMMUNOFLUORESCENT HISTOCHEMISTRY

The localised expression of clock proteins was further investigated by immunofluorescent histochemistry. Immunofluorescent histochemistry was used to co-localise clock proteins with cell type markers to luteal cell populations. The cell type markers used were: 1) cytochrome P450 aromatase, which localises to the granulosa-lutein cells, 2) cluster of differentiation molecule 31 (CD31), which localises to vascular endothelial cells, and 3) cluster of differentiation molecule 68 (CD68), which localises to macrophages. The usual theca-lutein cell marker is a 17α-hydroxylase antibody; this could not however be obtained for use in co-localisation. The cells were confirmed however, using 3βHSD antibodies in conventional IHC in serial sections, as they would be 3βHSD-positive and aromatase-negative, while granulosa-lutein cells would be both 3βHSD-positive and aromatase-positive. Alternatively, theca-lutein cells can be identified using their characteristic morphology and location in the layered structure of the human CL. They are considerably smaller than granulosa-lutein cells and lie between the stroma and granulosa-cell layers, invaginating into the granulosa-cell layer.

The pieces of human luteal tissue sampled were immediately immersion-fixed in 4% paraformaldehyde and processed into paraffin wax blocks. The blocks were sectioned at 5 μm thick on a Leica Jung RM 2035 microtome (Leica Microsystems, Milton Keynes, UK) and mounted on Menzel-Gläser Superfrost® Plus slides (BDH via VWR International Ltd, Leicester, UK), then left to dry and adhere at 40°C overnight. The dried sections were then stored at room temperature.

The sections were dewaxed in 100% xylene and rehydrated in a series of graduated alcohols then water. They were then antigen retrieved by pressure cooking in 0.01 M citrate buffer (pH 6) for 5 min at full pressure, then left to stand for 20 min and finally cooled under running tap water. Any endogenous peroxidase activity in the tissues was blocked by washing the sections in 3% (v/v) H_2O_2 in 40% methanol for 30 min at room temperature. The sections were then washed twice for 5 min in PBS. The blocking of endogenous peroxidise blocking is generally not required for immunofluorescent histochemistry (fluorescent IHC) as HRP-conjugated antibodies is generally not used. This was not the case here, when a Perkin Elmer Tyramide Signal Amplification™ (TSA) System (Perkin-Elmer Life Sciences, Boston, MA) was used, which employed an HRP-conjugated secondary antibody.

Any endogenous biotin or biotin-binding proteins, lectins, or nonspecific binding substances were blocked by applying, as per manufacturer's instructions, avidin (Vector Laboratories, Peterborough, UK) for 15 min followed by two washes with PBS for 5 min each. Biotin (Vector Laboratories, Peterborough, UK) was then added to block any remaining biotin-binding sites on the avidin. It was added, as per manufacturer's instructions, for 15 min followed by two 5-min PBS washes.

Any nonspecific antibody-binding sites were blocked by incubating sections in blocking serum composed of NGS (Autogen Bioclear UK Ltd, Wiltshire, UK) diluted 1:4 in PBS containing 5% BSA (Sigma, Dorset, UK). The sections were then incubated overnight in humidity chambers at 4°C with the primary antibody diluted in blocking serum (Table

3.2). Two types of negative control were included: one with control peptide pre-absorption and the other with the omission of the primary antibody.

Excess primary antibody that had not bound to the sections overnight was washed off using two 5-min PBS washes. The sections were incubated for 30 min at room temperature with GARB secondary antibody, diluted 1:500 in blocking serum. Unbound antibody was removed by two 5-min PBS washes. The chromagens could now be added. These chromagens are composed of fluorescently labelled avidin or streptavidin, which can bind onto the biotin that is conjugated to the secondary antibody. The chromagens used were either AlexaFlour® 488 (Invitrogen, Paisley, UK) or AlexaFlour® 546 (Invitrogen, Paisley, UK), which were conjugated to streptavidin (Table 3.2). The Streptavidin-AlexaFlour was diluted 1:200 in the PBS. The sections were incubated with the chromagens for 1 h at room temperature. The slides were incubated in the dark to prevent bleaching of the light-sensitive chromagens. Unbound chromagen was removed by washing twice for 5 min with PBS.

The sections were blocked a second time with blocking serum for 30 min at room temperature. The second primary antibody was added, at various dilutions, diluted in blocking serum (Table 3.2). The slides were incubated in humidity chambers, overnight at 4^{o}C. Unbound primary antibody was removed with a 5-min wash in PBS with 0.05% Tween-20 detergent (PBST) followed by a second 5-min wash in PBS. The HRP-conjugated secondary antibody was added. The sections were incubated with the secondary antibody, diluted 1:200 in blocking serum, for 30 min at room temperature. Unbound secondary antibody was the removed by washing for 5 min, firstly in PBST then secondly, in PBS.

The secondary antibody signal was enhanced using either a Perkin Elmer TSA™ Plus Flourescein (TSA Flr) System (Perkin-Elmer Life Sciences, Boston, MA) or a Perkin Elmer TSA™ Plus Cyanine 3 (TSA Cy3) System (Perkin-Elmer Life Sciences, Boston, MA) (Table 3.1). The Tyramide is the amplification agent. It is activated by HRP in

order to bind to protein residues in the tissues. In this way, it only binds to areas of the section that are attached to the HRP-conjugated secondary antibody. The Cyanine fluorescent dye is attached to the Tyramide and so, allows the visualisation of the Tyramide. The Flourescein Amplification Reagent or Cyanine 3 Amplification Reagent was diluted 1:50 in the 1x Plus Amplification Diluent provided. This was added to the sections and incubated in the dark for 10 min at room temperature. Unbound chromagen was removed by washing for 5 min, firstly in PBST then secondly, in PBS.

1ST PRIMARY ANTIBODY	CONC	SECONDARY ANTIBODY	CHROMAGEN	2ND PRIMARY ANTIBODY	CONC	SECONDARY ANTIBODY	TSA-DYE
CD31	1:20	GAMB	Streptavidin Alexa 546	BMAL1	1:120	GARP	TSA Flr
CD68	1:20	GAMB	Streptavidin Alexa 546	BMAL1	1:120	GARP	TSA Flr
PER1	1:16	GAMB	Streptavidin Alexa 488	AROM-ATASE	1:100	GAMP	TSA Cy3
PER1	1:16	GAMB	Streptavidin Alexa 488	CD31	1:80	GAMP	TSA Cy3
PER1	1:16	GAMB	Streptavidin Alexa 488	CD68	1:50	GAMP	TSA Cy3
CD31	1:20	GAMB	Streptavidin Alexa 546	PER2	1:200	GARP	TSA Flr
CD68	1:20	GAMB	Streptavidin Alexa 546	PER2	1:200	GARP	TSA Flr
CD31	1:20	GAMB	Streptavidin Alexa 546	CRY2	1:150	GARP	TSA Flr
CD68	1:20	GAMB	Streptavidin Alexa 546	CRY2	1:150	GARP	TSA Flr

Table 3.2 Co-localised primary antibodies used in this study, indicating the dilution used and the appropriate secondary antibody and chromagen.

The sections were then counterstained with the nuclear stain: 4'-6-diamidino-2-phenylindole (DAPI), diluted 1:1000 in PBS, by incubating for 10 min at room temperature. They were washed twice for 5 min with PBS. The sections were mounted (Cover Glass; VWR International Ltd, Leicester, UK) using Shandon Permaflour™ aqueous-based mounting medium (Fisher Scientific UK Ltd, Loughborough, Leicester, UK). The cellular localisation of the immunofluorescent-protein was examined and

photographed, using a Zeiss LSM 510 Meta Confocal microscope (Carl Zeiss Ltd, Welwyn Garden City, Hertfordshire, UK).

3.3 RESULTS

3.3.1 CLOCK PROTEIN IN THE HUMAN CORPUS LUTEUM

The human CL was successfully visualised using IHC. The gross appearance of the human CL can be observed in photomicrographs, taken with relatively low power magnification (Figure 3.1). The human CL is organised into layers of cells. The granulosa-lutein cell layer is the largest of the cell layers. The theca-lutein cells are generally distributed at the edge of the granulosa-lutein cell layer. The granulosa-lutein cell layer is invaginated by theca-lutein cells and stromal fibroblasts. The fibroblasts mostly surround the steroidogenic cell layers. They are contained mostly in the peripheral stromal cell layer, though there are also some located between the central clot and the steroidogenic cells. They invaginate into the steroidogenic cell layers from both these areas. Blood vessels can also be distinguished, in the stroma and in the steroidogenic cell layers. The central clot, that once comprised the follicular antral cavity, lies at the centre of the CL structure.

The principle canonical clock proteins: PER1, PER2, CRY1, CRY2 and BMAL1 were localised to the human CL using immunohistochemistry (IHC) (Figure 3.1). CLK could not be visualised in these or any other tissue sections using the antibodies available. The anti-CRY1 antibodies were also difficult to use as the positive staining that they provided of the putative CRY1 protein was not removed by pre-incubation with excess control peptide (Figure 3.1 Panel C inset). Although the failure of this negative control does effectively invalidate the CRY1 localised using IHC, the images of these potentially false-positive staining has been included as the staining patterns appeared to be specific with some cells clearly not immunoreactive adjacent to clearly positively stained cells (Figure 3.1). The general staining pattern was much more similar to that of CRY2 than that of PER1 and PER2, as would be expected as the *cry* genes are homologs of each other and are known to have closely related circadian roles. Furthermore, the

negative controls omitting the primary antibody was clear of any staining (Figure 3.1 Panel F).

The staining patterns of each of the clock proteins were, at first glance, generally very similar to each other in all of the CL sections stained. There were however, overall differences in the degree of staining observed between the clock proteins, which are illustrated in one example of a single CL, which was stained for the clock proteins in serial sections (Figure 3.1). Overall, the clock proteins were found in all the major cell types in the human CL. These cell types were discerned using their morphology, relative size, location in the layered human CL structure and detection with co-localisation markers (Maybin and Duncan, 2004). With these criteria, the cells identified were luteal fibroblasts, granulosa-lutein cells, theca-lutein cells, vascular endothelial cells and macrophages. Specific nuclear and cytoplasmic localisation of all the clock genes that were examined was detected in all these cell types. The clock proteins were present in various amounts between cells of the same cell type as well as between cell types. The presence and absence of the clock proteins, and the degree to which they were present differed between cells of the same cell type in single fields of view. This heterogeneity in clock protein localisation did not conform to any detectable pattern between cell types or between CL samples, or indeed between the specific clock proteins. It may be that the degree of heterogeneity observed would differ between luteal phases, perhaps pertaining to the timing of the luteal lifespan and luteolysis. In order to assess whether this was the case, it was necessary that the localisation of the clock proteins, and the heterogeneity so far inherent in the human CL, be examined in human corpora lutea from throughout the luteal cycle.

Where there was a marked difference between the cytoplasmic staining and nuclear staining, the nucleus being much more darkly stained than the cytoplasm, indicating a higher concentration of protein located in the nucleus, the difference was referred to as the ratio between the nuclear and the cytoplasmic degree of staining. When there was a large difference, this ratio was said to be relatively high, and when there was less

obvious difference between the nuclear versus cytoplasmic compartmentalisation of the protein, the nuclear:cytoplasmic ratio was said to be relatively low.

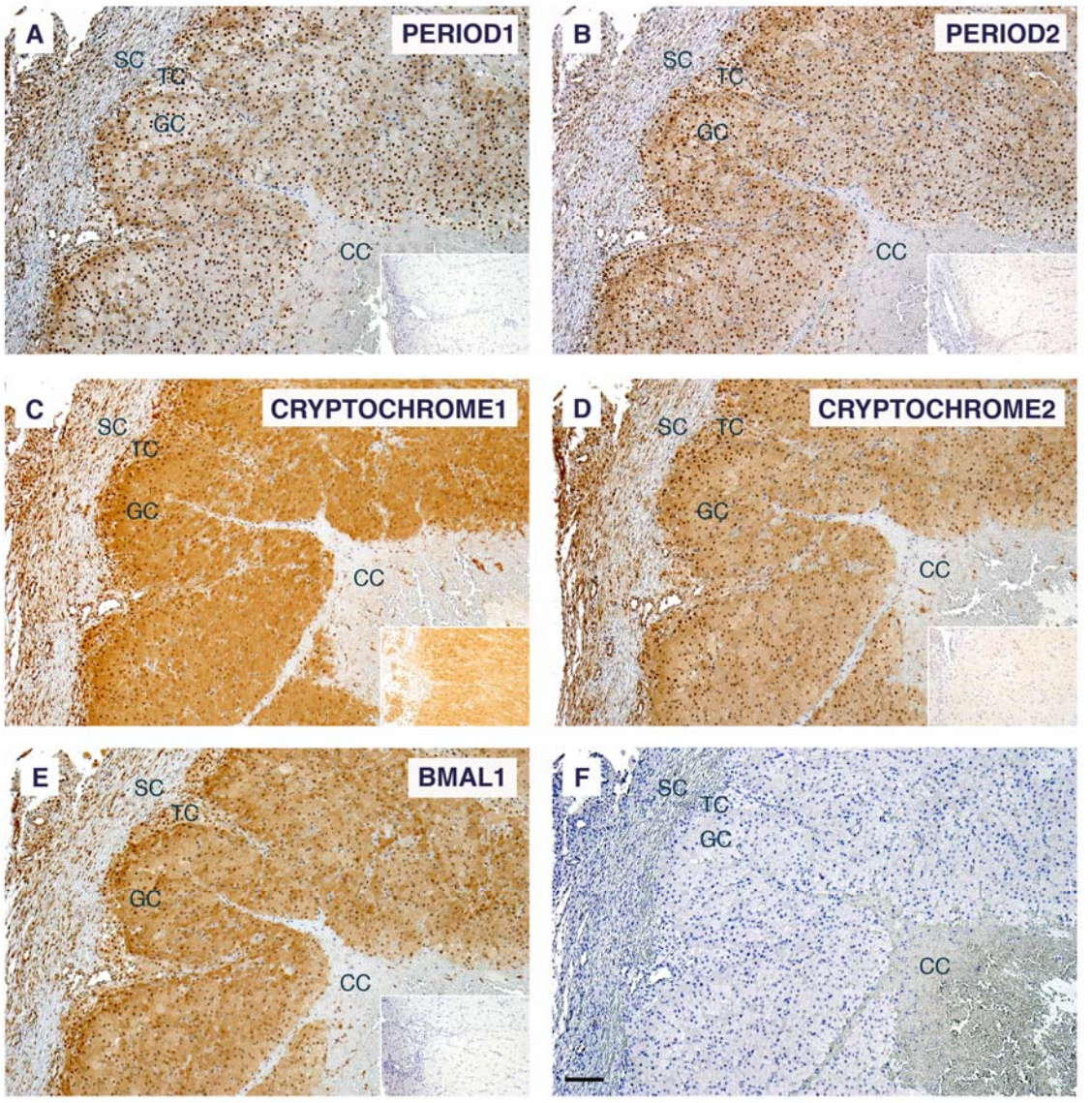

Figure 3.1 Photomicrographs of immunohistochemistry of the clock proteins in serial sections of a mid-luteal phase human CL. Each photomicrograph is labelled as follows: A: PER1, B: PER2, C: CRY1, D: CRY2, E: BMAL1 and F: negative control lacking primary antibody with scale bar for 100 μm. The insets are of control peptide pre-absorption negative controls. Luteal cell layers are labelled as follows: SC: stromal cell layer, TC: theca-lutein cell layer, GC: granulosa-lutein cell layer and CC: central clot.

Although all of the clock proteins successfully examined were found to be located in every discernible luteal cell type, not every cell within each cell type displayed these proteins. Some cells were not immunoreactive and no overall pattern could be clearly elucidated for these cells. Closer examination of the CL sections was conducted using higher microscope magnification (Figure 3.2). Generally, the PER1 and PER2 staining was more distinct than that of CRY1, CRY2. The staining of Per1, PER2 and CRY2 were also all much more distinct than that of BMAL1.

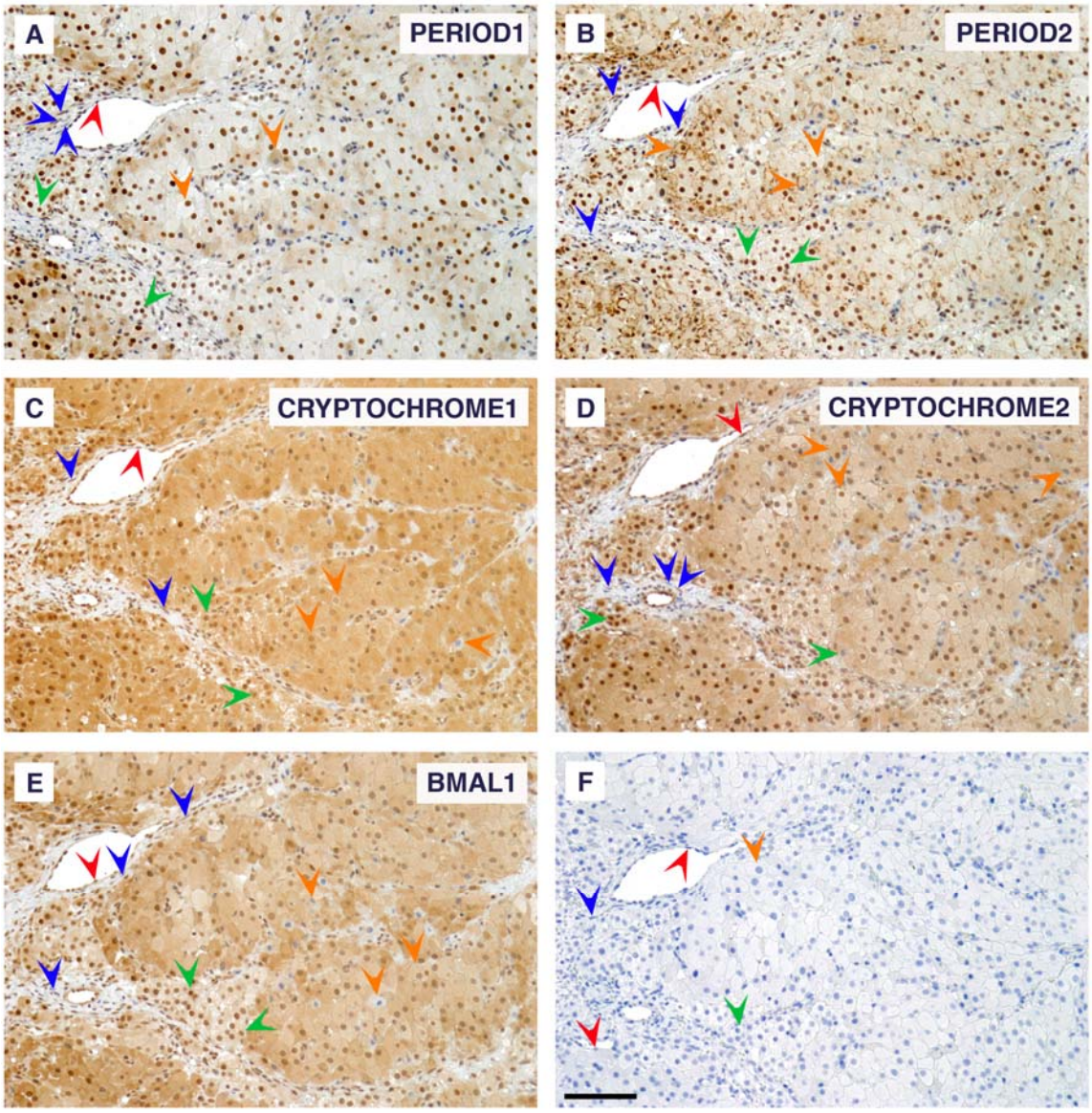

Figure 3.2 Higher magnification photomicrographs of immunohistochemistry of the clock proteins in mid-luteal human CL at 20x magnification. Each photomicrograph is labelled as follows: A: PER1, B: PER2, C: CRY1, D: CRY2, E: BMAL1 and F: negative control lacking primary antibody with scale bar for 100 μm. Various luteal cell types are indicated by colour-coded arrowheads, with the colours corresponding to individual cell types, as follows:- blue: stromal cells, green: theca-lutein cells, orange: granulosa-lutein cells and red: vascular endothelial cells.

PER1 can be seen to be clearly and strongly nucleic in its localisation with some cytoplasmic staining, in all cell types (Figure 3.1 Panel A and Figure 3.2 Panel A). The most pronounced cytoplasmic staining was in the steroidogenic cells: particularly in the theca-lutein cells. There was however a handful of not immunoreactive theca-lutein

cells embedded deep into the granulosa-lutein cell layer. The fibroblasts in general were more likely to be negative for PER1 than the steroidogenic cells, which were mostly PER1-positive. The weakest nuclear:cytoplasmic signal was also that of the fibroblasts. The fibroblasts located more internally within the CL, close to the central clot and invaginating deeply into the steroidogenic layers appeared to have a higher incidence of PER1-negative staining than those located in the peripheral stroma. The heterogeneity in the degree of staining and in the cellular compartmentalisation of the protein between cells of the same cell type was particularly evident in the granulosa-lutein cells, two of which have been marked out by arrows in Figure 3.1 Panel A. One of these cells has a distinct and strong nuclear staining with some cytoplasmic staining in a relatively high nuclear:cytoplasmic ratio of staining strength. The other cell has mostly cytoplasmic staining, which is much stronger than in the first cell described. It also has no or barely discernible nuclear staining, thus again presenting a relatively high nuclear:cytoplasmic staining strength ratio, although this ratio is lower than that for the first cell. The staining of the first cell described is more characteristic of the majority of the granulosa-lutein cells in this field of view, in this section. The overall degree of nuclear staining and the nuclear:cytoplasmic ratio of staining in the theca-lutein cells also varies, though not as much as in the granulosa-lutein cells. Some of the theca-lutein cells, along with fibroblasts, which were deeply embedded in the granulosa-lutein layer, were not immunoreactive. Many of the theca-lutein cells located closer to the outskirts of the granulosa cell layer had a lower nuclear:cytoplasmic ratio of staining strength compared to the adjacent granulosa-lutein cells. The fibroblasts were generally the most heterogeneous in their staining, with as many cells being not immunoreactive as there were positively stained, and with a highly variable degree of positive between cells. Examples of strong and faintly stained fibroblasts are depicted with arrows in the Figure 3.7 Panel A, alongside a non-immunoreactive fibroblast. PER1 was also observed in some but not all of the vascular endothelial cells (Figure 3.7 Panel A).

The staining pattern of PER2 was similar to that of PER1 (Figure 3.1 Panel B and Figure 3.2 Panel B). Again, all the cell types were PER2-positive, with a pronounced nuclear

signal and less pronounced cytoplasmic signal. There appeared to be more PER2 in the cytoplasm of the theca-lutein cells than in any other cell type, with a nuclear:cytoplasmic ratio in the strength of the staining that was very similar to that of PER1. This ratio however differs between these two proteins when the granulosa-lutein cells are inspected. Whereas a general difference could be discerned between the theca-lutein and granulosa-lutein cells in terms of nuclear:cytoplasmic ratios of staining strength with PER1, this was less evident when staining for PER2 (Figure 3.2 Panel B). Like the localisation of PER1, PER2 in the fibroblasts is clearly nuclear with much fainter cytoplasmic staining, and there appears to be more non-stained fibroblasts located closer to the central clot than the stromal fibroblasts closer to the outer boundary of the CL. Fibroblasts and theca cells observed in the midst of the steroidogenic cells appeared to also often be PER2-negative.

The staining pattern of PER2 was also unique in the granulosa-lutein cells (Figure 3.2 Panel B). Many cells demonstrated staining of cytoplasmic PER2, collected in foci radiating around the nucleus of some cells, and closely apposed to what appears to be the basement membrane of the cells. Not all cells however demonstrated the presence of the PER2 foci and indeed, their presence differed from CL sample to CL sample. There was also heterogeneity within samples, with some fields of view presenting no such staining and with other fields of view from the same sample, presenting many instances of foci staining. Indeed, in a single field of view, some granulosa-lutein cells can be seen to have no foci, while others do. Those that do can also differ in terms of degree of cytoplasmic staining, suggesting that the amount of PER2 detected in the cytoplasm varied from cell to cell. The nuclear staining in these cells could also vary. In Figure 3.2 Panel B, three examples of heterogeneous granulosa-cell staining have been picked out: 1) with nuclear and cytoplasmic staining, with the nuclear staining predominating and without any foci staining, 2) with nuclear and cytoplasmic staining, with the nuclear staining predominating but not as much as in the cell in example 1, and with cytoplasmic foci staining as strongly as the nucleus and 3) with cytoplasmic staining to a degree that is akin to that in example 1 but with foci staining as in example 2 and with very faint or

virtually no nuclear staining. Fibroblasts were found to stain equally heterogeneously, with examples of a strongly PER2-positive, a less strongly PER2-positive and a PER2-negative fibroblast indicated in Figure 3.2 Panel B. The theca-lutein cells were largely PER2-positive with most cells demonstrating stronger nuclear staining than cytoplasmic staining. The vascular endothelial cells were also mostly PER2-positive with generally much less heterogeneity observed in their staining between cells within individual fields of view. Some cells closely apposed to the positively-stained vascular endothelial cells and which may be pericytes, appear to be PER2-negative.

The staining of CRY1 was very diffuse in the steroidogenic cells, with a relatively low nuclear:cytoplasmic ratio in the degree of staining observed between these cell compartments in these cell types (Figure 3.1 Panel C and Figure 3.2 Panel C). The theca-lutein cells were again more homogeneously stained than the granulosa-lutein cells, both in terms of positive versus negative staining as well as in terms of degree of staining in the cytoplasm and nucleus. Most theca-luteal cells were CRY1-positive with a discernible nuclear:cytoplasmic ratio in the degree of staining, with the nucleus more strongly stained. Only a few theca-lutein like cells found in the midst of the granulosa-lutein layer could be seen to be either CRY1-negative or to have very little nuclear staining although cytoplasmic staining was present. The granulosa-lutein cells were also mostly CRY1-positive although there were some CRY1-negative cells. The non-immunoreactive cells appeared to account for a larger proportion of the granulosa-lutein cell population than the non-immunoreactive theca-lutein cells accounted for in the theca-lutein cell population. The staining of the CRY1-positive granulosa-lutein cells was much more mixed in terms of their nuclear:cytoplasmic staining strength ratio. To illustrate this, three granulosa-lutein cells have been pointed out in Figure 3.2 Panel C: 1) a strongly nuclear and almost-as-strongly cytoplasmic CRY1-positive cell, 2) a strongly nuclear but much fainter CRY1-positive cell and 3) a cytoplasmic CRY1-positive cell with very little if any nuclear CRY1. The fibroblasts were mostly CRY1-positive, both those associated with the peripheral stroma as well as those associated with the central clot and infiltrating into the steroidogenic cell layers, although there

were more CRY1-negative evident closer to the central clot. Although higher than that of the granulosa-lutein and theca-lutein cells, the nuclear:cytoplasmic ratio of staining strength in the fibroblasts was lower than that seen with PER1 and PER2. The nuclear staining of the stromal fibroblasts was very pronounced, but so was the cytoplasmic staining compared to that of PER1 and PER2 in the fibroblasts. The vascular endothelial cells appeared to be mostly CRY1-positive. It is notable that the primary antibody-omitting negative control in Figure 3.2 Panel F was clear, although the control peptide pre-absorption negative control for CRY1 was not (Figure 3.1 Panel C inset).

CRY2 was expressed in all the luteal cell types with staining that was much less diffuse than that of CRY1, and more closely resembled that of BMAL1 than that of CRY1 (Figure 3.1 Panel D and Figure 3.2 Panel D). Although its staining pattern in general had a lower nuclear:cytoplasmic signal strength ratio than that of PER1 and PER2, it was not as low as that of CRY1. The cytoplasmic compartmentalisation of CRY2 was much less than the nuclear compartmentalisation of BMAL1 in all the cell types. Once again, the theca-lutein cells were the most strongly stained for nuclear clock protein. There was also strong nuclear staining in the granulosa-lutein cells and the fibroblasts, with virtually all the granulosa-lutein cells being CRY2-positive. The nuclear:cytoplasmic signal strength ratio was no less variable in the stroma-associated theca-lutein cells than the granulosa-lutein cells. The theca-lutein cells found amidst the granulosa-lutein cell layer were much more likely to be CRY2-negative then the stroma-associated theca-lutein cells. There appeared to be a greater proportion of CRY2-negative theca-lutein cells in the granulosa-lutein cell layer than CRY1-negative cells in the same location. The staining of the granulosa-lutein cells did however still provide instances of cells that were 1) strongly positive in both nuclear and cytoplasmic compartments, with nuclear staining predominating, 2) strongly nuclear and faint cytoplasmic staining and 3) cytoplasmic staining with little or no nuclear staining (Figure 3.2 Panel D). The nuclei of positively stained steroidogenic cells were, for the most part, more densely stained than the cytoplasm. The nuclear:cytoplasmic ratio of the staining strength in the fibroblasts was very similar to that of CRY1. It was also

heterogeneous, with strongly CRY2-positive, faintly CRY2-positive and CRY2-negative cells pointed out in Figure 3.2 Panel D. The fibroblasts near the central clot, and particularly those invaginating into the steroidogenic layers from the central clot, were largely CRY2-negative. This was also the case for fibroblasts that were deeply embedded in the steroidogenic layers, even those in tracts originating from the peripheral stroma. The theca-lutein cells that were found in invaginating tracts deeply embedded in granulosa-lutein cell layer also tended to be CRY2-negative. The vascular endothelial cells were generally CRY2-positive.

The BMAL1 staining, like the CRY1 and CRY2 staining, was more diffuse than the PER1 and PER2 staining (Figure 3.1 Panel E and Figure 3.2 Panel E). The nuclear:cytoplasmic ratio in the strength of staining in the steroidogenic cells was relatively low and was slightly greater than that of CRY1 but slightly less than that of CRY2. The theca-lutein cells were again distinctly stained, with nuclear staining being greater than cytoplasmic staining, providing a higher nuclear:cytoplasmic signal strength ratio than the granulosa-lutein cells. The theca-lutein cells in the midst of the granulosa-lutein cell layer were however more variable in their positive versus negative BMAL1 staining, with a larger proportion of these cells being BMAL1-negative than the stroma-associated theca-lutein cells and granulosa-lutein cells. The granulosa-lutein cells were also virtually all positively-stained. There were small number of granulosa-lutein cells being BMAL1-negative, accounting for a larger proportion of the granulosa-lutein cell population than those not stained for of PER1, PER2 and CRY1. The degree of cytoplasmic staining in the steroidogenic cells was however quite varied, with the cells closest to the folds in the invaginating steroidogenic cell layers being more strongly stained than the cells in the midst of the steroidogenic layers (Figure 3.1 Panel E). The fibroblasts were mostly BMAL1-positive, albeit with some heterogeneity in the degree of staining, although most had stronger nuclear staining than cytoplasmic staining. The ratio between the strengths of these stains was relatively similar to that observed with CRY2. The few fibroblasts that were BMAL1-negative were mostly those invaginating

from the central clot into the steroidogenic cell layers as well as those deeply embedded in these layers. The vascular endothelial cells were mostly BMAl1-positive.

Figure 3.2 Panel F shows the negative control that lacked incubation with the primary antibody. The negative control is devoid of any DAB staining, demonstrating the specificity of the clock protein antibodies in the CL tissue with the protocol used. All the CL sections depicted in Figure 3.1 and Figure 3.2, alongside sections from other corpora lutea, were also processed with negative controls that were incubated with the primary antibody, pre-absorbed with control peptide. These negative controls were also clear of any specific clock protein staining (Figure 3.1 insets).

3.3.2 SPECIFIC CELL TYPES IN THE CORPUS LUTEUM

It was clear rhat the clock proteins were present in multiple cell types. Some cells can be identified by morphology more easily than others. Therefore, to ascertain which cell types the clock proteins were present in, it was necessary to identify as many cell types as possible, using IHC with antibodies raised against cell type marker proteins. The CL consists of different cell types in addition to the steroidogenic cells derived directly from the follicular granulosa cells and the steriodogenic cells derived directly from the follicular theca cells, such as fibroblasts, endothelial cells, pericytes and immune cells, including macrophages (Duncan et al., 1998a). The cell types which could not be identified using visualisation of marker peptides were identified by virtue of their characteristic morphology and location in the layered structure of the human CL. The cell types thus identified were fibroblasts and where appropriate, granulosa-lutein cells, theca-lutein cells, vascular endothelial cells and erythrocytes (Maybin and Duncan, 2004). The cell types that could be identified using marker peptides were the granulosa-lutein cells, theca-lutein cells, vascular endothelial cells and macrophages.

The granulosa-lutein cells were identified using antibodies raised against P450 aromatase. This enzyme catalyses the aromatisation of androgens into œstrogens, that occurs only in the granulosa-lutein cell type in the CL. This reaction occurs in the cytoplasm and so the peptide is only observed in the cytoplasmic compartment of the cell. A commercially available anti-P450 aromatase antibody was successfully used in an immunofluorescent IHC protocol with a DAPI nuclear counterstain (Figure 3.3 Panel A).

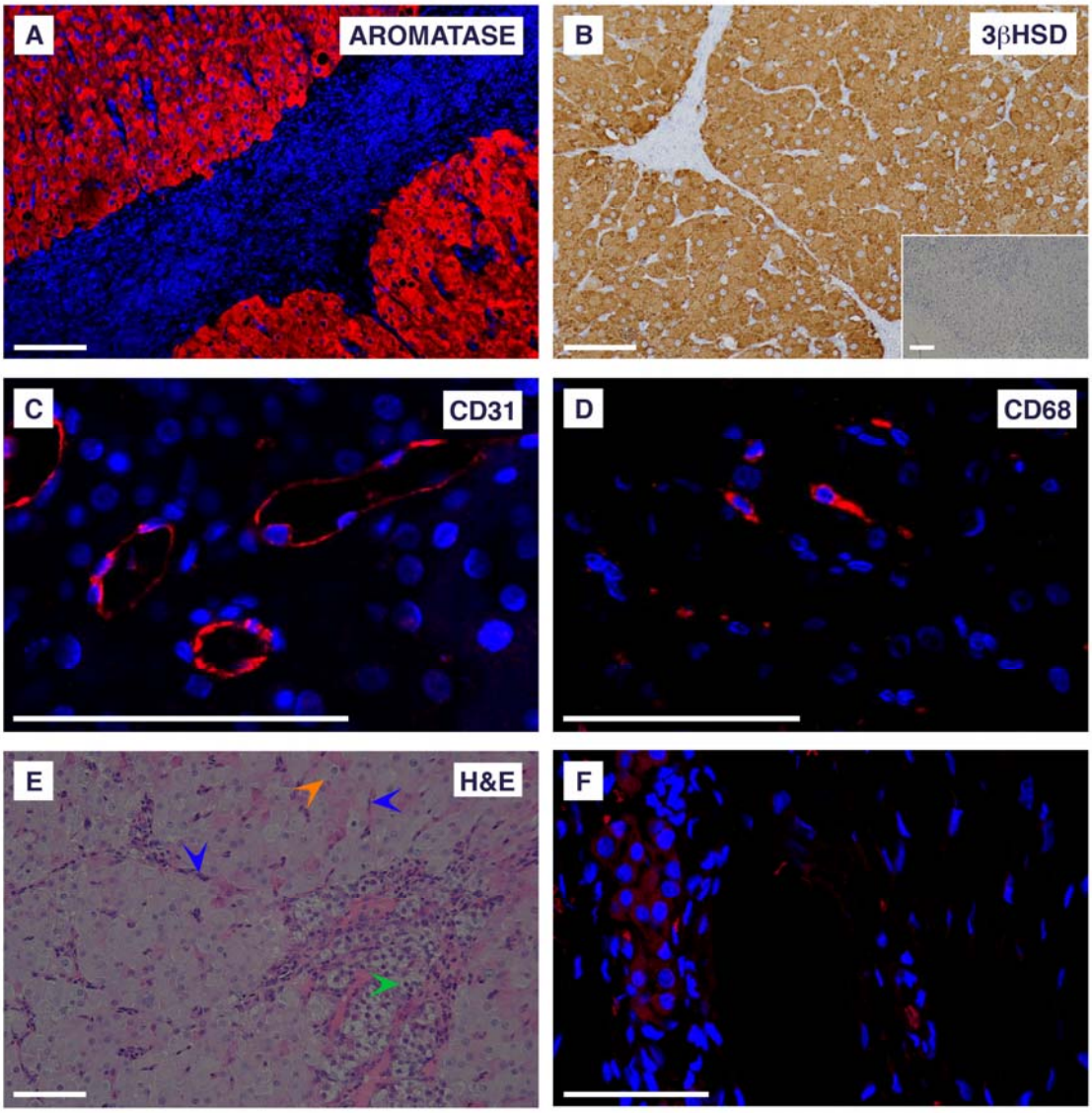

Figure 3.3 Photomicrographs of different cell types in the human CL at 20x and 60x magnification. A: Confocal image of red-staining P450 aromatase-positive granulosa-lutein cells with blue DAPI nuclear counterstain. B: brown-staining 3βHSD-positive steroidogenic cells revealed using a standard DAB detection system, with an inset image of a negative control lacking primary antibody, counterstained with haemotoxylin (blue). C: Confocal image of red-staining CD31-positive vascular endothelial cells with blue DAPI nuclear counterstain. D: Confocal image of red-staining CD68-positive macrophages with blue DAPI nuclear counterstain. E: a standard haematoxylin and eosin (H&E) stain showing all the luteal cells: granulosa-lutein cells (orange arrowhead), theca-lutein cells (green arrowhead) and fibroblasts (blue arrowheads). F: Confocal image of a double negative control lacking primary antibody with blue DAPI nuclear counterstain. The scale bars are for 100 μm.

The theca-lutein cells, being steroidogenic, can be identified along with the granulosa-lutein cells using IHC with antibodies against the 3βHSD enzyme. This was employed as it proved difficult to source a specific theca-lutein cell marker, such as a 17α-hydroxylase antibody, and it was decided that in order to identify these cells, sections stained for aromatase would be 'subtracted' from serial sections stained for 3βHSD, which localises to both types of steroidogenic cell. The enzyme, like aromatase, also localised to the cytoplasmic compartment. The comparison of serial sections was further made necessary, because the 3βHSD antibody could not be successfully used in an immunofluorescent protocol, and only worked in a conventional IHC protocol. The inset photomicrograph in Figure 3.3 Panel B is the negative control, which omitted a primary antibody. It successfully demonstrated the specificity of the primary antibody, as it was clearly not stained by DAB, and showed only the haematoxylin nuclear counterstain.

The CL contains a large number of blood vessels, which are lined by vascular endothelial cells. These cells have a characteristic morphology. They are very flat, elongated cells with long intercellular junctions and distinct nuclei. They occur in a single layer around the blood vessel. They were identified in the human CL using the cytoplasmic marker: CD31. The CD in its name refers this marker being a cluster of differentiation molecule. These molecules are located on cell surfaces and are often cell surface receptors or ligands. CD31, also known as platelet/endothelial cell adhesion molecule-1 (PECAM-1), is an endothelial cell adhesion molecule. The surface of the luteal vascular endothelial cells was successfully visualised using an antibody raised against CD31, using single immunofluorescent IHC (Figure 3.3 Panel C).

The CL also contains various immune cells, including macrophages. Macrophages phagocytose (engulf then digest) pathogens and cellular debris as well as stimulate other immune cells to mount a defence against pathogenic infection. Macrophages also have a characteristic morphology. They are round, mononuclear cells with one or two elongated tail-like extensions. In humans, they are approximately 21 μm in diameter.

Macrophages in the human CL were identified using another CD marker: CD68. CD68 is a glycoprotein that binds low-density lipoproteins, and is only expressed on macrophages. The outline of these cells can be clearly seen using single immunofluorescent IHC (Figure 3.3 Panel D).

The general architecture of the human CL is revealed in a section stained with haematoxylin and eosin (Figure 3.3 Panel E). Eosin is a dye that stains cytoplasm, collagen and muscle while haematoxylin stains basophilic molecules such as nucleic acids, which are found in cell nuclei. The photomicrograph in Figure 3.3 Panel E shows the invagination of the granulosa-lutein cell layer by vein-like tracts of theca-lutein cells and fibroblasts. The fibroblasts have a characteristic flat and elongated morphology, which was used to identify them.

Figure 3.3 Panel F shows a negative control, lacking primary antibody, photographed at the same settings as those in Figure 3.3 Panel C and D. It shows minimal red background fluorescence and demonstrates the specificity of the antibodies using single immunofluorescent IHC.

3.3.3 CLOCK PROTEINS IN SPECIFIC LUTEAL CELL TYPES

In order to definitively identify the cell types in which the various clock genes could be seen, co-localisation of the clock genes and cell marker peptides was performed using dual immunofluorescent histochemistry. This required the use of higher antibody concentrations, which precluded some of the clock protein antibodies. Some of the clock protein antibodies were also unsuitable as they were raised in the same animal species as that of the marker peptide antibody, making it impossible to distinguish the two antibodies using a secondary antibody that simply recognises proteins from the antibody donor-animal species. The use of late luteal phase human luteal tissue was also

preferred as this better enabled the identification of the various cell types based on their morphology, relative size and relative location. The clock proteins that were successfully co-localised with some of the marker peptides were: PER1, PER2, CRY2 and BMAL1.

PER1 co-localised with aromatase in the granulosa-lutein cells in the late luteal phase human CL (Figure 3.4 Panel A). In this section, most of the granulosa-lutein cells contained strong nuclear PER1 fluorescence. A few cells however were much less fluorescent, showing nuclei with more predominant nuclear DAPI fluorescence than that of PER1, although there did appear to be some nuclear PER1 present. Interestingly, the nucleoli of the nuclear PER1-positive granulosa-lutein cells were often negative for PER1. The theca-lutein cells were identified using their morphology, location and size, relative to the other cells, particularly the granulosa-lutein cells. The nuclei of the theca-lutein cells were also heterogeneously fluorescent for nuclear PER1, demonstrating strong staining, faint staining and no staining in various cells in the same field of view (Figure 3.4 Panel B). In the field of view in Figure 3.4 Panel B, there were as many nuclear PER1-positive theca-lutein cells as nuclear PER1-negative theca-lutein cells. The fibroblasts were similarly heterogeneously fluorescent, with some staining predominantly with DAPI and others predominantly with PER1. PER1 was also co-localised with CD31 in some of the vascular endothelial cells (Figure 3.4 Panel D), while other CD31-positive cells were PER1-negative (Figure 3.4 Panel C). PER1 did not co-localise with CD68 in the macrophages in this field of view (Figure 3.4 Panel E). A negative control omitting primary antibody showed relatively very low background red fluorescence and no green fluorescence, and no specific fluorescence of any particular cell or cell type, thus demonstrating the specificity of the antibodies in this protocol for visualising their cognate proteins (Figure 3.4 Panel F).

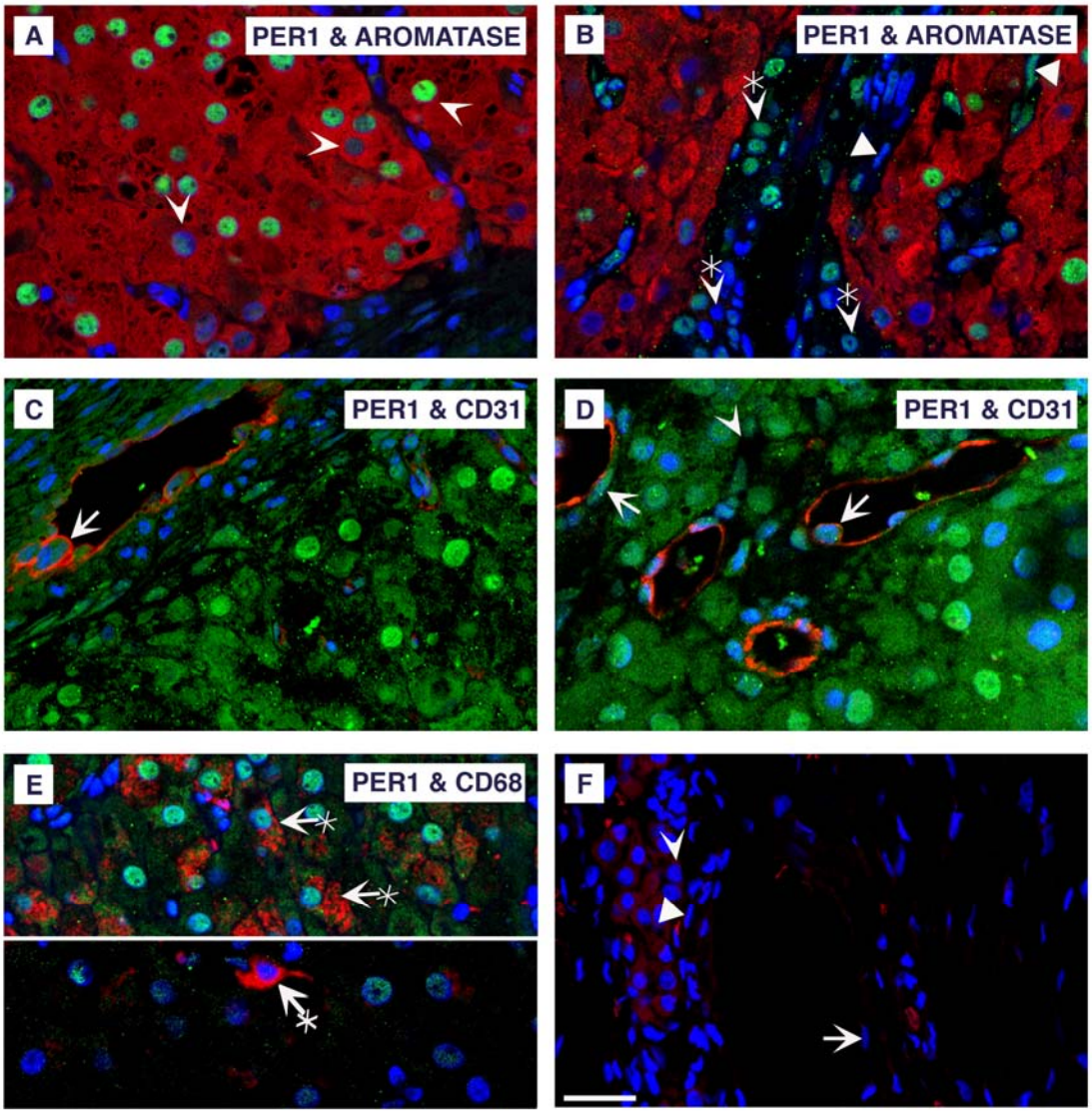

Figure 3.4 Confocal photomicrographs of immunohistochemistry of PER1 (green) co-localising with A and B: P450 aromatase (red), C and D: CD31 (red) in vascular endothelial cells and E: CD68 (red) in macrophages. F is the negative control lacking primary antibody. A DAPI nuclear counterstain (blue) was used in all sections. The arrowheads indicate granulosa-lutein cells, the arrowheads with asterisks indicate theca-lutein cells, the arrows indicate vascular endothelial cells, the arrows with asterisks indicate macrophages and the triangles indicate fibroblasts. The scale bar represents 100 μm.

PER2 also co-localised to luteal cell markers in the late phase human CL. It was found in many, but not all, the vascular endothelial cells, which were identified by CD31

fluorescence (Figure 3.5 Panel C). The inset image shows a higher magnification of the CD31-positive vascular endothelial cells containing PER2.

PER2 could not be co-localised with aromatase, as it would require too high a concentration than that which was available, in order to definitively characterise the presence of PER2 in the granulosa-lutein cells. Figure 3.5 Panel A however, although showing the co-localisation of PER2 and CD31, could be used for the purpose of illustrating the PER2 fluorescence in the granulosa-lutein cells. These cells were identified by their characteristically large size and cuboidal shape, as well as their layered location in relation to the other surrounding cells of different cell type. The aggregates of PER2 in foci, radiating around the nucleus and closely apposed to the outer boundary of the cell, which were previously described (Figure 3.2 Panel B) were again observed in some, but not all, of the granulosa-lutein cells, using dual immunofluorescent histochemistry. Some of the foci-laden cells were strongly PER2-positive in the nuclear compartment as well as in the cytoplasmic compartment. Other foci-laden cells appeared to have virtually no nuclear PER2 while others still appeared to have only a faint fluorescence of PER2, indicating that there was only relatively small amounts of PER2 in their nuclei (Figure 3.5 Panel B). The staining of the foci also varied, with some cells demonstrating thick rings of highly fluorescent PER2 in the cytoplasm, while other cells demonstrated only a light peppering of fluorescent foci, arranged in a very thin ring, close to the edge of the cells. In general, the foci-laden cells were arranged in close proximity to each other, occurring in small clusters. Granulosa-lutein cells that did not contain foci were also loosely arranged together in small clusters. This unusual pattern of staining appears to be unique to this protein in these cells, as they have not been previously reported.

Theca-lutein cells were also visible in confocal photomicrographs of PER2 co-localised with CD31 (Figure 3.5 Panel D). The theca-lutein cells were identified by their morphology, size and location, relative to the other cells in the CL. PER2 could be seen in the nuclei of some, but not all, of these cells. It could also been seen in some, but not

all, of the fibroblasts, which were also identified by their characteristic morphology, size and relative location in the CL.

PER2 was also successfully co-localised to CD68, indicating its expression in macrophages. It was both nuclear and cytoplasmic, appearing green in the nucleus and orange when co-localised with the red fluorescent cytoplasmic CD68 (Figure 3.5 Panel E). The inset image is a confocal photomicrograph taken at a higher power, depicting a PER2-positive macrophage. Figure 3.5 Panel F is a confocal photomicrograph, which better shows the cytoplasmic CD68 fluorescence demarcating the characteristic flame-like shape of the macrophages with DAPI nuclear counterstain and without the somewhat masking fluorescence of PER2.

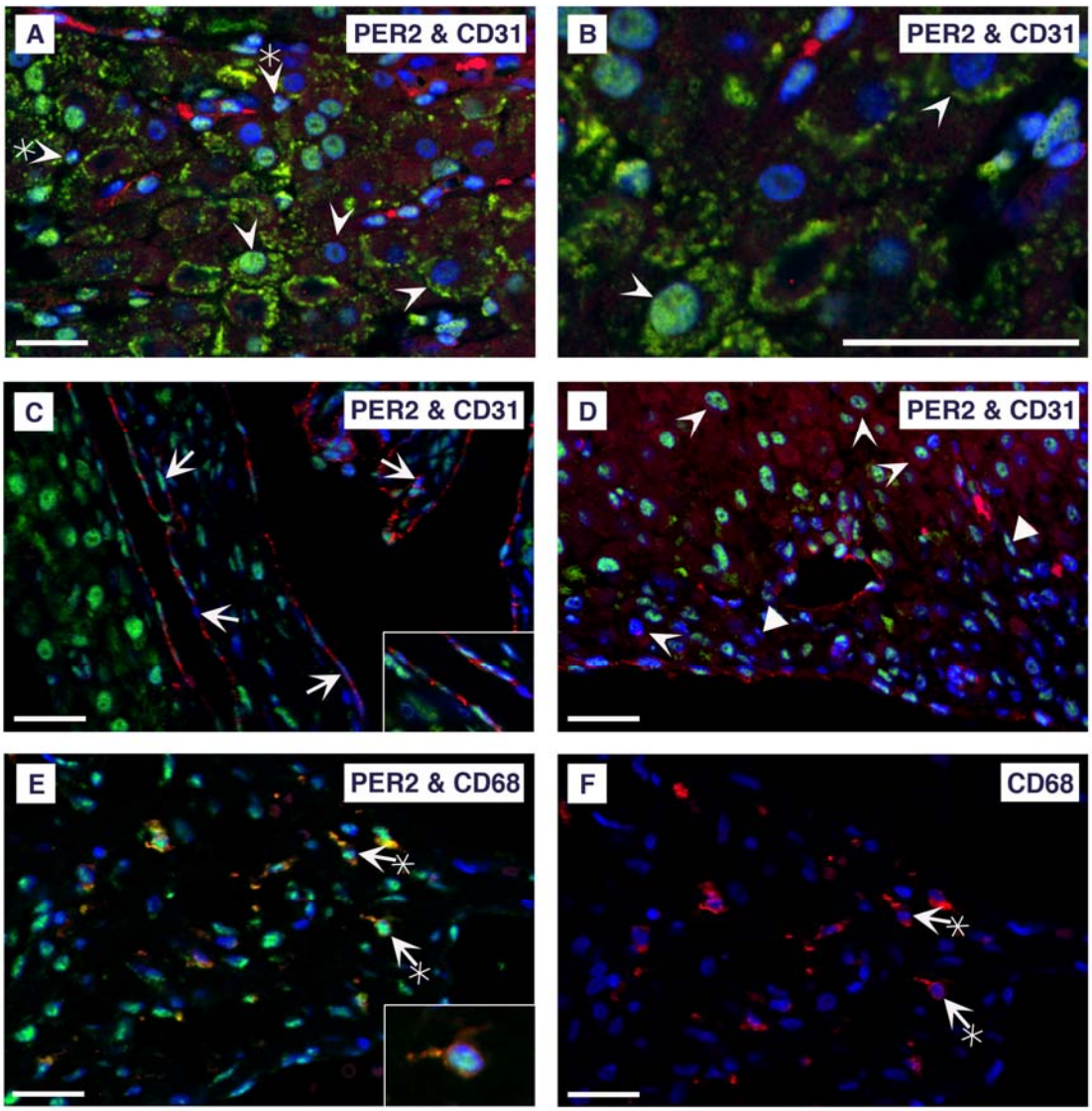

Figure 3.5 Confocal photomicrographs of immunohistochemistry of PER2 (green) co-localising with various peptides (red) and nuclear counterstained with DAPI (blue). A: PER2 co-localised with CD31 (red) in macrophages (arrows with asterisks), with an inset image of a magnified macrophage. B: CD31 (red) staining with DAPI and without PER2 staining. C: PER2 co-localised with CD31 (red) in vascular endothelial cells (arrows), with an inset image of a magnified vascular endothelial cells. D: PER2 co-localised with CD31 (red) in granulosa-lutein cells (arrowheads) and fibroblasts (triangular arrowheads). E: PER2 co-localised with CD68 (red) macrophages (arrows with asterisks), with an inset image of a magnified macrophage. F: CD68 (red) localising to macrophages (arrows with asterisks). No clear theca-lutein cells could be identified. The scale bars represents 100 μm.

CRY2 was also successfully co-localised to the CD31 and CD68 markers. The co-localisation of CRY2 with CD31 appears as orange in the vascular endothelial cells seen

in Figure 3.6 Panel A. The nuclei of some of these cells were predominantly CRY2-negative, while others were clearly CRY2-positive in both nuclear and cytoplasmic compartments. This is particularly obvious when the field of view is expanded using a lower power magnification, as demonstrated in Figure 3.6 Panel B. This also enables the observation of CRY2 in many of the granulosa-lutein cells, as well as, in the theca-lutein cells. The theca-lutein cells appeared to have a much fainter CRY2 signal with a more cytoplasmic distribution. The fibroblasts also demonstrated heterogeneous CRY2 localisation, with some fibroblasts being CRY2-positive and others being CRY2-negative.

CRY2 co-localised with CD68 in some of the macrophages. The degree of CRY2 staining in these macrophages was heterogeneous with fainter CRY2 fluorescence observed in some cells (Figure 3.6 Panel C) than in other cells (Figure 3.6 Panel D). The CRY2 protein was both nuclear and cytoplasmic, with a varied nuclear:cytoplasmic signal strength ratio. The nuclear compartment was more strongly fluorescent in some macrophages (Figure 3.6 Panels C and D) while in others, the cytoplasmic compartment was more fluorescent (Figure 3.6 Panel B).

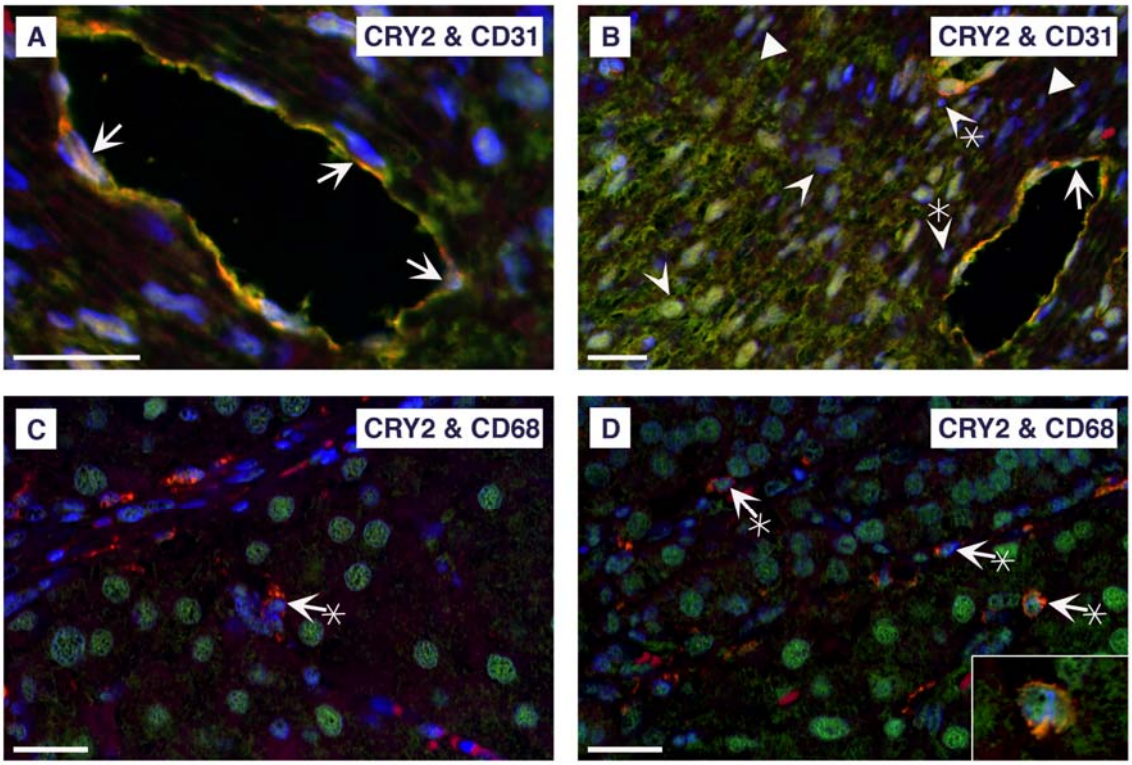

Figure 3.6 Confocal photomicrographs of immunohistochemistry of CRY2 (green) co-localising with various peptides (red) and nuclear counterstained with DAPI (blue). A and B: CRY2 co-localised with CD31 (red) in macrophages (arrows with asterisks), with an inset image of a magnified macrophage. C and D: CRY2 co-localised with CD31 (red) in vascular endothelial cells (arrows). The granulosa-lutein cells (arrowheads) also appear to be CRY2-positive while the theca-lutein cells (arrowheads with asterisks) were less easily identified as CRY2-positive. The scale bars represents 100 μm.

BMAL1 also successfully co-localised with the vascular endothelial cell marker peptide, CD31 and the macrophage marker peptide, CD68 (Figure 3.7). BMAL1 was mostly nuclear in the vascular endothelial cells (Figure 3.7 Panel A), which were virtually all BMAL1-positive in this field of view. BMAL1 was also present in the luteal macrophages, in both nuclear and cytoplasmic compartments: fluorescing green in the nucleus and orange (a combination of the red fluorescence of the CD68 and green fluorescence of the BMAL1) in the cytoplasm (Figure 3.7 Panel B). The steroidogenic cells could also be identified by their size and location (Figure 3.7 Panel A). They were found to be mostly BMAL1-positive, although there were also a few putative theca-lutein cells that were BMAL1-negative. The fibroblasts were also identified by their

classic morphology; some of which were BMAL1-negative and some of which were BMAL-positive (Figure 3.7 Panel A).

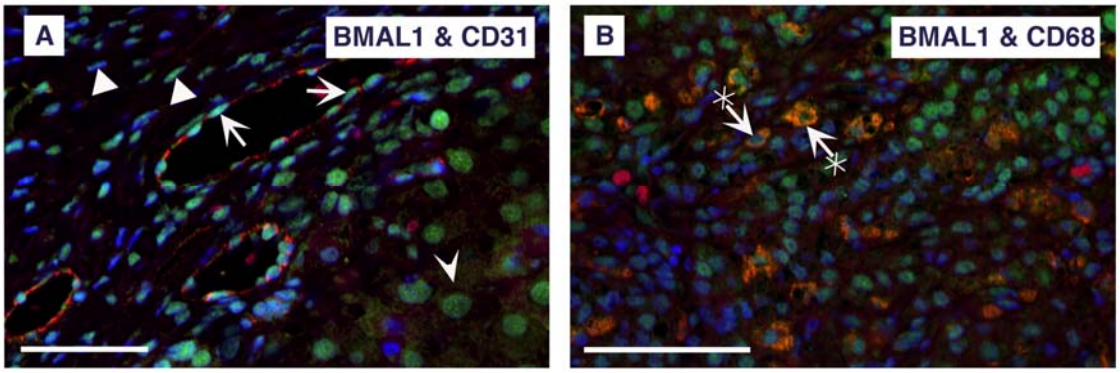

Figure 3.7 Confocal photomicrographs of immunohistochemistry of BMAL1 (green) co-localising with A: CD31 (red) in vascular endothelial cells (arrows) and B: CD68 (red) in macrophages (arrows with asterisks) with DAPI nuclear counterstain (blue). BMAL1 could also been seen in some steroidogenic cells, some of which were granulosa-lutein cells (arrowhead), as well as fibroblasts (triangular arrowheads). The scale bar represents 100 μm.

3.3.4 CLOCK PROTEINS THROUGHOUT THE LUTEAL PHASE

Sections from early, mid- and late luteal phase human corpora lutea were examined using conventional IHC of the clock proteins. This revealed that the clock proteins were present in the human CL at each of the phases of the luteal cycle. The heterogeneity in the localisation of the clock genes that was observed in the late luteal phase corpora lutea was also evident in the early and mid-luteal phase corpora lutea. No gross differences could be found between the corpora lutea of different phases that could not also be found between corpora lutea of the same phase. Therefore, the degree of heterogeneity observed in the clock protein localisation was not noticeably different between the luteal phases.

3.3.5 PERIOD1 IMMUNOSTAINING

In all the luteal phases, PER1 was found located predominantly in the nucleus though also, more faintly staining, in the cytoplasmic compartment of theca-lutein, granulosa-lutein and vascular endothelial cells. Virtually all the granulosa-lutein cells contained PER1, as did most theca-lutein cells. There were a few, isolated PER1-negative theca-lutein cells (Figure 3.8). The vascular endothelial and perivascular cells were more variable in their staining, with the cells of some blood vessels staining positive while cells of other blood vessels were less strongly stained and others still, were negative (Figure 3.8 Panels A and E). There was also the occasional blood vessel lined with an admixture of PER1-positive and PER1-negative cells (Figure 3.8 Panel C). Staining in the fibroblasts was mostly only nuclear with a few exceptions displaying both nuclear and cytoplasmic staining. The fibroblasts were stained in all samples but the proportion of fibroblasts positive for PER1 varied from sample to sample (Figure 3.8 Panels A and E). This variation was also evident between different areas of the same section in some samples (Figure 3.8 Panel D). PER1 was also found in some macrophages but was generally infrequent. The strength of staining in both the nucleus and cytoplasm varied greatly between individual cells of each cell type, within and between samples. The degree of heterogeneity in such staining was also variable within and between samples. No evident trends emerged over the luteal lifespan. The negative controls, which used the control peptide to occupy the primary antibodies, were entirely not immunoreactive.

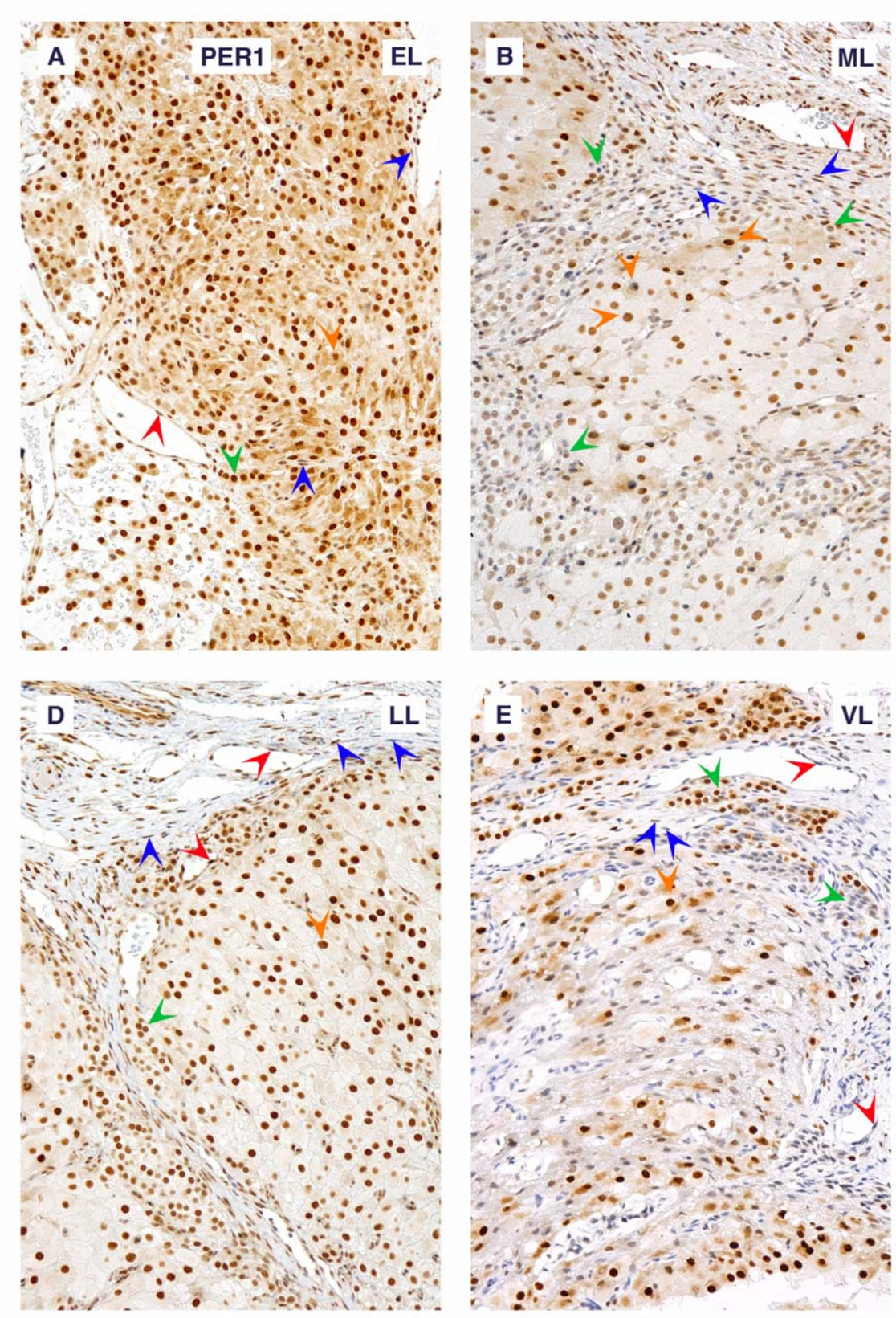
A
PER1
EL
B
ML
D
LL
E
VL

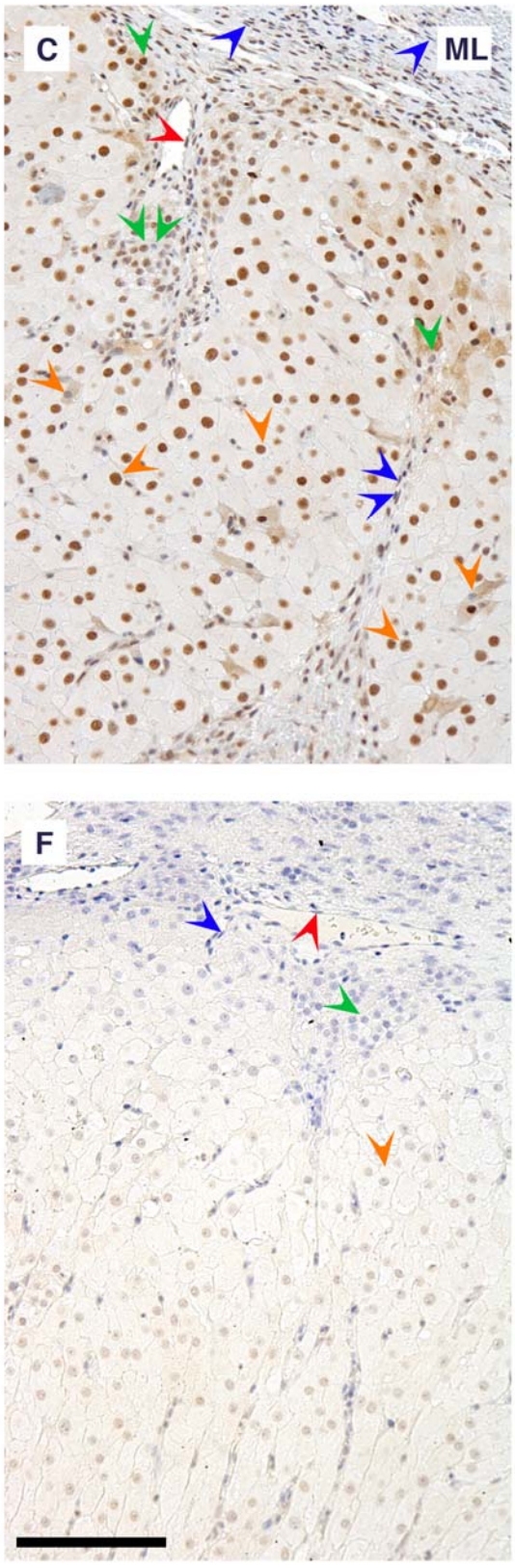

Figure 3.8 Photomicrographs of immunohistochemistry of PER1 in human CL throughout the luteal cycle: A: early, B and C: mid-,D: late and E: very late luteal phases. F is the control peptide pre-absorption negative control of the late luteal phase human CL. Various luteal cell types are indicated by colour-coded arrowheads, with the colours corresponding to individual cell types, as follows:- blue: stromal cells, green: theca-lutein cells, orange: granulosa-lutein cells and red: vascular endothelial cells. The scale bar represents 100 μm.

3.3.6 PERIOD2 IMMUNOSTAINING

PER2 was found throughout the luteal phases, in all cell types; in most granulosa-lutein cells and theca-lutein cells. The amount of positively staining cells amongst the fibroblasts, vascular endothelial, perivascular cells and macrophages, was more heterogeneous than with PER1 (Figure 3.9). There may have been a slight trend towards more PER2-negative fibroblasts, vascular endothelial, perivascular cells and macrophages cells in the late luteal than the mid-luteal phase samples. The mid-luteal samples also appeared to have more PER2-negative cells than the early luteal samples. The degree of heterogeneity in the nuclear:cytoplasmic signal strength ratio was therefore also increased over time. This trend however was based on a purely subjective observation. The degree of staining of the cells of each cell type was also very variable. It varied greatly among the individual steroidogenic cells in a single population, with different groups of steroidogenic cells displaying various ratios of nuclear:cytoplasmic staining strength. The fibroblasts associated with blood vessels appeared to cluster loosely into local groups of solely positive or negative cells within each cell type. The vascular endothelial cells around single blood vessels were also largely composed of solely PER2-positive or PER2-negative cells.

The PER2 staining in the granulosa-lutein cells, again demonstrated the unusual staining pattern of cytoplasmic foci, radiating around the nuclei of cells. These foci were again in some, but not all, of the cells and in some, but not all, of the CL samples. The nuclei of the foci-laden cells were often also PER2-positive, though sometimes, the foci appeared without nuclear staining (Figure 3.9 Panel F). The cells containing foci often clustered loosely in local groups of adjoining foci-laden granulosa-lutein cells. These foci-laden cells were however heterogeneously distributed with sometimes, large clusters of foci-laden granulosa-lutein cells, and other times, lone foci-laden cells occurring sporadically amongst granulosa-lutein cells that contained no foci. There were also clusters of granulosa-lutein cells that all contained no foci. This heterogeneity in PER2 localisation in the granulosa-lutein cells was observed in individual samples as

well as between samples, with some samples containing no foci-laden cells at all (Figure 3.9 Panel D). These foci were however found in samples of all the luteal phases examined. The strength of the staining of the foci and of the granulosa-lutein cell nuclei was also very variable, even in the groups of adjoining cells. This heterogeneity in the nuclear:cytoplasmic signal strength ratio was observed in many samples but to various degrees, with no overt patterns emerging over time. This was also true of the other cells types that were examined. The strength of the staining of the cell nuclei in all of the cell types tended to vary, within individual fields of view, to varying degrees between different fields of view and different CL samples. There were again no trends or patterns in the staining of PER2 that could be detected within or between the cell types, which changed between samples or with time.

The sample from the CL that was from a very late phase in the luteal cycle clearly showed cells dying, presumably by apoptosis (Figure 3.9 Panel G). The photomicrograph shows what appear to be healthy PER2-positive cells and apoptotic PER2-negative cells. The control peptide pre-absorption negative control was entirely negative of any specific DAB staining, which indicates that the PER2 staining observed is specific (Figure 3.9 Panel F).

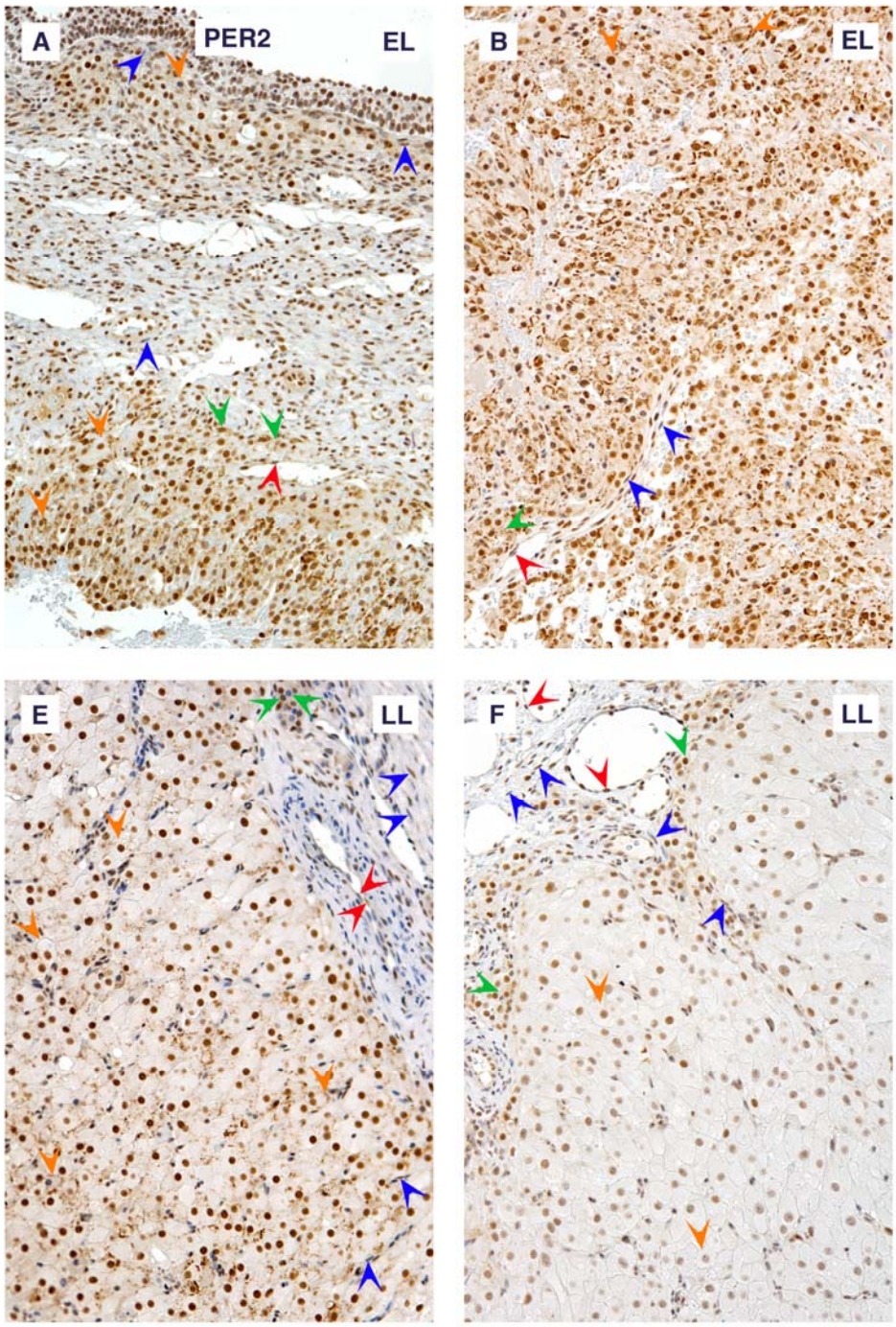
A
PER2
EL
B
EL
E
LL
F
LL

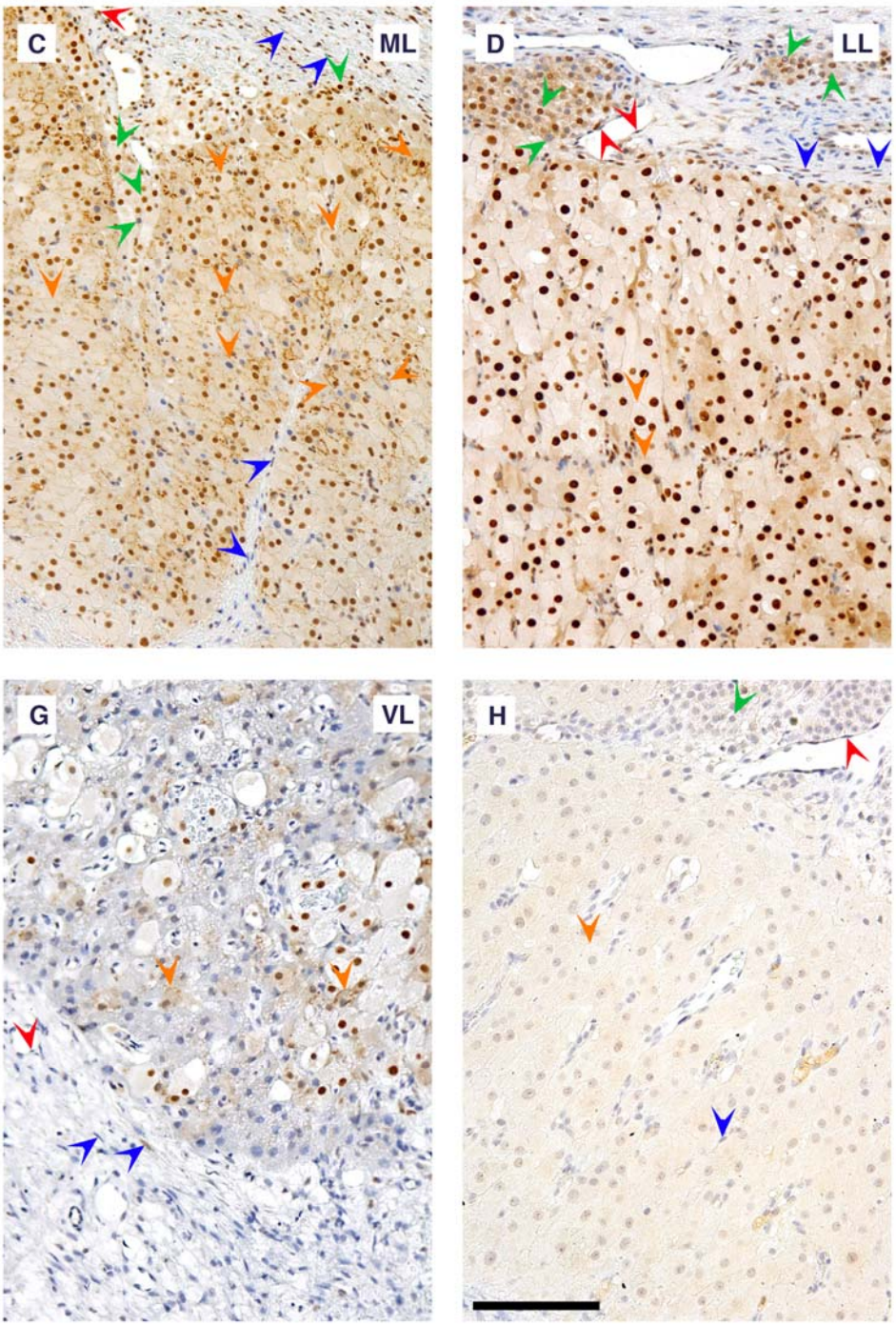

Figure 3.9 Photomicrographs of immunohistochemistry of PER2 in human CL throughout the luteal cycle: A and B: early, C: mid-, D, E and F: late and G: luteolytic luteal phases. H is the control peptide pre-absorption negative control. Various luteal cell types are indicated by colour-coded arrowheads, with the colours corresponding to individual cell types, as follows:- blue: stromal cells, green: theca-lutein cells, orange: granulosa-lutein cells and red: vascular endothelial cells. The scale bar represents 100 μm.

3.3.7 CRY1 IMMUNOSTAINING

There were no trends evident with luteal phase (Figure 3.10). The nuclear:cytoplasmic ratio in the staining of the cells did not appear to vary between the luteal phases. Nuclear staining was often stronger than cytoplasmic staining in all of the cell types in all of the phases. The vascular endothelial cells tended to be CRY1-positive (Figure 3.10 Panels A, B, C and D), although this was not the case in the VL CL (Figure 3.10 Panel E). The very late luteal phase CL was slightly different to the other corpora lutea, in that there appeared to be apoptotic cells. These cells were generally CRY1-negative, while apparently healthy cells were CRY1-positive (Figure 3.10 Panel E). The fibroblasts did not aggregate into like-staining groups, rather they were more heterogeneously intermingled with each other, across the luteal phases (Figure 3.10 Panels C and D). Not all cells were positively stained within each cell type, and the proportion of unstained cells did not appear to vary particularly with luteal phase. The cell types that tended to have the largest proportion of positively stained cells did not differ between the luteal phases. The specificity of the CRY1 staining was confirmed by the negative control that lacked primary antibodies was entirely devoid of staining, but not by the negative control that employed pre-absorption with the control peptide, which was not devoid of staining, although the staining that was present was much more diffuse and generalised (Figure 3.10 Panels F and G).

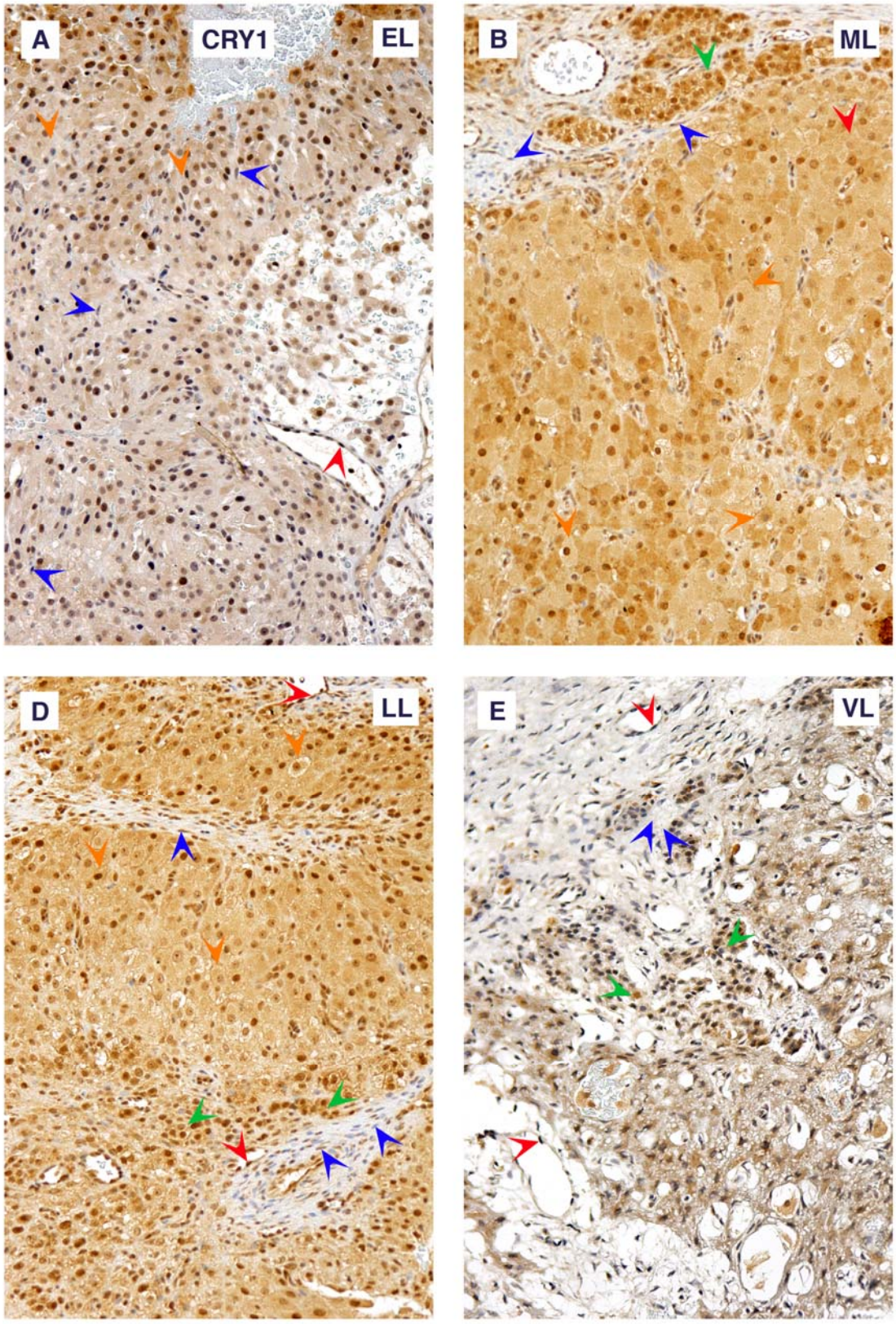
A
CRY1
EL
B
ML
D
LL
E
VL

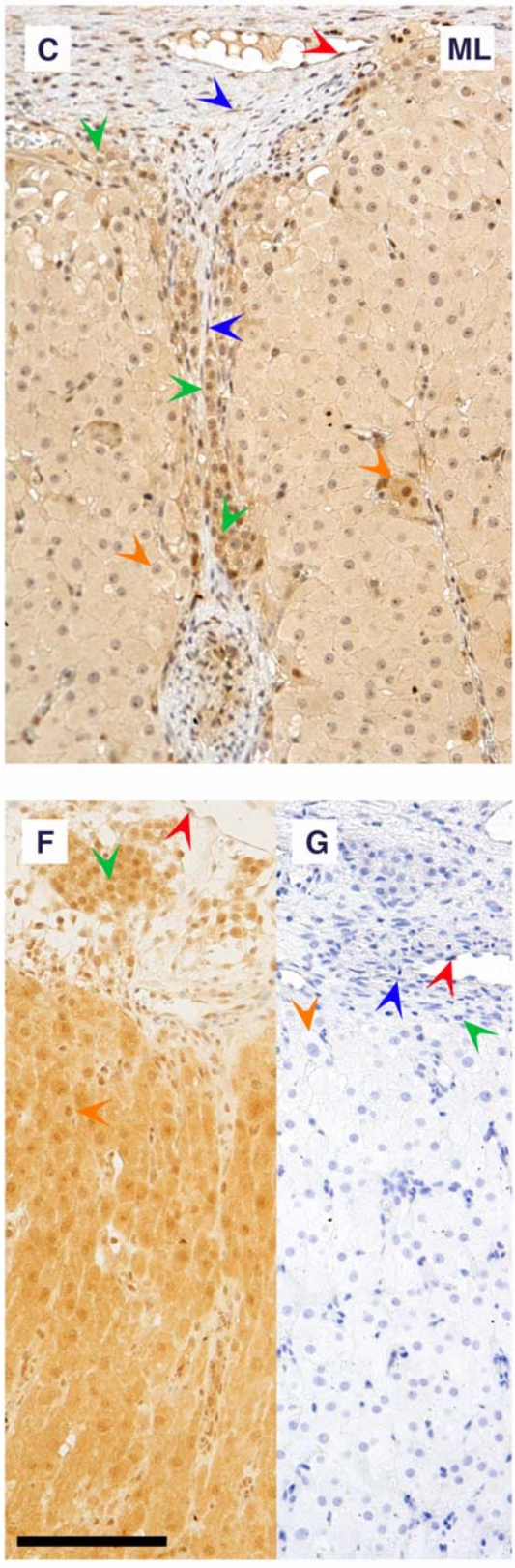

Figure 3.10 Photomicrographs of immunohistochemistry of CRY1 in human CL throughout the luteal cycle: A: early, B and C: mid-, D: late and E: luteolytic luteal phases. F is the pre-absorption negative control and G is the negative control omitting primary antibody. Various luteal cell types are indicated by colour-coded arrowheads, with the colours corresponding to individual cell types, as follows:- blue: stromal cells, green: theca-lutein cells, orange: granulosa-lutein cells and red: vascular endothelial cells. The scale bar represents 100 μm.

3.3.8 CRY2 IMMUNOSTAINING

CRY2 in most of the sections, throughout the luteal phases, was found in all the cell types at all luteal stages, in both nuclear and cytoplasmic compartments (Figure 3.11). The distribution of the staining was very much the same as with CRY1 (Figure 3.10). CRY2 was more diffusely staining in cytoplasmic and nuclear compartments, with mostly stronger nuclear signals than cytoplasmic signals. This was clearly evident with the granulosa-lutein cells. The fibroblasts near the outer stroma tended to show more clearly nuclear staining. Virtually all the cells were CRY2-positive with a few exceptions. The steroidogenic cells contained the occasional, single isolated, non-staining cell while the fibroblasts near the stroma layer and vascular endothelial cells were less infrequently negative (Figure 3.11 Panel D). The non-staining fibroblasts tended not to be isolated and were often observed with other non-staining fibroblasts integrated with positively staining fibroblasts, in a mixed population (Figure 3.11 Panel C). The fibroblasts did not aggregate into like-staining groups, but rather were more heterogeneously intermingled with each other (Figure 3.11 Panels B and D).

The degree of staining in each cell type was less heterogeneous than with BMAL1, PER1 and PER2. The very late luteal phase sample showed apparently healthy cells containing CRY2 and the apoptotic cells lacking CRY2. There were no trends evident with luteal phase. The negative control, which used the control peptide to occupy the primary antibodies, was entirely not immunoreactive (Figure 3.11).

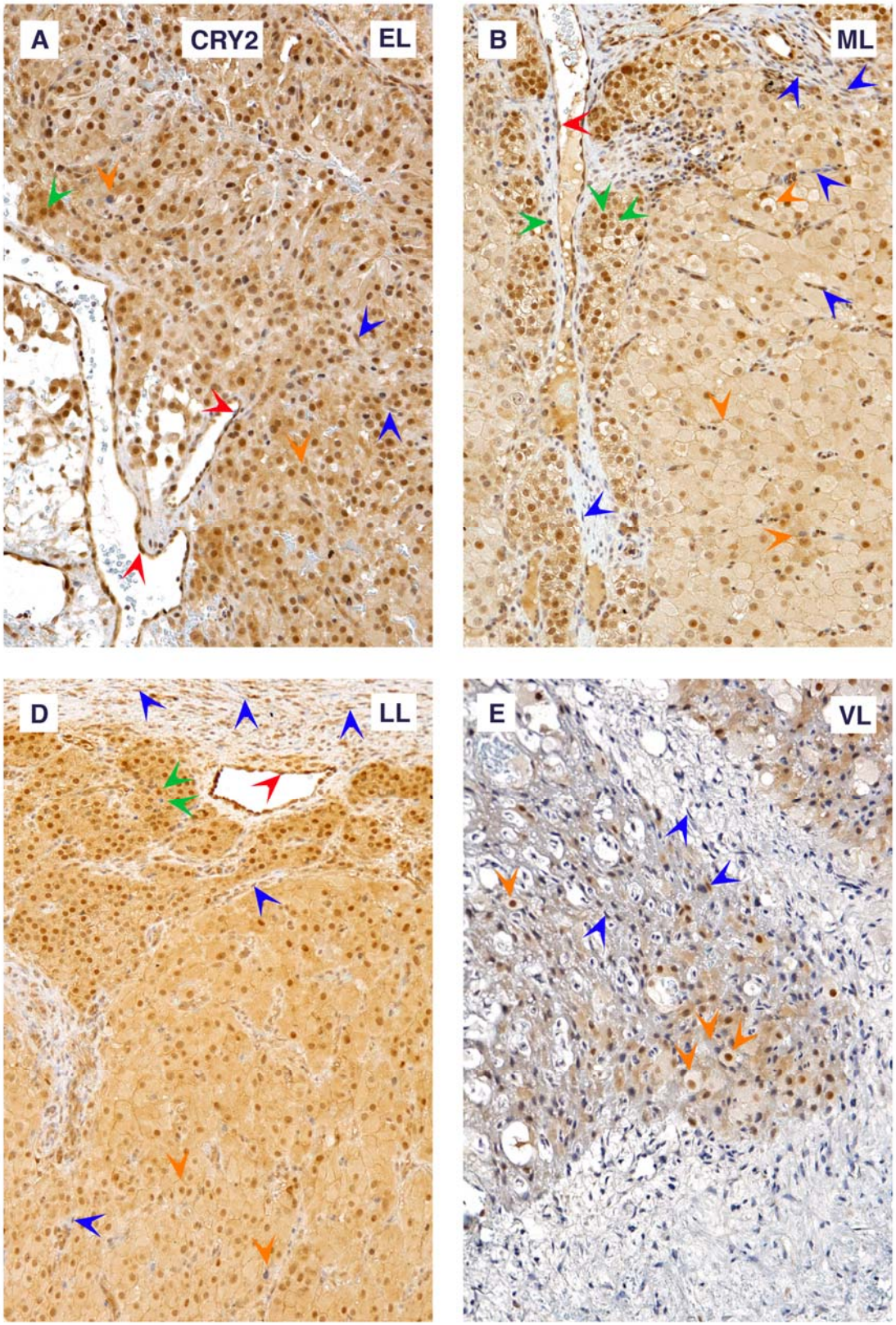
A
CRY2
EL
B
ML
D
LL
E
VL

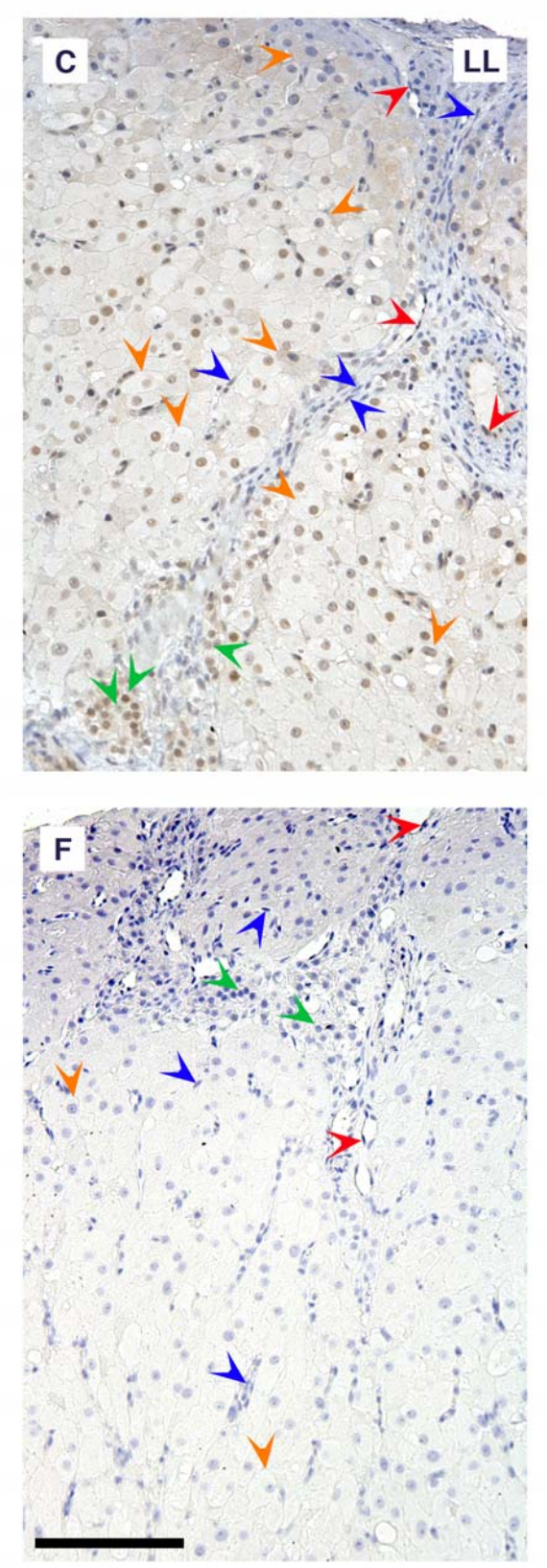

Figure 3.11 Photomicrographs of immunohistochemistry of CRY2 in human CL throughout the luteal cycle: A: early, B: mid-, C and D: late and E: luteolytic luteal phases. F is the control peptide pre-absorption negative control. Various luteal cell types are indicated by colour-coded arrowheads, with the colours corresponding to individual cell types, as follows:- blue: stromal cells, green: theca-lutein cells, orange: granulosa-lutein cells and red: vascular endothelial cells. The scale bar represents 100 μm.

3.3.9 BMAL1 IMMUNOSTAINING

BMAL1 was found in all cell types, across the early, mid and late luteal phases. Granulosa-lutein cells were mostly positive with the odd, isolated negative cells. These cells stained positive most consistently across the luteal lifespan. Theca-lutein cells were also predominantly positive for BMAL1. When they could be distinguished from granulosa cells, in the mid and late luteal phases, it was clear that the theca-lutein cells were less consistent in their staining, both within samples and between samples. There were areas where small groups of theca-lutein cells were negative, often when close to stromal cell layer. Theca-lutein cells could be seen as mostly negative then becoming mostly positive as they were positioned further from the stroma (Figure 3.12 Panel D). This pattern was not dependent on the stage of the luteal phase.

Vascular endothelial cells were also heterogeneously stained between sections, being completely negative around some blood vessels (Figure 3.12 Panel C) while completely positive around other blood vessels (Figure 3.12 Panel D). This was confirmed using co-localisation with CD31 markers. The perivascular cells were also heterogeneously stained, often negative around negative vascular endothelial cells and positive around positive vascular endothelial cells. It was also not uncommon that these perivascular cells were negative around positive vascular endothelial cells. This was also the case in all the luteal phases examined.

The stromally stained were also in some samples mostly not immunoreactive and in other samples, mostly positive, with no clear correlation to luteal phase. The stromal cells could also change the ratio of positive to negative cells, similarly to the theca-lutein cells, as they became increasingly embedded in the steroidogenic cell layers. The number of cells staining also differed between fibroblasts occurring close to the central clot and those occurring close to the outer stroma in some samples.

There was no overt trend in any of the BMAL1 staining over the luteal lifespan. The protein was located both in cytoplasmic and nuclear compartments, though it was predominantly nuclear in the fibroblasts. In one sample, the late-luteal phase CL appeared to be undergoing luteolysis. In this sample, it looked like the apoptotic cells were mostly BMAL1-negative whilst the cells that appeared healthy were BMAL1-positive (Figure 3.12 Panel E). The negative control, which used the control peptide to occupy the primary antibodies, was entirely negative, thus indicating the specificity of the BMAL1-positive staining (Figure 3.12 Panel F).

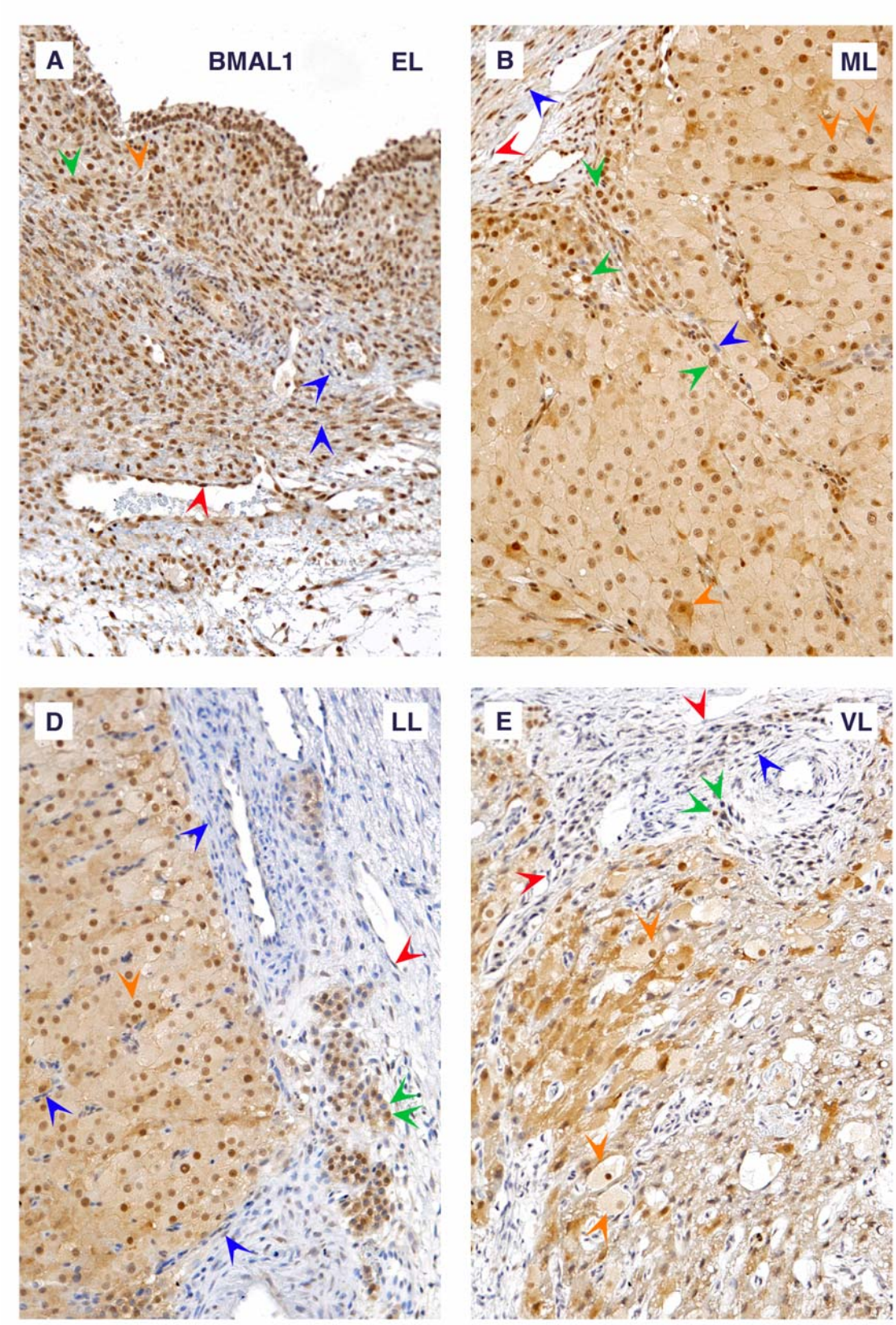
A
BMAL1
EL
B
ML
D
LL
E
VL

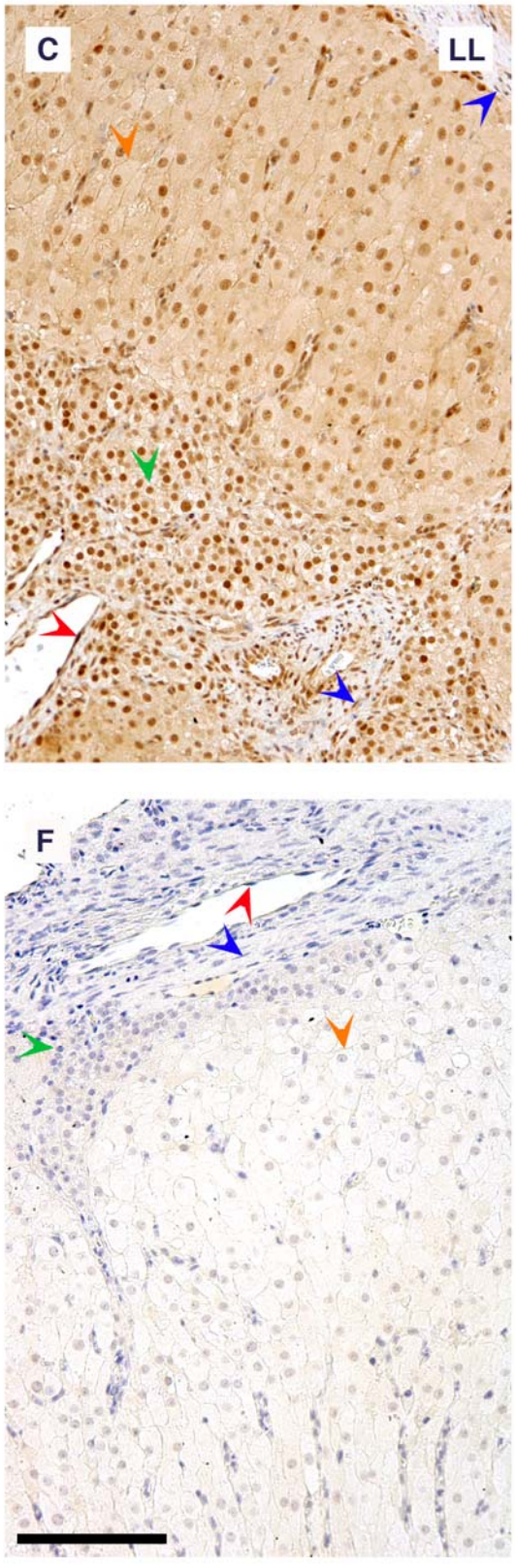

Figure 3.12 Photomicrographs of BMAL1 expression in human CL throughout the luteal cycle: A: early, B: mid-, C: late, D: late and E: very late (Day 14) luteal phases. F is a control peptide pre-absorption negative control of BMAL1 in a human corpus luteum at late luteal phase. Various luteal cell types are indicated by colour-coded arrowheads, with the colours corresponding to individual cell types, as follows:- blue: stromal cells, green: theca-lutein cells, orange: granulosa-lutein cells and red: vascular endothelial cells. The scale bar represents 100 μm.

3.4 DISCUSSION

The clock proteins: PER1, PER2, CRY2 and BMAL1 were all evident in the human CL. They were localised to each of the luteal cell types that could be discerned and were detected throughout the luteal phases. The cell types identified were: theca-lutein cells, granulosa-lutein cells, fibroblasts, vascular endothelial cells and macrophages. A full complement of clock genes and proteins have now also been detected in the CL of rodents, with PER1, PER2 and ARNTL (BMAL1) localising to the steroidogenic cells (Karman and Tischkau, 2006, Boden and Kennaway, 2006, He et al., 2007a, Fahrenkrug et al., 2006).

CRY1 also appeared to be localise to all the discernible cell types in the human CL, throughout the luteal cycle. The detection of CRY1 using IHC was however difficult to validate as the staining of the protein was not removed by pre-absorption with control peptide. This could be because the binding of the antibody was not specific to the CRY1 protein. The pre-absorption was conducted with ten times more control peptide than antibody, which would be more than sufficient to occupy all the antigen-recognition sites of the antibodies so that they would be unable to bind to any CRY1 protein in the tissue. Pre-absorption with fifty times more control peptide than antibody would more likely produce a successful negative result. However, at such high control peptide concentrations, it would highly possible that any failure of antibody binding to CRY1 in the tissue was due to stearic hindrance rather than any specific interaction between the control peptide and the antibody. It is not known whether the individual batches of these polyclonal anti-CRY1 antibodies, reported to work reliably in murine and human tissues, were tested with control peptide pre-absorption before being sold. If not, it may be that the polyclonal IgG population of this particular batch resulted in non-specific binding of the human luteal tissue. In order to test this, it is possible to use an isotype of the IgG to see whether a similar distribution of non-specific binding was observed to that with CRY1. Another explanation, given that these antibodies are polyclonal, is that one or

more of the clonal population bound with greater affinity to the native CRY1 in the luteal tissue than to the control peptide.

Despite these difficulties, the distribution pattern observed with the anti-CRY1 antibody in the human CL, using conventional IHC was very similar to that observed with the anti-CRY2 antibodies. This would be consistent with the idea that these two proteins, derived from genetic homologs, are similar in their structure and function, and also in their localisation in the human CL. The staining was also clearly a direct result of the action of the primary antibody as its omission resulted in the absence of staining. It was therefore possible that the staining observed with the anti-CRY1 antibodies was specific to luteal CRY1 and as such, the use of anti-CRY1 antibodies was included in the runs with conventional IHC. Another antibody that proved difficult to use was the polyclonal anti-CLK IgG. This antibody failed to work in any of the human, ovine and murine tissues tested.

Although the lack of success achieved in visualizing the CLK and CRY1 localisation in the human CL precluded the detection of the full complement of six canonical clock proteins, four of these proteins were successfully and robustly detected. PER1, PER2, CRY2 and BMAL1 were all detected in the human CL, evident in both nuclear and cytoplasmic compartments of all the luteal cell types that could be identified. The distribution of the clock proteins did not show any trends in terms of cellular compartmentalisation, between cells of the same cell type or between CL samples. Neither were there any patterns apparent between the clock proteins of the nuclear versus cytoplasmic compartmentalisation of the proteins. It would have been expected that while the clock proteins belonging to the negative limb of the circadian clock mechanism were nuclear, the clock proteins belonging to the positive limb of the circadian clock mechanism would be cytoplasmic; or *vice versa*. This did not appear to be the case, though direct co-localisation experiments could not be carried out because the species that the antibodies were raised in were the same. The cellular compartmentalisation of each of the clock genes was not uniform in any cell type with

any single CL section or indeed any single field of view. This lack of uniformity made it difficult for any conclusions to be drawn regarding the cellular compartmentalisation of PER1, PER2 and CRY2 versus that of BMAL1, which should be largely opposite to each other. This has not however yet been demonstrated using IHC in existing literature. The presence of the clock proteins in both compartments of the cell however, is consistent with the idea that these proteins function as transcription factors - activating and repressing gene expression in the nucleus, while also being timed to do so in a specifically circadian fashion, by their sequestration in dimerised forms in the cytoplasm. It is therefore very possible that these cells, which are clock protein-positive, possess circadian clocks.

The robust detection of the clock proteins: PER1, PER2, CRY2 and BMAL1, demonstrate that the distribution of the clock proteins was very heterogeneous. It could be argued that the heterogeneity is a result of the method used; that the staining is in fact an artifact of the IHC and that the heterogeneity is an indication of this. This argument can be convincingly rebutted by the very clear absence of staining in the negative controls, particularly where the specificity of the polyclonal IgG antibodies was tested, using pre-absorption with control peptides. The observed heterogeneity could also be argued to support the *bona fide* detection of the clock genes, as they are likely to be distributed in a similar manner and to largely the same degree; functioning, as they do, as components of the circadian clock mechanism that resides and functions autonomously in individual cells.

It seems likely that the individual luteal cells possess circadian clocks. These clocks time the biochemical processes of the cell and can run independently and autonomously from the clocks in the other luteal cells. This would account for the observed heterogeneity, where some cells possess higher nuclear:cytoplasmic ratios in clock protein abundance than other, possibly adjacent, cells. The advantage of running so many separately timed clocks within the same tissue could be the sustained and constant provision of a cellular product, such as progesterone, which is required continuously but

which may be produced in a circadian manner. The expression of the steroidogenic acute regulatory protein (StAR) for example, a rate-limiting enzyme involved in progesterone synthesis, is now known to occur in a circadian rhythm in poultry (Nakao et al., 2007, Ratajczak et al., 2008, Devoto et al., 2001, Devoto et al., 2002). Thus, although the output of each cell is liable to increase and decrease over time, the output of the entire tissue is constant. The continuous provision of progesterone by the CL is vital for the conceptus as the drop in progesterone levels is what initiates parturition at the end of gestation.

This loose or non-existent coupling of the putative luteal cellular clocks is consistent with reports of other peripheral clocks. Tissues outside of the brain, and the SCN in particular, have been observed to possess significantly weaker coupling between cells than in that of the SCN cells, which has been argued to provide greater flexibility in incorporating temporal information from diverse sources, such as the SCN and the food-entrainable oscillator (Balsalobre, 2002, Nagoshi et al., 2004, Stephan, 2002). The flexibility, conferred by loosely coupled clocks within a tissue, is likely to be important in the CL for its function within reproduction, a process that is composed of many parts that are temporally regulated and subject to temporal perturbation by other physiological processes. Stress is well-known to affect the duration of the reproductive cycle as well as the hormonal milieu of the ovary (Kaplan, 2008, Smith et al., 2003, Karsch et al., 2002). As such, the CL needs to be able to function accordingly to any hormonal changes in the ovary and temporal changes in the reproductive cycle. It could be argued that the loosely coupled cellular clocks help enable the luteal tissue to do this, and that the flexibility and responsiveness of the CL to its temporal environment is crucial for its efficient functioning and for its timing, particularly with regard to its lifespan.

No differences in clock protein distribution in the corpora lutea between the early, mid- and late luteal phases were detected. This could indicate that no such differences exist in the human CL; despite the changes that occur in the luteal cells, which differentiate and regress, with time. Alternatively, the changes in clock protein distribution over the lifespan of the human CL were not detected in these studies. This may be because the

windows during which these changes occur are of relatively short duration. This could be supported by the observation that many cells in parts of the section, from the very late stage CL which appeared to be undergoing luteolysis, were clock protein-negative. It stands to reason that the human CL, being a strictly regulated tissue in terms of its lifespan, would form and regress relatively rapidly, ensuring that the majority of its lifespan is spent in a fully functional state. This would be a very efficient use of time; with the processes of luteogenesis and luteolysis occurring in short time windows that are regulated by a luteal clock, which may already exist to regulate the duration of the luteal lifespan.

The human corpora lutea were collected for practical reasons between 10:00 am and 3:00 pm. The circadian changes of these clock proteins could not therefore be assessed, nor could whether the circadian time of sampling be implicated in the heterogeneity observed between the samples. The heterogeneity inherent within the samples however suggests that the time of day may only impact on the degree of inherent heterogeneity rather than on any synchronisation of the cellular clocks with each other within and between the tissues. This impact may however be significant in the regulation of luteal function and reproductive timing.

The local staining pattern of PER2 in some of the granulosa-lutein cells has not been previously reported. No evidence could be found of a similar staining pattern with any other clock protein, or indeed with any other protein in general. The *per2* gene has often been reported to be special amongst the other canonical clock genes in its myriad roles, for example, it is able to function as a tumour suppressor gene and it may play a role in regulating cell division (Albrecht et al., 2007). It may be that the PER2 aggregates observed in some of the granulosa-lutein cells, throughout the luteal lifespan, are related to the mitotic index of these cells, which is known to be particularly high in the granulosa cells of a maturing follicle. However, their persistence throughout the luteal phases in the absence of ongoing proliferations argues against this. PER2 may also function in the granulosa-lutein cells in an extra-circadian clock role, which may

requires it to aggregate in cytoplasmic foci. This aggregation of the PER2 could be the encapsulation of the protein in vesicles, emanating from the Golgi apparatus, where proteins are post-translationally modified and packaged. The vesicles are however unlikely to be excretory as no PER2 was detected outside of the luteal cells. PER2 is thus an unlikely candidate for signalling between cells, unless the PER2 secreted exists in a truncated form or in a tertiary conformation that rendered it undetectable by the anti-PER2 antibody in IHC.

Ultimately, these studies have revealed conclusively so far, is that the clock proteins: PER1, PER2, CRY2, BMAL1 and possibly CRY1 are present in the human CL, and that they are present in all the discernible luteal cell types, throughout the lifespan of the CL.

In summary, this chapter demonstrated for the first time that:

1. the canonical clock proteins: PER1, PER2, CRY2, BMAL1 and possibly CRY1 were expressed in the human corpus luteum;

2. this expression was localised to multiple luteal cell types including the steroidogenic cells, fibroblasts, vascular endothelial cells and macrophages; with the most consistent and strongest staining in the theca-lutein and granulosa-lutein cells;

3. the clock proteins are expressed throughout the human luteal lifespan;

4. the localisation of the clock proteins was heterogeneous, both spatially and temporally, in the human CL.

The presence of the clock proteins from both limbs of the circadian clock mechanism indicate that a circadian clock may potentially exist in the cells of the human CL. Using IHC methods, it was not possible to address the question of whether the overall clock protein levels changed across the luteal cycle in the human CL. In order to do this, clock

gene mRNA expression would be measured quantitatively in the human CL samples used in this study.

4 CLOCK GENE mRNA EXPRESSION IN THE HUMAN CORPUS LUTEUM THROUGHOUT THE LUTEAL LIFESPAN

4.1 INTRODUCTION

The clock proteins: PER1, PER2, CRY2 and BMAL1 have been observed in the human CL. These proteins belong to both the positive and the negative limbs of the circadian clock mechanism, and localise to the same cell types; suggesting that a functional cell-based circadian clock exists in these cells. If this were the case, these cell-based circadian clocks are likely to be involved in temporally regulating the functional processes of the CL, including its relatively fixed 14-day lifespan. In order to elucidate more information in support of this hypothesis, quantitative measurement of the clock gene mRNA in human corpora lutea, sampled from across the luteal cycle was performed. These are the same corpora lutea that were used in the previous chapter that are therefore known to express the clock genes, at a protein level. The quantitative molecular method will be tested to ensure that it is sensitive enough to detect any changes in clock gene expression by applying it to analyse the clock gene expression in cultured luteal fibroblast-like cells, derived from pre-ovulatory follicles under an assisted reproduction protocol, which is likely to be circadianly rhythmic. If no rhythm is detected, other cells well-known to express clock genes in a robustly circadian manner will be used.

Overt changes were not observed in the expression of the clock proteins throughout the luteal lifespan. This does not however indicate that there would be a corresponding lack of change in the expression of the clock genes, when measured using the messenger RNA (mRNA) concentration. It has been widely reported that many post-transcriptional and post-translational mechanisms exist, which can alter the temporal pattern of protein expression in cells from that of their cognate mRNA expression (Okamura, 2003, Zwiebel et al., 1991). Furthermore, there has been report

of clock protein expression differing from that of the clock gene in cells across 24 hours (Jilg et al., 2005). Therefore, it is possible that, changes exist that may be detected in the mRNA levels of the human CL across the luteal cycle. It could even be said to be very likely, as there is clearly a requirement for temporal regulation of the CL as a whole tissue, in order to time its lifespan and regression; a regulation that does not appear to be provided by change in the clock proteins and therefore may well be provided by change at the level of the actual gene transcription. It is also likely that any changes that exist that direct the timing of the luteal lifespan will be more easily evident when examining the CL as a whole, rather than by examining it, cell by cell or cell type by cell type. Thus, there is an emergent property related to co-ordination of luteal timing and luteal regression, which may arise from the mass of luteal cells assembled in an intact tissue.

It is therefore proposed that the level of global clock gene expression of the human CL changes across the luteal cycle, whereby the advent of luteolysis is triggered by the gradual and global loss or gain in clock gene expression as the CL ages.

Therefore, this chapter aims:

1. to establish a positive control by measuring the mRNA expression of *per1*, *per2*, *per3*, *cry1*, *cry2*, *bmal1*and *clk* in luteal fibroblast-like cells;

2. to determine whether global mRNA expression of *per1*, *per2*, *per3*, *cry1*, *cry2*, *bmal1*and *clk* changed over the luteal phase.

4.2 MATERIALS AND METHODS

4.2.1 ETHICAL APPROVAL FOR CORPORA LUTEA COLLECTION

Ethical approval was obtained as described in the previous chapter from the Reproductive Medicine Subcommittee of the Lothian Medical Ethics Committee and the COREC on two further occasions. The collection of CL from patients with informed consent was again performed by Dr W. Colin Duncan as described in the previous chapter.

4.2.2 ETHICAL APPROVAL FOR FOLLICULAR CELL COLLECTION

The collection of ovarian and follicular cells from patients undergoing assisted conception at the Edinburgh Fertility and Reproductive Endocrine Centre (EFREC) was separately approved by the Reproductive Medicine Subcommittee followed by further approval by COREC. Informed consent was obtained from all patients and their consultant gynaecologists, notably Dr K. Joo Thong.

4.2.3 SAMPLING HUMAN CORPORA LUTEA

Human CL tissues were collected as previously described, with 8 early luteal phase corpora lutea obtained 1 – 5 days after the LH surge, 12 mid-luteal phase corpora lutea obtained to 6 – 10 days after the LH surge and 6 late luteal phase corpora lutea obtained from 10 – 14 days after the LH surge. Some of the tissue pieces were used for RNA extraction and some were used for immunohistochemistry.

4.2.4 SAMPLING HUMAN FOLLICULAR FIBROBLASTS

With patient consent, follicular fluid was collected from women undergoing transvaginal oocyte retrieval for *in vitro* fertilisation after ovarian stimulation using a standard procedure. Briefly, a long-protocol stimulated cycle was followed, using intranasal naferelin (Pharmacia Biotech, Milton Keynes, UK), a gonadotrophin-releasing hormone analogue for down-regulation and daily purified gonadotrophins (Menopur, Ferring Pharmaceuticals, Langley, UK) for ovarian stimulation. When at least three follicles reached 18 mm diameter, 10 000 IU hCG was administered in order to mimic the pre-ovulatory LH surge. The follicular cells were thus luteinised. Transvaginal oocyte collection was performed under sonographic guidance 35 hours later (Duncan et al., 2005b, Stamouli et al., 1996). The aspirate will contain non-dividing LGCs short-lived in culture and fibroblasts that divide and can be propagated to monolayers.

4.2.5 CELL CULTURE OF LUTEAL FIBROBLAST-LIKE CELLS

The cells were derived as described previously (Duncan et al., 2005b, Myers et al., 2007a, Dickinson et al., 2008). Briefly luteal fibroblasts were obtained from follicular aspirates after the removal of oocytes. Individual follicles were not distinguished, and all follicular fluid from the same individual was pooled and centrifuged at 1500 rpm for 10 min. The cells were resuspended and washed three times with PBS. The cells were then resuspended in culture medium (Dulbecco's Minimum Essential Medium/Ham's F-12 mixture, Invitrogen Life Technologies, Inc., Gaithersburg, MD), supplemented with 2 mmol l^{-1} glutamine (Sigma, Dorset, UK), 6.25 mg l^{-1} insulin, 6.25 mg l^{-1} transferrin, 6.25 µg l^{-1} selenious acid (Roche, Welwyn Garden City, UK), 2.5 mg l^{-1} amphotericin, 50 mg l^{-1} penicillin, 60 mg l^{-1} streptomycin and 10% fœtal bovine serum (Sigma, Dorset, UK), then transferred to a culture flask and incubated overnight at 37^{o}C in 5% CO_2 in air. The media was changed the next day, after which it was only changed weekly. The cells were passaged every two weeks thus removing granulosa cell and other debris and allowing the population to be split into separate

flasks. The cells are allowed to grow to confluence over 5-6 weeks, during which time, the luteinised granulosa cells would have disappeared.

The fibroblast-like cells were used as a cellular control as they reliably modelled luteal fibroblasts. This was previously demonstrated when these fibroblast-like cells were shown to immunostain uniformly. They were 3βHSD-negative, CD31-negative, alpha-smooth muscle actin (α-SMA)-positive, and leucocyte common antigen (LCA)-negative. Heterogeneous staining had been seen in the luteinised granulosa cell cultures. After 6-8 days of culture, 10.1% (range, 5.4–12.3%) of the cells were 3βHSD negative, 6.9% of cells (4.3–11.1%) were α -SMA positive, 5.7% of cells (3.4–8.3%) were CD-31 positive and 5.95% of cells (2.7–9.3%) were LCA positive. This confirmed that there was only very low levels of contamination by luteinised granulosa cells in the fibroblast-like cell cultures, once other cell types had been separated (Duncan et al., 2005b). Fibroblasts were used as luteal steroidogenic cells are terminally differentiated and do not divide.

4.2.6 TOTAL RNA EXTRACTION II

Total RNA was purified from homogenised tissues using TRI Reagent™ RNA Isolation Reagent (Sigma-Aldrich, Poole, Dorset, UK) according to the standard method published by Chomczynski and Sacchi (Chomczynski and Sacchi, 1987). Briefly, 50-100 mg of each corpora lutea was homogenised with a pestle in sterile 2 ml microfuge tubes with 500 µl TRI Reagent. The remaining 500 µl of TRI Reagent was added to the tissue homogenate. These were then left to incubate on ice for 5 min, in order to allow the complete dissociation of nucleoprotein complexes.

Total RNA was purified from the fibroblasts using TRI Reagent™ RNA Isolation Reagent (Sigma-Aldrich, Poole, Dorset, UK) according to the standard method published by Chomczynski and Sacchi (Chomczynski and Sacchi, 1987). The cells were rinsed with phosphate-buffered saline and 1 ml of TRI® Reagent added. The cells were quickly scraped off the plates and transferred with the TRI® Reagent into

sterile microfuge tubes. They were stored at -70°C until batch extraction of the RNA, when they were thawed.

Phase separation was then achieved by the addition of 0.2 ml chloroform (Fisher Scientific, UK), mixing the samples well by inverting the tubes and then leaving the samples to stand for 1 hour on ice. The samples were then centrifuged at 12 000 x *g* for 15 min at 4°C. This separates the mixture into 3 phases: an organic phase containing the proteins, an interphase containing DNA, and an aqueous phase containing RNA. The RNA was carefully pipetted off, without any DNA contamination, and transferred to a 2 ml microfuge tube. The RNA was precipitated by the addition of 0.5 ml propan-2-ol (isopropanol) which was mixed well, then left to stand for 5 min at room temperature. The RNA was pelleted by centrifuging at 12 000 x *g* for 10 min at 4°C. The supernatant was discarded and the RNA pellet washed twice with 1 ml of 75% ethanol (dissolved in DEPC-treated water), vortexed then centrifuged at 7 500 x *g* for 5 min at 4°C. The supernatant was discarded and any remaining ethanol allowed to evaporate completely. The pellet was then resuspended by pipetting in 50 µl of DEPC-treated water.

As the RNA was intended for use in quantitative real-time PCR, it was important to remove any contaminating DNA. This was achieved by treating the RNA with 1 U deoxyribonuclease I (Ambion, Inc., Applied Biosystems, Warrington, UK) per 1 µg RNA for 30 min at 37°C. The deoxyribonuclease (DNase) cleaves the DNA at phosphodiester bonds in its backbone, rendering it useless as a template for PCR. The DNase reaction was terminated by the addition of DNase Stop Solution containing 50mM EDTA, 1.5M NaOAc (pH 5.2) and 1% SDS. The DNase was inactivated by denaturing at 70°C for 10 min. The DNase would then be unable to cleave newly-formed DNA in the RT-PCR reaction.

The total RNA yield was then quantified using a small aliquot of each sample. The optical density or absorbance of the RNA was measured using ultraviolet spectrophotometry on a GeneQuant™ *pro* RNA/DNA Calculator (Amersham Pharmacia Biotech, Little Chalfont, UK). The absorbance at 260 nm was used to automatically calculate the RNA concentration in the following equation:

RNA concentration = $Absorbance_{260}$ x Dilution factor x 40 µg/ml

because 40 µg/ml of RNA has an absorbance at 260 nm of 1. The ratio of absorbance between the 260 nm and 280 nm wavelengths provided an indication of RNA purity. The RNA was stored at – 80°C until use.

4.2.7 MESSENGER RNA PURIFICATION

Some of the total RNA was purified further. QuickPrep™ mRNA Purification Kit (Amersham Pharmacia Biotech, Little Chalfont, UK), which employed oligodeoxythymidylate (oligo(dT))-cellulose spin columns, were used to isolate messenger RNA (mRNA) from ribosomal and other ubiquitous small RNA. Messenger RNA generally contains long tracts of polyadenylate (poly(A^+)) at its 3' end. This allows the purification of these poly A^+ RNA away from other nucleic acids by hybridisation of the poly(A^+) 'tails' to oligo(dT) in oligo(dT)-cellulose spin columns.

Total RNA (1.25 mg) from each sample was purified for poly(A^+) RNA. The oligo(dT)-cellulose spin columns were prepared by inverting several times to resuspend the resin in the columns. The top and bottom closures of the spin columns were removed and the columns placed upright in sterile 15 ml centrifuge tubes. They were then centrifuged at 350 x *g* for 2 min at room temperature. The columns were removed from the centrifuge tubes and the tubes and eluted liquid discarded. The bottom closure was replaced onto the drained columns. The columns were placed into sterile 15 ml tubes containing open sterile 1.5 ml screw-top microfuge tubes, so that the tip at the bottom of the column is in the opening of the microfuge tube. The tubes were then placed upright in a rack.

Elution buffer containing 10 mM Tris-HCl (pH 7.4) and 1 mM EDTA was added to the total RNA samples so that each sample constituted 1 ml. The samples were incubated at 65°C for 5 min then chilled on ice for 5 min. Sample Buffer containing 10 mM Tris-HCl (pH 7.5), 1 mM EDTA and 3 mM NaCl (0.2 ml) were added to the

samples and mixed gently before placing on ice. The samples were then added to the top of the column bed and allowed to enter the resin under gravity. The bottom closure of the column was removed and the columns centrifuged at 350 x *g* for 2 min at room temperature.

The poly(A^+) RNA on the columns were washed with high and low salt washes. High Salt Buffer (0.25 ml) containing 10 mM Tris-HCl (pH 7.4), 1 mM EDTA and 0.5 M NaCl was added to each column. The columns were centrifuged at 350 x *g* for 2 min at room temperature. The high salt wash was then repeated with a second 0.25 ml of High Salt Buffer. The same was then repeated twice with the Low Salt Buffer, which contained 10 mM Tris-HCl (pH 7.4), 1 mM EDTA and 0.1 M NaCl.

The 1.5 ml microfuge tubes containing eluted wash buffer were discarded and replaced with new sterile 1.5 ml microfuge tubes. The poly(A^+) RNA bound to the column is eluted by the addition of 0.25 ml Elution Buffer, pre-warmed to 65^{o}C, followed by centrifugation at 350 x *g* for 2 min at room temperature. Subsequently, 0.75 ml of eluate should be obtained from the elution and this was repeated twice. A total of 2.25 ml of eluant containing poly(A^+) RNA was extracted from each sample of total RNA. The RNA was then centrifuged at maximum speed in a bench microcentrifuge for 1 min to remove any residual cellulose. The supernatant containing the poly(A^+) RNA was transferred into sterile 1.5 ml microfuge tubes, quantified using a standard spectrophotometry method and stored at -80^{o}C. The pellet was discarded.

4.2.8 PREPARATION OF COMPLEMENTARY DNA BY REVERSE-TRANSCRIPTION

The RNA was batch reverse transcribed using GeneAmp® RNA PCR Kit (Applied Biosystems, Warrington, UK) with random hexamers. Total RNA (200 ng) was added to a reaction mix containing 5.5 mM $MgCl_2$, 2.5 µM random hexamers, 500 µM of each deoxy-NTP, 0.4 U μl^{-1} RNase inhibitor, and 1.25 U μl^{-1} Multiscribe reverse

transcriptase (Applied Biosystems, Warrington, UK). The samples were incubated at room temperature for 10 min. They were then heated to 42°C for 60 min in order to provide the optimum temperature for enzymatic action. The reaction was then stopped and the enzyme denatured by incubating at 95°C for 10 min. Two types of negative control were used. One involved reactions performed on 3-5 randomly selected test samples with RT mix that was extracted prior to the addition of the reverse transcriptase. The other involved reactions with RT mix that omitted the template RNA, which was replaced by the same volume of RNase-free water. The resulting cDNA was stored short-term at 4°C or long-term at -80°C until subsequent PCR.

4.2.9 PRIMER DESIGN

Gene sequences were obtained from the National Center for Biotechnology Information (NCBI) GenBank nucleotide database, available online http://www.ncbi.nlm.nih.gov/. This database lists sequences by ascribing them Accession Numbers. Primers were designed as standard using primer design software. The software used was Primer3, available online at www-genome.wi.mit.edu/cgibin/primer/primer3_www.cgi. Primers were checked for specific binding by using the NCBI Basic Local Alignment Search Tool (BLAST), available online at http://blast.ncbi.nlm.nih.gov/Blast.cgi. This tool enables the identification of regions that are the same or similar between nucleotide sequences. It does this by mining genome and other nucleotide databases which are published online, using a search-term sequence. To minimise amplification of genomic DNA, the forward and reverse primers for each gene were chosen from different exons where possible. The sizes of the polymerase chain reaction (PCR) products were designed to be less than 250 bp to optimise the real-time quantification of the amplified DNA during reverse-transcribed polymerase chain reaction (RT-PCR). The RT-PCR technique quantifies the PCR products in real-time, using fluorescent SYBR Green I dye, that fluoresces when it is incorporated into newly-made DNA. The amplicon sizes must therefore be designed to be approximately the same, between the gene of interest and the gene standard, in order that kinetics within each amplification

reaction is relatively the same; so that the quantification of the PCR products are comparable between the various reactions.

As many of the clock genes have different RNA transcripts, the primer sequences were compared to these transcript sequences. This ensured that the PCR products would be of consistent size and that, as much as possible, the total transcript expression of each gene would be measured. The primers were also checked to see if they were intron-spanning. This would be a further way of ensuring the amplification of only the template DNA derived from RNA. Fully annotated transcript sequence data was obtained as standard from the Ensembl database using the Ensembl Genome Browser, available online at http://www.ensembl.org/index.html.
The *per1* primers did not span an intron but the PCR product did, according to the Ensembl Gene Report for ENSG00000179094. Sections of both *per1* transcripts (Ensembl Gene Report for ENST00000354903 and ENST00000317276) would be amplified, producing products that were 133 base pairs (bp) in size. The *per2* reverse primer and PCR product were both intron-spanning, according to the Ensembl Gene Report for ENSG00000179094. Sections of all three *per2* transcripts (Ensembl Gene Report for ENST00000254657, ENST00000254658 and ENST00000355768) would be amplified, producing products that were 154 bp in size.

Neither the *per3* primers nor the PCR product were intron-spanning, according to the Ensembl Gene Report for ENSG00000049246. Sections of four *per3* transcripts (Ensembl Gene Report for ENST00000168666, ENST00000361923, ENST00000377527 and ENST00000377532) would be amplified, producing products that were 150 bp in size. A fifth, short-sequence transcript however was not amplified, according to ENST00000377541. It took two attempts to design and optimise primer pairs for this gene.

The *cry1* primers did not span any introns but the PCR product did, according to the Ensembl Gene Report for ENSG00000008405. Sections of, only one of the two, *cry1* transcripts (Ensembl Gene Report for ENST00000008527) would be amplified, producing 128 bp products. The other transcript (ENST00000319645) was not amplified. It took two attempts to design and optimise primer pairs for this gene. The *cry2* primers did not span an intron but the PCR product did, according to the

Ensembl Gene Report for ENSG00000121671. Sections of the only known *cry2* transcript (Ensembl Gene Report for ENST00000263762) would be amplified, producing 142 bp products.

The *bmal1* (also known as the *aryl hydrocarbon receptor nuclear translocator-like protein 1* (*arntl*) gene) forward primer was intron-spanning, according to the Ensembl Gene Report for ENSG00000133794. Sections of all three *bmal1* transcripts (Ensembl Gene Report for ENST00000256172, ENST00000339640 and ENST00000361003) would be amplified, producing 175 bp products. Neither the *clk* primers nor product were intron-spanning, according to the Ensembl Gene Report for ENSG00000134852. Sections of all three *clk* transcripts (Ensembl Gene Report for ENST00000309964, ENST00000381322 and ENST00000381325) would be amplified, producing 147 bp products. It took three attempts to design and optimise primer pairs for this gene.

In order to perform real-time quantitative PCR, a standard endogeneous control was required. This would be a gene which is constantly expressed at constant levels in the tissue or cells of interest. The quantification of this gene expression provides a baseline for comparing the quantification of the genes of interest, which were expected to fluctuate. The gene chosen was the, constitutively expressed, housekeeping gene: *glucose 6-phosphate dehydrogenase* (*g6pdh*). Its PCR products but not primers were intron-spanning, according to the Ensembl Gene Report for ENSG00000160211. Sections of three of the four *g6pdh* transcripts (Ensembl Gene Report for ENST00000291567, ENST00000343440 and ENST00000369624) would be amplified, producing 215 bp products. One of the four transcripts would not be amplified (Ensembl Gene Report for ENST00000369620).

The primer sequences and corresponding gene sequences are listed below (Table 4.1):-

GENE	ACCESSION NUMBER	FORWARD PRIMER 5'-3'	REVERSE PRIMER 5'-3'
per1	NM_002616	cagcagttccattgcctaca	gagctctcgaagtgctgtca
per2	AB002345	gccaagtttgtggagttcct	cactgacacggcaaaagaaa
per3	AB047686	gatttcccaccttccagtga	actcaaaagggcaacagcac
cry1	NM_004075	ttggaaaggcatttggaaag	cgacatgacaaacaaccaaa
cry2	AB014558	tcctgccgcctcttctacta	ggtcaaacctggggttgtt
bmal1	AF070917	ctccaggaggcaagaagattt	ctactt*gatccttggtcgttg
clk	AB002332	ccagaaggggaacattcaga	tggctcctttgggtctattg
g6pdh	NM_000402	cggaaacggtcgtacacttc	ccgactgatggaaggcatc

* t was added to the sequence listed with the accession number to correspond with human *bmal1* (also known as *arntl*)

Table 4.1 The gene sequence accession numbers and PCR primer sequences for the clock genes.

The primers were synthesised by MWG-AG Biotech (Milton Keynes, UK). All the PCR products were sequenced using ABI PRISM Big Dye Terminator Sequencing Kits (Applied Biosystems) to confirm that the sequence of the PCR-amplified fragments matched that of the gene to which the primers were designed.

4.2.10 CONVENTIONAL POLYMERASE CHAIN REACTION

Before real-time quantitative gene expression analysis was performed, the primers were tested using conventional PCR. Briefly, 1 µl of cDNA was added to a PCR mix containing 0.25 U µl-1 of thermostable *Thermus aquaticus* DNA polymerase (*Taq*) (Promega, Southampton, Hampshire, UK), 0.5 µM each of forward and reverse primer, 0.2 mM deoxynucleotide triphosphates (dNTPs), 0.1% Triton X-100 detergent, 50 mM potassium chloride (KCl), 10 mM Tris-HCl, 2.5 mM $MgCl_2$ and nuclease-free water to achieve a final reaction volume of 10 µl. Complementary DNA template from cultured luteal fibroblast-like cells was used as an exogenous positive control, known to express clock genes. Negative controls employed the same PCR mix but substitute nuclease-free water for the template cDNA. The tubes

containing test samples mixed with PCR mix were briefly vortexed then collected by brief centrifugation in a bench microcentrifuge. Mineral oil was then laid over the mixes in each tube to minimise the dispersion of the reaction mix by evaporation and condensation during the PCR. The samples were then placed in a DNA Engine Peltier Thermal Cycler PTC-200 (MJ Research, Inc., Watertown, MA) and incubated at 95^{o}C for 5 min to activate the polymerase. The PCR then consisted 35 cycles of denaturation at 95^{o}C for 30 s, annealing at the optimal primer pair temperature for 90 s and elongation at 72^{o}C for 90 s, followed by a final denaturation step at 72^{o}C for 10 min. The optimal PCR annealing temperatures are listed below alongside corresponding PCR product sizes (Table 4.2):-

GENE	ANNEALING TEMPERATURE (^{o}C)	PRODUCT SIZE (bp)
per1	64	133
per2	64	154
per3	62	150
cry1	60	128
cry2	61	142
bmal1	56	175
clk	62	147
g6pdh	62	215

Table 4.2 Conventional PCR primer-pair annealing temperatures and product sizes.

The PCR products were visualised using electrophoresis to separate the DNA fragments on a 1% agarose gel submerged in a 1x Tris-acetate-EDTA (TAE) buffer with 100 volts (V) for 75 min. The agarose gel contained 0.002% ethidium bromide, which intercalates into the DNA and can be observed and photographed fluorescing under ultraviolet (UV) transillumination. Products were verified using a 100-bp DNA ladder composed of several reference size standards of 100*x* base pairs as well as by sequencing.

4.2.11 REAL-TIME QUANTITATIVE REVERSE TRANSCRIBED POLYMERASE CHAIN REACTION USING THE ROCHE LIGHTCYCLER® SYSTEM

Real-time quantitative reverse-transcribed polymerase chain reaction (qRT-PCR) was performed using, using a two-step RT-PCR protocol, in the Roche LightCycler® system, which was comprised of the carousel-based LightCycler® 2.0 instrument with reagents from the LightCycler® FastStart Kit. This system follows the standard principles behind real-time qRT-PCR, using the incorporation of the fluorescent SYBR Green I binding dye into double-stranded DNA during the PCR transcription process to monitor the amount of template amplification. The procedure involved adding the LightCycler FastStart polymerase enzyme to the LightCycler FastStart Reaction Mix SYBR Green I solution. This mixture was then referred to as the LightCycler FastStart Reaction Mix SYBR Green I and contained 'hot-start' FastStart *Taq* DNA polymerase buffer, DNA double-strand specific SYBR Green dye and 1 mM magnesium chloride ($MgCl_2$). Additional $MgCl_2$ was added to achieve the magnesium ion (Mg^{2+}) concentration that was optimal for each of the clock gene primer pairs.

GENE	ANNEALING TEMPERATURE (^{O}C)	MAGNESIUM CONCENTRATION (mM)	MEASURE (^{O}C)	PRODUCT SIZE (bp)
per1	64	3	84	133
per2	64	4	83	154
per3	62	3	76	150
cry1	60	5	77	128
cry2	61	3	82	142
bmal1	56	4	80	175
clk	62	3	76	147
g6pdh	62	3	76	215

Table 4.3 Real-time qRT-PCR primer-pair annealing temperatures, Mg^{2+} concentrations, measurement temperatures and product sizes.

The annealing temperature and Mg^{2+} concentrations for each primer pair were optimised using either human placental cDNA or previously extracted and characterised human luteal cDNA (Table 4.3). These optimisation PCRs were

performed using Thermo-Start™ *Taq* DNA polymerase (ABgene Ltd, Epsom, UK) in a DNA Engine Peltier Thermal Cycler PTC-200 (MJ Research, Inc., Watertown, MA). Eight PCRs of each primer pair, using the gradient annealing temperature facility of the cycler, were performed to observe the PCR efficiency of annealing temperatures between 52^{o}C and 68^{o}C. PCR products were examined using gel electrophoresis with UV transillumination of ethidium bromide in the DNA. The brightest, most well-defined single band of PCR product corresponding to the expected size was an indication of the optimal PCR conditions. The presence of single bands of the expected size along with low amounts of primer-dimer further confirmed the specificity of the primers.

Magnesium concentrations of 3-5 mM were used to identify the optimal Mg^{2+} concentrations for the most efficient PCR reaction using the LightCycler® 2.0 instrument (LightCycler). The DNA amplification step enabled the identification of the optimal temperature required for quantifying the level of gene expression. This meant that the artefact caused by background fluorescence from non-specifically amplified DNA was minimised. A DNA melting curve analysis could then be performed at the optimal quantification temperature. A single DNA melting curve peak indicated a single real-time qRT-PCR amplified product. This was used to confirm the specificity of the primers.

A standard curve was required for quantification of the gene expression from the test samples. It was generated using serial dilutions of standardised cDNA, derived from human placental RNA, in real-time qRT-PCR in the LightCycler. The cDNA was derived from RNA of known concentration. A dedicated LightCycler program (version 3.3) using the second derivative maximum method (Kubista et al., 2006).

Briefly, 1 µl cDNA was added to a PCR mix consisting of 1 µl each of the forward and reverse primers, 1 µl LightCycler FastStart Reaction Mix SYBR Green I solution containing SYBR Green, 3 mM Mg^{2+} and LightCycler FastStart polymerase, 5 µl nuclease-free water and any extra Mg^{2+} that was required. The final reaction volume was 10 µl. The reaction mixes and test samples were carefully transferred into LightCycler capillary tubes, which were then closed. The tubes were briefly

centrifuged then loaded into the LightCycler. The PCR was then implemented using the standard LightCycler protocol.

The PCR product concentrations were automatically calculated for each sample using the dedicated LightCycler software. It compared the sample threshold cycle (C_T) number to those of the standard curve. As the standard curve was produced using cDNA derived from RNA of known quantity, the test sample RNA levels could thus be extrapolated by comparison with the standard curve. In all cases the level of gene expression within the samples fell within the boundaries of the corresponding standard curve. All the samples were analysed in duplicate and assay variation was typically within the accepted standard 10%. The expression levels of the genes of interest were normalised to the expression level of *g6pdh* for each sample. Each sample was amplified in duplicate. The PCR products were then extracted from the LightCycler capillary tubes and run on 2% agarose gels using electrophoresis, in order to confirm their size and the primer specificity.

4.2.12 STATISTICS

The assumption of homogeneity of variance was confirmed for all the data. This meant that the variance within each of the data sets (*n*) was equal. The statistical computer program: SPSS was used test the homogeneity of variances of these data sets. This program employed Levene's test of homogeneity of variance. The variances within these data sets were homogeneous. This data could then be tested using analysis of variance (ANOVA). ANOVA assumes that the data sets are normally distributed and that the samples are independent.

ANOVA is a collection of statistical models and procedures which use variances to test the equality of multiple mean values. The null hypothesis predicts that all the means will be equal. This will be disproved if at least one mean is different from the others. A difference is detected if a mean value is sufficiently higher or lower than its value predicted using variance and normal distribution. If this difference is detected in a sufficient number of data sets, statistical significance of this difference can be

calculated. A statistically significant difference is one that is unlikely to have occurred by chance.

The real-time qRT-PCR data was analysed using one-way ANOVA that provides an F statistic from which probability was calculated. Statistical difference was set at a probability (*P*) value of 0.05. Where significant differences were detected, pairwise comparisons were conducted using the Bonferroni *post hoc* test. This test compares all possible pairs of means to find differences, while taking into account the fact that more than two samples were taken. The standard error of the mean was also calculated. The data was assumed to be normally distributed and was not transformed.

RESULTS

The expression of the clock genes, *clk*, *bmal1*, *per1*, *per2*, *per3*, *cry1* and *cry2* was successfully detected in the human CL, indicated here by images obtained from the electrophoresis of PCR products from conventional RT-PCR (Figure 4.1). The electrophoresis of the PCR products from real-time qRT-PCR, using the LightCycler® system provided the same result. The amplicons were of the expected size and the PCR products were sequenced to confirm their identity. Template from the luteal fibroblast-like cells, obtained from extended cultures of cells from luteinised pre-ovulatory follicles, was used to provide an exogeneous positive control for clock gene expression. The housekeeping gene, *g6pdh*, was used as an endogenous positive control for the real-time quantitative PCR and the expression of the clock genes was normalised to the *g6pdh* expression (Myers et al., 2007a). By using the band intensity of the amplicons from the luteal fibroblast-like cells as a baseline, it was noted that the level of clock gene expression varied between the early, mid- and late luteal phases (Figure 4.1).

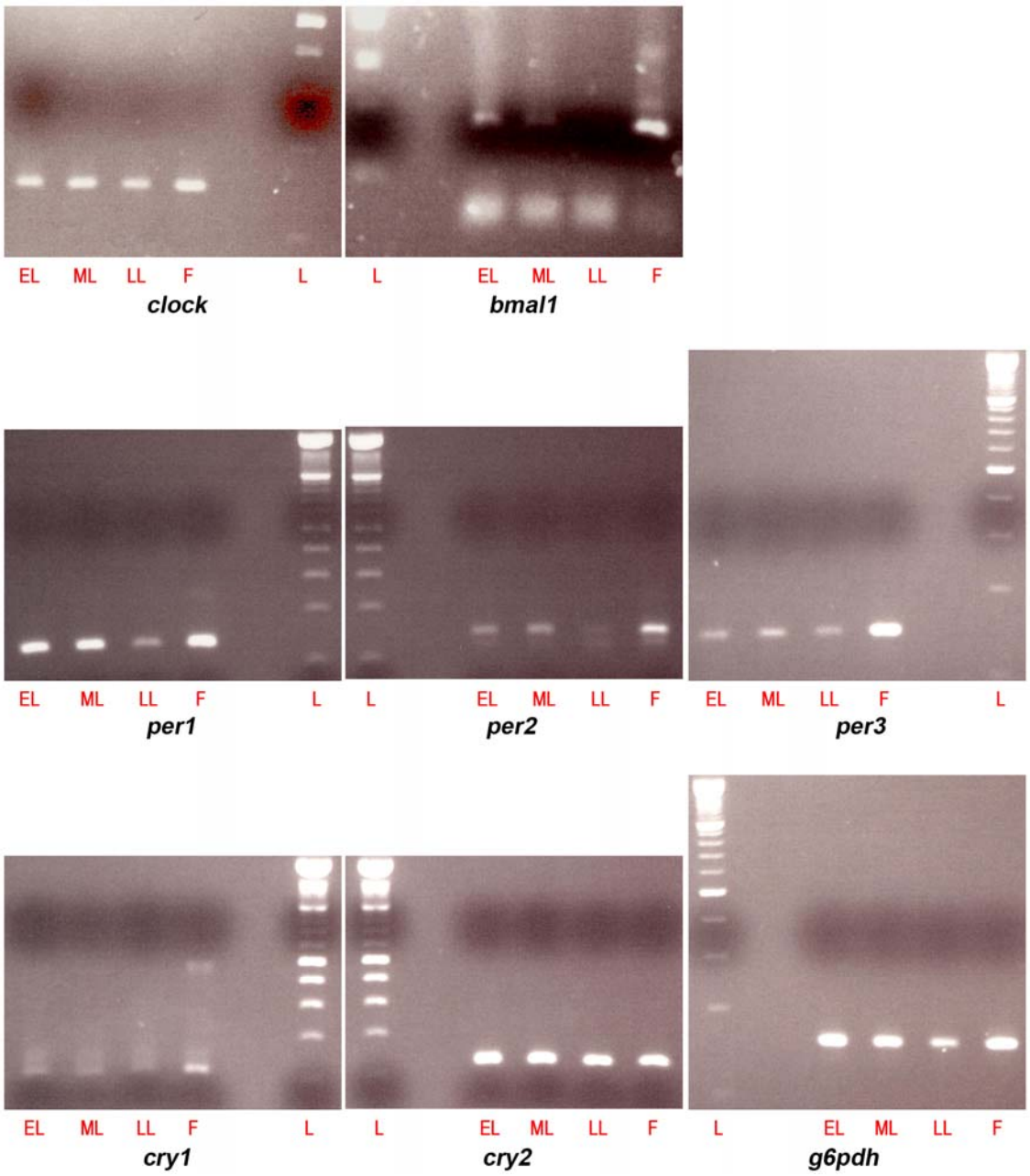

Figure 4.1 Agarose gel electrophoresis of clock gene PCR products. The expression of *clk*, *bmal1*, *per1*, *per2*, *per3*, *cry1* and *cry2* and, positive control standard gene, *g6pdh* was evident in the PCR-amplified cDNA obtained from human intact CL tissue, at early (EL), mid- (ML) and late (LL) luteal phases and from human luteal fibroblast-like cells (F), which were used as a positive control DNA template. All the amplicons localised to the correct size on the gel when lined up with a 100 bp DNA ladder (L) and were further identified by sequencing.

The use of ethidium bromide in agarose gels is however not robustly quantitative and better measures can be obtained using real-time qRT-PCR. The amount of clock gene expression in the intact human CL was therefore quantified at three stages across the luteal lifespan, using real-time qRT-PCR with the Roche LightCycler® 2.0 system.

The overall level of *clk* and *bmal1* gene expression did not alter significantly throughout the three stages of the luteal phase. There was a trend for the *clk* expression to increase over time, from the early luteal phase to the late luteal phase, but this was not significant due to the relatively large errors of the mean, which can be seen as overlapping error bars in the *clk* histogram depicted in Figure 4.2.

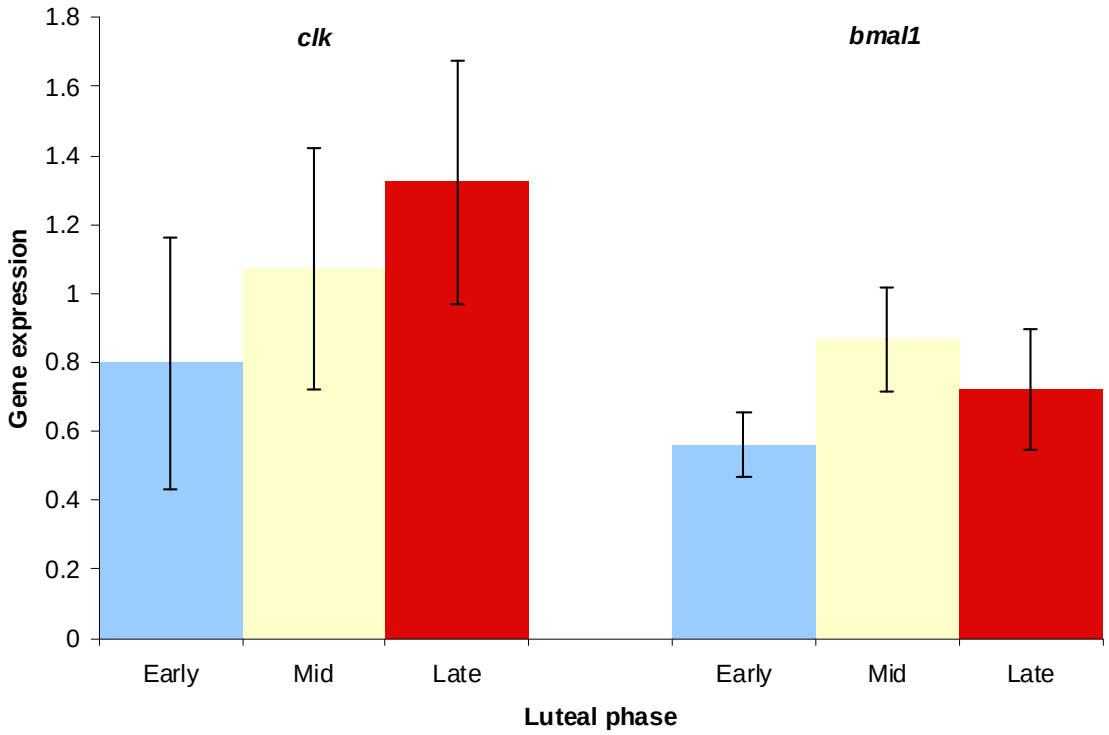

Figure 4.2 Histogram of *clk* and *bmal1* gene expression in the human intact CL, normalised to *g6pdh* gene expression. The gene expression levels were quantified using cDNA concentration extrapolated from a standard curve using real-time qRT-PCR; and statistically analysed with ANOVA with Bonferroni pairwise comparisons. Neither *clock* nor *bmal1* gene expression was significantly different between any of the three luteal phases: early, mid- and late (P>0.05). The error bars refer to the standard error of the mean.

The level of gene expression of all the *per* genes changed over the luteal lifespan. The *per1* gene was significantly increased between the mid-luteal phase and the late luteal phase (P=0.035), *per2* between the early and late luteal phase (P=0.026), and *per3* between the early and late luteal phase (P=0.043) (Figure 4.3). There was overall an increase in the *per1* mRNA expression with time. The level of clock gene expression relative to that of the housekeeper control gene was greater for *per3* than for the other two *per* homologs.

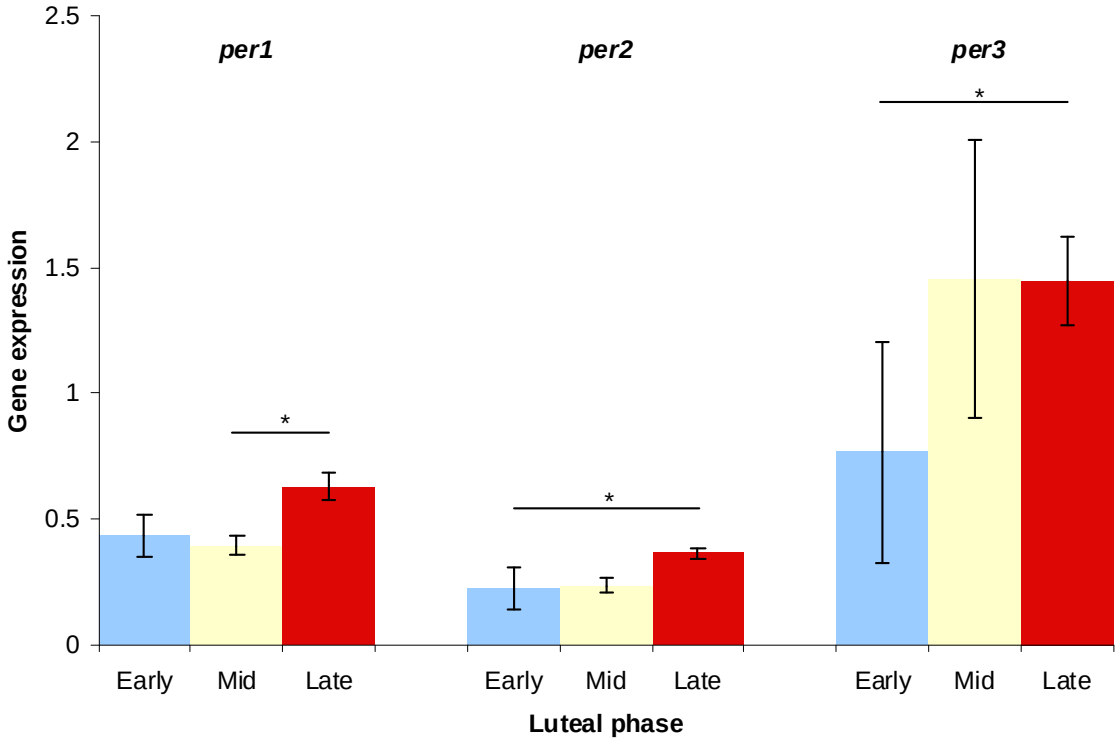

Figure 4.3 Histogram of *per1*, *per2* and *per3* gene expression in the human intact CL, normalised to *g6pdh* gene expression. The gene expression levels were quantified using cDNA concentration extrapolated from a standard curve using real-time qRT-PCR; and statistically analysed with ANOVA with Bonferroni pairwise comparisons. The late luteal *per1* gene expression was significantly greater than that of the mid-luteal phase (P = 0.035). The late luteal *per2* gene expression was significantly greater than that of the early luteal phase (P = 0.026). The late luteal *per3* gene expression was significantly greater than that of the early luteal phase (P = 0.043). The error bars refer to the standard error of the mean.

Likewise, both the *cry1* and *cry2* genes were expressed at higher levels during the late-luteal phase when compared to the early luteal phase. Expression of *cry1* was significantly higher (P=0.045) whereas *cry2* showed a more marked change in gene expression levels between the early and late luteal phases (P=0.006) (Figure 4.4). The level of *cry* expression relative to that of *g6pdh* was much less than that of *per3*, *clk* and *bmal1*.

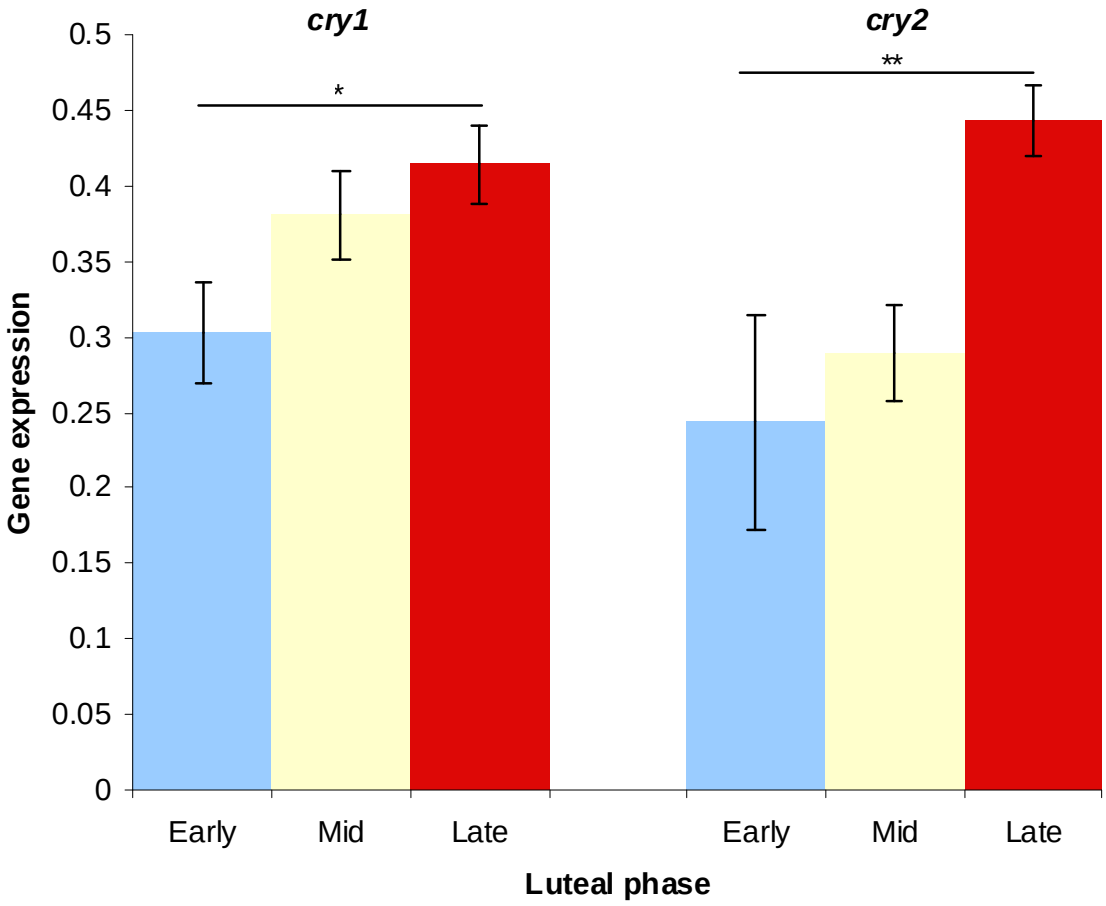

Figure 4.4 Histogram of *cryptochrome1* and *cryptochrome2* gene expression in the human intact CL, normalised to *g6pdh* gene expression. The gene expression levels were quantified using cDNA concentration extrapolated from a standard curve using real-time qRT-PCR; and statistically analysed with ANOVA with Bonferroni pairwise comparisons. The late luteal *cryptochrome1* gene expression was significantly greater than that of the early luteal phase ($P = 0.045$). The late luteal *cryptochrome2* gene expression was significantly greater than that of the early luteal phase ($P = 0.006$). The error bars refer to the standard error of the mean.

4.3 DISCUSSION

The mRNA expression of all the clock genes investigated: *per1*, *per2*, *per3*, *cry1*, *cry2*, *bmal1* and *clk*, was successfully detected and quantified in the human CL, across the luteal cycle.

In the absence of any corroborating independent evidence found in literature to date, the question of the reliability of the results presented in this chapter must be addressed. Firstly, the primers were specific and successfully amplified the cDNA into amplicons of the correct size and sequence identity. The PCR reactions were designed to be approximately the same between the reactions of the clock gene amplification and the standard gene amplification. This was important for reliable normalisation with the endogenous control gene standard curve. The running of these two amplification reactions in separate tubes was not ideal, but the reactions were performed in parallel and in duplicate to ensure any errors that may have been introduced were minimised. The melting curve analysis that was performed after each real-time qRT-PCR run further validated the accuracy of the nucleic acid quantification. The successful amplification of all seven genes investigated, in the luteal fibroblast-like cells, derived from pre-ovulatory follicles under an assisted reproduction protocol, successfully established an exogenous positive control that added confidence to the results obtained with the human CL. The luteal fibroblast-like cells were found to robustly express all of the clock genes, and the successful detection of these genes further validated the primers and PCR protocols using them. The use of the same standard endogenous control in every run also enabled the comparison and validation of the separate PCR runs against each other, so that they could be combined into a single data set. The negative controls were also successfully devoid of any PCR reaction. Thus, the data generated is a real representation of the global clock gene expression of the intact human CL.

These demonstrate the global expression of clock genes in the intact human CL, throughout the early, mid- and late luteal phases. Significant changes were observed in the level of mRNA expression in the genes belonging to the negative limb of the circadian clock mechanism: *per1*, *per2*, *per3*, *cry1*and *cry2*, between the early luteal

phase and the late luteal phase. All these negative limb clock genes were generally found to increase their level of mRNA expression as the CL aged, from the early luteal phase through the mid-luteal phase and into the late luteal phase. The pattern was marginally less clear for *per1* since the difference between the early luteal phase and late luteal phase gene expression levels was not significant, although the level of expression in the late luteal phase was greater than that of both the other two luteal phases.

There was no significant change observed in the level of mRNA expression in the genes belonging to the positive limb of the circadian clock mechanism: *bmal1*and *clk* between any of the luteal phases. The mRNA level of *clk* though, did demonstrate an upward trend with time, which was similar to those observed in with the negative limb clock genes (Figure 4.2 *clk*).

The general difference in the increasing levels of mRNA expression between the genes of the negative limb of the circadian clock mechanism and the genes of the positive limb is notable. This is similar to the events occurring in a cell-based circadian clock, where it has been shown that only one set of genes: the negative limb genes need to oscillate in a circadian rhythm, while the other set of genes: those of the positive limb of the circadian clock mechanism are constitutively expressed, in order to generate a circadian clock (Sumova et al., 2003, King and Takahashi, 2000, Oishi et al., 1998, Sato et al., 2006, Ueda et al., 2005, Ko and Takahashi, 2006). The significant change in expression of only the negative limb genes may be the related to the function of producing clockwork that is able to regulate the longer term timing of the luteal lifespan. The increased levels of clock gene expression observed may be an artefact of the changing cellular composition of the CL as it ages. It could be argued that the clock gene expression detected in this study is the result of an increasing proportion of a particular cell type, for example, macrophages which are known to be more prevalent as the CL ages (Duncan et al., 1998b). However, the IHC studies in the previous chapter do not demonstrate any particular cell type predominantly contributing to the clock gene expression in the corpora lutea, as they aged.

The working hypothesis is that the level of global clock gene mRNA expression changes across the luteal lifespan. This is so far supported by the clock gene

expression levels increasing with time rather than decreasing. There was no evidence for any loss of clock gene expression as the CL aged, and approached the time of luteolysis. This is similar to other reports on clock gene expression in the rodent ovary *in vitro* (He et al., 2007b, He et al., 2007a, Karman and Tischkau, 2006). The clock genes: *per1*, *per2*, *cry1*, *arntl* (*bmal1*) and *clk*, were all expressed in the intact rodent CL (Karman and Tischkau, 2006). The corpora lutea employed in these studies though were not staged, nor the animals assessed for œstrous cycle staging. What was observed however, may relate to the timing of the CL and its lifespan was the discovery of circadian variation in the level of *bmal1* expression in large antral follicles but not in corpora lutea. This suggests that the next logical step, in elucidating more about the temporal regulation of the human CL and its lifespan, should be the investigation of 24-hour clock gene expression of mRNA levels in the human CL.

In summary, this chapter has demonstrated for the first time that:

1. the clock genes: *per1*, *per2*, *per3*, *cry1*, *cry2*, *bmal1*and *clk* are expressed in the human CL and luteal fibroblast-like cells;

2. these genes are expressed throughout the luteal cycle, in the early, mid- and late luteal phases;

3. the level of global of *per1*, *per2*, *per3*, *cry1* and *cry2* gene expression increased significantly across the luteal cycle;

4. the expression of *clk* and *bmal1* did not change significantly across the luteal cycle;

5. there was no decrease or loss of global clock gene expression across the luteal cycle.

Although the level of global gene expression has now been elucidated, and some of that clock gene expression has been found to change significantly across the human luteal cycle, it has still not been established whether these genes are circadianly expressed in the human CL. The investigation of 24-hour clock gene expression in human luteal cells will be the focus of the next chapter.

5 CLOCK GENE EXPRESSION ACROSS 24-H IN HUMAN LUTEINISED GRANULOSA CELLS IN CULTURE

5.1 INTRODUCTION

The previous two chapters established that clock genes are expressed in the human CL and that the expression changes across the luteal lifespan. There is robust expression of the clock proteins in the steroidogenic cells of the human CL, including the granulosa-lutein cells. This is relevant because, in order to assess the clock gene expression in the human CL across 24 hours, an *in vitro* model is needed, as it is not possible to sample corpora lutea from women at different times of the day due to logistical and ethical considerations. It is still crucial however, that the 24-hour expression of the clock genes is investigated in the human CL, as this is the main function of these genes in virtually all the cells of the body. It is also likely that the gene expression profiles that emerge for these genes will pertain to the temporal regulation of luteal function and lifespan.

The *in vitro* model proposed for establishing the 24-hour mRNA expression of the clock genes in luteal cells employs the LGCs. These are the cells that are developing into the granulosa-lutein cells of the CL. These cells are obtained from the follicular fluid from follicles that have been surgically enucleated of their oocytes, under an assisted conception cycle. The follicular fluid or aspirate therefore contains a mixture of cells, from a mixture of follicles, from a single individual woman. These follicles are large and have been exposed to a high dose of hCG that was administered to mimic the pre-ovulatory LH surge. The follicular fluid was obtained 35 hours after the pseudo-LH surge from three or more large follicles, which were generated under a programme of hormonal treatment using fertility drugs that stimulate the maturation of several follicles, rather than the usual single dominant follicle, in the ovaries.

During oocyte retrieval, cell culture media is used to flush out the cells from the enucleated follicles. It is from this aspirate, that the LGCs are extracted. As these cells are not required for the *in vitro* fertilisation (IVF) process, they are usually discarded and therefore are relatively readily available.

The use of this cell culture system as a model of the human CL has been validated by numerous other studies (Dickinson et al., 2008, Duncan et al., 2005b, Duncan et al., 2005a, van den Driesche et al., 2008, Madhra et al., 2004, Myers et al., 2007a, Myers et al., 2007b, Myers et al., 2008). Many of these studies have shown that these cells express genes that are characteristic and specific to human granulosa-lutein cells. The LGCs have also been shown to synthesise and secrete progesterone, functioning steroidogenically like human granulosa-lutein cells (Ivell et al., 1999). Moreover, and very importantly, these cells have been shown to persist in culture for approximately 14 days, the same time period as that of the intact human luteal lifespan, before spontaneously degenerating and disappearing. This suggests that whatever temporal regulation there is in the intact human CL that controls the timing of luteolysis and thus, the luteal lifespan is preserved largely intact, in the cultured LGCs. Furthermore, the lifespan of these cells can be extended and their demise forestalled by treatment with hCG, which mimics the effect of hCG in the intact human CL. Human chorionic gonadotrophin is a luteotrophic maternal recognition of pregnancy signal that is emitted by the conceptus and acts on the LH receptor, to ensure the continued survival and function of the CL during early gestation. The hCG effect in the LGCs further replicates the *in vivo* situation of the intact human CL, by being required in increasing amounts for the continued maintenance of the LGCs as they age. The intact human CL of pregnancy similarly requires and receives increasing amounts of hCG from the growing conceptus.

The follicular aspirates are also a source of another cell type that resembles human luteal cells, as described in the previous chapter. Human luteal fibroblast-like cells can be obtained from the cultures of LGCs, after the demise of the LGCs, which occurs after around 14 days (Duncan et al., 2005b, Myers et al., 2007a). These luteal fibroblast-like cells, like the fibroblasts of the intact human CL, do not possess hCG/LH receptors. They are therefore not directly affected by the exogenous hCG surge. The enrichment of the LGC cultures for LGCs does not completely eliminate

the presence of a small number of these luteal fibroblast-like cells. These cells are able to proliferate and do so in abundance after the demise of the LGCs, which occurs after ~14 days without hCG-rescue. They are able to grow to confluence, producing a cell population that possesses cell-to-cell communication. These cells are not terminally differentiated and can be maintained in primary cell culture. They may therefore be used to represent another human luteal or luteal cell-like cell type, other than the LGCs, for the purpose of elucidating more about the potentially circadian expression of the clock genes in the human CL. The fact that this other population of cells is fibroblast-like is also particularly useful, as fibroblasts have generally been shown to possess individual cell-based circadian clocks, which can be synchronised by a variety of zeitgebers, including serum shock *in vitro* (Balsalobre et al., 1998, Kaeffer and Pardini, 2005).

Thus, the use of both these cell culture models promised to provide useful insight into the 24-hour expression of clock genes in the human CL, as it ages. The working hypothesis is that the expression of the clock genes is linked to the temporal regulation of the luteal lifespan. It is proposed that all of the clock genes may be expressed in the LGCs and luteal fibroblast-like cells, seeing that they are expressed in the granulosa-lutein cells and fibroblasts in the intact human CL. It is further proposed that the expression of some if not all of these clock genes will be rhythmic across 24-hours and may change with the time spent in culture, representing the time elapsed in the progression of the luteal cycle. The hCG-rescue of the LGCs may affect the clock gene expression of these cells. The clock gene expression in the luteal fibroblast-like cells will also be altered, by serum shock, resulting in the emergence of more overtly rhythmic pattern of gene expression in their, collectively arrhythmic or dampening, circadian rhythms. This will likely be due to better synchrony of the cellular clocks, mediated by the hCG.

Thus, this chapter aims:

3. to determine whether the clock genes: *clk*, *bmal1*, *per1*, *per2* and *cry1* are expressed in cultured human LGCs and luteal fibroblast-like cells;

4. to assess whether the clock gene expression in the LGCs and luteal fibroblast-like cells is rhythmic across 24-hours;

5. to determine whether the 24-hour clock gene expression in the LGCs changes with time, between the first (D1) and eighth (D8) day of culture;

6. to determine whether hCG treatment of the LGCs affects clock gene expression;

7. to assess whether serum shock affects 24-hour clock gene expression in the luteal fibroblast-like cells.

5.2 MATERIALS AND METHODS

5.2.1 ETHICAL APPROVAL

The collection of ovarian and follicular cells from patients undergoing assisted conception at the EFREC was separately approved by the Reproductive Medicine Subcommittee followed by further approval by COREC. Informed consent was obtained from all patients and their consultant gynaecologists, notably Dr K. Joo Thong.

5.2.2 SAMPLING

With patient consent, follicular fluid was collected from women undergoing transvaginal oocyte retrieval for *in vitro* fertilisation after ovarian stimulation using a standard procedure. Briefly, a long-protocol stimulated cycle was followed, using intranasal naferelin (Pharmacia Biotech, Milton Keynes, UK), a gonadotrophin-releasing hormone analogue for down-regulation and daily purified gonadotrophins (Menopur, Ferring Pharmaceuticals, Langley, UK) for ovarian stimulation. When at least three follicles reached 18 mm diameter, 10 000 IU hCG was administered. This large hCG dose mimicked the pre-ovulatory LH surge that triggers ovulation. Transvaginal oocyte collection was performed under sonographic guidance 35 hours later (Duncan et al., 2005b). The follicular fluid that was flushed from the follicles was reserved and used as a source of LGCs and luteal fibroblast-like cells (Stamouli et al., 1996).

The follicular fluid or aspirates that were obtained from three separate women were kept separate. Each follicular aspirate was used for culturing a single set of LGCs for 24-hour sampling. Each set generated was a single *n* number. These sets were referred to as *individual* samples (Figure 5.1). There were three individual samples (n=3). The follicular aspirates of two or three women were combined to culture a single set of LGCs. This set of LGCs, comprising LGCs from multiple women,

generated a single *n* number, and was referred to as a *pooled* sample (Figure 5.1). Three pooled samples were used (*n*=3). Samples were pooled because demand for these cells was fierce, and there was not enough time to wait for follicular aspirates that contained sufficiently large quantities of LGCs to comprise a single individual sample. Therefore, follicular aspirates with too few LGCs for a single sample were combined with other, similarly low LGC yielding, follicular aspirates, to produce a sample that was composed of a sufficient amount of LGCs. The pooling of the follicular aspirates was only possible with follicular aspirates that were obtained on the same day. Luteal fibroblast-like cells were all obtained from pooled follicular aspirates, that were not used for LGC isolation.

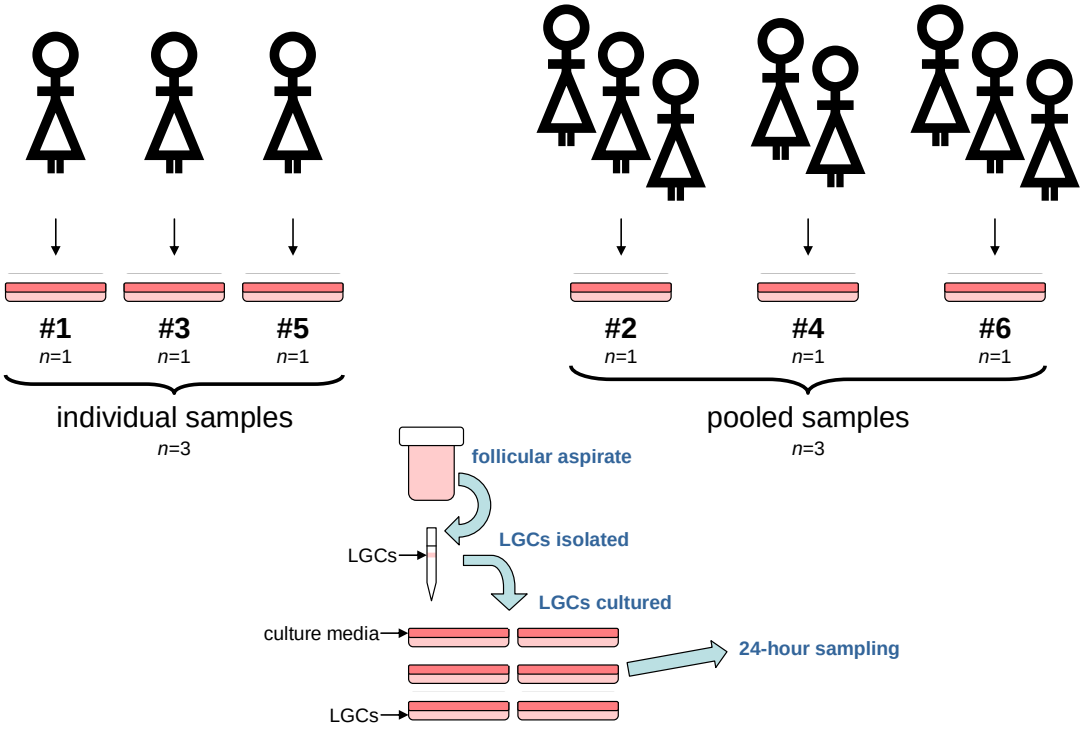

Figure 5.1 Diagram showing the acquisition of individual and pooled LGC samples. There are three samples; each composed of LGCs from a single individual woman, in this case, samples #1, #3 and #5. There are three pooled samples, each sample composed of LGCs from several women, in this case, sample #2 is composed of cells from three individual women, sample #4 is composed of cells from two individual women and sample #6 is composed of cells from three individual women. A diagram of the process of cell culture is also depicted, showing a pot of follicular aspirate, from which the LGCs are extracted, and then cultured in pre-coated cell culture plates, containing cell culture media.

5.2.3 LUTEINISED GRANULOSA CELL CULTURE

LGCs were obtained from follicular aspirates after the removal of oocytes. Individual follicles were not distinguished, and all follicular fluid from the same individual were pooled and centrifuged at 1500 rpm for 10 min. The cells were resuspended in culture medium (Dulbecco's Minimum Essential Medium/Ham's F-12 mixture, Invitrogen Life Technologies, Inc., Gaithersburg, MD) supplemented with 2 mmol l^{-1} glutamine (Sigma, Dorset, UK), 6.25 mg l^{-1} insulin, 6.25 mg l^{-1} transferrin, 6.25 μg l^{-1} selenious acid (Roche, Welwyn Garden City, UK), 2.5 mg l^{-1} amphotericin, 50 mg l^{-1} penicillin and 60 mg l^{-1} streptomycin, layered over a 45% Percoll/culture medium mixture, and centrifuge at 1200 rpm for 30 min to pellet the blood cells. LGCs, visible in the interface, were collected by pipette and washed three times in PBS. The cells were resuspended in culture medium, and viable cells were counted using a trypan blue exclusion test (van den Driesche et al., 2008). Where possible, the cells from individual patients were used for an entire experiment, (individuals data set, n =3) but failing that, cells from several patients were pooled to achieve a sufficient quantity of viable cells for an experiment, n=3 (pooled data set, n=3). Each time course experiment comprised six sets of 350 000 cells, plated onto 2 wells of 15-mm round-well plates precoated with BD Matrigel™ Basement Membrane Matrix Extracellular Matrix Proteins (Biotrace International, Brigend, UK). The cells were cultured using 0.5 ml culture medium at 37^{o}C in 5% CO_2 in air (Figure 5.1).

Individual 66-mm round well plates containing 350 000 cells in 2 wells were sampled every 4 h for 24 h after 12 h of culture. Remaining plates of cells were maintained with daily media changes, timed to coincide with the time of initial culture, as there were reports of media changes being sufficient for re-entraining circadian rhythms in cultured cells (Welsh et al., 2004). The cells were then sampled on day 8 post-culture. Human chorionic gonadotrophin treatment involved the addition 1000 μg ml^{-1} of recombinant hCG (Profasi, Serono Laboratories, Welwyn Garden City, UK) for 2 h then replacement with the usual media. The 2-h treatment was started at a time 2 hours prior to the usual time for daily media change. Untreated controls were given media changes at times of treatment addition and withdrawal.

The plates were removed from the incubator and the medium carefully pipetted off. The media was frozen until the progesterone concentrations were measured using RIAs, adapted from routine methods previously described (Gault et al., 2003). RNA was then extracted from the cells, which were harvested every four hours on day 1 and day 8 post-culture (Figure 5.2).

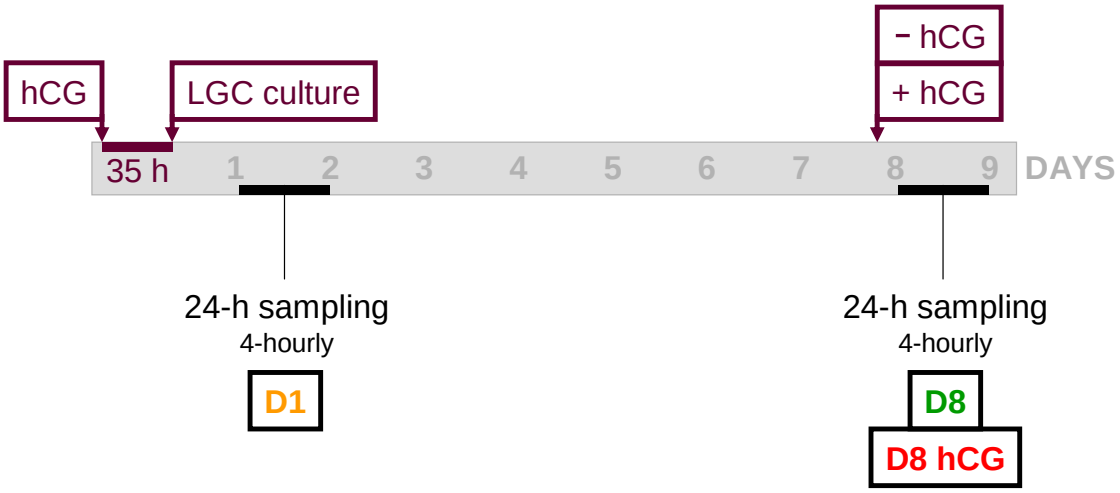

Figure 5.2 Timeline of the LGC culture. The diagram indicates when the timing of cell culture, treatment with (+ hCG) and without (- hCG) and 4-hourly sampling over 24 hours on the first (D1) and eighth (D8) day of culture, with (D8 hCG) and without (D8) hCG.

5.2.4 LUTEAL FIBROBLAST CELL CULTURE

The reproductive medicine subcommittee of the Lothian medical ethics committee approval included the culture of luteal fibroblast-like cells from the follicular aspirates collected during assisted conception. The cells were derived as described previously and reported in the previous chapter (Duncan et al., 2005b, Myers et al., 2007a, Dickinson et al., 2008).

For the 24-h time course experiments, the luteal fibroblast-like cells were cultured in 66-mm round well plates (Fisher Scientific, Leicester, UK) and allowed to grow to confluence with daily media changes timed to the same time of day or to coincide with that of any concurrent LGC cultures (n=3). Once the cells were confluent, they

were treated with 50% fœtal bovine serum for 2 h then the media replaced with serum-free media. Untreated controls were given media changes consistent with the treatment volumes and times. Individual plates were sampled every 4 h for 24 h. The cells were harvested by removing the medium, which was discarded. RNA was then extracted from the cells at each time point.

5.2.5 TOTAL RNA EXTRACTION

RNA was extracted using an RNeasy® Micro RNA extraction kit (Qiagen Ltd, West Sussex, UK) using the Total RNA Isolation from Animal Cells spin protocol with the on-column DNase treatment (Qiagen Ltd, West Sussex, UK). There were less than 1 x 10^5 cells in each sample. Briefly, once the media had been removed from the cells, they were disrupted and lysed by the direct addition of 350 µl Buffer RLT containing 1% β-mercaptoethanol to the plate. The cells were scraped using sterile pipette tips and the cell lysate pipetted into a microfuge tube. The lysate was vortexed to ensure it was well-mixed and that any clumps of cells would be disintegrated. To homogenise the sample, the cell lysate was pipetted directly into a QIAshredder spin column (Qiagen Ltd, West Sussex, UK) which was placed in a 2 ml microfuge tube, then centrifuged for 2 min at maximum speed in a bench microcentrifuge. The QIAshredder was removed and discarded, leaving the homogenised lysate in the 2 ml microfuge tube.

One volume (usually 350 µl) of 70% ethanol was then added to the homogenised lysate and mixed well with pipetting. This precipitates the RNA. The sample, including any precipitate that had formed, was then carefully pipetted into an RNeasy MinElute Spin Column in a 2 ml collection tube. The tube was then centrifuged for 15 s at 8 000 x *g*. The RNA was now bound to the silica-gel membrane in the RNeasy MinElute Column. The flow-through was discarded.

Buffer RW1 (350 µl) was then added to wash the RNeasy MinElute Spin Column. The tube was centrifuged for 15 s at 8 000 x *g* and the flow-through discarded. The RNA was then treated with deoxyribonuclease (DNase) to remove any template DNA,

using a Qiagen RNase-free DNase set (Qiagen Ltd, West Sussex, UK). Next, 10 µl DNase I stock solution (Qiagen Ltd, West Sussex, UK) was mixed gently with 70 µl of Buffer RDD and added directly onto the RNeasy MinElute silica-gel membrane. The DNase was left to work in the column for 15 min at room temperature. The column was then washed by adding 350 µl of Buffer RW1 to the column and centrifuging for 15 s at 8 000 x *g* and the flow-through was discarded.

The column was transferred into a new 2 ml collection tube. Buffer RPE (500 µl) was then pipetted into the column and centrifuged for 15 s at 8 000 x *g*. The flow-through was discarded. The silica-gel membrane was then dried by the addition of 500 µl of 80% ethanol to the column, which was then centrifuged for 2 min at 8 000 x *g*. The flow-through and collection tube were discarded. The column was then dried more thoroughly. It was transferred to a new 2 ml collection tube. The cap was left open and then the tube centrifuged at maximum speed for 5 min in a bench microcentrifuge. The flow-through and collection tube were discarded.

The RNA was then eluted. The column was transferred to a 1.5 ml collection tube and 14 µl of RNase-free water was pipetted directly onto the centre of the silica-gel membrane. The tube was closed and left to incubate on ice for 10 min. The tube was then centrifuged for 1 min at maximum speed on the bench centrifuge. This step was repeated with a second 10 µl volume of RNase-free water. The RNA was then quantified on an Agilent 2100 Bioanalyzer (Agilent Technologies UK Ltd, Wokingham, Berkshire, UK). RNase-free water was added to the RNA to achieve a final concentration of 50 ng/µl and RNA was stored at -80^{o}C until analysis.

5.2.6 RNA QUANTIFICATION

RNA was quantified using an Agilent RNA 6000 Nano LabChip® kit (Agilent Technologies UK Ltd, Wokingham, Berkshire, UK) on an Agilent 2100 Bioanalyzer (Agilent Technologies UK Ltd, Wokingham, Berkshire, UK). The Agilent assay works using capillary electrophoresis and so, not only quantifies the RNA, but simultaneously provides an assessment of the RNA purity. The purity measurement

works in much the same way as using sodium dodecyl sulphate polyacrylamide gel electrophoresis (SDS-PAGE). The Bioanalyzer contains software that generates electropherograms of each sample and ladder as well as an RNA Integrity Number (RIN) that is a quantification estimate and calculates the ribosomal ratios of total RNA samples.

Each RNA sample (1 µl) and an Agilent RNA 6000 Nano Marker ladder (1 µl) were denatured by heating at 70^{o}C for 2 min before rapidly chilling on ice. The RNA samples and ladder were loaded into an Agilent RNA 6000 Nano LabChip containing microfluidic gel freshly mixed with fluorescent dye. The dye binds to nucleic acids and so allows the fluorescent detection of the RNA fragments, as well as any contaminating template DNA. Each LabChip is made up of an interconnected set of micro-channels that are used to separate the nucleic acid fragments, based on their size as they are driven through the chip electrophoretically.

5.2.7 PREPARATION OF COMPLEMENTARY DNA BY REVERSE-TRANSCRIPTION

The RNA was batch reverse transcribed using GeneAmp® RNA PCR Kit (Applied Biosystems, Warrington, UK) with random hexamers. Total RNA (125 µg) was added to a reaction mix containing 1x RT Buffer, 5 mM magnesium chloride ($MgCl_2$), 1 mM dNTPs, 1.25 µM random hexamers, 1 U μl^{-1} recombinant RNasin® ribonuclease (RNase) inhibitor and 1 µl recombinant Moloney murine leukaemia virus (MuLV) reverse transcriptase in a final reaction volume of 20 µl. The reverse transcriptions were performed in duplicate, with positive controls using human placental RNA. Negative controls comprising reactions performed without the addition of template RNA as well as using a 3-5 randomly selected test samples with a reaction mix lacking reverse transcriptase were included.

The samples were incubated at room temperature for 10 min. They were then heated to 42^{o}C for 60 min in order to provide the optimum temperature for enzymatic action.

The reaction was then stopped and the enzyme denatured by incubating at 95°C for 10 min. The resulting cDNA was stored short-term at 4°C or long-term at -80°C until subsequent PCR.

5.2.8 PRIMERS

In order to quantify the expression levels of the clock genes, specific PCR primers designed to amplify the clock gene DNA was required. TaqMan® Gene Expression assays were used which provided commercially available primers and probes for human clock genes. The TaqMan® system employing these primers and probes was preferred as it offered higher throughput than the LightCycler® system, as well as enabled the use of a heterologous endogenous control in a multiplex amplification reaction with the gene of interest. These TaqMan® Gene Expression Assays used included *clock*, *bmal1*, *per1*, *per2*, *cry1* and *cry2*. The details are listed below (Table 5.1):-

GENE	ASSAY NUMBER	FLUORESCENT DYE	AMPLICON SIZE (bp)
clock	Hs00231857_m1	FAM	88
bmal1	Hs00231048_m1	NED	61
per1	Hs00231857_m1	FAM	88
per2	Hs00256143_m1	FAM	121
cry1	Hs00172734_m1	NED	84

Table 5.1 List of the TaqMan® Gene Expression Assays used, including catalogue numbers, fluorescent dye label and amplicon size.

The primers and probes were intron-spanning where possible to better ensure the amplification of only cDNA template rather than any contaminating genomic DNA. The probes were TaqMan® MGB™ probes. These probes incorporate a 5' reporter dye and a 3' non-fluorescent quencher (NFQ). The NFQ produces a lower background signal, which increases the precision of the gene expression

quantification. The major groove binder (MGB) moiety works by stabilising the probe when it is hybridised by binding to the major groove of the DNA. This increases the melting temperature (T_m) of the probe to improve the specificity of the unquenching of the fluorescent label by the endonuclease activity of the *Taq* polymerase.

An internal control PCR reaction was required to run in duplex with the PCR amplification of the gene of interest. Ribosomal 18S RNA was selected for the internal control. It is used routinely and is abundant in cells. It would therefore provide a reliably detectable level of gene expression. It was also found not to be circadianly expressed in sheep, nor was it affected by photoperiod in sheep (Dupre et al., 2008). The crossing threshold (C_T) of the 18S reaction was also not predicted to be too distant from that of the clock genes in the ovine CL. The 18S primers and probe selected were the standard ones which are routinely used (Applied Biosystems, Warrington, UK). They were fluorescently labelled with the VIC dye and are used in conjunction with an MGB probe.

The primer and probe concentrations were then optimised. The optimal concentrations for the primer pairs were determined using a range of concentrations. The primers were used in ratios of 1:1, 3:1, 6:1 and 18:1 reciprocally between the forward and reverse primers and the T_m was varied by ± 2^oC increments. The primer pair concentrations were optimised using temperature gradients. The probe concentrations were then optimised by titrating against the primer pairs at their optimised concentrations, to ensure that the probe does not limit the fluorescence in the PCR due to its more abundant template: ribosomal 18S cDNA. The primers and probes were performed in singleplex PCRs initially then in duplex PCRs which included the internal control primers and probes. The optimal conditions resulted in the lowest C_T value without excess primer or probe.

5.2.9 REAL-TIME QUANTITATIVE REVERSE TRANSCRIBED-POLYMERASE CHAIN REACTION USING THE APPLIED BIOSYSTEMS TAQMAN® SYSTEM

Once the primers were selected, they were used in real-time qRT-PCR to amplify up the clock gene DNA. The qRT-PCR was performed, using a two-step RT-PCR protocol, in the Applied Biosystems TaqMan® system, which was comprised of the TaqMan® 3700HT instrument with reagents from the AmpliTaq Gold® Fast PCR Master Mix kit. This system follows the standard principles behind real-time qRT-PCR, as described previously. It uses quenched fluorescent probes that hybridise between the forward and reverse primers and which become unquenched when cleaved by the nuclease activity of the polymerase during the PCR amplification process. The amount of fluorescence detected is used to monitor the amount of template amplification.

The duplex qRT-PCR reaction was made up of 1.5 µl cDNA, 1x AmpliTaq Gold® Fast PCR Master Mix, UP, 1x each of forward and reverse primers, 1x probe, 0.02 µM each of forward and reverse 18S primers, 0.08 µM 18S probe to a final reaction volume of 10 µl. The AmpliTaq Gold® Fast PCR Master Mix, UP is a solution containing hot start *Taq* polymerase, dNTPs, magnesium and buffer. It is used in fast PCR reactions, which take approximately 40 min rather than the standard 2 h. Reactions were loaded into 96-well plates and the PCRs performed in a TaqMan® 3700HT instrument, using a fast protocol. Complementary DNA from ovine adrenal gland was used as a positive control. Negative controls included reactions omitting the template which was replaced by nuclease-free water. PCR reactions were performed in triplicate with each of the duplicate cDNA.

The C_T values were then used to calculate the relative gene expression of each gene of interest, using the second derivative method with the adrenal gland positive control as the reference sample (Kubista et al., 2006).

5.3 RESULTS

5.3.1 PROGESTERONE FROM LUTEINISED GRANULOSA CELLS

The media extracted from the LGCs prior to RNA extraction were assayed using radiolabelled immuno-assays (RIA) to quantify the progesterone (P_4) concentration. This provided an indication of the steroidogenic function of the cells, which, as expected, showed a decrease in P_4 levels from D1 to D8 (Figure 5.3). This meant that the LGCs had lost some of their steroidogenic function with time, as is the case in the intact human CL of the reproductive cycle. The hCG treatment of the LGCs on D8 shows the restoration of P_4 secretion to levels akin to those on D1, and which are higher than those of the D8 LGCs without hCG treatment. The P_4 levels indicate that the LGCs are healthy, steroidogenically functional and hCG responsive.

It is important to note that the changes reported in the P_4 levels between the LGC populations between D1 and D8, with and without hCG, were not statistically significant. This was disregarded though, because the failure to detect any statistical significance is due the relatively low levels of P_4 that the LGCs are producing. This is due to the absence of a substrate from which P_4 can be synthesised. Cholesterol, in the form of low-density lipoprotein (LDL), is often used to supplement the culture media of the LGCs in order to provide such a substrate for P_4 synthesis. Its addition to LGC cultures is well known to produce relatively high levels of P_4, particularly after hCG-rescue (Duncan et al., 2005a).

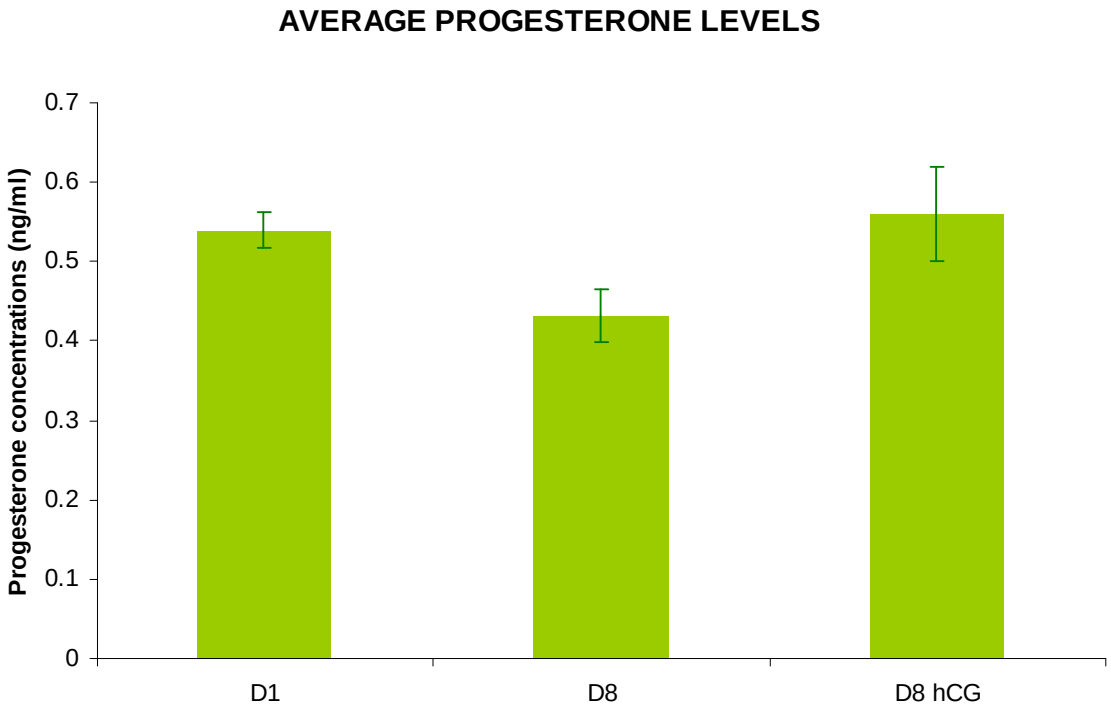

Figure 5.3 Histogram of progesterone levels. This shows the progesterone concentrations in the media from LGC on days one (D1) and eight (D8) of culture, with (D8 hCG) and without hCG (D8). The error bars refer to the standard error of the mean.

5.3.2 24-HOUR CLOCK GENE EXPRESSION IN LUTEINISED GRANULOSA CELLS

5.3.2.1 GENE EXPRESSION BETWEEN INDIVIDUAL AND POOLED SAMPLES

There was an increased level of *clk* expression across 24-hours in five out of six of the samples (exception sample #6), which peaked at ZT 10 – 14 on D1 and at ZT 10 – 22 on D8, but with marked variation both in the timing of the maximum and in the absolute level of expression (Figure 5.4). Sample #4 was notable in having a much higher overall level of gene expression than any of the other samples. Samples #5 and #6 were also notable in that they shared no clear peak that was consistent with any of the other samples.

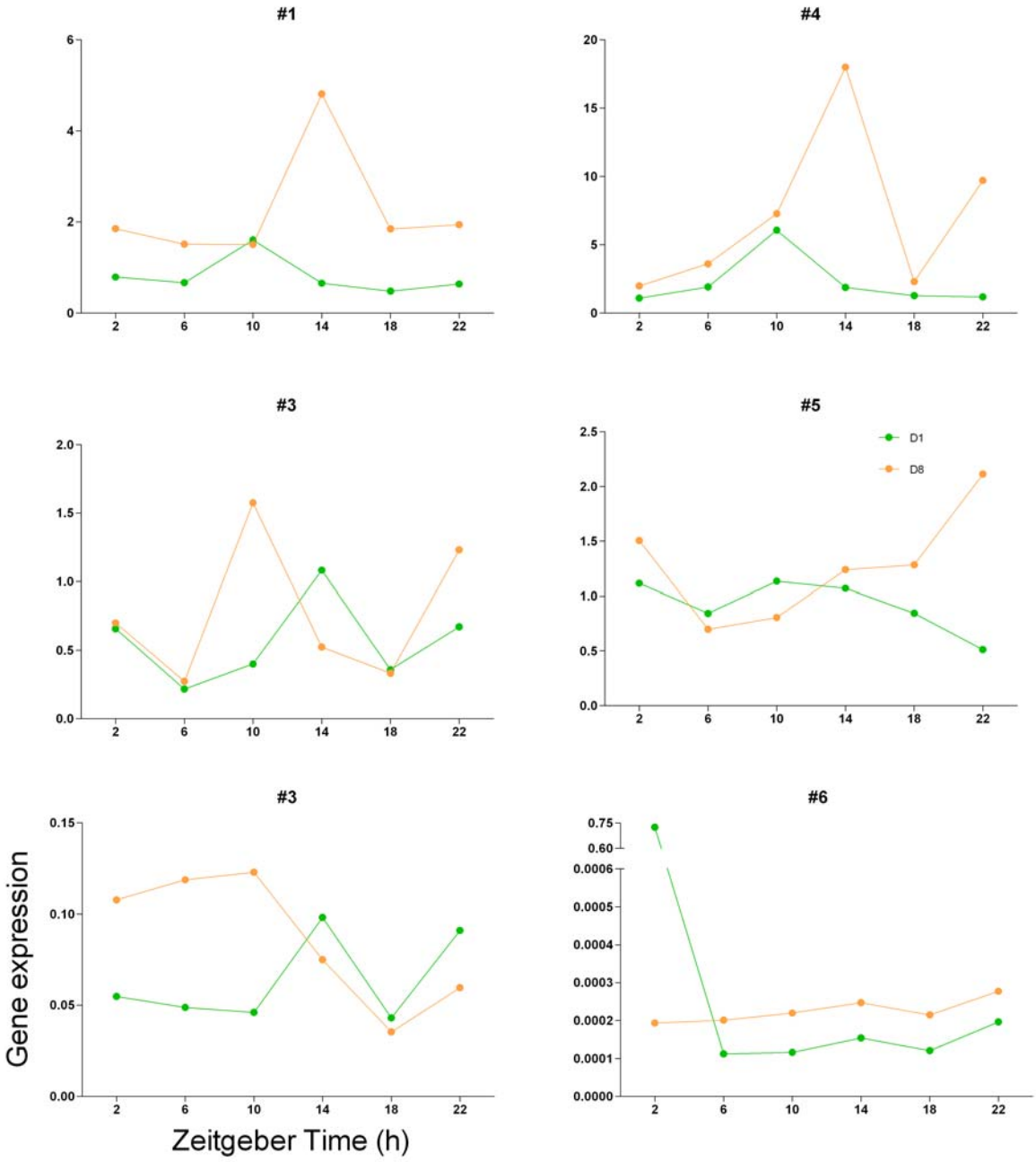

Figure 5.4 The gene expression of *clk* in individual (#1, #3 and #5) and pooled (#2, #4 and #6) LGC samples, demonstrating the increased rhythmicity of the gene expression on D8 (orange) compared to that on D1 (green).

The expression profiles of *clk* loosely segregate into three characteristic 24-hour gene expression patterns: 1) high expression, 2) rhythmic and 3) arrhythmic (Figure 5.4). The high expression profile was typified by the *clk* expression of sample #4, which revealed a maximum at ZT 10 on D1 and at ZT 14 on D8, with robust expression. The rhythmic *clk* gene expression profile was typified by sample #1 and sample #2. This was classified according to the clear evidence of peaks and troughs in the 24-hour profiles that fitted relatively closely with a sigmoid curve. The arrhythmic gene

expression profile was typified by sample #5 and sample #6 (with the ZT 2 data point excluded), with a relatively small change in the level of *clk* gene expression across 24 hours.

After this arbitrary classification, the 24-h expression of the other four clock genes were then examined in relation to the pattern of *clk* rhythmicity using the three categories: sample #4 – high expression (Figure 5.5), sample #1 – rhythmic (Figure 5.6) and sample #5 – arrhythmic (Figure 5.7).

5.3.2.2 HIGH EXPRESSION PROFILE

Sample #4 expressed particularly high *clk* gene expression and the rhythmic expression on D1 and D8 were very robust. The 24-hour expression of the other clock genes was also very robust in this sample (Figure 5.5). The D8 24-hour profiles of gene expression corresponded more closely to sigmoid curves, with the peaks of all but *cry1* occurring at higher levels of gene expression than on D1. All the D8 peaks occurred at either ZT 10 or ZT 14 while all the D1 peaks occurred at ZT 10, except for *per1* which peaked earlier at ZT 6. There appeared to be a phase delay of ~4 hours in the D8 expression of *clk*, *per1* and *per2*, based on the time of peak gene expression (acrophase). The acrophases did not shift between D1 and D8 of *bmal1* and *cry1* gene expression, nor was there a marked increase in the level of gene expression between the acrophases on D1 and D8. Contrary to expectation, there was no evidence of antiphasic timing in the 24-hour profiles of expression for the genes comprising the negative limb of the circadian clock mechanism (*per1*, *per2* and *cry1*) and the genes comprising the positive limb of the circadian clock mechanism (*clk* and *bmal1*).

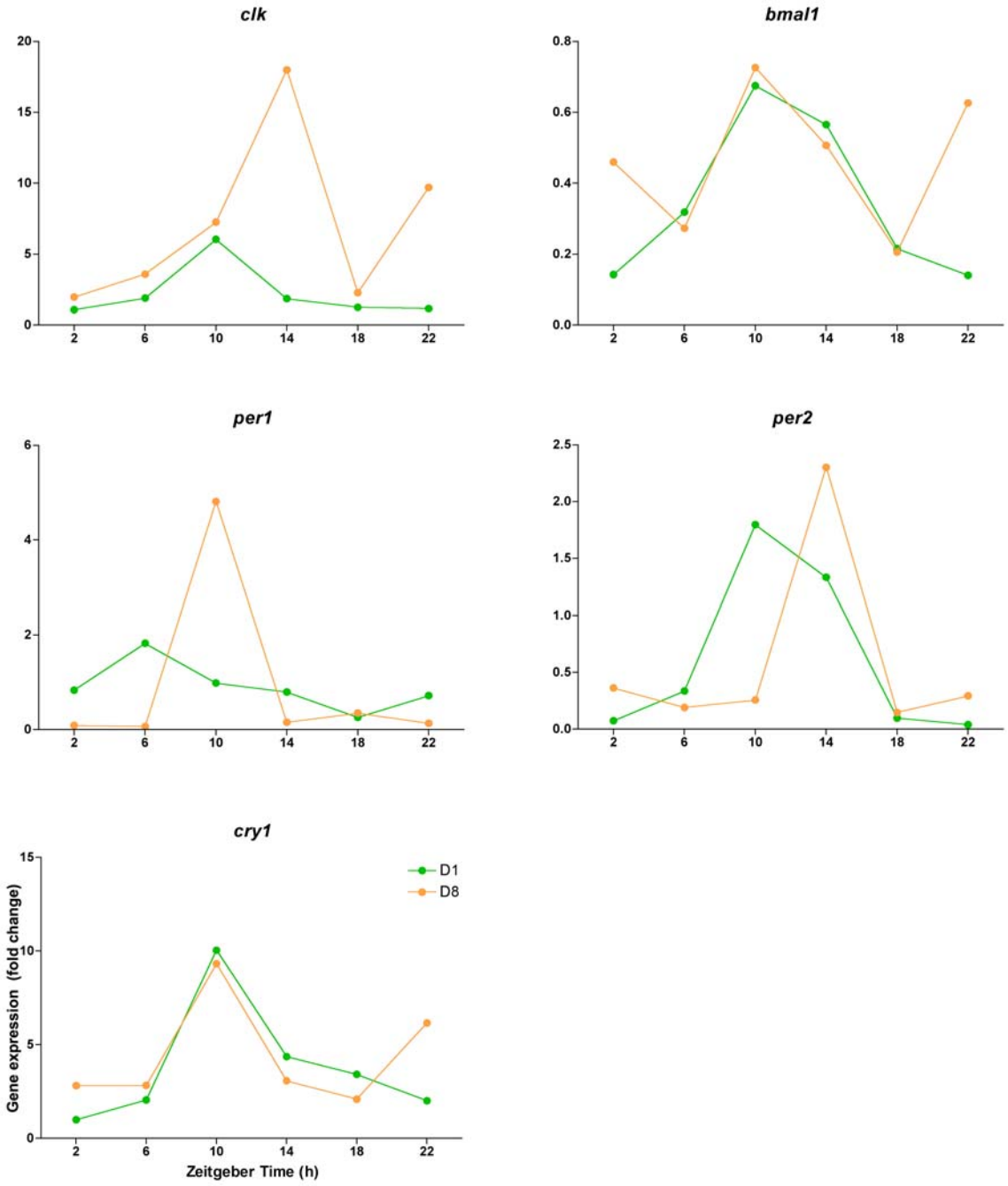

Figure 5.5 This individual sample, sample #4, shows relatively high gene expression of *clk*, *per1* and *cry1*, as demonstrated by the relatively high amplitudes (fold change), on both D1 (green) and D8 (orange).

5.3.2.3 RHYTHMIC PROFILE

The rhythmic profile of gene expression was demonstrated by sample #1, where all of the graphs of the 24-hour profiles of clock gene expression relatively closely resembled a sigmoid curve (Figure 5.6). All the D8 acrophases occurred at ZT 14, showing a ~4 hour phase delay of the D1 acrophases, except for *per1*, which was delayed by a further ~4 hours. The level of gene expression was increased in general and also higher at the peaks of the D8 circadian expression of *clk*, *bmal1* and *cry1*. This was not the case for the *per* genes, which appeared to have a decrease in the general level of clock gene expression on D8, as well as lower amounts of gene expression at its D8 acrophase. The general level of the expression of the clock genes were largely in line with those of the other samples, except the expression of *per2*, which was quite high on D8 in this sample compared to *per2* expression on D1 and D8 in all the other samples. The acrophase of the D8 *cry1* rhythm was also the highest of all the samples, taking into account the D1 and D8 acrophases. Again, no antiphasic relationships were observed between the rhythmic expression of the genes belonging to the negative limb of the circadian clock mechanism and the genes belonging to the positive limb of the circadian clock mechanism, on either D1 or D8.

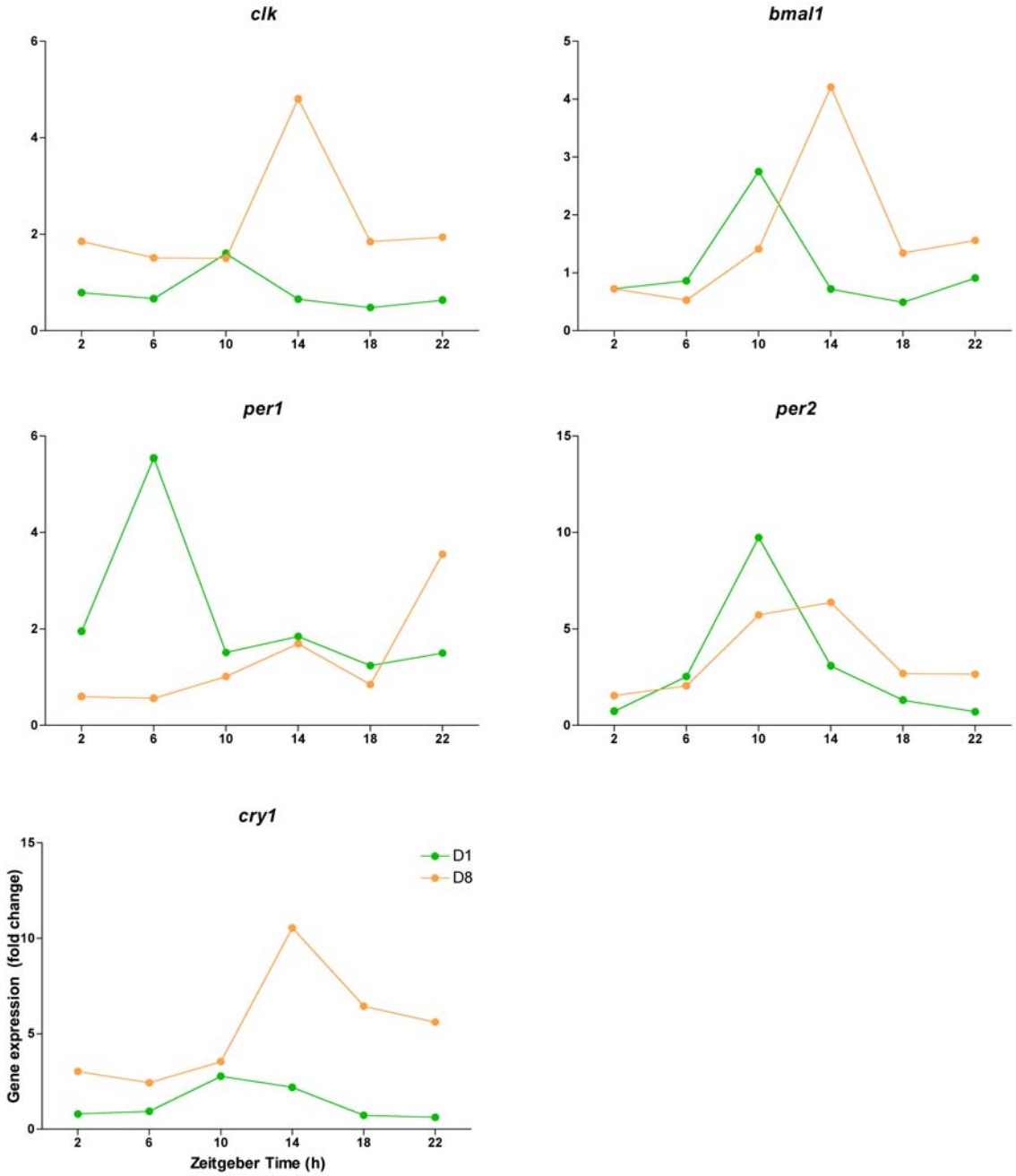

Figure 5.6 This pooled sample, sample #1, shows relatively rhythmic gene expression of all the clock genes on both D1 (green) and D8 (orange).

5.3.2.4 ARRHYTHMIC PROFILE

The arrhythmic profile of gene expression is characterised by very low general levels of clock gene expression, typified by sample #5 (Figure 5.7). The pattern of 24-hour gene expression of all of the clock genes on D1 and D8 did not closely resemble a sigmoid curve, and the peaks of expression throughout the 24-hour period were not as immediately obvious as they were in other samples, except sample #6, which also had

relatively low general levels of clock gene expression. Bearing in mind the low levels of gene expression denoted by the *y* axes, there was a downward trend in gene expression from ZT 2 to ZT 22 across the 24-hour period on D1 and an upward trend between ZT 2 and ZT 22 on D8. On D1, the lowest level of gene expression occurred at ZT 22 for all the clock genes, except *per1* which had its lowest level of expression occurring earlier, at ZT 18. The highest level of clock gene expression on D1 tended to occur at either ZT 2 or ZT 10. On D8, the highest level of expression was observed with all the clock genes at ZT 22. The lowest level of gene expression occurred at ZT 6 in all of the clock genes, except *per2* which occurred earlier at ZT 2. As noted, in both the high expression and the rhythmic profiles was evident, there was again an increase in the general level of clock gene expression on D8 compared to that of D1, except for *per1*, which demonstrated the reverse.

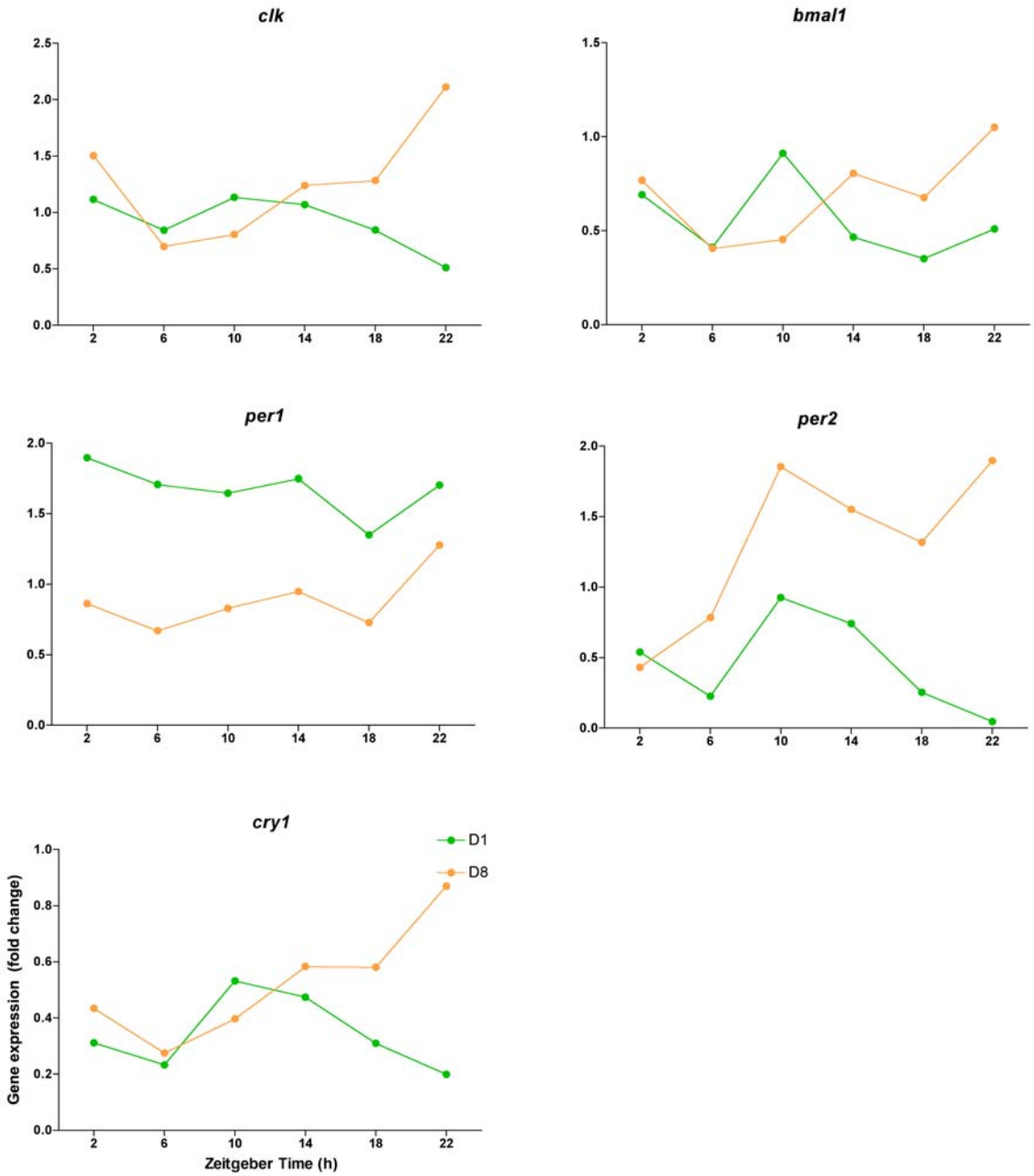

Figure 5.7 This pooled sample, sample #5, shows relatively arrhythmic gene expression of all the clock genes, with very low fold-change in the level of gene expression.

5.3.2.5 THE *per1* GENE EXPRESSION

It was noticed that the expression profile of *per1* differed from that of the other clock genes on D1, the acrophase occurring earlier than those of the other clock genes in both the high expression profile (sample #4) and the rhythmic profile (sample #1), and with its level of general gene expression decreasing from D1 to D8, reverse to the

trend that was observed with the other clock genes in the arrhythmic profile (sample #5). The 24-hour expression profiles of *per1* on D1 and D8 were therefore examined to see if they bucked the trend in all of the samples. This did indeed turn out to be the case. The general level of gene expression on D8 was found to be lower than that on D1, in all the samples (Figure 5.8).

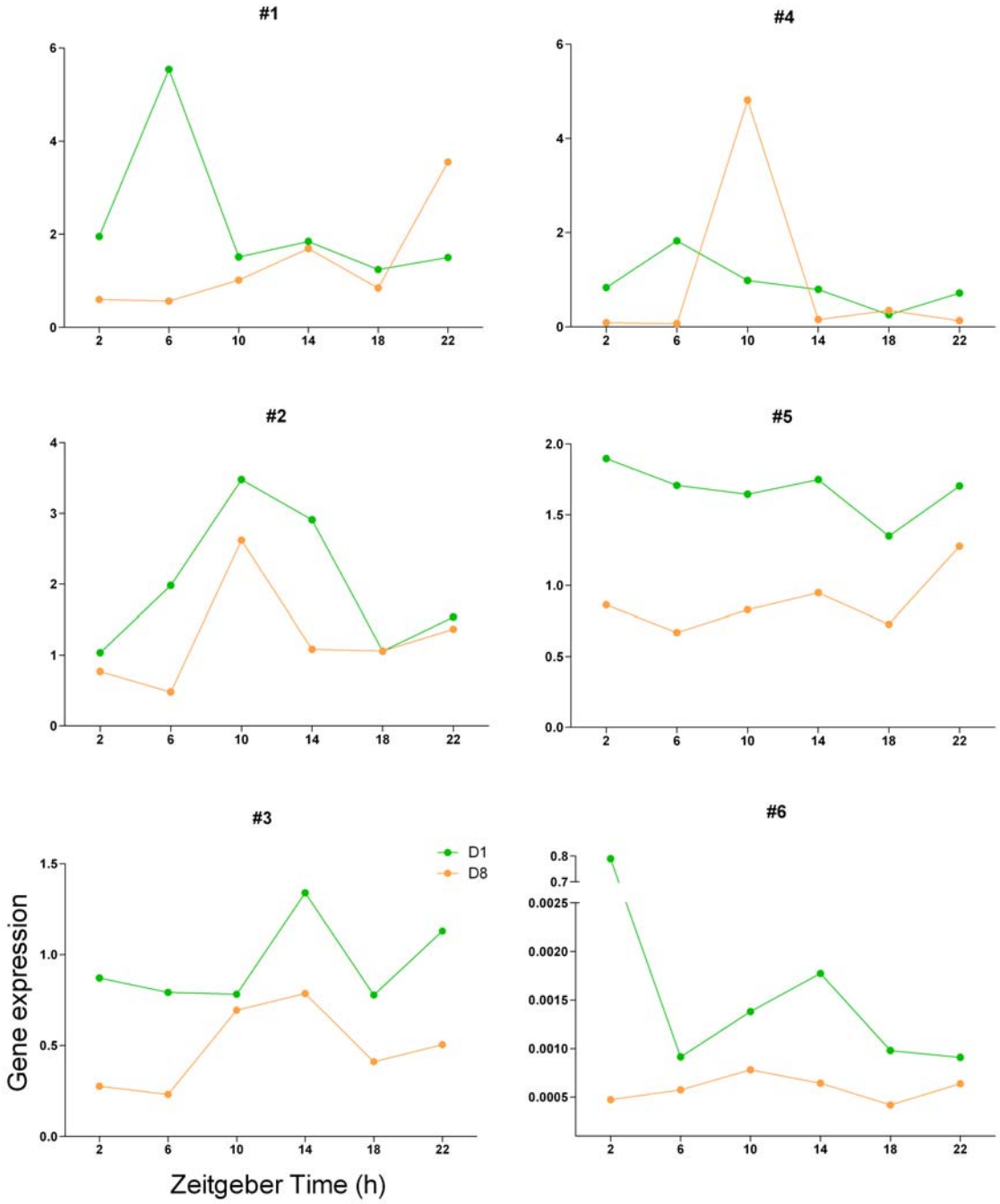

Figure 5.8 24-hour *per1* gene expression in the different LGC samples, on D1 (green) and D8 (orange).

5.3.2.6 CHANGES IN ACROPHASE

Differences in the acrophase of the 24-hour profiles of the different clock genes were analysed in all of the samples, from D1, D8 and D8 with hCG treatment (Figure 5.9). The differences in the acrophases may represent phase shifts in the circadian rhythms of the clock genes in the LGCs. All of the clock gene acrophases were phase delayed, occurring later on D8 than they did on D1. This phase delay is likely to be *bona fide* as the standard errors of the mean, indicated by the error bars generally do not extend beyond the line that separates phase advances from phase delays (Figure 5.9). This line is demarcated by the dotted line that lines up with zero on the *y* axis.

Treatment with hCG on D8 phase advanced the acrophases and putative circadian rhythms of all of the clock genes (Figure 5.9). This phase advance is again, likely to be *bona fide*, as the standard errors of the mean, indicated by the error bars, do not extend over the line between phase advance and phase delay.

Whether the hCG treatment restored the timing of the D8 acrophases to that of D1 was then assessed (Figure 5.9). If the hCG treatment advanced the acrophases to the same degree as they were delayed from D1 to D8, no change should be observed between the acrophase timing on D8 hCG and D1. This was generally the case. Although, not all the data points fell exactly on the zero-line that indicated no change, the standard errors of the mean all, except that of *per1*, fell across this line. Therefore there is no net change in the timing of the acrophases of the circadian rhythms of *clk*, *bmal1*, *per2* and *cry1* between D8 hCG and D1. The hCG treatment did effectively restore the timing of the acrophases of these genes to that of D1. The *per1* gene is the only exception, once again bucking the trend.

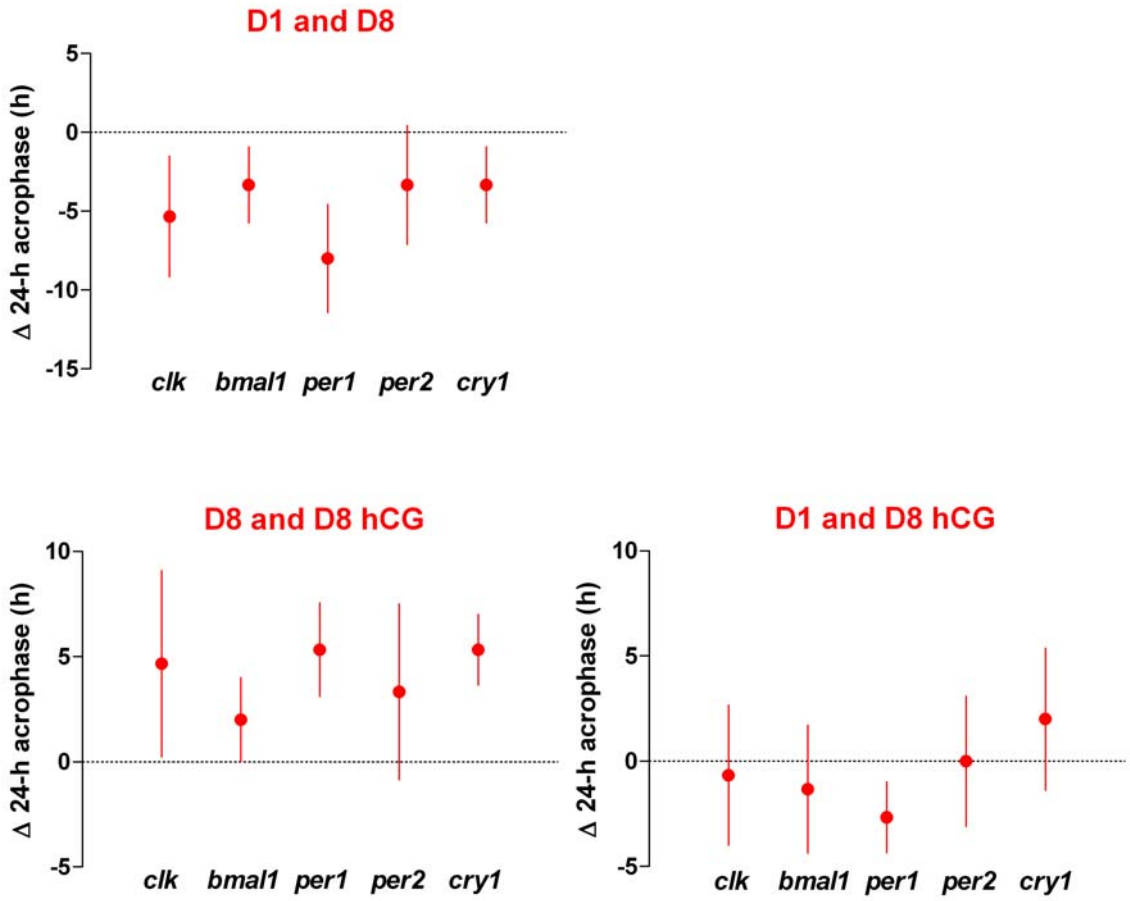

Figure 5.9 Changes in acrophase of 24-hour clock gene expression from LGCs between days one (D1) and eight (D8) of culture, with (D8 hCG) and without hCG (D8). The error bars refer to the standard error of the mean.

5.3.2.7 CHANGES IN MEAN 24-HOUR GENE EXPRESSION LEVELS BETWEEN D1, D8 AND D8 hCG

There appeared to be differences in the degree to which the levels of gene expression of the clock genes in the LGCs changed across the 24-h profiles, between D1 and D8. The mean levels of gene expression were calculated for all the 24-hour gene expression profiles of all of the clock genes, on D1 and D8, with and without hCG treatment. These were then compared to see if any consistent changes could be detected between the means of the D1 and D8 circadian rhythms. It is assumed that the greater the mean level of gene expression, the more robust the gene expression, and the more reliable the result. The comparison of the mean values between D1 and D8 revealed that there was effectively no change in the general level of the *bmal1*, *per1* and *per2* gene expression (Figure 5.10). This is demonstrated by the extension

of the standard errors of the mean beyond the boundary that demarcates the increase from the decrease in the general amount of gene expression. This boundary can be seen in the graph as a dotted line, which lines up with zero on the *y* axis, indicating that there is zero or no change in the average level of gene expression. The means of the *clk* and *cry1* gene expression however increased after eight days in culture.

The treatment of the LGCs with hCG on D8 increased the mean level of gene expression of all of the clock gene rhythms, excluding *clk* compared to D8 without hCG (as well as compared to D1) (Figure 5.10 and Figure 5.11). The *per2* gene was particularly affected by hCG treatment, although the large standard error of the mean indicated that there was a large variation in the extent of the increase. The hCG-induced increase of the level of the clock gene expression was sufficiently great that virtually all of the clock gene means were greater than those of D8 as well as those of D1. The hCG therefore increased the general level of gene expression of the *bmal1*, *per1* and *per2* genes from those of D8, that had remained unchanged from those of D1, while increasing even further the level of the *clk* and *bmal1* gene expression that had already increased after eight days spent in culture.

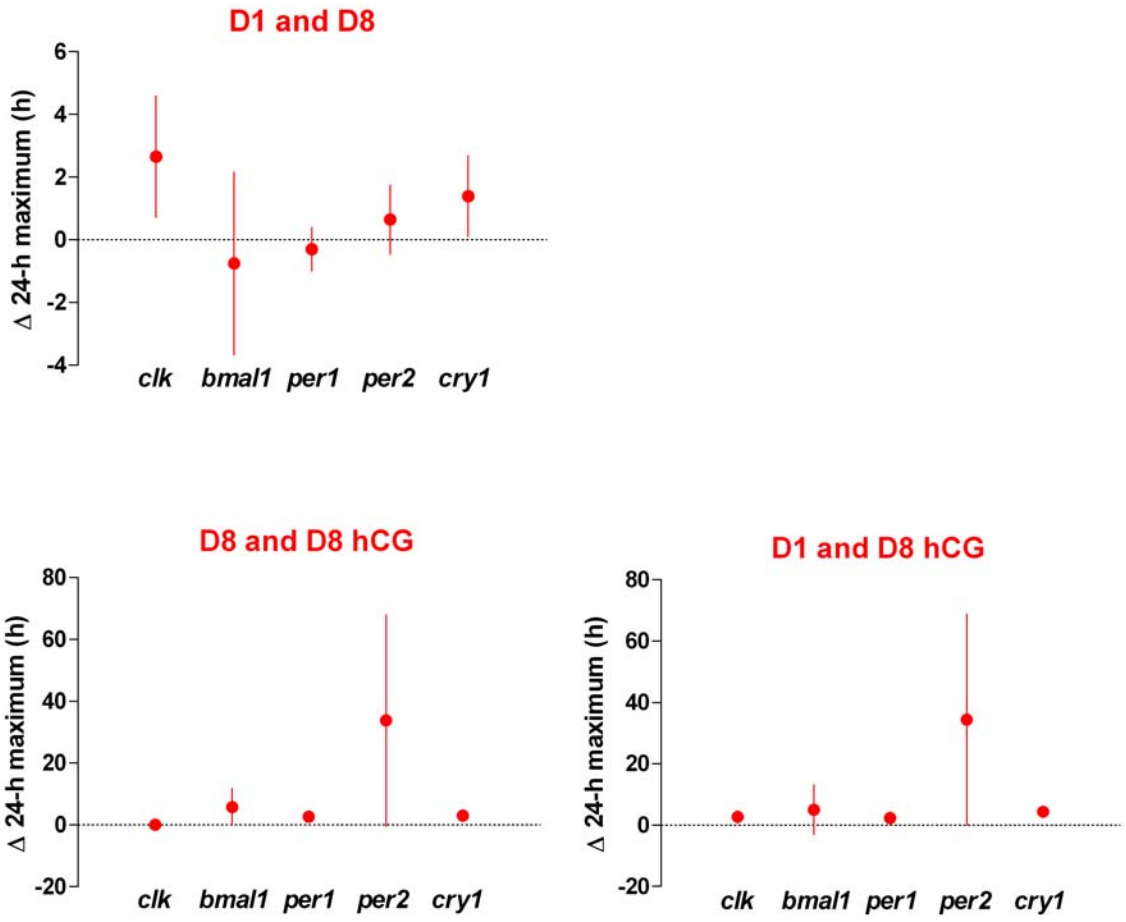

Figure 5.10 Changes in the average 24-hour level of clock gene expression in the LGCs between days one (D1) and eight (D8) of culture, with (D8 hCG) and without hCG (D8). The error bars refer to the standard error of the mean.

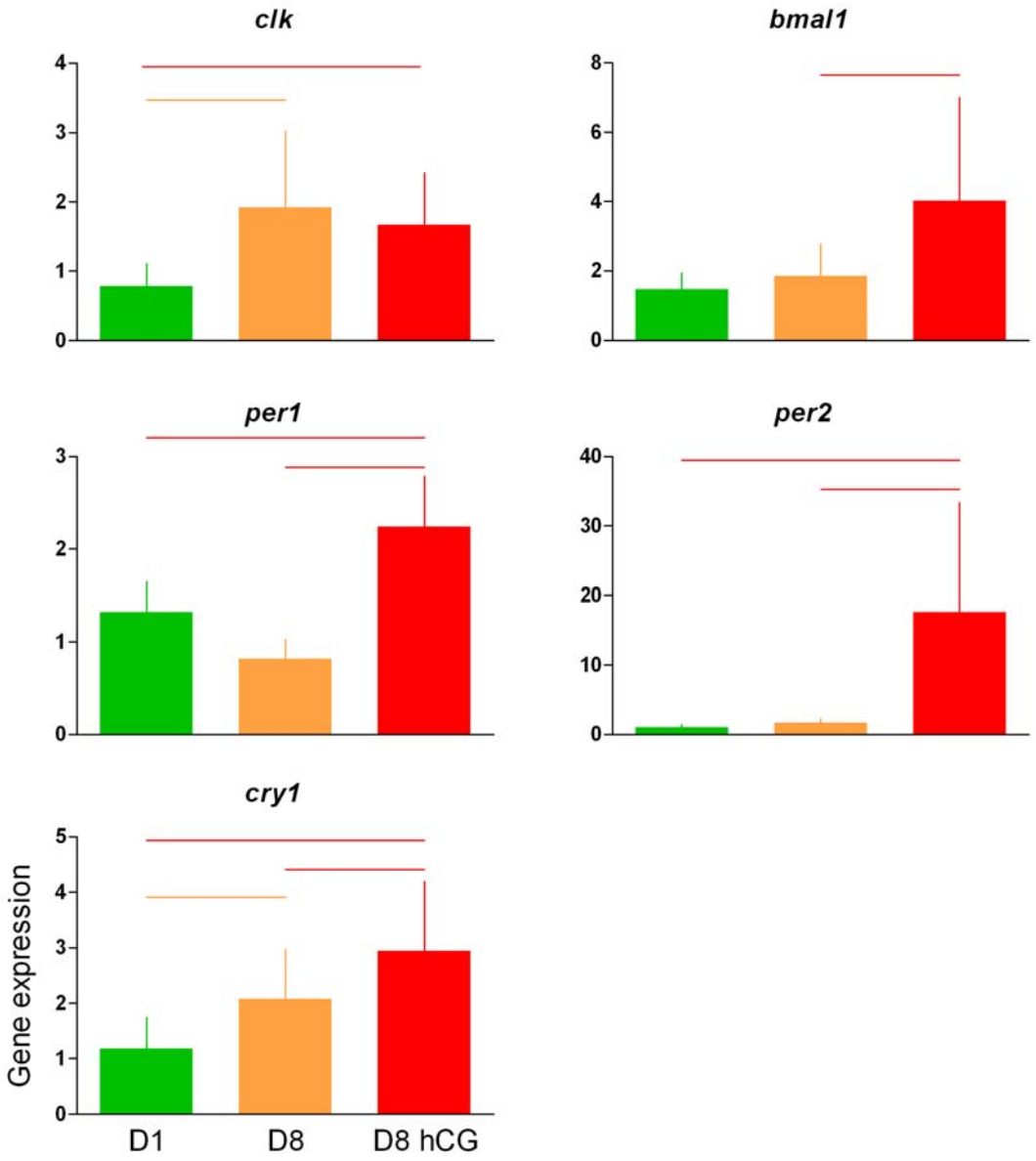

Figure 5.11 Histograms of the mean level of 24-hour gene expression of each of the clock genes on days one (D1) and eight (D1) of culture, with (D8 hCG) and without hCG (D8). The horizontal bars represent differences that were flagged in Figure 5.10 as lying away from zero on the *y* axis. The error bars refer to the standard error of the mean.

5.3.2.8 STATISTICAL ANALYSIS

In order to further analyse the quantitative gene expression data, using statistics, an analysis of the variance (ANOVA) was conducted. This involved the analysis of the individual and pooled samples together, in a data set that comprised an *n* number of 6 (n=6).

One-way ANOVA assessed whether the amount of expression of one of the clock genes varied significantly across the 24-hour period, in all six samples, on either D1 or D8, with or without hCG treatment. No significant variances could be found in the 24-hour gene expression profiles of any of the clock genes, during D1 or D8, with or without hCG treatment (Figure 5.12).

Two-way ANOVA assessed whether the 24-hour gene expression variances of one of the clock genes varied significantly between D1 and D8, with or without hCG treatment. The 24-hour variances of the clock gene expression profiles were not significant between D1, D8 and D8 hCG (Figure 5.12).

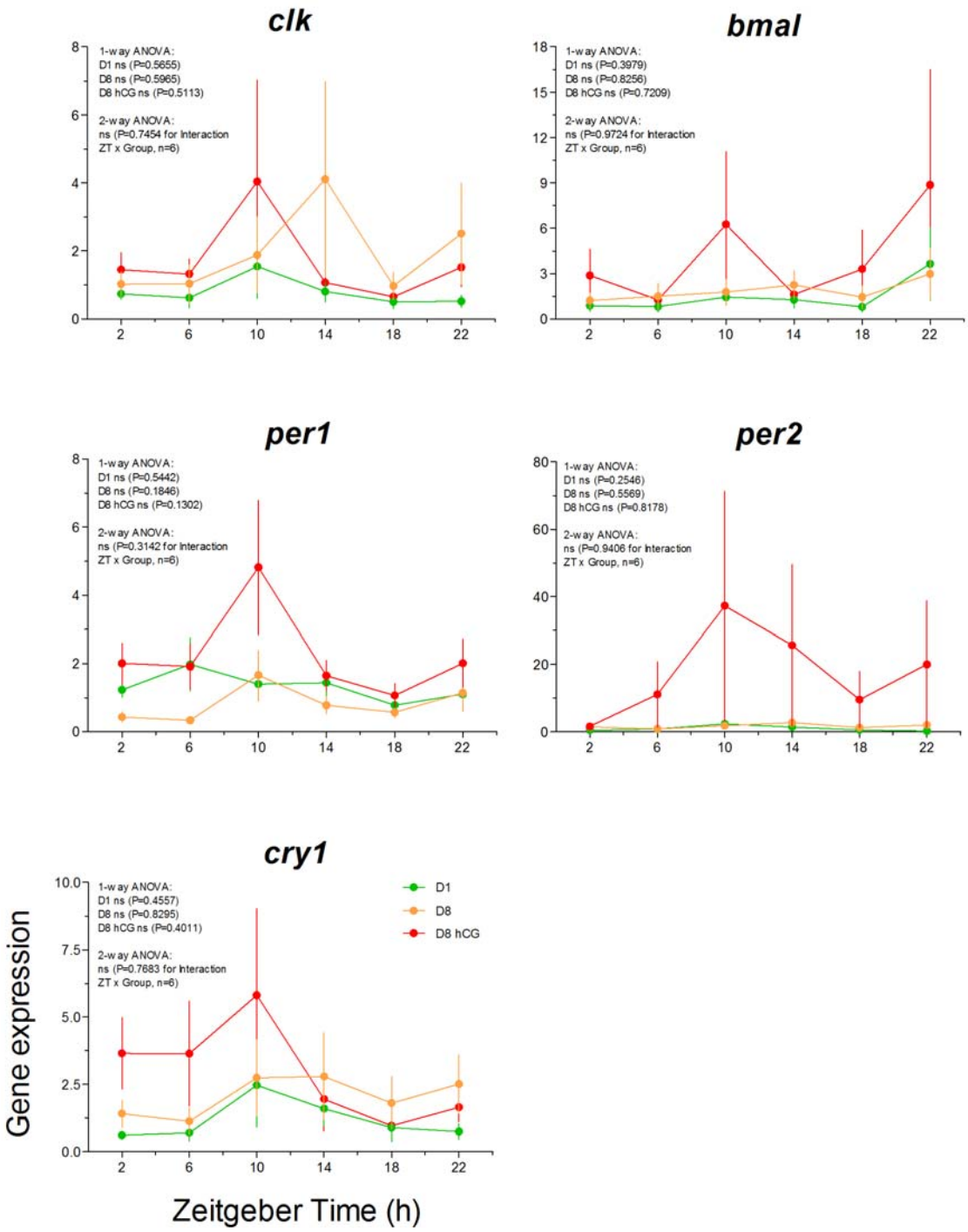

Figure 5.12 The data from the pooled and individual samples were placed into a single data set (*n*=6) and analysed statistically using one-way analysis of variance (1-way ANOVA) to ascertain whether the gene expression profile varied significantly across 24 hours, and using two-way analysis of variance (2-way ANOVA) to ascertain whether the 24-h profiles varied significantly between D1 (green), D8 (orange) and D8 hCG (red) for each clock gene. The error bars refer to the standard error of the mean.

Overall, there were no significant changes in 24-h clock gene expression of any of the measured clock genes, *clk*, *bmal1*, *per1*, *per2* and *cry1*, after 1 day (D1) or 8 days (D8) of culture or with hCG treatment after 8 days (D8 hCG) of culture. This is likely

to be due to the large standard errors of the mean, which indicate a relatively large variation in the levels of gene expression elicited by the different samples. Despite this, trends could be observed. The peak levels of gene expression across 24 hours tended to be delayed by eight days spent in culture, and this delay could be reversed by hCG treatment on the eighth day of culture. The maximal differences between the peak and trough levels of clock gene expression across 24 hours on D1 and D8 were diminished by hCG treatment on D8. The expression of the *per1* gene tended to differ from the expression of the other clock genes.

5.3.3 24-HOUR CLOCK GENE EXPRESSION IN LUTEAL FIBROBLAST-LIKE CELLS

The clock genes: *clk*, *bmal1*, *per1*, *per2* and *cry1*, were all expressed in the luteal fibroblast-like cells. The 24-hour expression profiles varied greatly between samples; and a representative data set of one study is illustrated in Figure 5.13. The circadian rhythmic expression was evident for all of the clock gene profiles. Serum shock increased the amplitudes of the circadian expression of *clk*, *bmal1*, *per2*, *cry1* and possibly *per1*. The serum shock-induced increase in amplitude may indicate the successful resynchronisation of the cell-based circadian clocks with the luteal fibroblast-like cell populations. The acrophases of *clk*, *bmal1* and *per2* coincided at ZT 14. The serum shock did not alter the timing of these acrophases, nor did it appear to phase shift any of these circadian rhythms. The acrophase of *cry1* also occurred at ZT 14 without serum shock, but was phase advanced to ZT 10 by the serum shock. The acrophase of *per1* occurred at ZT 22 after serum shock but the level of expression was very low compared to that of the other clock genes.

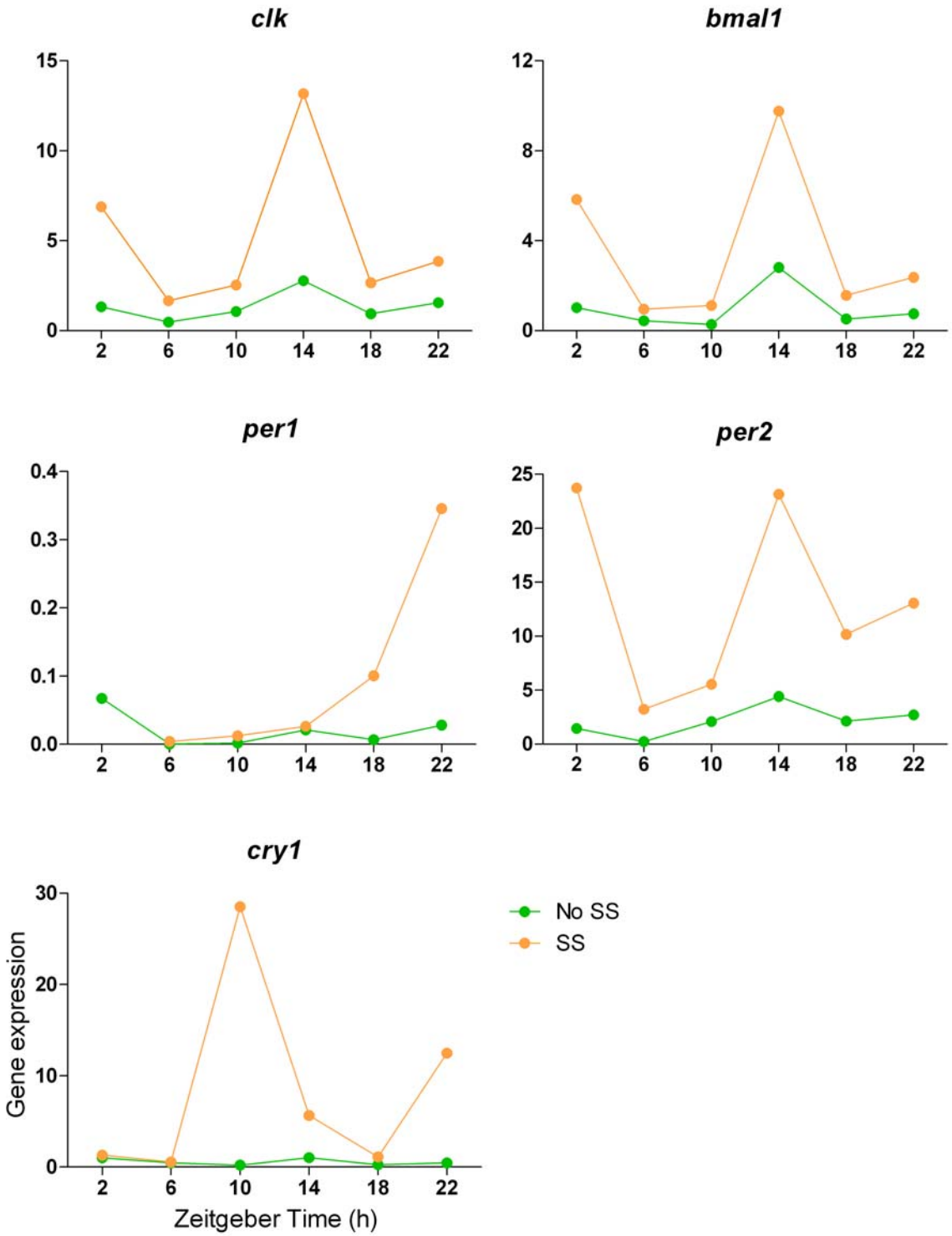

Figure 5.13 Graphs of clock gene expression, measured using fold change, in cultured luteal fibroblast-like cells over 24 h, treated with (SS) (orange) and without serum shock (No SS) (green) (*n*=1).

5.4 DISCUSSION

All the five clock genes investigated: *clk*, *bmal1*, *per1*, *per2* and *cry1*, were found to be expressed in the LGCs and the luteal fibroblast-like cells. The 24-hour patterns in the level of mRNA expression of these genes were found to vary greatly between individual samples of the LGCs. Although these 24-hour patterns were categorised into high expression, rhythmic or arrhythmic profiles, there was however, no significant change in the level of gene expression of any of the five clock genes, across 24 hours, on either D1 or D8, with or without hCG treatment. The lack of statistical evidence supporting a change in the level of gene expression over the 24-hour period however precludes the strict appellation of *circadian* gene expression to the clock gene expression profiles.

It could be argued however that, even with the lack of statistical support, the gene expression that was observed in the LGCs is rhythmic. This argument hinges on the consistent phase shifts of the putative acrophases in the 24-hour expression of all of the clock genes between D1 and D8 and between D8 with and D8 without hCG. This >4 hour phase delay occurs consistently for all five clock genes over eight days between D1 and D8, and is compatible with the existence of an endogenous oscillation in the 24-hour expression of all of the clock genes. Furthermore, this phase delay is reversed by hCG treatment, which phase advances the expression of all the clock genes, such that their putative acrophases are phase shifted by >4 hours. This hCG-mediated phase advance, in the opposite direction to the time-mediated phase delay, consistently appears to be of the same magnitude as the phase delay for each of the individual clock genes. Thus, hCG reverses the effect of time on the phase, the actual timing, of the clock gene circadian rhythms.

A constant oscillation time period, in effect, *tau,* can be calculated for these rhythms. *Tau* is often used in circadian physiology to describe a free-running period, the portion of time taken to complete one oscillation in the absence of entraining zeitgebers. The average human *tau* is 24.2 hours (Czeisler and Gooley, 2007). The *tau* in this case is not precisely free-running, but can still be calculated for the circadian oscillations, which are phase-responsive to hCG. *Tau* is calculated here,

based on the knowledge that the phase shifts by approximately five hours over the course of eight days, and presuming that the D1 oscillation was that of the entrained period and circadian, so 24 hours, rather than ultradian or infradian. The tau therefore, of the LGC endogenous oscillation, is ~24.6 hours. This indicates that 0.6 hours, has been added every day, for eight days, to produce a >4 hour-delay in the timing of the clock gene expression in the LGCs. It is notable that the period of the LGCs is, like the free-running *tau* of the human as a whole, slightly longer than the period of a geophysical day: 24 hours.

The oscillations in the clock gene expression were however difficult to quantify in combination. There was a relatively great range of expression profiles, in terms of timing of the acrophase, frequency and amplitude of the oscillations, as well as in terms of effect of time spent in culture and hCG treatment. The extent to which the clock gene 24-hour expression profiles varied may be a real representation of the gene expression in the samples of cultured LGCs and luteal fibroblast-like cells. This variability may arise from a population of cells, possessing cell-based clocks, which run autonomously of each other. The autonomy of the endogenous clocks may be normally overrided by an entraining signal in the intact CL. The requirement of extrinsic rather than intrinsic entrainment is a feature of peripheral clocks. Looser coupling of the cellular circadian clocks is thought to confer greater flexibility, allowing these cell-based clocks to respond more rapidly and less noisily to temporal stimulus. This enables the better integration and co-ordination of temporal information from and to the various other clocks and pacemakers around the body, in order to orchestrate their various temporally regulated processes into a harmonious and unified whole-body physiology.

The human CL could therefore be a novel peripheral clock tissue. Consider that each luteal cell in an intact CL contains a circadian clock, and that these clocks are able to run autonomously, and do so, in order to provide the constant synthesis and secretion of progesterone. The gene of the StAR protein, which provides the rate-limiting step in steroid hormone production, has been reported to be rhythmically expressed, in a circadian fashion in poultry (Nakao et al., 2007). StAR is involved in the transport of the steroid substrate, cholesterol, from the outer membrane of the mitochondria to the inner membrane of the mitochondria. This is where cholesterol side chains are

cleaved to produce pregnenolone, which is an intermediate metabolite of the progesterone synthesis pathway. The circadian expression of StAR has been proposed to be clock gene driven and is responsive to LH signalling. This implies that there is a temporal component involved in the regulation of steroidogenesis. Time is often used to segregate biochemical processes that would be incompatible were they to occur simultaneously in the cell. Therefore, it is possible that individual steroidogenic cells can synthesise P_4 only at certain times, or only at a certain rate at certain times. Undoubtedly, there is a wave-like pattern to the P_4 concentrations that are secreted from the CL, which occurs as a result of pulsatile LH signalling to the CL. However, this P_4 secretion pattern is not pulsatile, nor is it circadian. It would appear rather, that it is secreted relatively constantly. The provision of a relatively constant concentration of P_4 is probably crucial because a drop in P_4 levels can result in increased uterine activity that can end gestation and cause the failure of the pregnancy (Mesiano, 2004). P_4 may even be involved in the regulation of the uterine endometrial clock genes, which are likely to be involved in the regulation of the proliferation, differentiation and function of the endometrium during pregnancy as well as during the non-conceptive menstrual cycle. This is supported by evidence that P_4 administration was able to synchronise the circadian rhythms of *per2* in rodent uterine endometrial stromal cells *in vivo* (Hirata et al., 2008).

It is hypothesised that clock genes function to regulate the rhythmic synthesis and secretion of P_4 from individual luteal cells, such that the P_4 output from the whole CL tissue is relatively constant. It is probable that clock genes function to modulate the circadian expression and possibly also the post-translation modification of StAR, which in turn regulates the rhythmic synthesis of P_4. As there is no evidence of P_4 being stored in large amounts in the steroidogenic cells, it is likely that the P_4 is thus, also rhythmically secreted by cells (Niswender et al., 2000). The clock genes are therefore likely to also mediate the co-ordination of the rhythmic P_4 secretion from individual cells, such that a relatively constant provision of P_4 is produced by the CL tissue as a whole. In order for there to be a constant provision of P_4 from the CL, there must at any one time be a proportion of steroidogenic cells actively secreting P_4. Thus, in order to ensure that the rhythmic cellular P_4 output of the entire CL is kept relatively constant, in the face of pulsatile inputs such as LH, the individual steroidogenic cells must therefore time their putatively temporally regulated P_4

synthesis and secretion, so that at any one time, there is a relatively constant proportion of the steroidogenic cell population secreting P_4. These necessarily discordant cellular clocks must therefore be co-ordinated to a certain degree, by extrinsic or intrinsic signals or perhaps a combination of both.

A candidate signalling molecule that may co-ordinate the timing of the discordant luteal clocks is hCG, which has been reported to be released in a temporally regulated manner from placental tissue *ex vivo* (Barnea et al., 1992, Barnea and Kaplan, 1989). The putatively pulsatile hCG may act to resynchronise the luteal clocks, thereby facilitating the maintenance of co-ordinated temporal luteal steroidogenic function. However, the accepted wisdom is that hCG, unlike LH, is not pulsatily released. It is however very possible that it interacts in another, as yet unknown, way with the luteal cell clocks, to mediate some temporal co-ordination. It has been observed in the current study that hCG treatment of the LGCs on D8 at ZT 0 restores certain features to 24-hour clock gene expression, along with steroidogenic function. The timing of the acrophases of all of the clock genes shifted from the first to the eighth day in culture. The treatment of the LGCs on D8 with hCG however, returned the timing of these acrophases from the shifted D8 times to the previous D1 times. It would appear therefore that the hCG treatment is effectively *resetting* the clock gene-driven timers in the LGCs. The same could be true in the intact human CL of pregnancy. The hCG treatment also affected the average 24-hour level of gene expression of the putative rhythms in the clock gene expression of all five genes. The average amounts of gene expression were increased by the hCG treatment, which is consistent with the hCG synchronising the LGC clocks, so that they function more effectively and thus, collectively produce a higher level of gene expression.

It is also notable that there was no real change in mean levels of *bmal1*, *per1* and *per2* gene expression between D1 and D8. D1 may mark the time during which the LGCs are maturing from, effectively, the early luteal phase to a time of full function. D8 may represent the time when the cells of an intact human CL start to decline, as they move from the mid-luteal to the late luteal phase. The same level of clock gene expression on D1, which was sufficient for fully functional luteal P_4 synthesis and secretion, may no longer be sufficient by D8 for the synthesis and secretion of P_4 to the same concentrations. The hCG treatment increased the level of gene expression in

all the clock genes, which corresponded to the resumption or maintenance of fully functional P_4 synthesis and secretion to the same levels as those produced on D1. It would therefore appear that the increased requirement for hCG that these LGCs exhibit over time may be related to the requirement for increasing levels of clock gene expression over time. This may also explain the requirement for increasing amounts of hCG with time. If a certain amount of hCG produced a corresponding amount of clock gene expression, then the need for increasing amounts of clock gene expression would require correspondingly increasing amounts of hCG. In this way, the gradient of hCG concentrations needed to maintain the LGCs and the intact human CL may reflect the a gradient of increasing clock gene expression that is required by the LGCs and CL *in vivo* with time. However, the LGC system may still be employed. If these hypotheses were true, increasing levels of clock gene expression should be detected in the LGCs, the longer they are maintained in culture by sufficient, and therefore increasing amounts of hCG. The increase in clock gene expression could also impact on the overall amount of P_4 secretion, which has been observed to increase with time, in hCG-rescued LGCs that have been supplemented with LDL. These cells have been observed to produce P_4 concentrations greater than those of D1. There may therefore exist a mechanism, where increasing P_4 levels from the CL act to provide temporal information, in the form of a timer (accruing in time rather than oscillating in time), to the uterus to synchronise its endometrial clock gene expression, which then effects the provision of hCG in increasing amounts from the feto-placental unit to the CL, where the hCG resets the rhythmic expression of clock genes and where the temporal information from the hypothalamus can be integrated in the form of pulsatile LH. In this way, the timing of the various temporally regulated processes of the reproductive tract can be co-ordinated and integrated with the timing in the rest of the body.

There co-ordination of the putative discordant luteal clocks may also be intrinsically regulated by timing information emanating form the luteal cells themselves. Autocrine and paracrine interactions amongst luteal cells have already been shown to be crucial for luteal function (Duncan et al., 2009). The response of the luteal fibroblast-like cells to serum shock indicates that these cells, which model luteal fibroblasts, are able to receive entraining signals and respond by increasing the amplitudes of their rhythmic clock gene expression. The entrainment of cellular circadian clocks by serum shock can be reproduced *in vitro* by a variety of chemicals

and acute perturbations of the cell culture system (Schibler et al., 2003). The luteal fibroblast-like cell response to serum shock is therefore unlikely to be restricted to serum shock, and is probably elicited *in vivo* by other signalling molecules. This means that their clocks may be somewhat enslaved by the circadian outputs of the cells immediately around them. If this were true of luteal fibroblasts *in vivo*, these cells may be well placed to integrate the temporal information emitted by neighbouring cells via paracrine signalling; cells such as other fibroblasts and steroidogenic cells. Luteal fibroblasts are known to possess P_4 receptors and P_4 is known to be LH/hCG responsive (Maybin and Duncan, 2004, Duncan et al., 2005a). Furthermore, P_4 is involved in paracrine signalling and has also been reported to entrain *per2* expression in uterine endometrial stromal cells (Duncan et al., 2009, Hirata et al., 2008).

The fibroblasts may also be able to emit temporally-entraining paracrine factors, which affect other fibroblasts and other cells of various luteal cell types. It could be imagined therefore, that an auto-regulated system exists in the CL, co-ordinated by the variously timed cellular clocks, for the maintenance of loose temporal synchrony between cells. The exceptional expression of *per1* may also be involved in some way as it does not seem to be as robustly circadian or as responsive as the other clock genes, suggesting that it may have a stabilising influence on the luteal clocks, which might otherwise be too responsive. The classic two-cell theory of œstradiol synthesis already establishes a precedent for the co-ordination of a crucial and complex biochemical process, using communication, which is essential, between two types of cell, within the CL (Johnson and Everitt, 2000). It describes the process of œstrogen synthesis, which is performed jointly by the theca cells and granulosa cells of the ovarian follicle. The theca-lutein and granulosa-lutein cells, derived from these same follicular cells, are thought to maintain this relationship, in addition to the independent granulosa-lutein cell steroidogenesis, which evolved when they acquired LH receptors. This mechanism may also then be co-opted by the luteal cells for the establishment of communication networks between multiple cell types, which are used to provide temporal regulation of luteal function and lifespan.

Although a link between circadian rhythmicity and steroidogenesis in the mammalian ovary has not yet been discovered, one has been revealed in the avian ovary (Nakao et

al., 2007). The mature pre-ovulatory follicles of chickens develop synchronised clock gene rhythms in their granulosa cells, which regulate the rhythmic secretion of P_4 and affect the timing of ovulation. This circadian clockwork is not evident in the early ovarian follicle, indicating that it develops with the proliferation of the granulosa cells during follicular development, under gonadotrophin regulation. Gonadotrophins may thus affect the expression of circadian clockwork. The effect of hCG on the LGCs may therefore represent the first example of a similar link between circadian rhythmicity, steroidogenesis and gonadotrophins in the mammalian female reproductive system.

Overall, the results of this chapter, though largely speculative, have been potentially very informative, though statistically robust corroboration would be preferred. It may be that the variation proposed to arise from discordant cellular clocks arises from a functionally heterogeneous cell population, composed as they are of LGCs from different follicles at varying stages of maturity, which in some instances, have been obtained from more than one woman. It could also be argued that the culturing of the LGCs abolishes the cell-to-cell communication channels that are clearly essential for the full function of the CL as a whole. This argument could even be supported by the more robust circadian-like gene expression profiles observed in the confluent cultured luteal fibroblast-like cells. It is possible that the increase in the level of clock gene expression and in the robustness of the putatively rhythmic gene expression in these cells, is due to the establishment of the cell-to-cell communication, which occurred as the cells were able to proliferate. It is also notable that the there was no tissue-wide synchrony in the clock protein levels and cellular compartmentalisation observed in the intact CL in Chapter 2.

One final point of interest was that there was also no antiphasic relationship in the 24-hour clock gene expression profiles between the genes belonging to the negative limb and the positive limb of the circadian clock mechanism. This may indicate that the time delay from the peak mRNA expression to the peak protein accumulation in the cytoplasm and nucleus varies for the different clock genes. The regulation of the luteal clock may thus be largely post-translational. This equivocal evidence coupled with the lack of statistical significance in the results of this chapter, means that it has not been possible to establish whether any of the five clock genes are expressed in a

circadian rhythm in the cells representing the human CL. The findings of this chapter do however indicate that there is a likely interaction between the expression of the clock genes and luteal steroidogenic function, survival and lifespan, particularly with regards to the effect of gonadotrophin action.

In summary, this chapter has demonstrated for the first time that:

1. the clock genes: *clk*, *bmal1*, *per1*, *per2* and *chy1*, are expressed in the human LGCs and luteal fibroblast-like cells;

2. these genes appear to be rhythmically expressed across 24 hours;

3. the clock gene expression in the LGCs appeared to be affected by time spent in culture and hCG treatment:

    a. with the timing of the acrophases of the apparently rhythmic clock gene expression becoming phase delayed after eight days in culture, and being phased advanced by hCG;

    b. with the mean amount of clock gene expression increasing in response to hCG treatment;

4. the mean levels of rhythmic clock gene expression was increased by serum shock of the luteal fibroblast-like cells;

5. the peaks in apparently rhythmic clock gene expression between the transcriptional activators (*clk* and *bmal1*) and transcriptional repressors (*per1*, *per2* and *cry1*) were not in antiphase in the LGCs.

The question of whether the clock genes are circadian rhythmically expressed in the CL is still a crucial one which needs to be answered. Therefore, another model was employed, one that samples intact corpora lutea, preserving the intercellular communication channels that may be crucial for luteal function and

for the transmission of temporal information in the regulation of the CL and its lifespan. This is the focus of the next chapter.

The question of whether the clock genes are circadian rhythmically expressed in the CL is still a crucial one that needs to be answered. Therefore, another model was employed, one that samples intact corpora lutea, preserving the intercellular communication channels that may be crucial for luteal function and for the transmission of temporal information in the regulation of the CL and its lifespan. This is the focus of the next chapter.

6 CLOCK GENE EXPRESSION IN THE OVINE CORPUS LUTEUM

6.1 INTRODUCTION

It has not yet been possible to establish whether the clock genes in the CL are expressed in circadian rhythms and whether these rhythms segregate antiphasically, between the transcriptional activator genes: *clk* and *bmal1* representing the positive limb of the circadian clock mechanism, and the transcriptional inactivator genes: *per1*, *per2*, *cry1* and *cry2* representing the negative limb of the circadian clock mechanism, which would indicate the presence of a circadian clock in this tissue. As it was not possible to sample corpora lutea from women across a 24-hour time course, more readily available corpora lutea will be sampled from sheep.

Sheep are a long-lived, diurnal mammalian species, which possess a seasonally regulated reproductive axis. The Soay breed is particularly useful as it is relatively primitive and as such, still possesses much of the strict temporal regulation of reproduction that more commercial breeds have been outbred to lose. The sheep species has been successfully used in many previous studies, modelling the reproductive axis and ovarian function (Spencer and Bazer, 2002, Campbell et al., 2003).

The sheep CL is generated in much the same way as it is in humans. It is formed from the follicular cells after ovulation, which has occurred following a pre-ovulatory LH surge. The follicular cells rapidly differentiate and proliferate and the tissue remodels to form a steroidogenically active CL, that secretes P_4 (Niswender et al., 2000). The corpora lutea of sheep have a lifespan of approximately 14 ± 2 days. This lifespan is regulated in a fundamentally different way from that of humans. Humans employ a luteotrophic mechanism while sheep employs a luteolytic one, so pregnancy in humans is luteotrophic while in sheep, it is antiluteolytic. The key signalling

molecule is hCG in humans and $PGF_{2\alpha}$ in sheep. Ovine P_4 secretion inhibits uterine $PGF_{2\alpha}$ release and with time, the endometrial tissue loses its sensitivity to P_4 and so, $PGF_{2\alpha}$ is increasingly secreted. Thus, by virtue of its initial and continued secretion, P_4 is considered the key regulator of luteal lifespan in sheep (Schams and Berisha, 2004).

It is not just the uterine endometrial cells that secrete $PGF_{2\alpha}$; the CL itself secretes $PGF_{2\alpha}$. The effect of the luteal $PGF_{2\alpha}$ however is unlike that derived from the endometrium. The luteal $PGF_{2\alpha}$ is luteotrophic during the early and mid-luteal phases. Progesterone is again involved in regulating the $PGF_{2\alpha}$ secretion, this time from the CL. It has been observed that the inhibition of P_4 has produced opposite effects on $PGF_{2\alpha}$ release, depending on the luteal phase. Antagonism of P_4 during the EL phase results in a reduction of luteal $PGF_{2\alpha}$ secretion. Antagonism of P_4 during the mid-luteal phase however results in an increase in luteal $PGF_{2\alpha}$ secretion (Skarzynski et al., 2001). This apparently bimodal effect of P_4 on luteal $PGF_{2\alpha}$ clearly relates to its role in the regulation of luteolysis. This bimodal effect seems dependent on luteal phase. It follows then that the regulation of luteolysis and thus, luteal lifespan by P_4 is dependent on the luteal phase and ergo, timing. It is also possible that the exogeneous control of luteal lifespan, via the uterine and endometrial $PGF_{2\alpha}$, is regulated in a time-dependent manner. In other words, there could be a clock working at the level of the ovine uterus, endometrium and/or CL, that regulates the timing of the luteal lifespan. This is however less likely to be the case in humans, where the clock-control is more likely to be intrinsic to the CL alone. Despite the potential, the timing mechanism itself is likely to be conserved.

It must also be considered that the sheep is a seasonal animal which is only reproductively active during the winter months. Therefore, the animals in this study were kept under short day conditions to maintain the ovarian cycle. A well-known observation in sheep is the relay of photoperiodic information via the 24-hour melatonin rhythm. The melatonin signal is decoded in the brain and PT of the pituitary gland to affect the reproductive axis (Malpaux et al., 1999, Hanon et al., 2008). In the PT, the melatonin is able to directly activate *cry1* expression (Lincoln, 2006). Melatonin receptors have also been observed in luteal cells, though no clear

role for melatonin has been elucidated in the CL (Woo et al., 2001, Soares et al., 2003). This study therefore measured the melatonin concentration in the sheep, to investigate whether there was a temporal relationship between melatonin and clock gene expression in the CL.

This chapter aims to:-

1. characterise the expression of the clock genes: *bmal1*, *per1*, *per2*, *cry1* and *crye2* in the ovine CL across 24 hours and establish whether the phase relationships between the 24-hour gene expression profiles were consistent with a classical circadian clock;

2. determine whether the expression of clock genes, *bmal1*, *per1*, *per2*, *cry1* and *cry2* would differ between early and late luteal phases, either in terms of:-

    - overall levels of gene expression
    - phase shifts and/or phase relationships of gene expression;

3. investigate the relationship between luteal clock gene expression and melatonin secretion to see if *cry1* activation was consistent with that of a melatonin-target tissue, such as the PT.

6.2 MATERIALS AND METHODS

6.2.1 ANIMALS

All animals were treated and experimental procedures performed in compliance with the UK Animals Scientific Procedures Act of 1986.

Forty-five pubertal, yearling ewes of the Soay breed of feral sheep (16.54 ± 17.75 kg body weight), born in April and May were allowed to live and graze freely outdoors for the summer months. They were then brought indoors in November and housed in a barn area. They were then moved to light-controlled rooms at the start of December. They were maintained under short days (LD 8:16), mimicking the winter photoperiod. The time of daily lights-on (ZT 0) was constant at 0800 h (CT 8). They were fed a standardised diet of grass pellets: 500 g per animal (Vitagrass, Cumbria) daily, 1 h into the light phase (ZT 1). Hay and water were available *ad libitum*. White fluorescent strip lights provided approximately 160 lux at the animals' eye level during the light phase, whereas dim red light of less than approximately 5 lux was provided during the dark phase. Temperature in the animal rooms was regulated with a variable airflow system and heating to maintain the ambient temperature between 10 and 20°C. Spontaneous locomotor activity was recorded every 10 min by using infrared sensors with a Mini Mitter VitalView recorder (Mini Mitter, Sunriver, OR) that plotted actograms.

The reproductive cycles of the sheep were synchronised using exogeneous $PGF_{2\alpha}$, which provides a mechanism of inducing luteal regression. The use of $PGF_{2\alpha}$ and progestogen for the synchronisation of ovine reproductive cycles is routinely practiced. This study achieved synchronisation between animals using two cycles of $PGF_{2\alpha}$ and progestogen treatment, with the sheep becoming synchronised with each other to within two days. From mid-winter (January), the Soay ewes were injected intramuscularly with 0.4 ml of $PGF_{2\alpha}$, three times with 14-day intervals, to induce and thus synchronise ovulation and œstrous cycles. To further potentiate the synchronised entry into the breeding season, the ewes were primed with intravaginal P_4 sponges for 12 days prior to the first $PGF_{2\alpha}$ injection. The removal of the sponges just before

$PGF_{2\alpha}$ administration causes a dramatic fall in P_4 levels, which precipitate hormonal events that lead to the onset of œstrus within the following 36-48 h. The ram effect was also employed, where a sexually active, vasectomised ram was introduced into the same housings as the ewes. The ram effect consists of male pheromones, released from sebaceous and scent glands in the skin, inducing a rapid increase in the frequency of pulsatile luteinising hormone secretion, which in turn, promotes the entry into œstrous. Blood P_4 concentrations were measured using RIAs to confirm the synchronised, sexually active status of the ewes. Melatonin RIAs were also performed, using blood samples collected at ZT 2 – 3 during the subjective day, to establish the circadian status of the ewes. The RIAs were routinely performed using methods previously described (Gault et al., 2003).

6.2.2 SAMPLING

Ovulation occurs 72 h after the $PGF_{2\alpha}$ treatment followed by the formation of the CL over the next 12 days. Approximately half the sheep were killed on Day 3 of the luteal phase, called the early luteal (EL) phase. The remainder were killed on Day 10 of the luteal phase, called the late luteal (LL) phase. The ewes were killed by pentobarbital injection into the jugular vein. On both occasions, groups of four animals were sampled at four-hourly intervals, over 24 hours, starting at ZT 3. Immediately before killing, a blood sample was collected from the jugular vein with a syringe or Vacutainer® (BD, Oxford, UK). This was heparinised and centrifuged immediately after collection, and used for the measurement of P_4 and melatonin concentrations by RIA. The sheep killed during the dark phase of the LD cycle were killed without the lights on. An opaque black bag was placed over the head after death and remained in place until the brains were dissected from the skulls, to prevent any possible effect of light. The animals were weighed before removal of the ovaries. Not all of the sheep possessed a CL, which resulted in a *n* number of two for one of the time points: ZT 23 during the EL phase. The other *n* numbers during both EL and LL phases are also listed, in Table 6.1.

Zeitgeber time	EL phase sample *n* numbers	LL phase sample *n* numbers
3	4	4
7	3	4
11	3	4
15	4	4
19	3	5
23	2	5

Table 6.1 The *n* numbers of CL sampled at each 24-h time point during the EL and LL phases.

It is noted that the *n* of 2 can not provide a meaningful standard error of the mean, despite the presence of error bars for this time point in the graphical data presented in the Results section of this chapter.

The resected ovaries containing a CL were cut in half, so that the CL was also halved. The ovary halves were snap frozen on dry ice and once frozen, stored at -80^{o}C. RNase inhibitor solution was used on all surfaces and surgical instruments to help preserve the ovarian RNA. Care was taken to clean surfaces and surgical instruments between samples in order to avoid cross-contamination.

Pieces of adrenal gland and liver tissue were also randomly sampled from two sheep. These would be used as positive controls for the experiments.

6.2.3 TOTAL RNA EXTRACTION

To measure clock gene expression, total RNA was purified from homogenised luteal tissues using an RNeasy® Micro RNA extraction kit (Qiagen Ltd, West Sussex, UK) using the Total RNA Isolation from Animal Tissues spin protocol with the on-column DNase treatment (Qiagen Ltd, West Sussex, UK). A piece (5 mg) of each CL sample was thawed in 300 µl of Buffer RLT containing 1% β-mercaptoethanol, then disrupted and homogenised twice in an electronic Qiagen Tissue Lyser (Qiagen Ltd, West Sussex, UK), set at 10 000 revolutions per minute (rpm) for 3 min at room temperature. RNase-free water (590 µl) was then added to the sample. The

homogenate was pipetted into a sterile 2 ml microfuge tube. Proteinase K (Qiagen Ltd, West Sussex, UK) (10 µl) was then added to the homogenate and mixed thoroughly by pipetting. The homogenate was incubated with the enzyme for 10 min at 55°C. The sample was then centrifuged at 8 000 x *g* at room temperature. The supernatant was carefully pipetted into a sterile 2 ml microfuge tube and the pellet discarded.

Thereafter, 100% ethanol (450 µl) was added to precipitate the RNA. The sample (700 µl), including any precipitate that had formed, was then carefully pipetted into an RNeasy MinElute Spin Column in a 2 ml collection tube. The tube was then centrifuged for 15 s at 8 000 x *g*. The RNA was now bound to the silica-gel membrane in the RNeasy MinElute Column. The flow-through was discarded.

Buffer RW1 (350 µl) was then added to wash the RNeasy MinElute Spin Column. The tube was centrifuged for 15 s at 8 000 x *g* and the flow-through discarded. The RNA was then treated with deoxyribonuclease (DNase) to remove any template DNA, using a Qiagen RNase-free DNase set (Qiagen Ltd, West Sussex, UK). Next, 10 µl of DNase I stock solution (Qiagen Ltd, West Sussex, UK) was mixed gently with 70 µl of Buffer RDD, then added directly onto the RNeasy MinElute silica-gel membrane. The DNase was left to work in the column for 15 min at room temperature. The column was then washed by adding 350 µl of Buffer RW1 to the column and centrifuging for 15 s at 8 000 x *g*. The flow-through was discarded.

The column was transferred into a new 2 ml collection tube. Buffer RPE (500 µl) was then pipetted into the column and centrifuged for 15 s at 8 000 x *g*. The flow-through was discarded. The silica-gel membrane was then dried by the addition of 500 µl of 80% ethanol to the column, which was then centrifuged for 2 min at 8 000 x *g*. The flow-through and collection tube were discarded. The column was then dried more thoroughly. It was transferred to a new 2 ml collection tube. The cap was left open and then the tube centrifuged at maximum speed for 5 min in a bench microcentrifuge. The flow-through and collection tube were discarded.

The RNA was then eluted. The column was transferred to a 1.5 ml collection tube. RNase-free water (30 µl) was pipetted directly onto the centre of the silica-gel

membrane. The tube was closed and left to incubate on ice for 10 min. The tube was then centrifuged for 1 min at maximum speed on the bench centrifuge. This step was repeated with a second 30 µl volume of RNase-free water. The RNA was then quantified on an Agilent 2100 Bioanalyzer (Agilent Technologies UK Ltd, Wokingham, Berkshire, UK). RNase-free water was added to the RNA to achieve a final concentration of 100 ng/µl. The RNA was then stored at -80^{o}C.

6.2.4 RNA QUANTIFICATION

RNA extracted from the ovine corpora lutea was quantified using an Agilent RNA 6000 Nano LabChip® kit (Agilent Technologies UK Ltd, Wokingham, Berkshire, UK) on an Agilent 2100 Bioanalyzer (Agilent Technologies UK Ltd, Wokingham, Berkshire, UK).

Each RNA (1 µl) sample and an Agilent RNA 6000 Nano Marker ladder (1 µl) were denatured by heating at 70^{o}C for 2 min before rapidly chilling on ice. The RNA samples and ladder were loaded into an Agilent RNA 6000 Nano LabChip containing microfluidic gel freshly mixed with fluorescent dye. The dye binds to nucleic acids and so allows the fluorescent detection of the RNA fragments, as well as any contaminating template DNA. Each LabChip is made up of an interconnected set of micro-channels that are used to separate the nucleic acid fragments, based on their size as they are driven through the chip electrophoretically.

6.2.5 PREPARATION OF COMPLEMENTARY DNA BY REVERSE-TRANSCRIPTION

To generate cDNA, the RNA was batch reverse transcribed using GeneAmp® RNA PCR Kit (Applied Biosystems, Warrington, UK) with random hexamers. Total RNA (2 500 µg) was added to a reaction mix containing 1x RT Buffer, 5 mM $MgCl_2$, 1 mM dNTPs, 1.25 µ M random hexamers, 1 U μl^{-1} recombinant RNasin® RNase inhibitor and 1 µl recombinant MuLV reverse transcriptase in a final reaction volume of 50 µl.

The reverse transcriptions were performed in duplicate, with positive controls using ovine adrenal gland and liver RNA. Negative controls comprising reactions performed without the addition of template RNA as well as using 3-5 randomly selected test samples with a reaction mix lacking reverse transcriptase were included. The reactions were performed duplicate.

The samples were incubated at room temperature for 10 min. They were then heated to 42^{o}C for 45 min in order to provide the optimum temperature for enzymatic action. The reaction was then stopped and the enzyme denatured by incubating at 95^{o}C for 10 min. The resulting cDNA was stored short-term at 4^{o}C or long-term at -80^{o}C until subsequent PCR.

6.2.6 PRIMER AND PROBE DESIGN

The nucleotide sequences of the clock genes were obtained from the NCBI GenBank nucleotide database (http://www.ncbi.nlm.nih.gov/) and ENSEMBL database (http://www.ensembl.org/index.html.). This database lists sequences by ascribing them Accession Numbers. Primers were designed as standard using primer design software. The software used was Primer Express™ (Applied Biosystems, Warrington, UK). Primers were designed with various criteria in mind. For one, the guanine-cytosine (GC) content of the sequences were not to exceed 30-80% as this would make the primers anneal too unspecifically to itself forming primer-dimers as well as binding unspecifically to the template cDNA. Runs of four or more identical nucleotides, particularly guanine, were also avoided for the same reason. The T_m and annealing temperatures were kept in the range of 58-60^{o}C. The number of guanines or cytosines or both were limited to two or less in the last five bases at the 3' end of the primer sequences. The forward and reverse primers were designed to anneal as closely to the probe on the template as possible without overlapping it.

The probes used to quantify the clock gene expression were designed to be TaqMan® MGB™ probes. These probes incorporate a 5' reporter dye and a 3' NFQ. The NFQ produces a lower background signal, which increases the precision of the gene

expression quantitation. The MGB moiety works by stabilising the probe when it is hybridised and thus raises its T_m so that it is less likely that the fluorescence is unquenched by anything but the endonuclease activity of the *Taq* polymerase.

Primers and probes were then checked for specific binding by using the NCBI BLAST, available online at http://blast.ncbi.nlm.nih.gov/Blast.cgi. This tool enables the identification of regions that are the same or similar between nucleotide sequences. It does this by mining genome and other nucleotide databases which are published online, using a search-term sequence. To minimise amplification of genomic DNA, the primers and probes were designed to span intron sequences where possible. The sizes of the PCR products were designed to be less than 250 bp to optimise the real-time quantification of the amplified DNA during RT-PCR.

As many of the clock genes have different RNA transcripts, the primer sequences were compared to these transcript sequences. This ensured that the PCR products would be of consistent size and that, as much as possible, the total transcript expression of each gene would be measured. The primers were also checked to see if they were intron-spanning in all the transcripts. Transcript sequence data was obtained as standard from the Ensembl database using the Ensembl Genome Browser, available online at http://www.ensembl.org/index.html.

The ovine and bovine clock gene accession numbers and number of transcripts per gene are listed below (Table 6.2):-

GENE	ACCESSION NUMBER	NUMBER OF TRANSCRIPTS
oper1	AF044911	1
oper2	AY253914	1
ocry1	AY275673	1
bcry2	ENSBTAG00000021223	1
bbmal1	ENSBTAG00000013029	2
bclk	ENSBTAG00000001272	2
ogapdh	AF030943	1

Table 6.2 List of ovine and bovine clock gene accession numbers and number of transcripts per gene.

Where there was more than one transcript, primers designed to amplify both transcripts simultaneously were designed. An internal control PCR reaction was required to run in duplex with the PCR amplification of the gene of interest. The housekeeping gene: *glyceraldehyde-3-phosphate dehydrogenase* (*gapdh*) was initially tested as an internal control. It is used more routinely than ribosomal 18S in clock gene experiments of this nature. The ovine *gapdh* had also been independently validated to be unchanged, either by circadian time or photoperiod (Kubista et al., 2006). The test of *gapdh* versus 18S showed that they were equally good. It was decided that 18S would not be used although it had been used previously in the experiments with the luteinised granulosa cells to provide a reliably detectable level of gene expression. The C_T of the *gapdh* reaction was also not predicted to be too distant from that of the clock genes in the ovine corpus luteum. The *gapdh* primers and probe were commercially available as a TaqMan® Gene Expression Assay (Applied Biosystems, Warrington, UK). They were fluorescently labelled with the VIC dye and are used in conjunction with an MGB probe.

The primer and probe concentrations were then optimised. The optimal concentrations for the primer pairs were determined using a range of concentrations. The primers were used in ratios of 1:1, 3:1, 6:1 and 18:1 reciprocally between the forward and reverse primers. The T_m was also varied ± 2°C. The optimal probe concentrations were then optimised by titrating against the primer pairs at optimal concentration, to ensure that the probe does not limit the fluorescence in the PCR due to its more abundant template: *gapdh* cDNA. The primers and probes were performed in singleplex PCRs initially then in duplex PCRs which included the internal control primers and probes. The optimal conditions resulted in the lowest C_T value without excess primer or probe. These PCRs were performed with serial dilutions of cDNA template, producing standard curves that added further validation of the specificity of the amplification reactions (Figure 6.1, Figure 6.2 and Figure 6.3).

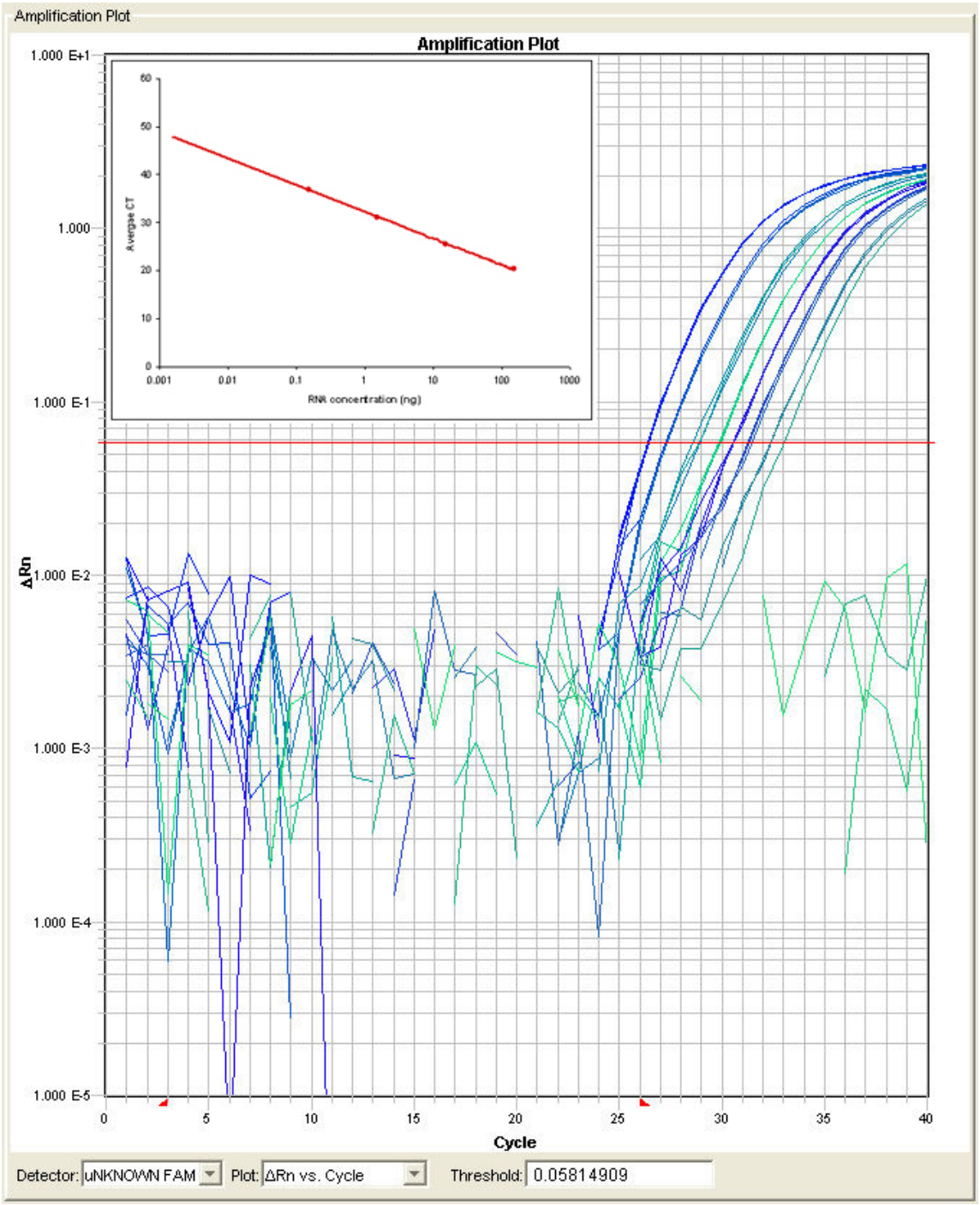

Figure 6.1 TaqMan® amplification plot of the *oper1* real-time PCR product concentration detected using an unquenched flourescent FAM dye signal, from a PCR duplexed with *og6pdh*, which was performed in triplicate with serially diluted cDNA. The red line demarcates the C_T threshold. The inset is the standard curve plotted using the C_T values and the $\Delta\Delta C_T$ method.

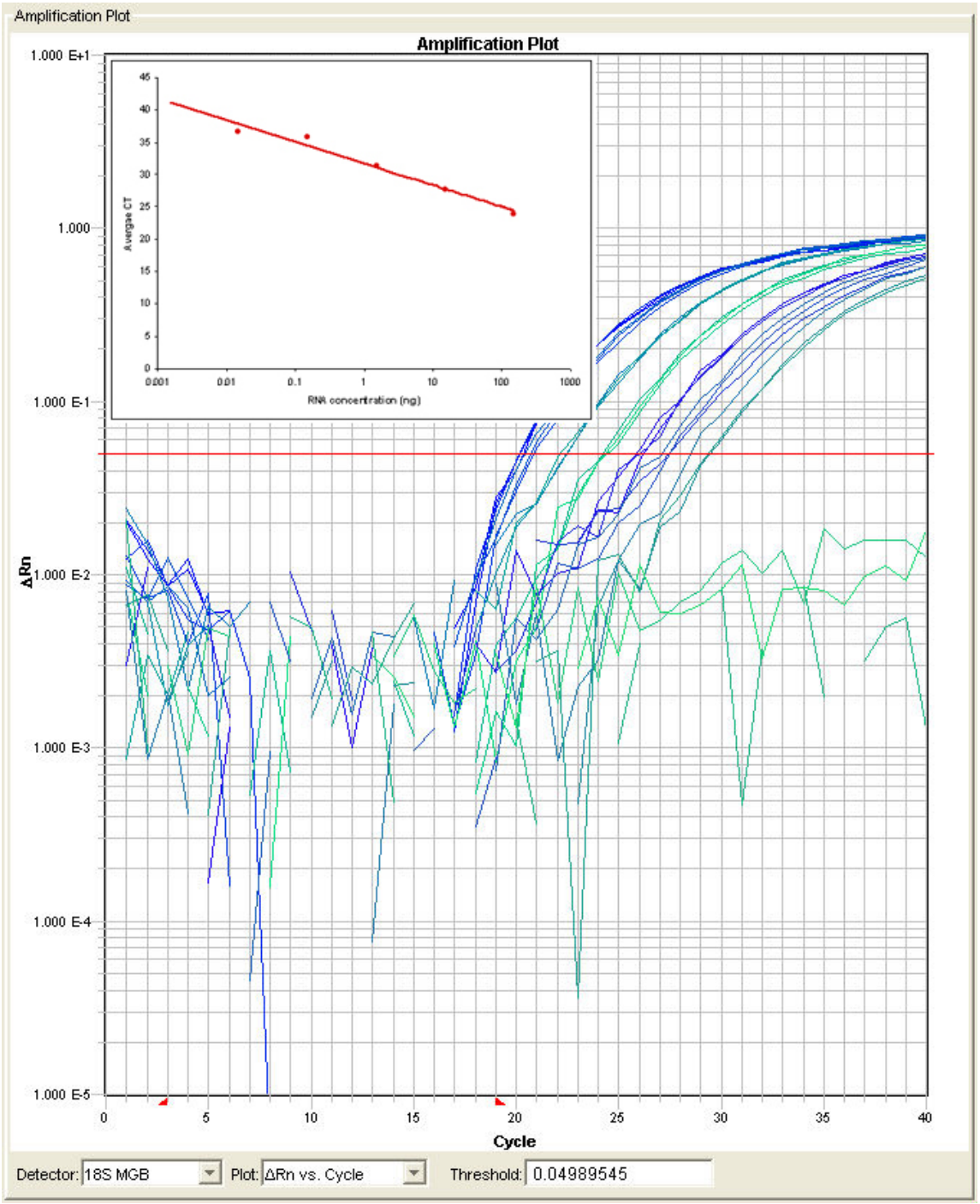

Figure 6.2 TaqMan® amplification plot of the *og6pdh* real-time PCR product concentration detected using an unquenched flourescent VIC dye signal, from a PCR duplexed with *oper1*, which was performed in triplicate with serially diluted cDNA. The red line demarcates the C_T threshold. The inset is the standard curve plotted using the C_T values and the $\Delta\Delta C_T$ method.

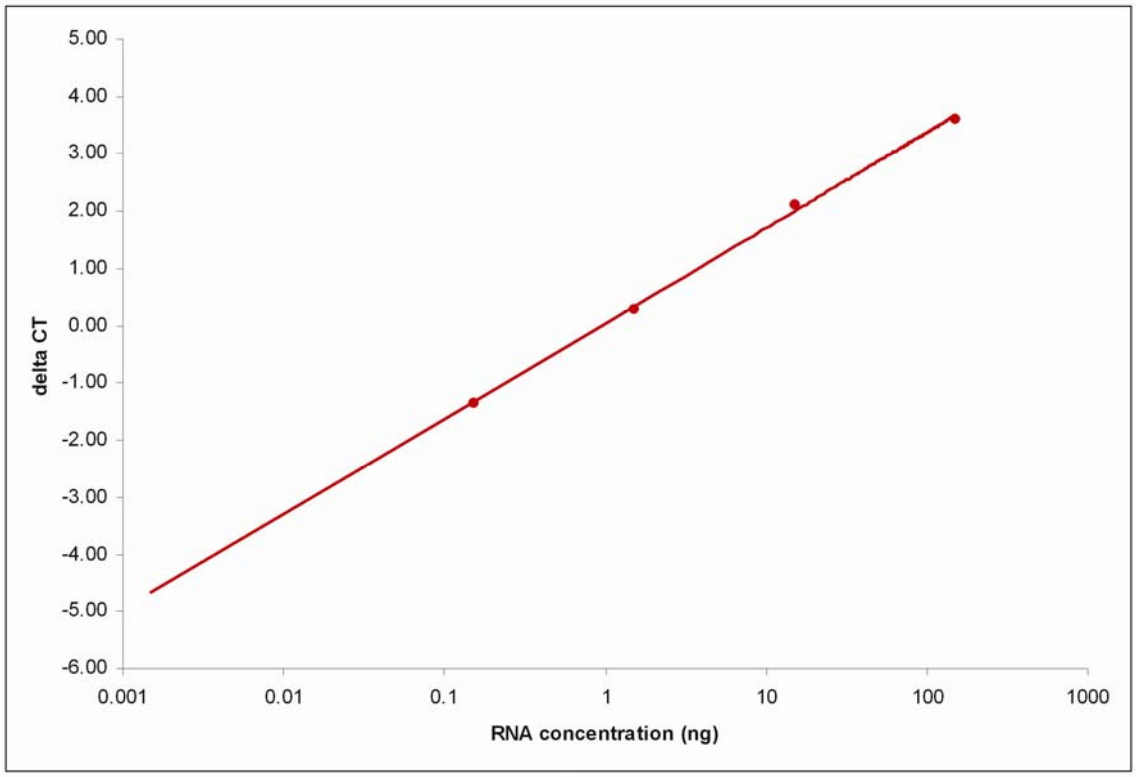

Figure 6.3 Standard curve of the difference between the duplexed *oper1* and *og6pdh* PCR C_T values (ΔC_T) using serial dilutions of cDNA.

The primer and probe sequences and PCR product sizes are listed below (Table 6.3):-

GENE	FORWARD PRIMER 5'-3'	REVERSE PRIMER 5'-3'	PROBE 5'-3'	SIZE
oper1	ccgtgtgccatggacatgt	aaccaggacaccttctccgtg	cacggagccggtgtcctggtt	93 bp
oper2	agggcatcacctctgagttca	ttgtggccgctgtgtcc	cgtgaagaatgtggatatg	59 bp
ocry1	ggtggagaaactgaagcacttaca	aagaaaagcttgggtggcaa	ttggaaaggcatttgg	64 bp
bcry2	ccgagssctcgcatactctctat	ctgaatgggcagaagccg	cctggacaagatcat	62 bp
bbmal1	ccctcacggaaggttagaataca	aaatgcaagggaagctcacag	caccaaggaagaataa	66 bp
bclk	ttaatgctagaggctcttgatggtt	tgtgtctgagagtgtaacttcattgc	ttttttagcaatcatgacagatg	88 bp
ogapdh	acgctcccatgtttgtgatg	ctcaagattgtcagcaatgcct	tgaaccacgagaagtat	71 bp

Table 6.3 List of ovine and bovine clock gene primer pairs and probe, including nucleotide sequence and amplicon size.

The primers were synthesised by Applied Biosystems (Warrington, UK). They were validated by performing duplex qRT-PCR with serial dilutions of adrenal and liver

RNA. The ΔC_T values were then plotted on the y axis against a logarithmic to the base 10 scale of the RNA concentration. A line of best fit was then fitted to the values plotted. An R^2 value was then obtained from the equation describing the gradient of the best fit line. The R^2 values were less than 0.1, indicating that any gradient in the best fit line was not significant. This meant that the C_T values did not significantly differ between PCR reactions of the serially diluted template cDNA.

All the PCR products were sequenced using ABI PRISM Big Dye Terminator Sequencing Kits (Applied Biosystems) to confirm that the sequence of the PCR-amplified fragments matched that of the gene to which the primers were designed. However, the PCR products were too small in all cases, except for *oper1*, to be sequenced directly. They therefore would have to be cloned into plasmids to produce longer plasmid-preparation DNA for sequencing. Alternatively or additionally, several of the products contained restriction endonuclease cleavage sites, which once cleaved by endonuclease treatment, would produce products of known size that may be separated and sized using a 4% agarose gel electrophoresis. It was decided that these not be done; that the specificity of the primer pair and MGB probe combination would suffice for confirming the specificity of the amplification reaction. This was decided because the cloning would be time-consuming and time was restricted. The endonuclease reaction would be less time-consuming but had a lower chance of success. The PCR products were already very small and so cleaving them might produce fragments that would not be disparate enough in size to be detectable on an agarose gel.

6.2.7 REAL-TIME QUANTITATIVE REVERSE TRANSCRIBED POLYMERASE CHAIN REACTION USING THE APPLIED BIOSYSTEMS TAQMAN® SYSTEM

Real-time qRT-PCR was performed using, using a two-step RT-PCR protocol, in the Applied Biosystems TaqMan® system, which was comprised of the TaqMan® 3700HT instrument with reagents from the AmpliTaq Gold® Fast PCR Master Mix

kit. This system follows the standard principles behind real-time qRT-PCR, as described in the General Materials and Methods. It uses quenched fluorescent probes that hybridise between the forward and reverse primers and which become unquenched when cleaved by the nuclease activity of the polymerase during the PCR amplification process. The amount of fluorescence detected is used to monitor the amount of template amplification.

The duplex qRT-PCR reaction was made up of 1.5 µl cDNA, 1x AmpliTaq Gold® Fast PCR Master Mix, UP, 1.125 µM each of forward and reverse custom primers, 0.75 µM custom probe, 0.02 µM each of forward and reverse 18S primers, 0.08 µM 18S probe to a final reaction volume of 25 µl. The AmpliTaq Gold® Fast PCR Master Mix, UP is a solution containing hot start *Taq* polymerase, dNTPs, magnesium and buffer. It is used in fast PCR reactions, which take approximately 40 min rather than the standard 2 h. Reactions were loaded into 96-well plates and the PCRs performed in a TaqMan® 3700HT instrument, using a fast protocol. Complementary DNA from ovine adrenal gland and liver were used as positive controls. Negative controls included reactions omitting the template which was replaced by nuclease-free water. PCR reactions were performed in triplicate with duplicate cDNA.

The C_T values were then used to calculate the relative gene expression of each gene of interest, using the second derivative method with the adrenal gland positive control as the reference sample (Andersson et al., 2005, Lincoln et al., 2002).

6.3 RESULTS

6.3.1 24-HOUR PROGESTERONE CONCENTRATIONS IN THE EARLY AND LATE LUTEAL PHASES

The blood P_4 levels were significantly increased from the EL to the LL phase (Figure 6.4). The EL and LL P_4 concentrations did not vary significantly over 24 hours.

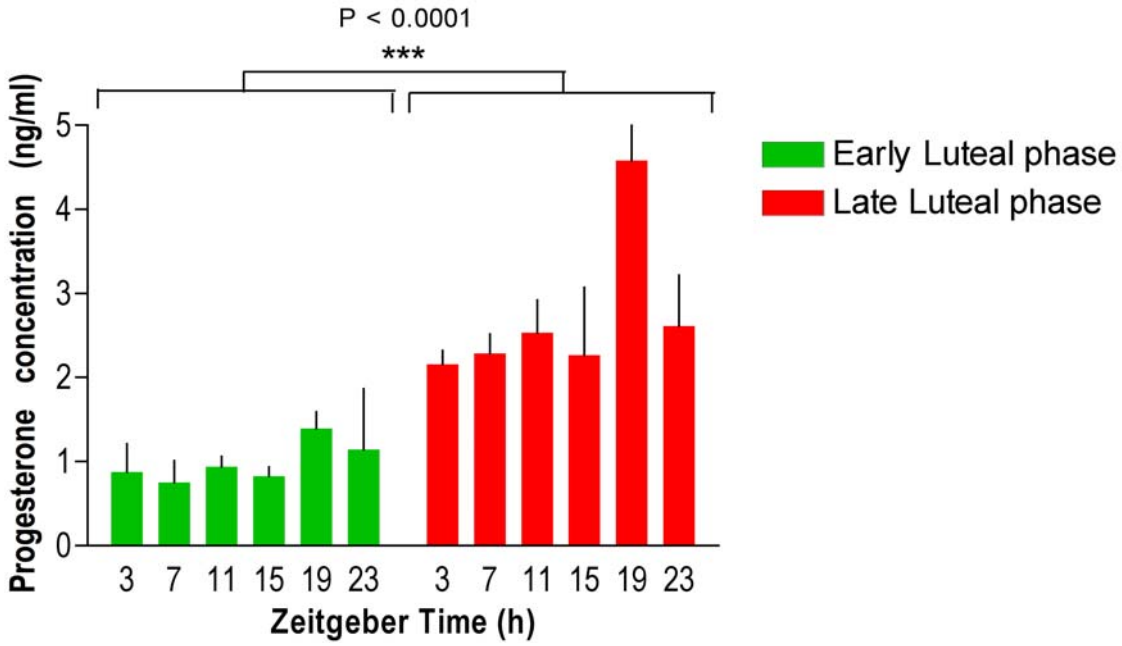

Figure 6.4 24-hour profiles of blood progesterone concentrations during the early and the late luteal phases. The EL concentrations were compared with the LL concentrations using Student's *t*-test. The error bars refer to the standard error of the mean.

This appropriate characterisation of the luteal phases was further supported by the macroscopic appearance of the corpora lutea when sampled. The corpora lutea contained both granulosa-lutein cells, better referred to as large lutein cells (LLC) in sheep and theca-lutein cells, better referred to as small lutein cells (SLC) in sheep, which were derived from the follicle, and in the sheep, were not organised in layers as in the human CL, but were randomly distributed.

6.3.2 24-HOUR CLOCK GENE EXPRESSION IN OVINE CORPUS LUTEUM

The expression of all five clock genes: *per1*, *per2*, *cry1*, *cry2* and *bmal1* were revealed in the ovine CL (Figure 6.5).

During the EL phase, the expression of *bmal1*, *per1*, *cry1* and *cry2* did not vary significantly over the course of 24 hours and were therefore, not circadian. The P values were all greater than 0.1 (P>0.1): *bmal1* P=0.616, *per1* P=0.610, *cry1* P=0.150 and *cry2* P=0.156. The expression of *per2* however, was robustly rhythmic, peaking at ZT 11 with its nadir ZT 3 (ANOVA P=0.037).

During the LL phase, the expression of *bmal1* (P=0.014), *per1* (P=0.013), *cry1* (P=0.007) and *cry2* (P=0.004) were discovered to be circadian. The one-way ANOVA indicated that the amount of gene expression, of each of these genes, varied significantly across the 24 hours. Conversely, the previously circadian expression of *per2* was now no longer circadian. One-way ANOVA of the 24-hour gene expression profile in the LL phase yielded a P value of 0.177, which was more than the 0.05 significance threshold (P>0.05). The circadian rhythm of *bmal1* was seen to peak at ZT 19, in conjunction with the acrophases of *cry1* and *cry2*. The expression of *per1* peaked 16 hours earlier, at ZT 3. The peak amount of *per2* gene expression also occurred at ZT 3. The nadirs of these rhythms converged less than the acrophases did between the clock genes, with *bmal1* and *cry2* at their lowest at ZT 7. The nadir of the *per1* rhythm was ZT 15, while that of *cry1* was at ZT 3. The phases of the circadian rhythms in the LL phase did not appear to be antiphasic between the transcriptional activator, *bmal1* and the other, transcriptional inactivator, clock genes. The curve of the *bmal1* circadian rhythm appeared to most closely resemble that of *per1*, while the two *cry* genes, appeared to be relatively similar. They were certainly more similar to each other than they were with either of the other two rhythmic genes.

The general level of gene expression of each clock gene was comparable between the EL and LL phases. The EL *per2* and *cry1*, along with the late luteal *cry1* profiles

demonstrated the highest levels of gene expression. These were all in the range of 1500-fold higher than the baseline, which was considerably greater than that of the other 24-hour profiles. The late luteal *per2* expression profile, though not circadian, was also relatively high, at an approximate 500-fold change, while the remaining clock gene profiles were all less than 5 folds higher than the baseline.

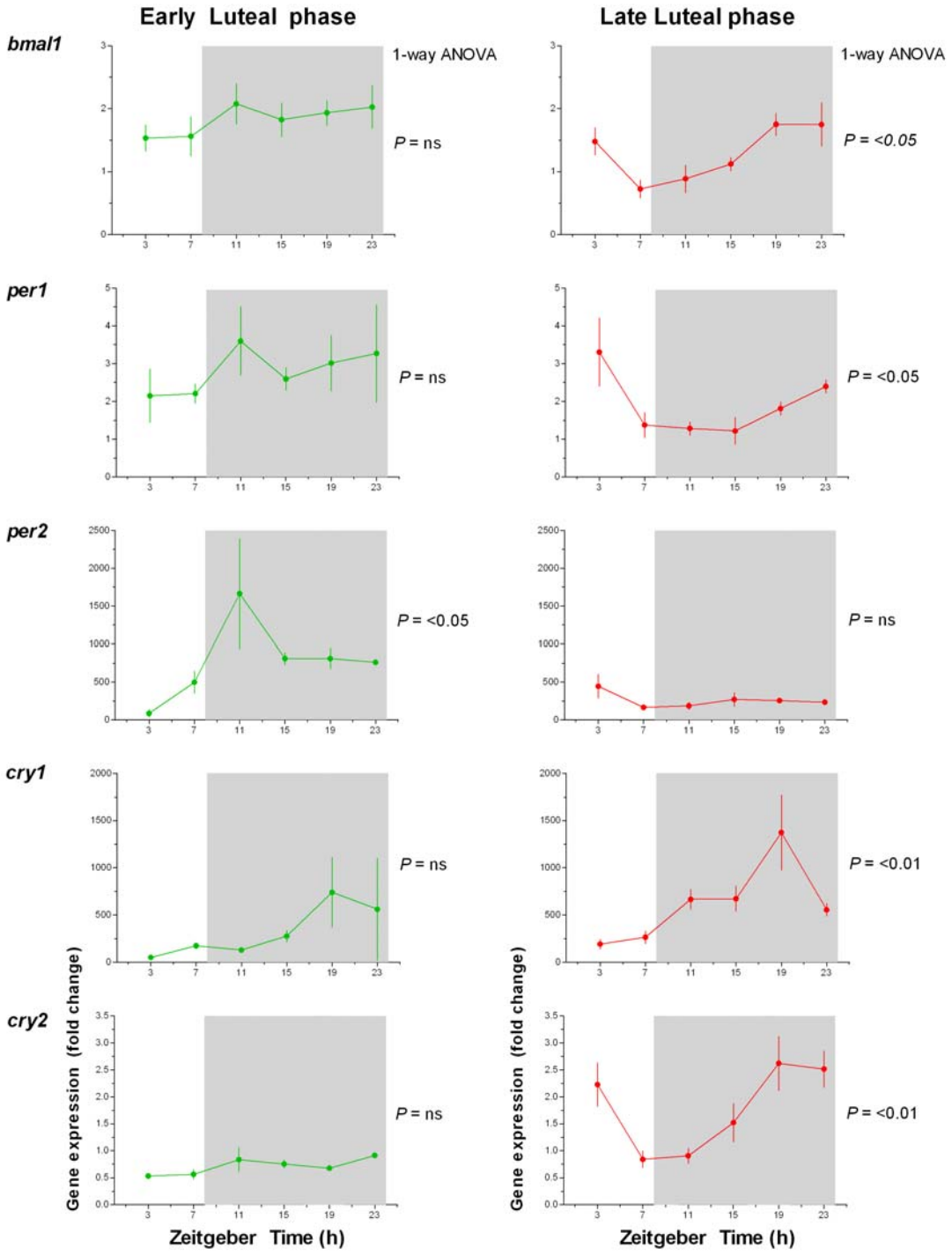

Figure 6.5 Graphs showing the amounts of gene expression of *bmal1*, *per1*, *per2*, *cry1* and *cry2* in the ovine CL, across 24-h, during the early (EL) and the late (LL) luteal phases. The gene expression was quantified using real-time qRT-PCR, measured in fold change and normalised to *ogapdh*. The data were statistically analysed for 24-hour variance using 1-way ANOVA assuming normal distribution and the *P* values indicated next to the corresponding graphs. The shaded area demarcates the night time dark phase. The error bars refer to the standard error of the mean. *n*=3-5.

The 24-hour clock gene expression profiles were then compared between the EL and the LL phases, to see whether there was a significant difference between the circadian gene expression of the clock genes between the two luteal phases (Figure 6.6). Two-way ANOVA was used to statistically compare the two sets of gene expression profiles. Although the expression of *bmal1* became circadian in the LL phase, it was not sufficiently divergent from the 24-hour profile of the EL phase, which did not vary significantly across the 24 hours (P=0.209). The emergence of the *per1* circadian rhythm in the LL phase though, was significant, although it only just fell below the 0.05 significance threshold (P=0.0497). The loss of the circadian rhythm in *per2* expression from the EL to the LL phase was also significant, and highly so at P=0.001. The EL and LL phase 24-hour profiles of *cry1* gene expression were strikingly similar, and sure enough, proved to not be significantly different (P=0.593). The *cry2* gene expression profiles however, were significantly different between the two luteal phases, with one being circadian and the other one, not (P=0.020).

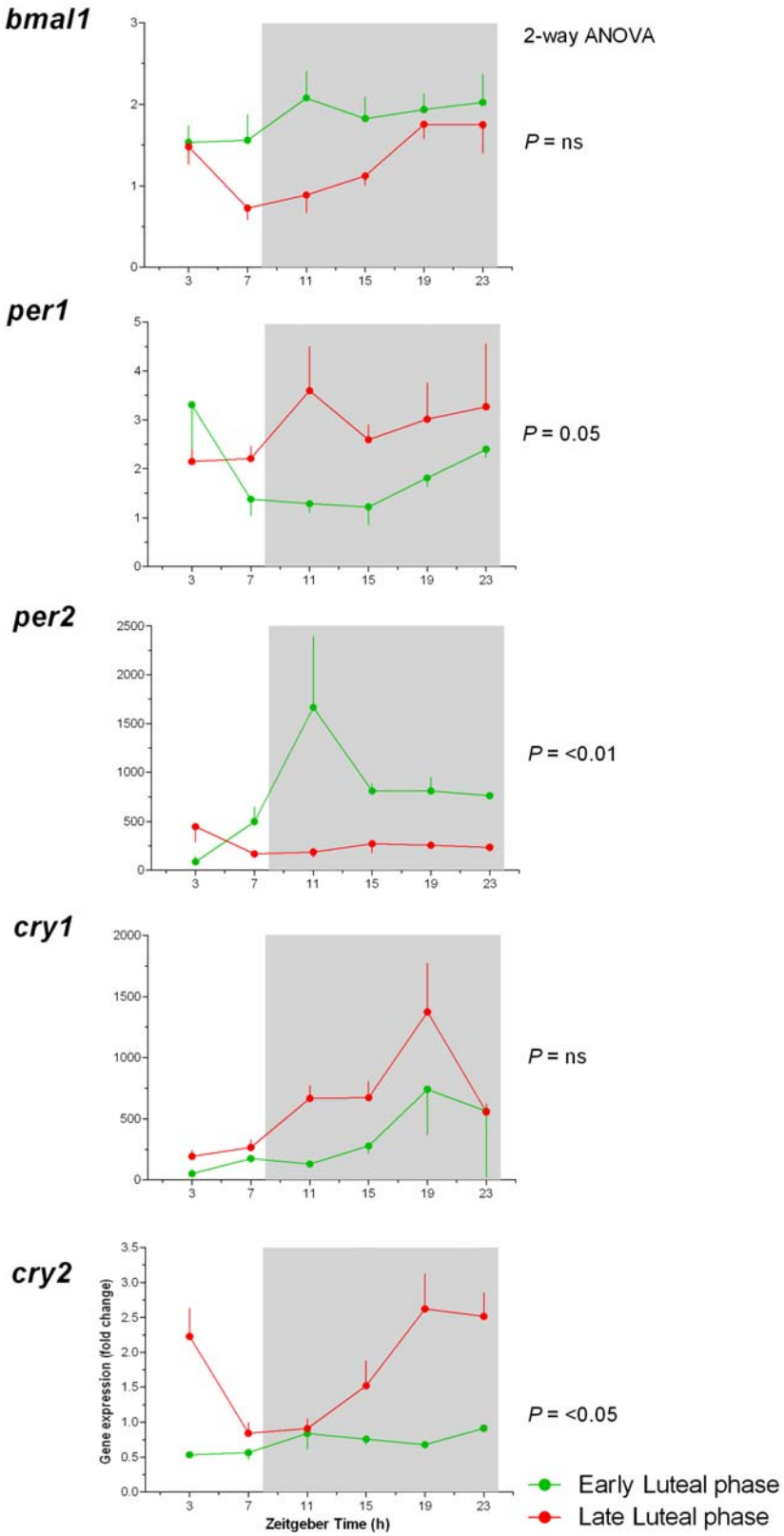

Figure 6.6 Graphs showing the amounts of gene expression of *bmal1*, *per1*, *per2*, *cry1* and *cry2* in the ovine CL, across 24-h, during the early (EL) and the late (LL) luteal phases. The gene expression was quantified using real-time qRT-PCR, measured in fold change and normalised to *ogapdh*. The 24-hour clock gene expression profiles were analysed for change between the EL and LL phases using 2-way ANOVA. The shaded area demarcates the night time dark phase. The error bars refer to the standard error of the mean. *n*=3-5.

6.3.3 24-HOUR MELATONIN CONCENTRATIONS IN THE EARLY AND LATE LUTEAL PHASES

The blood melatonin concentrations were significantly higher at night (ZT 8 - ZT 24/0) than during the day (ZT 24/0 - ZT 8) in both the EL (Student's *t*-test P = 0.0071) and the LL (Student's *t*-test P = 0.0015) phases (Figure 6.7). There was no significant difference between the 24-hour profiles in EL and LL.

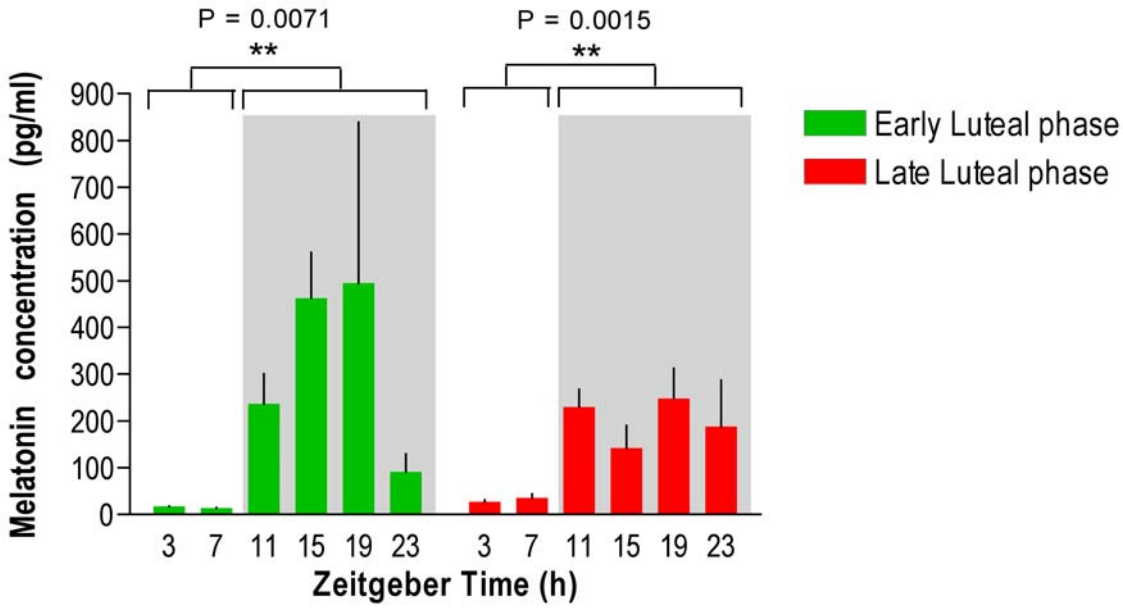

Figure 6.7 24-hour profiles of blood melatonin concentrations during the early and the late luteal phases. The daytime and the night time concentrations were compared using Student's *t*-test. The shaded area demarcates the night time dark phase. The error bars refer to the standard error of the mean.

The 24-hour blood melatonin levels were then compared to the corresponding 24-hour clock gene expression levels in the EL and LL phases. A correlation was observed between the melatonin and *cry1* 24-hour profiles, in EL and LL (Figure 6.8). The peak melatonin concentration in the EL phase coincided with EL peak in *cry1* gene expression, at ZT 19. This was also the case in the LL phase, with the coincident peaks occurring also at ZT 19. The timing of the nadirs in the melatonin concentrations and the level of *cry1* gene expression were also roughly coincident, in both the luteal phases. The LL nadirs of the melatonin levels and *cry1* expression were at ZT 3, where they were coincident.

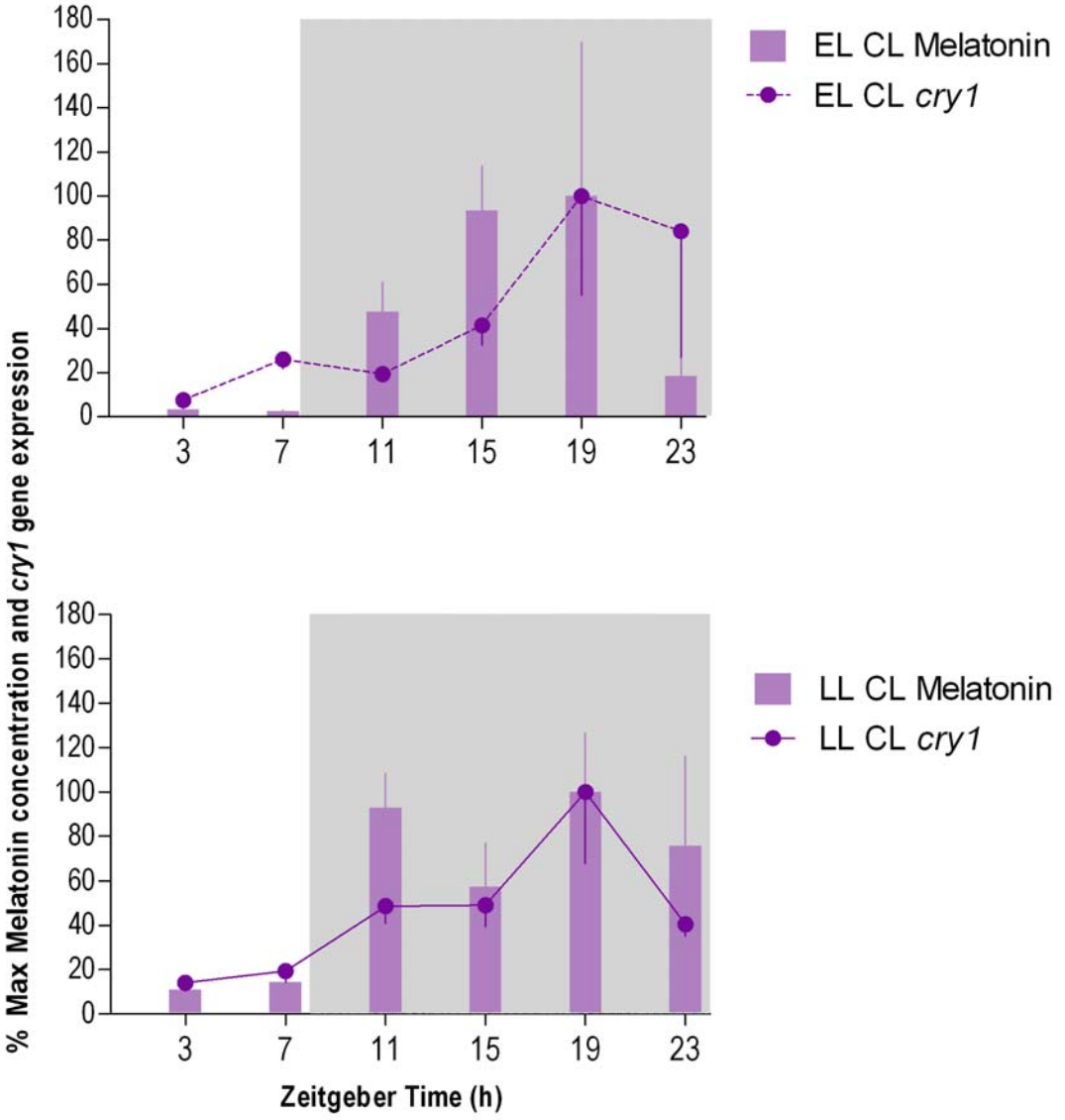

Figure 6.8 24-hour profiles of blood melatonin concentrations are shown as histograms. Corresponding 24-hour profiles of *cry1* gene expression in the ovine CL, during the early (EL) and the late (LL) luteal phases, are shown as line graphs. The shaded area demarcates the night time dark phase. The error bars refer to the standard error of the mean.

Previous studies have measured 24-hour clock gene expression rhythms in the SCN and PT in the Soay sheep (Lincoln et al., 2002). These provided two data sets with which the luteal data sets could be compared. This comparison was only performed using the late luteal data set, as this contained the majority of the circadian gene expression.

The correlation, observed in the current study, between the melatonin concentrations and the *cry1* gene expression levels, have already been observed in other studies. The correlation was initially noticed in the ovine PT and shown to be causally linked, by treatments with melatonin (Johnston et al., 2006). This correlation, which is evident in the late luteal CL and the PT of the sheep, is not seen in the ovine SCN. The circadian gene expression profiles of the other clock genes in the CL were also different to those in the PT and in the SCN (Figure 6.9). The circadian expression of one of the genes that comprises to the positive limb of the circadian clock mechanism: *bmal1* is expressed in antiphase with two of the genes comprising to the negative limb of the circadian clock mechanism: *per1* and *cry1* in the SCN. This antiphasic relationship is maintained in the PT, between *bmal1* and *per1*. The expression of *cry1* in the PT is no longer antiphasic to that of *bmal1*. It is now seen to peak at the same time as the blood melatonin concentration peak. The antiphasic relationships between the genes of the positive and negative limbs of the circadian clock are not maintained at all in the late luteal CL. In fact, by comparing the late luteal circadian expression profiles of the positive limb gene, *bmal1* versus negative limb genes, *per1*, *per2*, *cry1* and *cry2*, it is possible to see that the 24-hour expression profiles of the same limb genes tend to segregate together.

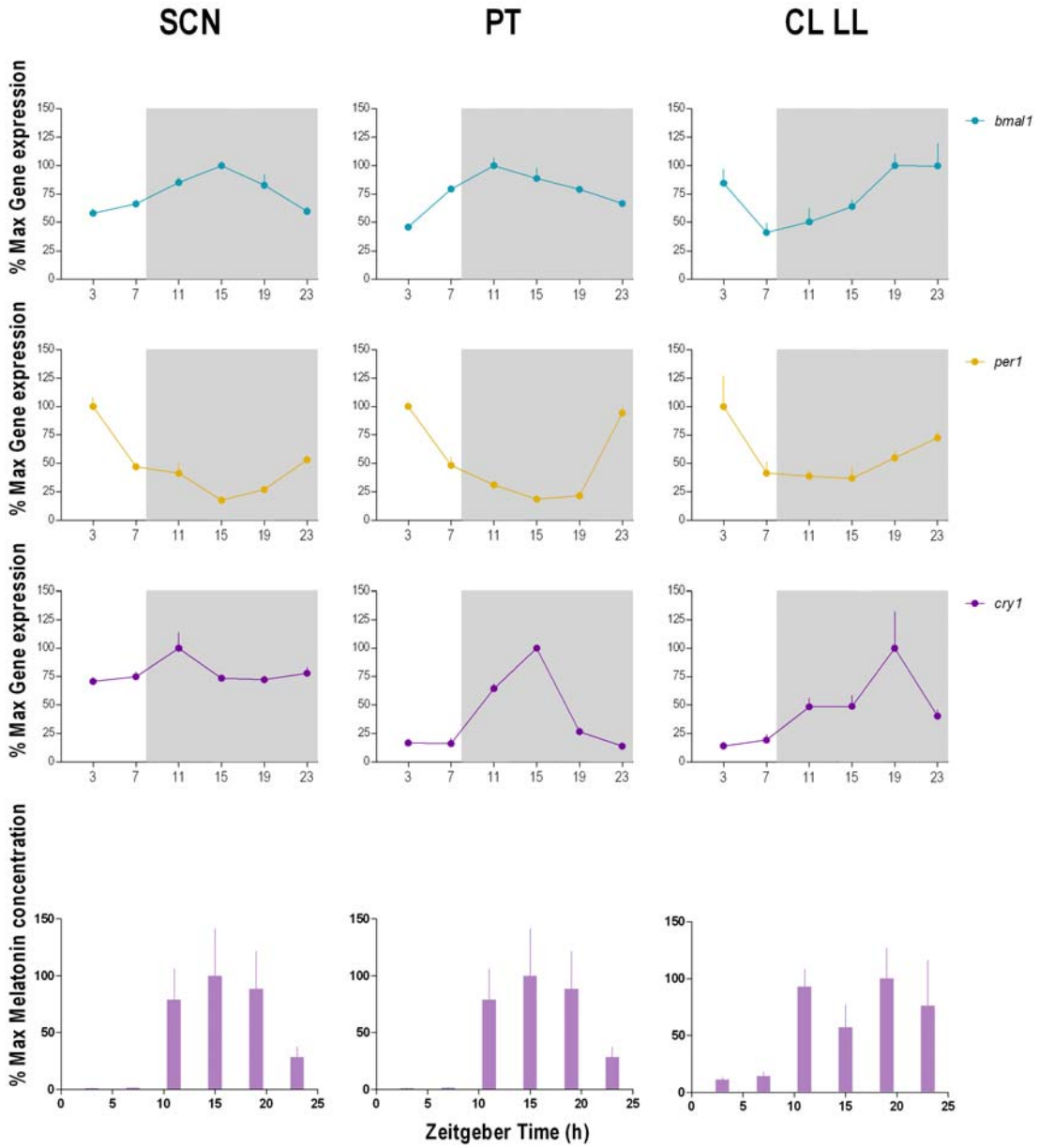

Figure 6.9 The comparison of melatonin and clock gene expression between the late luteal CL (CL LL), the PT and the SCN. The 24-hour *bmal1*, *per1* and *cry1* gene expression data and blood melatonin concentrations have been converted into percentages of the maximum gene expression level (% Max), such that the acrophase of each circadian profile is 100 %. These data have been converted for the purpose of normalising them for comparison. These are depicted by the line graphs. Corresponding blood melatonin concentrations from the same data sets are shown as histograms. The error bars refer to the standard error of the mean.

6.4 DISCUSSION

The 24-hour profiling of the clock gene expression in the ovine CL was determined. This procedure, where multiple individuals are used to constitute a single sampling time point in the 24-hour time course, has been previously used in numerous studies, to successfully define the circadian expression of clock genes in the ovine SCN and PT (Sladek et al., 2007, Johnston et al., 2006, Lincoln et al., 2005, Johnston et al., 2004, Lincoln et al., 2002, Dupre et al., 2008). The increased blood P_4 levels from the EL to the LL phase indicated that the corpora lutea were producing lower amounts of P_4 in EL than LL phases, as expected for the progression of the corpora lutea through the ovarian cycle. The increased night time blood melatonin levels indicated that the sheep were expressing normal rhythmic melatonin production.

The first aim was to establish whether the expression of the five selected clock genes: *bmal1*, *period1*, *period2*, *cryptochrome1* and *cryptochrome2* changed across 24 h, with a pattern reminiscent of a cell-based, endogenous circadian clock. The results, notably for the LL phase, revealed significantly rhythmic expression of all the clock genes with the exception of *per2*, which was rhythmic in EL. The phase relationships of the 24-hour profiles, which were only circadian for both the genes of the negative limb of the circadian clock mechanism and the genes of the positive limb of the circadian clock mechanism in the LL phase, were not consistent with those of a classical cell-based, endogenous circadian clock.

The gene *bmal1*, belonging to the positive limb of the circadian clock feedback loop was circadianly expressed in the CL during the LL phase. Its expression was relatively high in the late night, between ZT 19 – 23. This contrasts with the situation in the ovine SCN, where *bmal1* is maximal in the middle of the dark phase, and in the PT, where it is maximal during the early night (Figure 6.9). This information, taken together, is consistent with the view that peripheral tissues have different circadian timing to that of pacemaker tissues, and are regulated independently and differentially by neural and endocrine signals (Nakamura et al., 2005, Carr et al., 2003, Peirson et al., 2006, Hirota and Fukada, 2004). In the CL, the *bmal1* had a very similar timing to that for *cry2* which normally constitutes the negative limb of circadian clock

feedback loop. In addition, the 24-hour profile of *per1* and *cry1* showed increases during the night or early morning, to peak at either ZT 19 or ZT 3 respectively. There was no evidence of an inverse relationship between *bmal1* and the other (negative limb) clock genes, in contrast to the pattern previously reported in the ovine SCN and PT. Thus, the results are inconsistent with the idea that the classical circadian clock which drives *bmal1* expression and feedback, unless the feedback time relationships at the level of the circadian clock proteins are very different from that normally associated with a circadian clock. The results are more indicative of a situation where the clock genes are being driven by some additional, potentially extrinsic, factor.

There was very clear evidence that the 24-hour profiles of the clock gene expression differed between the EL and the LL phases. They differed in terms of circadian variation between the two luteal states, but not in the absolute level of gene expressions. The analysis revealed that the profiles for all the clock genes except *bmal1* were different between the EL and the LL phases. These data suggest that the cells of the CL are progressing during development of the CL and that *per2* behaves in a distinct fashion from the other clock genes. The 24-hour expression of *per2* transforms from arrhythmic to rhythmic as the luteal cycle progresses from the EL phase to the LL phase, whereas the reverse occurs for the other clock genes examined. It may be that this apparent acquisition of circadian rhythmicity in the clock genes bar *per2* is involved in the timing of luteolysis and therefore luteal lifespan. The loss of the EL phase *per2* circadian rhythmicity may also be part of the regulation of the luteal development and lifespan.

Clock genes have been observed acquiring *de novo* overt circadian rhythmicity in gene expression. Studies looking at clock gene expression during the ontogenesis of the rat liver showed the evolution of rhythmic clock gene expression from prenatal to postnatal stages (Sakamoto et al., 2002). Sladek *et al*. found that all the clock genes they examined, *per1, per2, cry1, clock, bmal1* and *rev-erbα* were expressed throughout their observation period from embryonic day 20 (E20), postnatal day 30 (P30). The rodent clock gene expression was measured from E20, through postnatal day 2 (P2), 10 (P10), 20 (P20), to adulthood on P30. In general, all the canonical clock genes (not including *rev-erbα*) took till P30 to establish overtly circadian rhythms, with high amplitude, of gene expression. The gene: *cry1* was rhythmic with

a low amplitude at E20 but then was not rhythmic at subsequent developmental stages until P30. The gene: *bmal1* was rhythmic with a low amplitude at P2 but again, was no longer rhythmic by P10. The rhythm was however re-established with greater amplitude by P20 and persisted with high amplitude till P30. The gene: *per1* became rhythmic with high amplitude by P10 and remained so through to P30. The gene: *per2* became overtly rhythmic at P20 through to P30. The gene: *cry1* and clock were the last to become overtly rhythmic, at P30. The gene: *rev-erbα* expressed overt circadian rhythms throughout, from E20 to P30. The authors resist much comment on the early, low amplitude rhythms of *cry1* and *bma1l*, implying that these rhythms were somewhat not equivocal, because of their low amplitude and the later emergence of overt, high amplitude rhythms. The authors concluded that only *rev-erbα* was rhythmically expressed throughout the entire observation period, while the other clock genes took more time to gradually attain their overtly rhythmic status.

This apparently gradual acquisition of overtly rhythmic clock gene expression may also occur in the ovine CL, with ovine luteal development recapitulating the ontogeny of the rodent liver (Sakamoto et al., 2002). The large amount of cell division and differentiation occurring in luteogenesis may be like that occurring in the formation of other organs during embryogenesis. The only exception here would be *per2,* which showed high amplitude variation during the EL phase but not the LL phase. The variation is overt and can not be dismissed as equivocal due to its amplitude. Furthermore, *per2* was found in the rat heart to have a circadian rhythm during early ontogenesis, that then disappeared but later re-emerged (Sladek et al., 2007).
Both *cry1* and *bmal1* also started circadianly rhythmic gene expression that then stopped and then re-started again, during the ontogenesis of the rat liver (Sakamoto et al., 2002). The *cry1* expression was circadian on E20 but was no longer detectable by P2, just three days later. The *cry1* rhythm re-emerged by P30 though it was undetectable ten days earlier. The *bmal1* rhythm was seen on P2 but then disappeared until around P20. The phases of these early rhythms that disappeared were phase delayed compared to the adult rhythm phases. There is no discussion of the phase relationships between the clock genes forming the negative and positive limbs of the circadian clock. It does appear however that by P30, there was a classical clockwork phase relationship between these genes. Even at P20, the genes expression phase

relationship between the *period* genes appeared to be somewhat in antiphase to *clk* and *bmal1*.

It was also observed in the ontogeny of the rat heart that *per2* took the longest out of all the clock genes to establish an overtly rhythmic 24-hour gene expression profile (Sakamoto et al., 2002). The phasing of the rhythmic *per2* expression also appeared to shift from postnatal day 20 to postnatal day 30, which was not the case for the rhythmic expression of *cry1*, *bmal1* and *clk* (Sladek et al., 2007). These data suggest that *per2* may differ in some way to the other clock genes, as it does in the EL and LL phase CL. The early establishment then loss of circadian *cry1* and *bmal1* in the rat liver during development also indicates that the loss of rhythmicity with time, like that of the *per2* expression in the EL and LL phase CL, may be meaningful. It may be a feature of developing peripheral clocks as this phenomenon has yet to be reported in the development of circadian clock gene expression in the SCN. The SCN also gradually develops circadian rhythmicity in its clock gene expression but it does so more rapidly than the peripheral clocks so far examined (Seron-Ferre et al., 2007). It established circadian rhythmicity long before the heart or liver does. It also establishes this rhythmicity with phases that are the same early on in development as they are later in the adult. This is not the case in peripheral tissues. Tissue specific differences in programming of the development of the molecular oscillations have been suggested (Tamura et al., 2008).

With the developing liver, it was also suggested that the clock genes were not initially strongly subject to the SCN signal. Rather, it was proposed that the circadian rhythms were food entrained. This was possible, though the constant rhythmicity of the *rev-erbα* gene from E20 through to adulthood would seem to belie that. It does however provide a possible cause for the different phases in circadian gene expression between early postnatal life and adulthood. One might speculate that the clock gene expression during development of peripheral tissues is subject to zeitgebers other than the SCN. If this were true, it may not only be the timing of meal times which can shift the phases of an emerging peripheral circadian clock. It is likely that the hormonal milieu could impact on the phasing of the peripheral circadian clocks of endocrine tissues such as the CL.

The mystery of how rhythmic gene expression is generated in the expression of the clock genes, in the apparent absence of a classical autoregulated, transcription-translation positive feedback loop may well be solved by addressing the possibility of post-translation modification of the clock proteins. The phases of circadian gene expression between the clock genes did not indicate the presence of a circadian clock but the observation that PER2 protein is able to oscillate in a circadian fashion in the absence of circadian *per2* expression indicates that post-translational modification may be able to produce circadian clockwork (Albrecht et al., 2007). This, coupled with the observation of the apparently unique localisation of the PER2 protein in the cytoplasm of the granulosa-lutein cells in the intact human CL, suggest that there may well be post-translational mechanisms operating in the provision of temporal regulation by the clock genes and their cognate proteins in the CL.

The third aim of this study was to assess whether the CL may be a melatonin-target tissue, with regard to its clock gene expression. This hypothesis was based on evidence that melatonin activates P_4 production in primates and regulates clock gene expression in melatonin-target tissues, such as the ovine PT (Woo et al., 2001, Jilg et al., 2005, Johnston et al., 2006). In the primate, melatonin affects steroid production, such as progesterone release. The CL expresses melatonin receptors and responds to melatonin (Albrecht et al., 2007). Additional evidence shows that the ovine PT, which expresses MT_1 receptors, responds to melatonin by activating its clock gene expression and using this to regulate its circadian clock. Melatonin activates *cry1* through a stimulatory mechanism at night and activates *per1* during the day through the removal of the inhibition of gene expression i.e. a 'de-repression' mechanism (Lincoln, 2006). The prediction of this hypothesis is that similar types of timing-control may occur in the CL as it does in the PT of the sheep.

In the ovine CL, *cry1* expression was maximal during the dark phase, when the melatonin concentrations were high, which may be consistent with a stimulatory role of melatonin on *cry1* expression. In both the EL and LL phases, *cry1* was maximal later in the night, at ZT 19, and this correlated with the time when blood melatonin concentrations were also at a maximum. In the ovine PT, a similar scenario occurs: with maximum levels of melatonin occurring at the same time as the *cry1* expression maximum, at ZT 15, in the early part of the night. Combined together, these results

are consistent with the view that melatonin may activate *cry1* in the ovine CL and be a significant regulator of clock gene expression. Moreover, for *per1*, in contrast to *cry1*, gene expression is elevated during the late night and was maximal in the morning, in the late luteal CL. The pattern was quite similar to that of the ovine PT and SCN. This was also consistent with the view that melatonin regulates *per1* through a 'de-repression' mechanism. Interestingly, the 24-hour profile of *per1* expression was very similar between the three ovine tissues, whereas this was not the case with *cry1* expression, suggesting that there is a specific relationship between melatonin and *cry1* expression.

Overall, the current study provides circumstantial evidence that daily clock gene expression in the ovine CL is potentially driven by melatonin rather than being merely an intrinsic clockwork mechanism and as such, the CL may be regarded as a melatonin-target tissue. In this respect, it is interesting that sheep are reproductively active under short winter photoperiods and thus, long-durational melatonin is likely to be permissive of full CL function. It could therefore be predicted that an ovine CL formed under long photoperiods, would not be able to function normally. A specific phase-relationship between *per1* and *cry1* expression may be required in the ovine CL, as proposed for the functional control of the ovine PT, for full P_4 secretion. A reproductively active short-day animal would by contrast appear different under long-day conditions and would not have fully functioning CL (Lincoln, 2006).

This study demonstrates, for the first time, that the five studied clock genes were all expressed across 24 h in the ovine CL, with a clearly defined rhythmicity, most robust for the clock genes in LL but with a paradoxical difference for *per2*, which was rhythmic in EL and not in LL. The lack of an inverse relationship between the rhythmic expression of *bmal1* and the other clock genes: *per* and *cry* is inconsistent with a classical endogenous clock. The results better supports a model in which clock gene expression changes during maturation of the tissue, regulated by extrinsic hormone factors, but still providing temporal control of the luteal lifespan.

In summary, this chapter has demonstrated for the first time, that:

1. the clock genes: *bmal1*, *per1*, *per2*, *cry1* and *cry2* are expressed in the ovine CL;

2. these genes are expressed throughout the luteal lifespan;

3. *bmal1*, *per1*, *cry1* and *cry2* are expressed in circadian rhythms during the LL phase but not during the EL phase;

4. *per2* is expressed in a circadian rhythm during the EL phase but not during the late luteal phase;

5. the phase relationships between these rhythmic gene expression profiles are not consistent with that of a classical circadian clock.

As endogenous clocks can be generated by clock protein oscillations in the absence of rhythmic mRNA expression, it is important that the clock protein expression in the CL is examined, across 24 hours, in order to establish more conclusively whether circadian clocks operate in the CL and in the regulation of its lifespan.

7 PRODUCING OVINE CLOCK PROTEIN ANTIBODIES

7.1 INTRODUCTION

The establishment of whether an endogenous, clock gene-driven circadian clock exists in the cells of the CL remains equivocal. Although circadian rhythms in clock gene expression were observed in the ovine CL, the phase relationships between them were not consistent with those of a classical circadian clock. There have however been reports of circadian clock work existing only at the level of the clock proteins (Axmann et al., 2007, Dong and Golden, 2008, Johnson, 2007). It is therefore essential that these proteins be better examined in the CL, to ascertain whether any circadian fluctuation can be identified in their quantity of cellular compartmentalisation, across a minimum period of 24 hours.

In order to do this, the corpora lutea sampled in the previous chapter from Soay sheep, across 24 hours, from the EL phase and the LL phase, will be examined. Each of these corpora lutea were divided at the time of sampling into two bilateral halves. One half was stored for mRNA extraction and gene expression analysis and the other half was immediately immersion fixed for IHC. As such, it was crucial that antibodies were found that would be able to visualise the clock proteins in the sheep. Furthermore, these would need to be sufficiently specific that they could be used in immunoflourescent histochemistry, co-localised to luteal cell type markers. This would be absolutely necessary as the cellular organisation of the ovine CL is much more random than that of the human CL. There are no layers of LLCs and SLCs; rather, these cells are freely mixed with each other in the mass of the ovine CL, along with fibroblasts and cells of other luteal cell types.

The gene expression analysis of the ovine corpora lutea, in the previous chapter,

established that circadian mRNA expression was evident, mostly in the LL phase. There was a high-amplitude circadian rhythm in *per2* expression during the EL phase which was then no longer detectable in the LL phase. The PER2 protein was observed in Chapter 1 as unusual in its cytoplasmic localisation, in the human granulosa-lutein cells, appearing to aggregate into foci that radiated around the nucleus, closely apposed to what appears to be the basement membrane. This suggests that there may be more than transcriptional regulation involved in the role of this clock gene, in potentially regulating temporal processes, in the CL.

The importance of protein-protein interaction in the functioning of the circadian clock has already been long established. The clock proteins, PER and CRY are known to both hetero- and homo-dimerise, in order to produce the necessary time lags required for the provision of a 24-hour period. The dimerisation of these proteins to each other is thought to prevent them from being ubiquitinylated and so, stop them degrading via the ubiquitin-proteosome protein-degradation pathway. The accumulation of these proteins is timed so that the dimers occur coincidently, only at specific intervals, thus constituting an internal coincidence timer, which has been proposed to be the mechanism by which the photoperiodic melatonin signal is decoded in the PT (Lincoln, 2006). This is highlighted by a study of the rodent PT, where the clock proteins could only be quantified in the nucleus and the rhythmic change did not reflect the mRNA rhythm. Peak PER1 protein levels occurred three hours later than the *per1* mRNA maxima and CRY1 protein occurred 14 hours later than the *cry1* mRNA maxima, and the timing of both protein maxima were found to be coincident (Jilg et al., 2005). These proteins clearly localised to the nucleus for a specific function, at timed intervals. These proteins and the timing of their interaction with each other and with DNA, when they function as transcriptional activators or repressors, are therefore essentially the components of the circadian system that give rise to the provision of the specific 24-hour period, that is circadian.

The visualisation of these proteins would also perhaps allow the characterisation of these interactions, which have previously not been clearly revealed. Although real-time imaging exists of the clock proteins function in living cells, these cells exist either *in vitro* or *ex vivo*. It has not yet been characterised in cells of an intact mammalian tissue, sampled across 24 hours, and most certainly not in the CL *in vivo*.

Initial attempts to visualise the clock proteins using the commercial antibodies that were successful in Chapter 2 met with mixed success. The BMAL1 antibody worked successfully, but it was the only one of the whole battery of antibodies that did. As such, it was decided that specific antibodies would be raised against the ovine clock proteins: PER1 and CRY1, as these constituted the negative limb of the circadian clock; BMAL1 representing the positive limb of the clock having already been visualised.

It was not however, possible to complete the systematic visualisation of the clock proteins in the ovine CL across 24 hours, due to time constraints. As such, this chapter will focus largely on successfully raising sheep-specific antibodies against clock genes, and testing them in ovine tissues, aiming ultimately at successfully visualising the clock proteins in the ovine CL.

Therefore, this chapter aims:

1. to identify ovine amino acid sequences for CRY1 and PER1 and assess sequence homology for protein specificity;

2. to identify putative epitopes in the selected ovine amino acid sequences, using epitope-mapping software;

3. to assess the likelihood of projection from the protein tertiary structure and plasma membrane of the putative epitopes amino acid sequence using hydrophobicity plot analysis;

4. to raise antibodies in pre-screened rabbits, using both commercial and in-house methods and testing the titre of the antibodies;

5. to establish a positive control using immunohistochemistry to test the ovine CRY1 and PER1 antibodies in ovine brain tissues known to robustly express circadian clock genes;

6. to investigate CRY1 and PER1 in the ovine CL using IHC with the ovine-specific antibodies.

7.2 MATERIALS AND METHODS

There is an element of Results in this Materials and Methods section, due to the arrangement of the aims of this chapter. The results derived in the process of raising the antibody, though addressing the direct aims listed in for this chapter, will be included in the Materials and Methods. The use of the anti-clock protein antibodies in the ovine CL will be described in the Results section. The results contained within both the Materials and Methods and the Results sections will then be discussed together in the Discussion.

7.2.1 PRODUCING OVINE PER1 AND CRY1 ANTIBODIES

Antibodies were produced specifically against ovine PER1 and ovine CRY1 peptides.

7.2.1.1 IMMUNOGEN DERIVATION

7.2.1.1.1 PEPTIDE-ANTIGENS

Arguably the most important aspect in the production of antibodies is the design of the peptide-antigen. A peptide-antigen is a small segment, approximately 15-18 amino acids long, of the protein sequence of interest. Peptide-antigens are used for immunisation of animals that then produce antibodies against the protein of interest. These antibodies can then be purified, titred and checked for activity against antigenic control peptides. Suitably active antibodies can then be assessed for use in immunochemistry. These antibodies are by nature, polyclonal, as a spectrum of antibodies is generated in response to the various epitopes in the immunogen recognised by the host's immune system.

7.2.1.1.1.1 OVINE CLOCK PROTEIN SEQUENCES

The published protein sequences for ovine PER1 and ovine CRY1 were obtained from the NCBI GenBank DNA databases, with the respective accession numbers: AAC03000 and AAQ62559 (Figure 7.1).

CRY1 *Ovis aries*

NCBI Protein Database Accession Nº: AAQ62559

irishtlydl dkiielnggq ppltykrfqt liskmeplei pvetitsevm ekcttplsdd hdekygvpsl eelgfdtdgl psavwpgget ealtrlerhl erkawvanfe rprmnansll asptglspyl rfgclscrlf yfkltdlykk vkknssppls l

PER1 *Ovis aries*

NCBI Protein Database Accession Nº: AAC03000

spsppsssia ysllsassep dnpstsgcss eqsarartqk elmtalrelk lrlpperrgk grsgtlatlq yalacvkqvq anqefyqqws leegepcamd mstytleele hvtseytlrn qdtfsvavsf ltgr

Figure 7.1 The amino acid sequences of the oCRY1 and oPER1 proteins.

The sequences were then aligned with those of CRY1 homologs in other species, as well as with ovine CRY2, using ClustalW software that was available online (http://www.ebi.ac.uk/Tools/clustalw2/index.html) and viewed with Jalview software (http://www.jalview.org/) (Figure 7.3 and Figure 7.3).

CRY1 ALIGNMENTS IN JALVIEW USING CLUSTALW

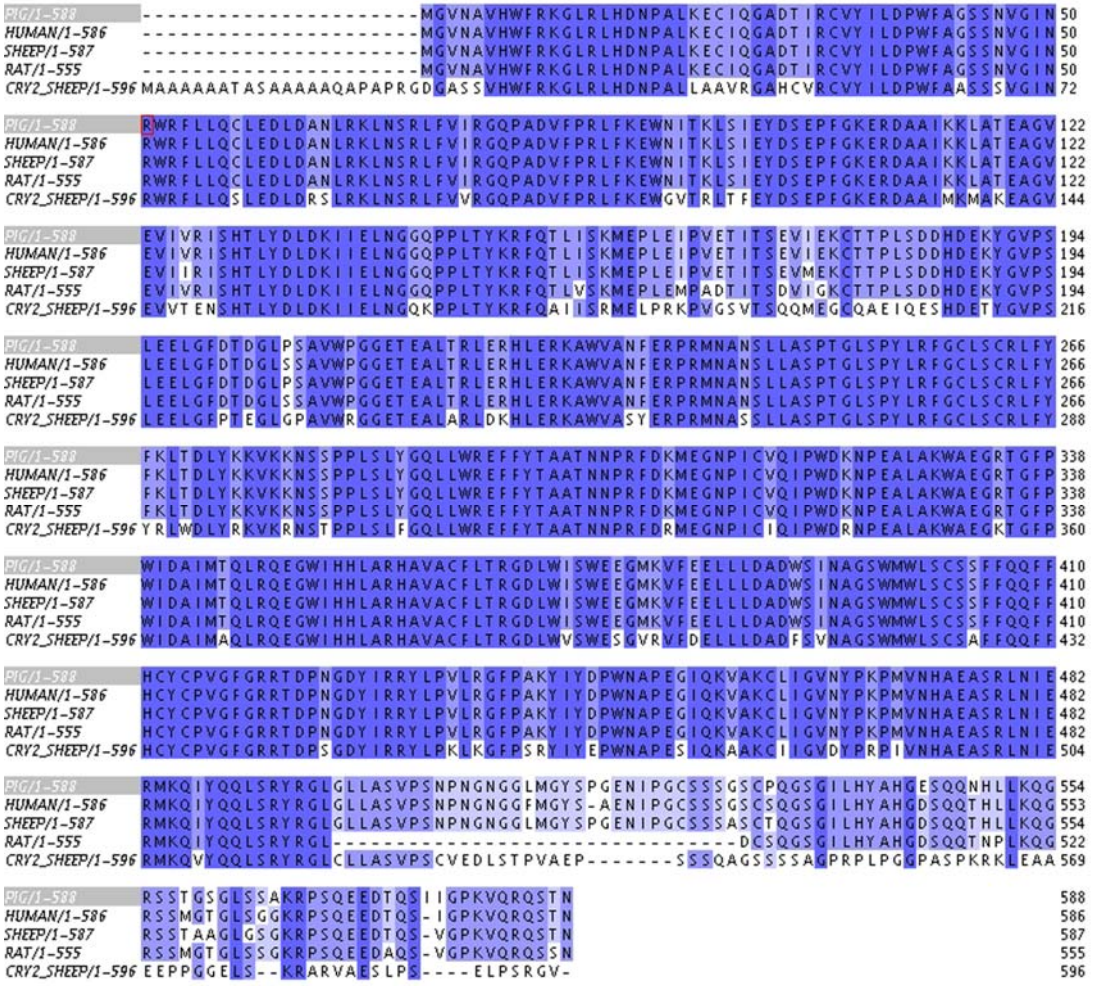

Figure 7.2 Diagrammatic representations of the homologous portions of oCRY1 amino acid sequence with other species and with the homologous ovine protein, oCRY2.

PER1 ALIGNMENTS IN JALVIEW USING CLUSTALW

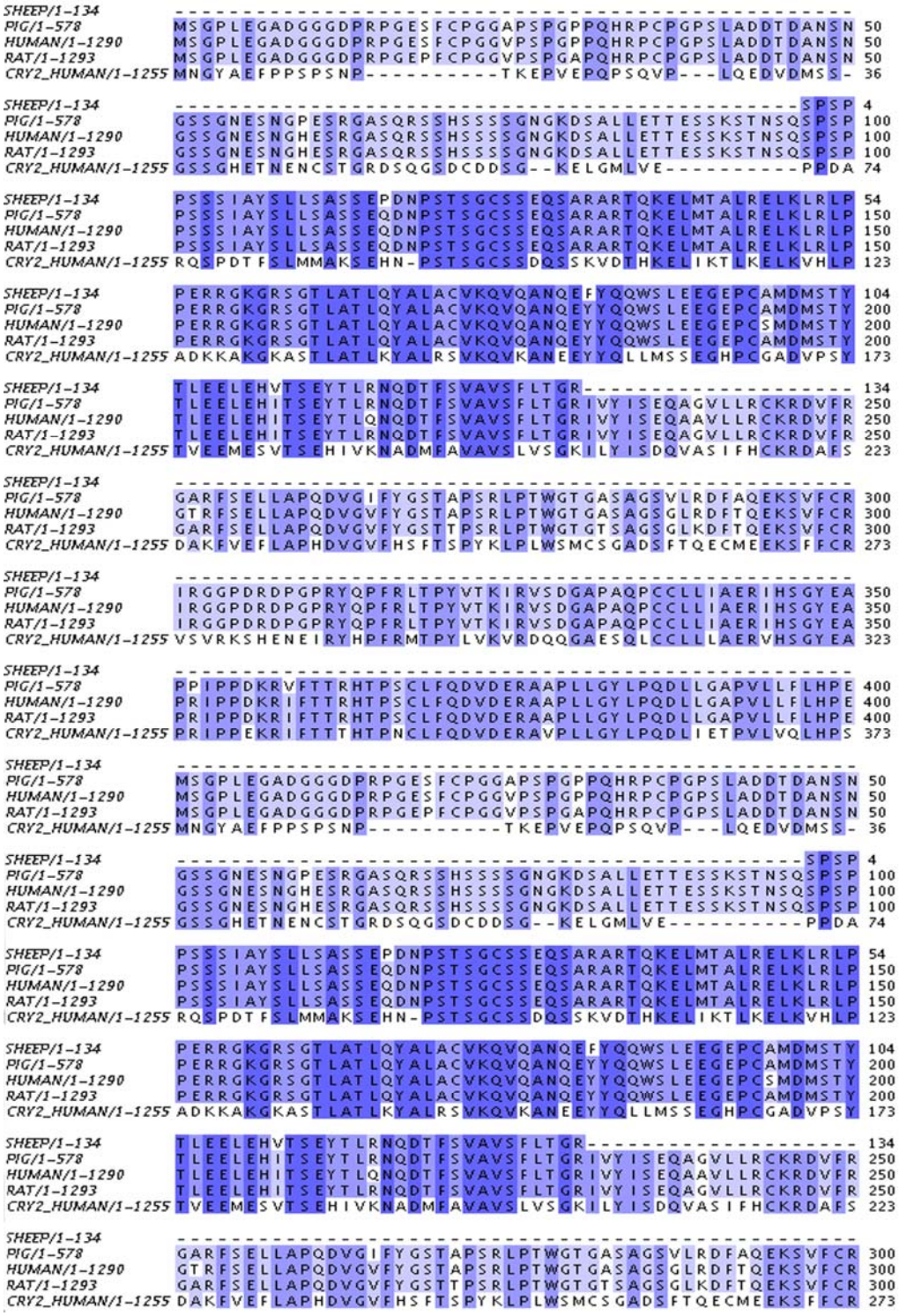

Figure 7.3 Diagrammatic representations of the homologous portions of oPER1 amino acid sequence with other species and with the homologous ovine protein, oPER2.

7.2.1.1.1.2 EPITOPE PREDICTION

The sequences were mined for putative epitope sequences using Epitope Locator epitope prediction software, available online (www.imtech.res.in). The potential of these sequences to be antigenic was then scored (Figure 7.4).

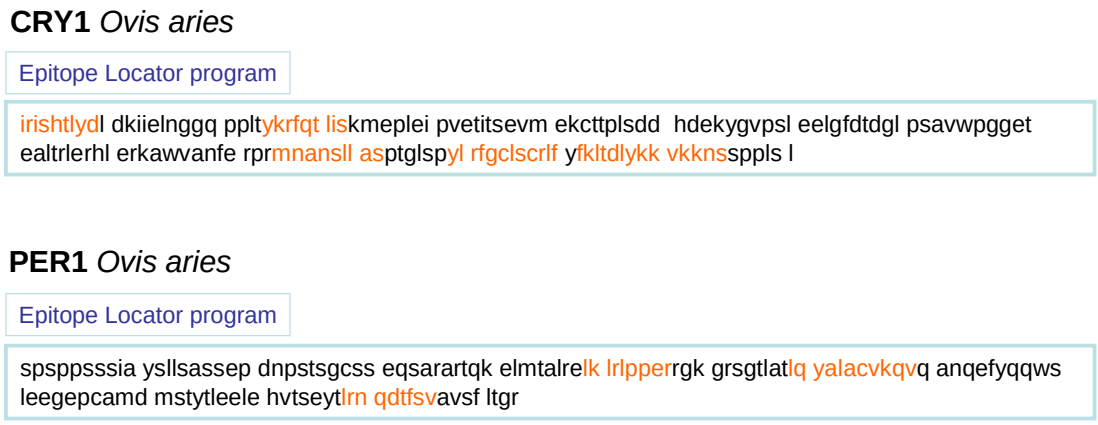

Figure 7.4 The putative epitopes in the known sequences of oCRY1 and oPER1 have been selected based on known epitope sequence, and have been highlighted in orange.

7.2.1.1.1.3 HYDROPATHY ANALYSIS OF PUTATIVE EPITOPES

Kyte-Doolittle hydrophobicity plots were generated for the protein sequences to try and identify hydrophilic regions that would be likely to protrude, epitope-like, from the protein mass (Figure 7.5). They were generated using software available online (http://gcat.davidson.edu/rakarnik/kyte-doolittle.htm).

CRY1 *Ovis aries*

Kyte-Doolittle Hydropathy Plot

irishtlydl dkiielnggq ppltykrfqt liskmeplei pvetitsevm ekcttplsdd * hdekygvpsl eelgfdtdgl psavwpgget ealtrlerhl * erkawvanfe rprmnansll asptglspyl rfgclscrlf yfkltdlykk vkknssppls l

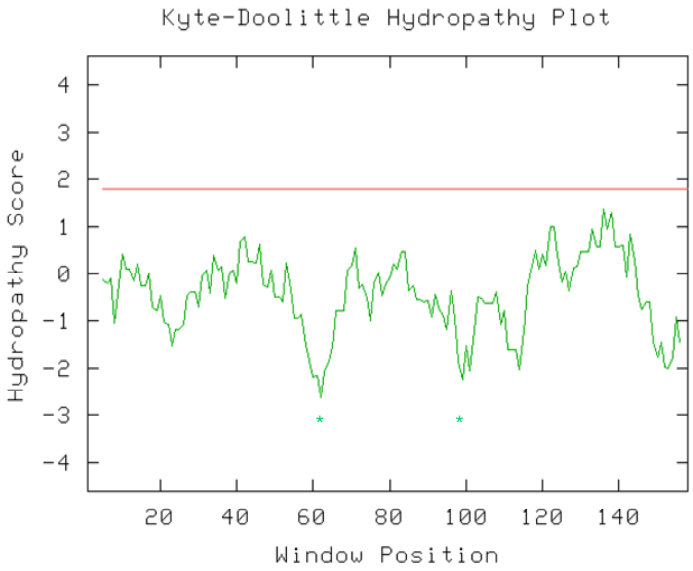

PER1 *Ovis aries*

Kyte-Doolittle Hydropathy Plot

spsppsssia ysllsassep dnpstsgcss eqsarartqk elmtalrelk lrlpperrgk * grsgtlatlq yalacvkqvq anqefyqqws leegepcamd mstytleele hvtseytlrn * qdtfsvavsf ltgr

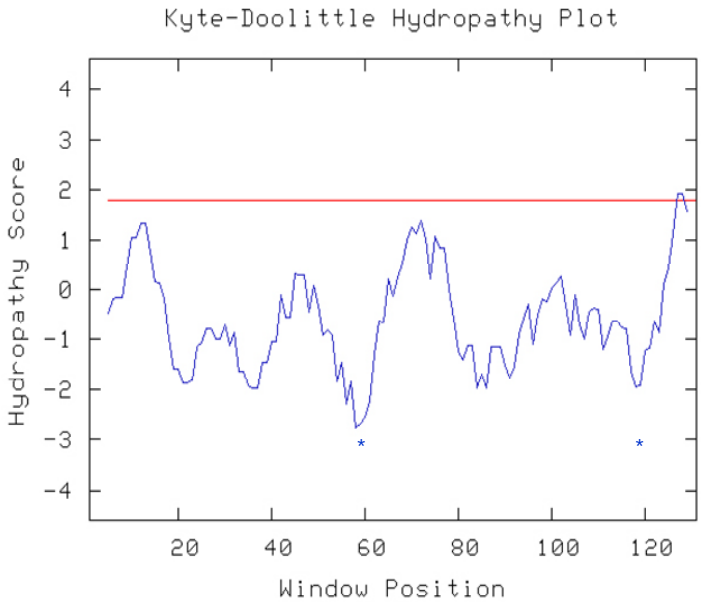

Figure 7.5 Kyte-Doolittle Hydropathy plots and amino acid sequences of oCRY1 and oPER1, with the most hydrophilic portions of the sequence marked with asterisks.

7.2.1.1.1.4 PEPTIDE-ANTIGEN SEQUENCE SELECTION

The high-scoring hydrophilic, epitopic sequences were then used to screen the NCBI databases for the same putative epitopes on other, undesired, proteins, in order to avoid antigenic sequences likely to produce cross-reactive antibodies. The databases were searched using BLAST software (National Institutes of Health). This also provided information regarding homologs in other species and tissue distribution. Two potential peptide-antigen sequences, per clock protein, were proposed and a final selection made, following advice, both, from in-house: Dr Kevin Morgan, Professors Rodney Kelly and Philippa Saunders and from the sequence spotter at Affiniti Research Products Ltd, Biomol International LP, Paul Sheppard (Figure 7.6).

CRY1 *Ovis aries*

Sequence selected

irishtlydl dkiielnggq ppltykrfqt liskmeplei pvetitsevm ekcttp**lsdd * hdekygvpsl ee**lgfdtdgl psavwpgget ealtrlerhl * erkawvanfe rprmnansll asptglspyl rfgclscrlf yfkltdlykk vkknssppls l

PER1 *Ovis aries*

Epitope Locator program

spsppsssia ysllsassep dnpstsgcss eqsarartqk elmtal**relk lrlpperrgk * gr**sgtlatlq yalacvkqvq anqefyqqws leegepcamd mstytleele hvtseytlrn * qdtfsvavsf ltgr

Figure 7.6 Amino acid sequences of oCRY1 and oPER1 with the final antigen-peptide sequence selection underlined and in bold font.

7.2.1.1.1.5 IMMUNOGEN CONSTRUCTION

To increase the immunogenic potential of the sequences, they are conjugated to keyhole limpet haemocyanin (KLH). KLH is a carrier protein, much larger than the oligopeptide sequences selected, and capable of solely, stimulating an immune response. The KLH is conjugated to the oligopeptide by a cysteine amino acid (C). As both of the selected sequences derive from the N-terminal of their respective proteins, the C is attached to the potentially less-antigenic C-terminal end of the

oligopeptide. It is supposed that the N-terminals are more likely to protrude, as they would in their *in vivo* conformation, while the more C-terminal oligopeptide parts would not as they would likely not *in vivo*.

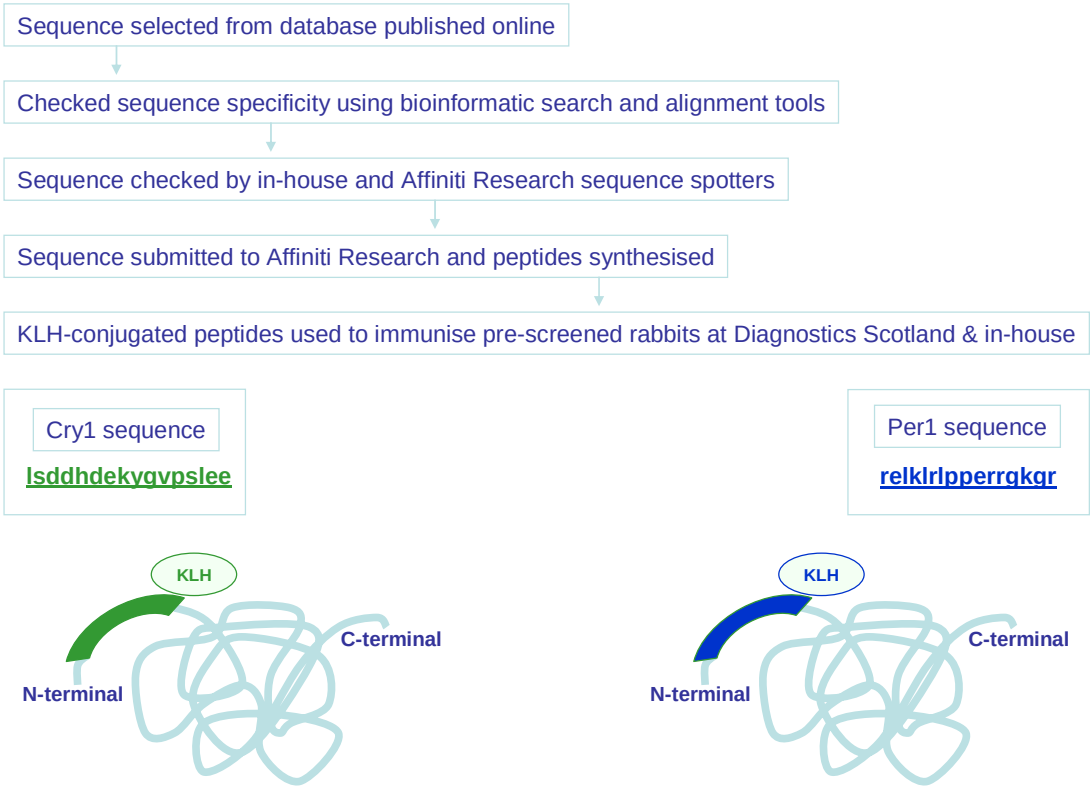

Figure 7.7 Sequence of events in the selection of the antigen-peptide sequence, with diagrams depicting the putative location of the KLH-conjugated antigen-peptide sequence corresponding to the native oCRY1 and oPER1 proteins.

The resulting immunogens (Figure 7.7), composed of oligopeptides coupled with carrier proteins, using a standard cross-linker: m-maleimidobenzoyl-N-hydroxysuccinimide ester (MBS), were then synthesised by the Peptide & Protein Research Services of Affiniti Research Products Ltd, Biomol International LP. Unconjugated oligopeptides were also synthesised for use when testing the reactivity of the antibodies.

7.2.1.2 ANIMAL IMMUNISATION

Rabbits were used as the hosts for immunisation. Their treatment and the experimental procedures performed using them were in compliance with the UK Animals Scientific Procedures Act of 1986 and with the regulatory board license awarded to Professor Alan M^{c}Neilly (project license number: PPL60/3232 19B, A12) for the production of polyclonal antibodies using rabbits.

Before immunisation with the immunogens, four rabbits from Diagnostic Scotland and three rabbits that were obtained for immunisation in-house were screened for any pre-existing cross-reactivity to clock gene peptides, using enzyme-linked immunosorbent assays (ELISAs). The pre-immune sera were substituted for primary antibodies, used in IHC with ovine and murine hypothalamic and PT sections. Primary antibodies raised against VIP (DiaSorin Ltd, Wokingham, UK) and αGSU were also used as positive controls in hypothalamic and PT sections respectively. The IHC protocol that was followed was the one incorporating thick 50 μm sections in free-floating conditions. The sections were treated both, with and without, antigen retrieval using pronase. The sera were tested over a range of dilutions: from 1:10 to 1:1 000. They and the positive control primary antibodies were incubated overnight at 4^{o}C. Both, SARB or GARB, secondary antibodies were used at a 1:500 dilution.

Two of the four rabbits from Diagnostic Scotland failed the test and were excluded from any further use. The remaining 2 rabbits from Diagnostic Scotland were inoculated with the CRY1 immunogen. All 3 rabbits obtained for immunisation in-house passed the pre-immunity test and were inoculated with the PER1 immunogen.

Each rabbit received approximately 2 mg peptide with 0.3 ml warm MPL® + TDM + CWS Adjuvant (Sigma, Dorset, UK) dissolved in 0.7 ml PBS. The MPL® + TDM + CWS Adjuvant is comprised of 0.5 mg monophosphoryl lipid A from *Salmonella minnesota* (MPL), 0.5 mg trehalose dicorynomycolate (TDM) and 0.5 mg cell wall skeleton from a tubercule bacillus (CWS) in 2% oil-Tween® 80-water. The CWS provides additional immunopotentiating activity. The rabbits were injected at multiple sites: 200 μl intramuscularly per hind leg, 100 μl subcutaneously in the neck and the remaining 300 μl subcutaneously in a further 6 sites. Re-inoculation was then

repeated approximately every 4 weeks. The rabbits receiving the PER1 immunogen were re-inoculated twice and the rabbits receiving CRY1 immunogen were re-inoculated four times. A 50 ml blood donation was taken after each re-inoculation, a week later, from each rabbit. The blood was left to clot: standing overnight at 4^{o}C. The straw-coloured serum was then decanted into sterile universal containers and the clot discarded. The sera were stored at 4^{o}C in the interim while they were initially tested for immunoreactivity and until they were cleared of serum proteins and their concentration. The final blood donation was obtained by exsanguinating the rabbits and thus provided the largest volume of blood and antibodies (Figure 7.8). As the antibodies produced are polyclonal, it was prudent to obtain antibodies from the rabbits before their exposure to the immunogen became chronic as this has been previously known to adversely affect the clonal population of the antibodies.

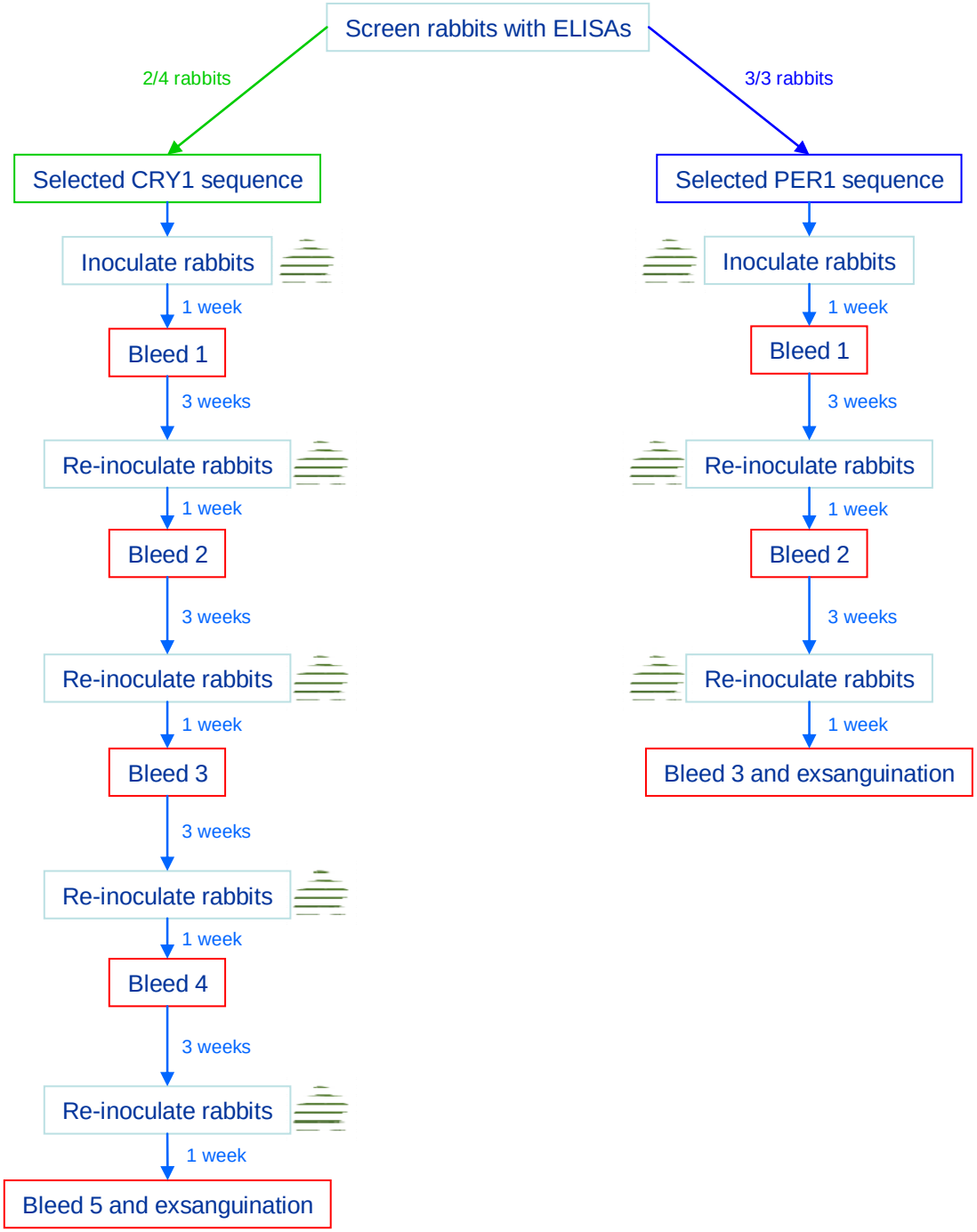

Figure 7.8 Timeline of rabbit immunisations and bleeds in the production of anti-oCRY1 and anti-oPER1 antibodies.

7.2.1.3 ANTIBODY PURIFICATION

The sera, prior to clearance of serum proteins, were tested with ELISAs. They were tested in a range of dilutions: from neat to 1:100 000, for reactivity against the unconjugated PER1 and CRY1 control peptide-antigens. The pre-immune sera were used as negative controls.

7.2.1.3.1 ENZYME-LINKED IMMUNOSORBENT ASSAY

The sera, prior to clearance of serum proteins, were tested with enzyme-linked immunosorbent assays (ELISAs). They were tested in a range of dilutions: from neat to 1:100 000, for reactivity against the unconjugated PER1 and CRY1 control peptide-antigens. The pre-immune sera, which had already been screened using ELISAs (at 1:10, 1:20, 1:50, 1:100, 1:200, 1:500 and 1:1 000 dilutions, with SARB diluted 1:50 and visualised using DAB), were used as negative controls.

Briefly: the lyophilised control peptides were reconstituted in distilled water to a 0.5 mg/µl concentration, maintained at pH 7. Peptide solution (100 µl) at a 0.5 mg/µl concentration was used to coat each well of a Reacti-Bind™ maleic anhydride activated polystyrene 96-well plate. Half the wells were coated with PER1 and the other half with CRY1. The plate was incubated on a microplate shaker for 1 h at room temperature. The maleic anhydride on the plate reacts and bonds with the largely basic PER1 and largely acidic CRY1 peptides. The wells were washed 3 x 200 µl of SuperBlock® Blocking Buffer then rinsed a further 3 x 300 µl PBS. The peptide or ligand was thus immobilised on the plates, which were used immediately for ELISAs.

The test sera, containing antibodies, were diluted 1:100, 1:1 000 and 1:10 000 in wash buffer consisting of 0.1% BSA and 0.05% Tween® 20 detergent in PBS. This primary or *capture* antibody (100 µl) was added to each well, in duplicate, and the plate incubated for 1 h at room temperature. This allowed the antibodies in the sera to bind to the peptide-antigen. Excess antibody was then rinsed off three times with 200 µl of wash buffer. HRP-labelled goat anti-rabbit immunoglobulin G (IgG) secondary or *detection* antibody (Amersham Biosciences, Buckinghamshire, UK) (100 µl)

dissolved 1:50 in wash buffer was added to each well and the plate incubated for 1 h at room temperature. The secondary antibody specifically binds to the primary antibody. Excess antibody was again rinsed off three times with 200 µl wash buffer. The amount of secondary antibody bound to the primary antibody-peptide-antigen matrix was then measured using a colorimetric substrate.

Colorimetric substrate solution (100 µl) was added to each well and the colour left to develop for 30 min. The reaction was stopped, by adding 50 µl of stop solution. The absorbance of the wells at 450 nm was measured using spectrophotometry. The greater the colorimetric reaction, the darker and more light-absorbent the liquid in the ELISA plate. A successful antibody reaction is demonstrated by a colorimetric reaction that is graduated, corresponding to the serial dilutions of the sera. The ELISA was performed in duplicate as a control.

The results of the ELISAs are as follows (Figure 7.9):-

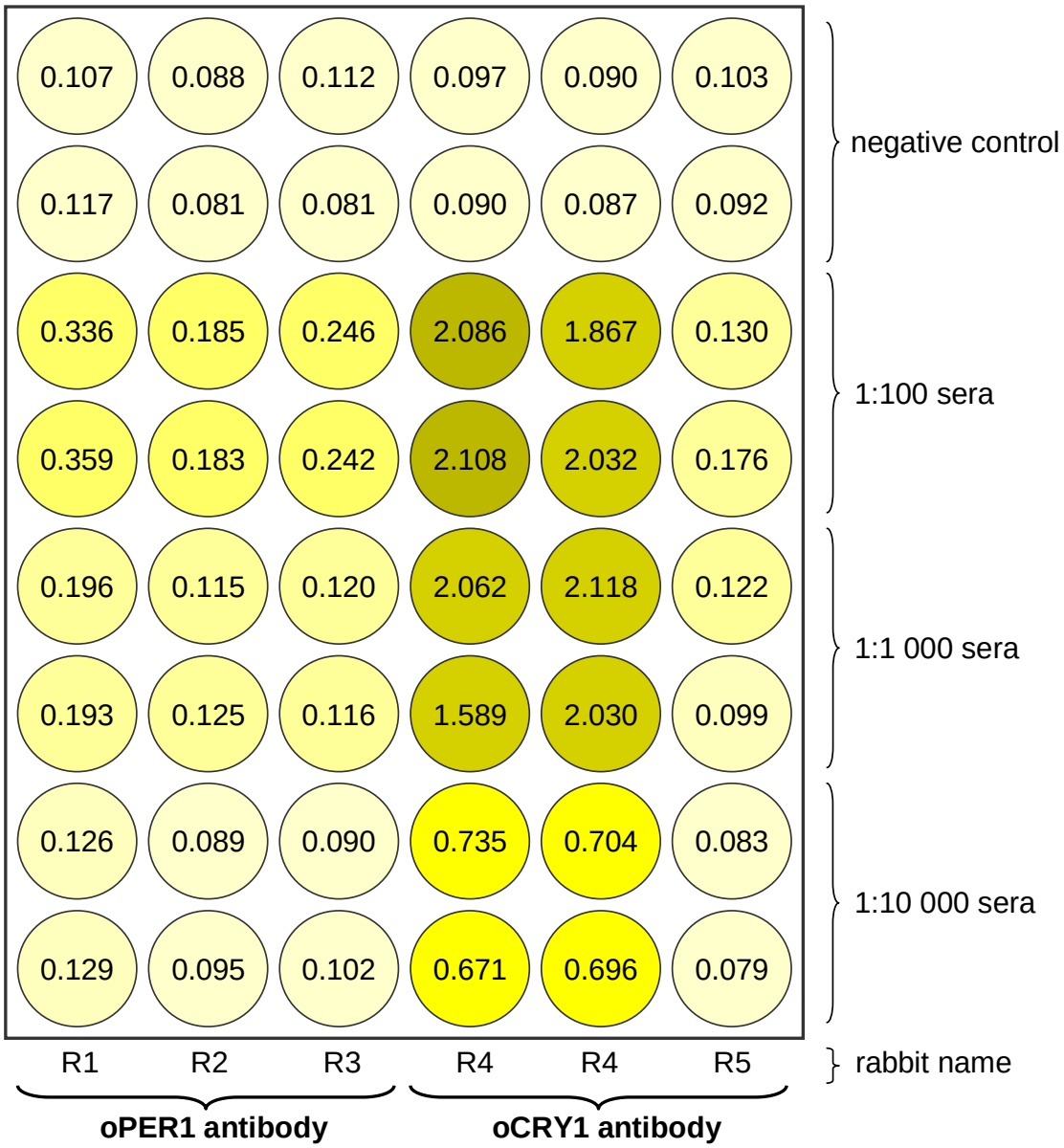

Figure 7.9 A schematic diagram of an ELISA plate with colorimetric detection of the oCRY1 antibodies from three rabbits: R1, R2 and R3 and the oPER1 antibodies from two rabbits: R4 and R5 binding to the unconjugated positive control peptide oCRY1 and oPER1 respectively, with corresponding absorbance values at 450 nm of the well contents.

7.2.1.3.2 CAPRYLIC ACID AND AMMONIUM SULFATE IMMUNOGLOBULIN G PURIFICATION

This protocol was adapted from standard published ones. The sera, from the exsanguination (final bleed) of each rabbit, were purified. The sera were each diluted with 2 volumes of 60 mM acetate buffer, comprised of 0.15% sodium acetate and 0.3% acetic acid in distilled water, pH 4.5 (titrated with 1 M Tris). Caprylic acid (25 µl) (Sigma, Dorset, UK) was added per ml of diluted sera. The acid was added slowly, drop-wise, using a syringe and 20-gauge needle, into constantly agitated sera. In mildly acidic conditions, the addition of short-chain fatty acids, such as caprylic acid, to serum will precipitate most serum proteins with the exception of the IgG. The sera were left stirring for 30 min at room temperature after the addition of caprylic acid, to allow the non-IgG serum proteins and albumin to completely precipitate out of solution. The solution was then centrifuged for 15 min at 3 000 *g* at 4°C. The supernatant was carefully decanted and filtered to remove any residual precipitate. The pellet was discarded and the supernatant dialysed for 2 days against PBS at 4°C. The resulting dialysed solution, containing IgG, was then quantified, using a Bio-Rad Protein Assay (Bio-Rad Laboratories (UK) Ltd, Hertfordshire, UK). The purified sera were suitably aliquoted and stored at -20°C.

7.2.1.4 TESTING ANTIBODIES WITH IMMUNOHISTOCHEMISTRY

The antibodies were tested using free-floating 50 µm-section and conventional 5 µm-section IHC protocols on ovine hypothalamus and PT sections. The hypothalamic sections contained the SCN, PeVN, PVN and SON. The antibodies were also control tested for specificity. Where there were some pre-immune sera left after the ELISAs, this was used as a negative control. Conventional IHC was performed using overnight pre-incubation of the primary antibody with 10 x antibody concentration of the unconjugated peptide-antigen. This 10-fold excess of antigen bound specifically to the antibodies, flooding their antigen epitope-recognition sites, thus inactivating the antibody's potential to bind to the native peptides in the tissue sections.

7.2.1.4.1 DERIVING POSITIVE CONTROLS

7.2.1.4.1.1 IMMUNOHISTOCHEMISTRY

The immunohistochemistry protocol was adapted from existing protocols practiced in-house. The technique employed 5 μm thin tissue sections. Antibodies were first used against SCN neuronal marker peptides, as they were reported to be more abundant than clock proteins. The marker peptide was VASOPRESSIN (VP). Antibodies against the clock protein, BMAL1 would also be used.

7.2.1.4.1.1.1 TISSUE SAMPLING

Normal healthy sheep scheduled for culling were used to provide tissue to test the antibodies, using IHC. The sheep were killed using pentobarbital injection, and their heads decapitated. The decapitated heads were perfused through both carotid arteries with 1 L PBS, then 1 L 4% NBF. The partially fixed brain was then resected with the PT attached. It was extracted with as much of the attached pituitary gland that could be prised out of the sella turcica. A hypothalamopitutiary block containing the SCN, PT and possibly some pituitary gland was resected (Figure 7.10). It was post-fixed by immersing immediately in 4% NBF for 6 h at 4^{o}C, then transferred to 70% ethanol at 4^{o}C.

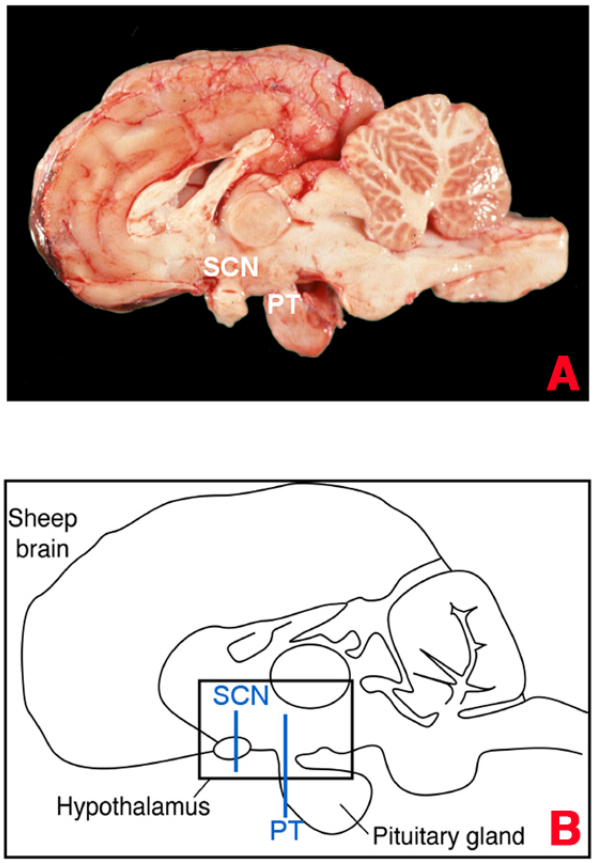

Figure 7.10 A: Photograph of ovine brain, sagitally sectioned along the midline. B: Schematic diagram of ovine brain, in sagital midline section. The rectangle indicates the hypothalamopituitary section that was resected during tissue sampling. The blue lines indicate the region that was sectioned for immunohistochemistry.

7.2.1.4.1.1.2 SECTIONING

The block was coronally re-blocked, along the coronal plane, into two smaller blocks: one containing the SCN and one containing the PT. The tissue was then saturated and embedded in paraffin wax. The wax-embedded blocks were sectioned at a relatively standard thickness of 5 μm on a Leica Jung RM 2035 microtome (Leica Microsystems, Milton Keynes, UK) mounted on Menzel-Gläser Superfrost® Plus slides (BDH via VWR International Ltd, Leicester, UK) and then left to dry and adhere at 40°C overnight (see Fig 1.2.3.1). The dried sections were then stored at room temperature.

7.2.1.4.1.1.3 IMMUNOHISTOCHEMISTRY WITH THIN MOUNTED SECTIONS

The sections were dewaxed in 100% xylene and rehydrated in a series of graduated alcohols then water. They were then antigen retrieved by pressure cooking in 0.01 M citrate buffer (pH 6). They were cooked for 5 min at full pressure then left to stand for 20 min and finally cooled under running tap water. Any endogenous peroxidase activity in the tissues was blocked by washing the sections in 3% (v/v) H_2O_2 in 40% methanol for 30 min at room temperature. The sections were then washed three times for 5 min in PBS. Any nonspecific antibody-binding sites were blocked by incubating sections in blocking serum composed of NGS (Autogen Bioclear UK Ltd, Wiltshire, UK) diluted 1:4 in PBS containing 5% BSA (Sigma, Dorset, UK). The sections were then incubated in humidity chambers overnight at 4°C with the primary antibody diluted in blocking serum. The primary antibodies against SCN marker peptides: VP and VIP (DiaSorin Ltd, Wokingham, UK) were used at various dilutions: VP at 1:1000 and VIP at 1:100,

Table 7.1). The primary antibodies against ovine clock proteins were used neat and the BMAL1 antibody (Autogen Bioclear UK Ltd, Wiltshire, UK) was used at a 1:20 dilution (

Table 7.1). Control sections were incubated with blocking serum to confirm the action of the primary antibody.

Antibody	**Catalogue No.**	**IHC Conc.**	**Secondary Antibody**
Rabbit anti-sheep PER1 IgG	-	neat	SARB
Rabbit anti-sheep CRY1 IgG	-	neat	SARB
Rabbit anti-*Drosophila* BMAL1 IgG	BMALD11-A	1:20	GARB
Rabbit anti-VP antisera	20069	1:1000	SARB
Rabbit anti-porcine VIP antisera	20077	1:100	GARB

Table 7.1 Caprylic-acid purified polyclonal ovine clock gene primary antibodies and affinity purified commercial primary antibodies used in this study: vasopressin (VP) and vaso-intestinal peptide (VIP), indicating the species the antibody was raised in and against, the antibody catalogue number where appropriate, the dilution used and the appropriate secondary antibody.

Excess primary antibody was washed off in three 10-min PBS washes. The sections were then incubated with the appropriate secondary antibody, either swine anti-rabbit biotinylated (SARB) (Dako, Cambridge, UK) or goat anti-rabbit biotinylated (GARB) (Vector Labs, California, USA), diluted 1:500 in blocking serum, for 1 h at room temperature. Unbound antibody was washed off in three, 10-min, PBS washes. ABC-HRP (Dako, Cambridge, UK), diluted in 0.05 M Tris-HCl (pH 7.4) according to the manufacturer's instructions, was added to the sections. They were incubated at room temperature for 30 min then the excess ABC-HRP was washed off in three, 5-min, PBS washes. The ABC-HRP was then detected using the peroxidase substrate, DAB (Dako, Cambridge, UK). When the brown DAB staining was optimal (neither too weak nor too strong), as detected under a Zeiss ICS KF2 light microscope (Carl Zeiss Ltd, Welwyn Garden City, Hertfordshire, UK), the peroxide reaction was stopped. It was stopped by immersing the sections in distilled water. The DAB stain was effectively of the immunoreactive-protein. The negative control should generally be devoid of any brown DAB staining.

The sections were then counterstained with a blue nuclear stain: Harris' haematoxylin (BDH via VWR International Ltd, Leicester, UK). The sections were then dehydrated in graduated alcohols and xylene. They were then mounted (Cover Glass; VWR International Ltd, Leicester, UK) with Pertex© mounting medium (Cell Path, Hertfordshire, UK). The cellular localisation of the immunoreactive-protein was examined and any staining photographed, using a Provis AX70 microscope (Olympus Optical, London, UK) fitted with a Canon DS6031 digital camera (Canon Europe, Amsterdam, The Netherlands).

7.2.1.4.1.1.4 IMMUNOHISTOCHEMISTRY RESULTS

7.2.1.4.1.1.4.1 CRY1

The polyclonal anti-oCRY1 antibodies raised were successfully used in positive control sections of hypothalamopituitary tissue (Figure 7.11). The antibodies visualised the oCRY1 in the ovine median eminence (ME) and PT. The neural ME staining was very different from that of the glandular-like PT. The staining in the ME was much sparser, as would be expected for neural tissue (Figure 7.11 Panels A and B). Individual oCRY1-positive neurones can be seen (Figure 7.11 Panel C). The PT staining was very dense and the oCRY1 appeared to localise specifically to cells, that were arranged in small clusters, that were then arranged in a striated pattern, virtually throughout the PT tissue (Figure 7.11 Panel D). The negative control omitting the primary antibody was clear (Figure 7.11 Panel E).

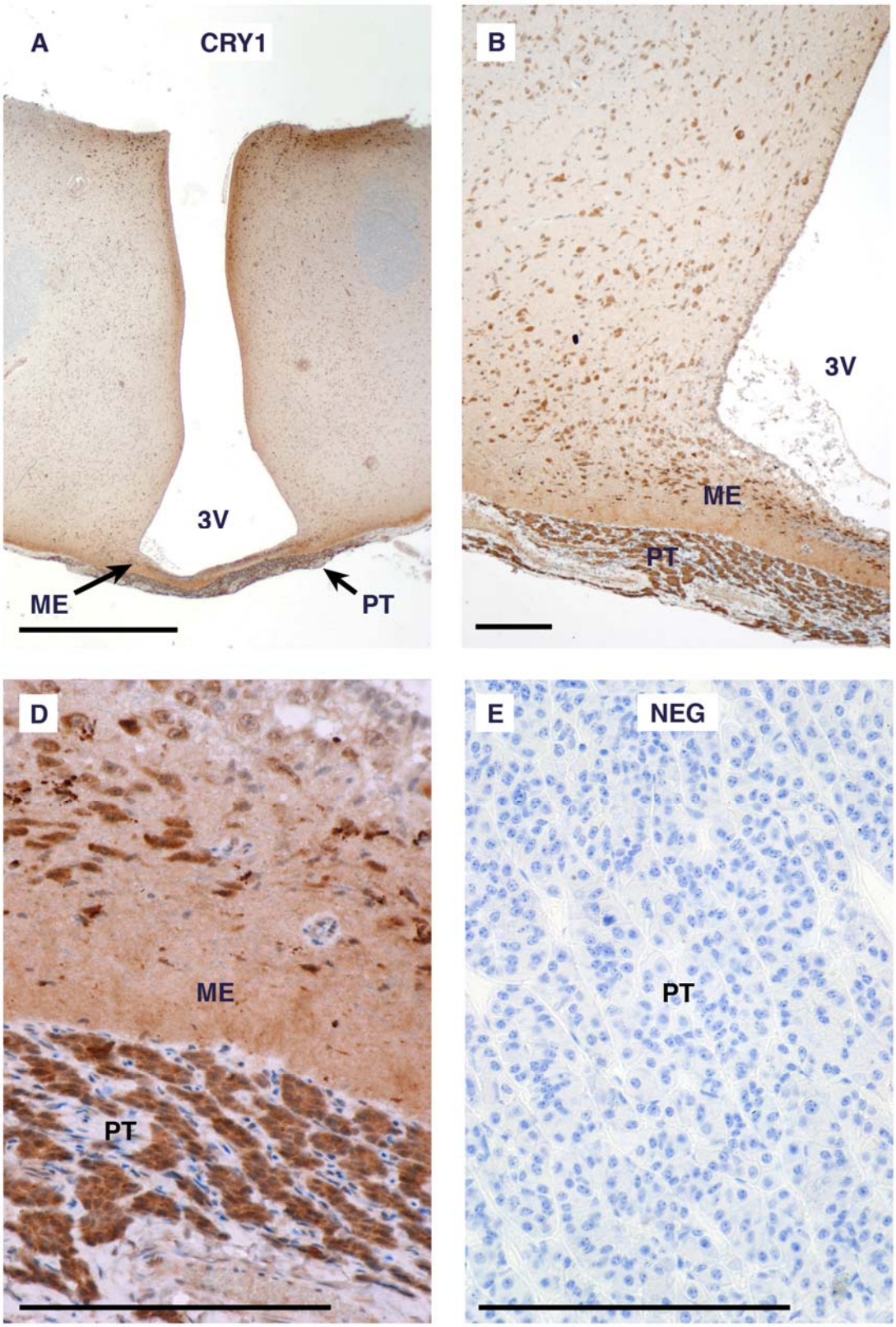
A
CRY1
3V
ME
PT
B
3V
ME
PT
D
ME
PT
E
NEG
PT

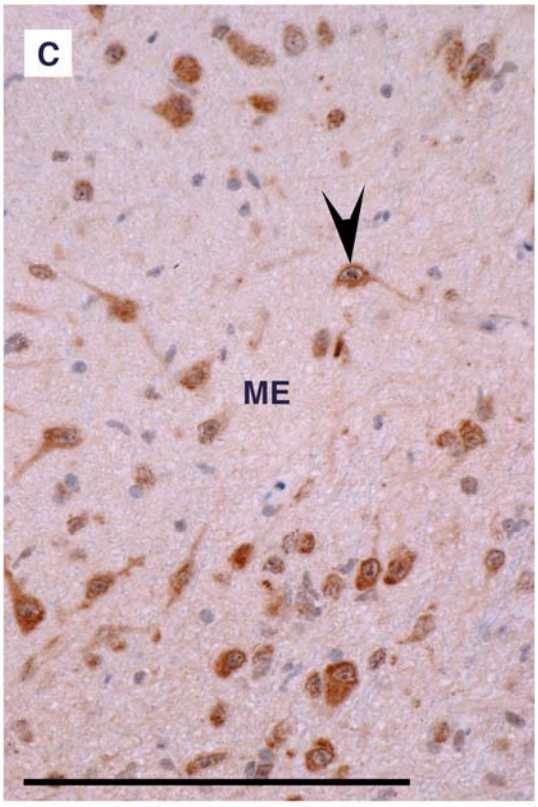

Figure 7.11 Photomicrographs showing ovine CRY1 staining (brown) in ovine hypothalamopituitary sections containing the third ventricle (3V), median eminence (ME) and PT. The arrowheads point to positively stained cells. CRY1 staining in the ME and PT are shown in the hypothalamopituitary section at low power in A and high power in B. C shows CRY1 in ME neurones and D shows CRY1 in the ME and PT. E is the negative control omitting primary antibody. The scale bars represent 100 μm except in A, where it represents 1000 μm.

The anti-oCRY1 antibodies also successfully localised the clock protein to the SCN and periventricular nucleus (PeVN) (Figure 7.12). The staining of the PeVN neurones can clearly been seen along with the smaller SCN neurones (Figure 7.12 Panel A). These can be seen more clearly at higher magnification, where the CRY1 protein appears to be mostly cytoplasmic in the SCN neurones (Figure 7.12 Panel B) as well as in the PeVN neurones (Figure 7.12 Panel C). The negative control omitting primary antibody is shown in Panel D. VP staining has been used to provide some idea of the anatomy and the location of the SCN (Figure 7.12 Panel E), which has been highlighted using the colour-replacement tool in Adobe Photoshop CS2 (Figure 7.12 Panel F).

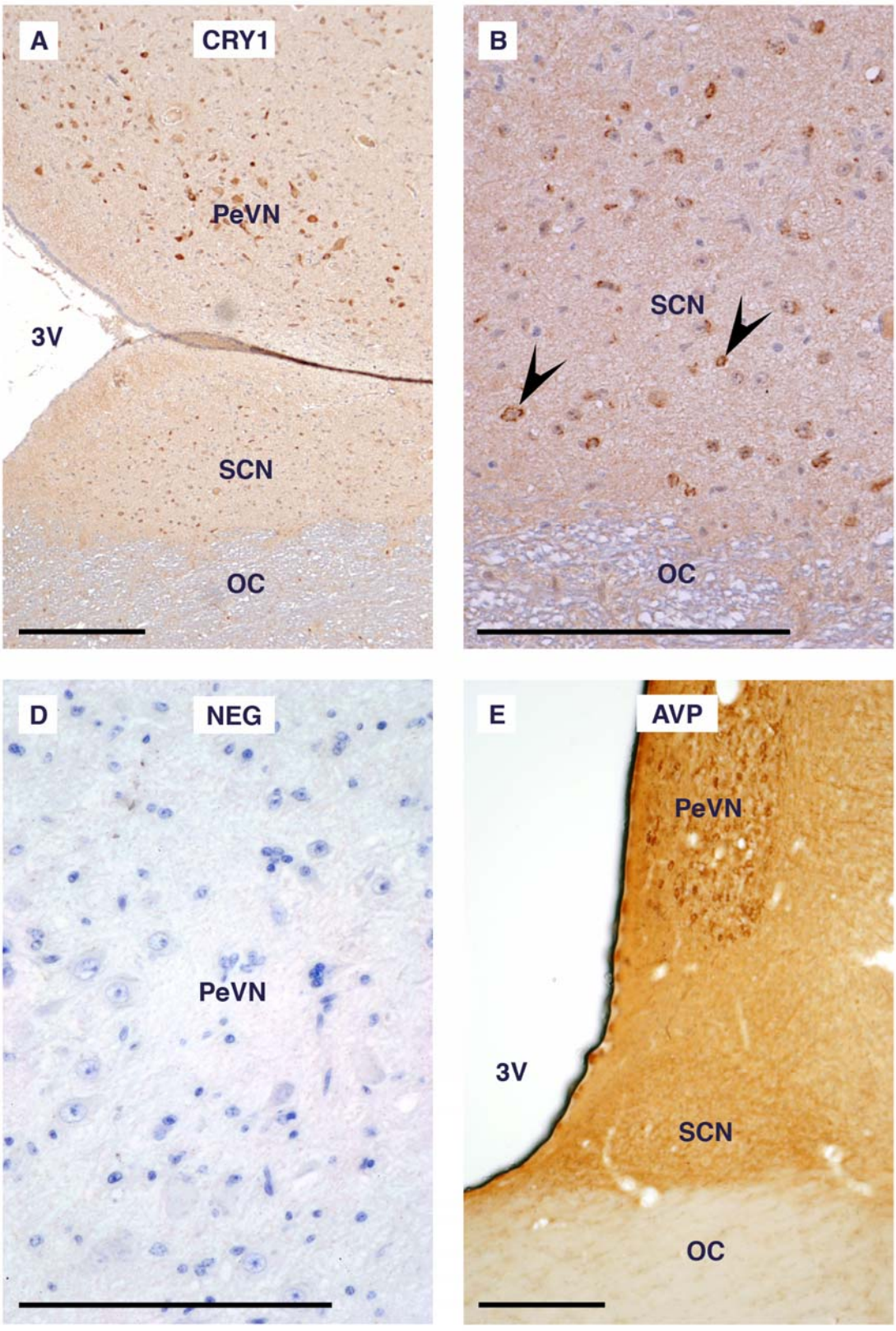
A
CRY1
PeVN
3V
SCN
OC
B
SCN
OC
D
NEG
PeVN
E
AVP
PeVN
3V
SCN
OC

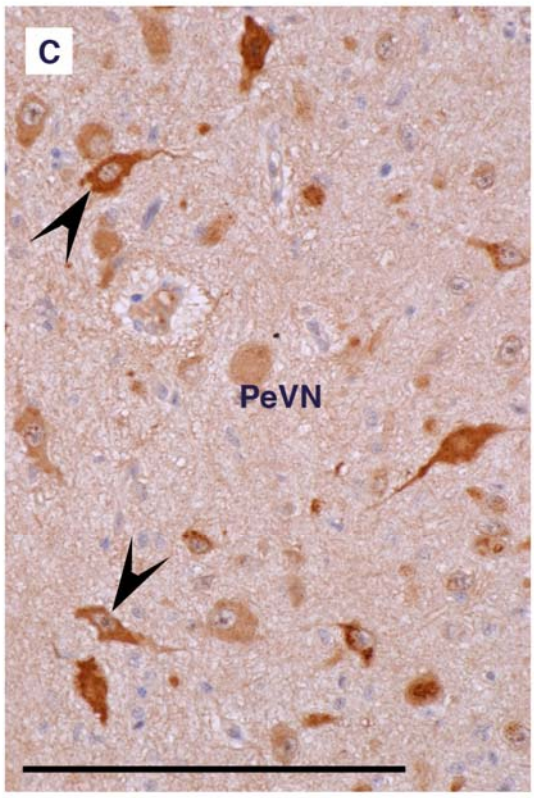

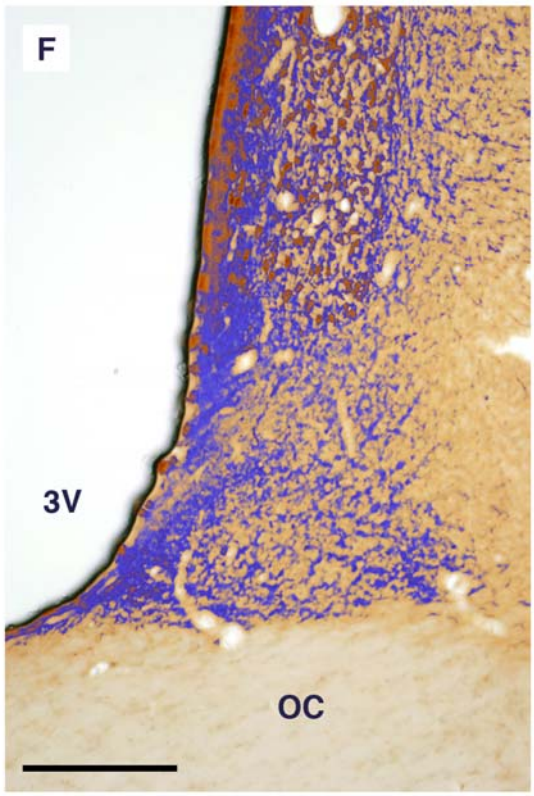

Figure 7.12 Photomicrographs showing ovine hypothalamic sections containing the third ventricle (3V), optic chiasm (OC), periventricular nucleus (PeVN) and SCN with ovine CRY1 staining (brown) in A, B and C, and VP staining(brown) in E and F, with a nuclear counterstain (blue). The staining of oCRY1 in neurones on the PeVN and SCN is shown at low power in A, and in higher power in the SCN neurones in B, and at higher power in PeVN neurones in C. The VP staining in the SCN has been highlighted (indigo) using the colour replacement function of the Photoshop CS2 image-processing software. The arrowheads point to neuronal staining. D is the negative control omitting primary antibody. The scale bars represent 100 μm.

7.2.1.4.1.1.4.2 PER1

The anti-oPER1 polyclonal antibodies produced very specific stain, in a small proportion of the cells in the hypothalamopituitary tissue (Figure 7.13). Cells that appear the same morphologically, differ in their oPER1 localisation. The stain appears to always be nuclear. The negative control omitting antibody was clear, so the staining observed is specific to the primary antibody. The staining patterns in the *pars distalis* of the pituitary gland appear more widely distributed than the staining in the PT (Figure 7.13 Panel A and B), ME (Figure 7.13 Panel A) and paraventricular nucleus (PVN) (Figure 7.13 Panels E and F). The cells that stain particularly densely appear to be corticotrophs, due to their sparse location on the edge of the main clusters of pituitary (lactotroph) cells (Figure 7.13 Panels C and D). The negative controls omitting primary antibody in the PT and neural tissue of the hypothalamopituitary sections were clear (Figure 7.13 Panels G and H).

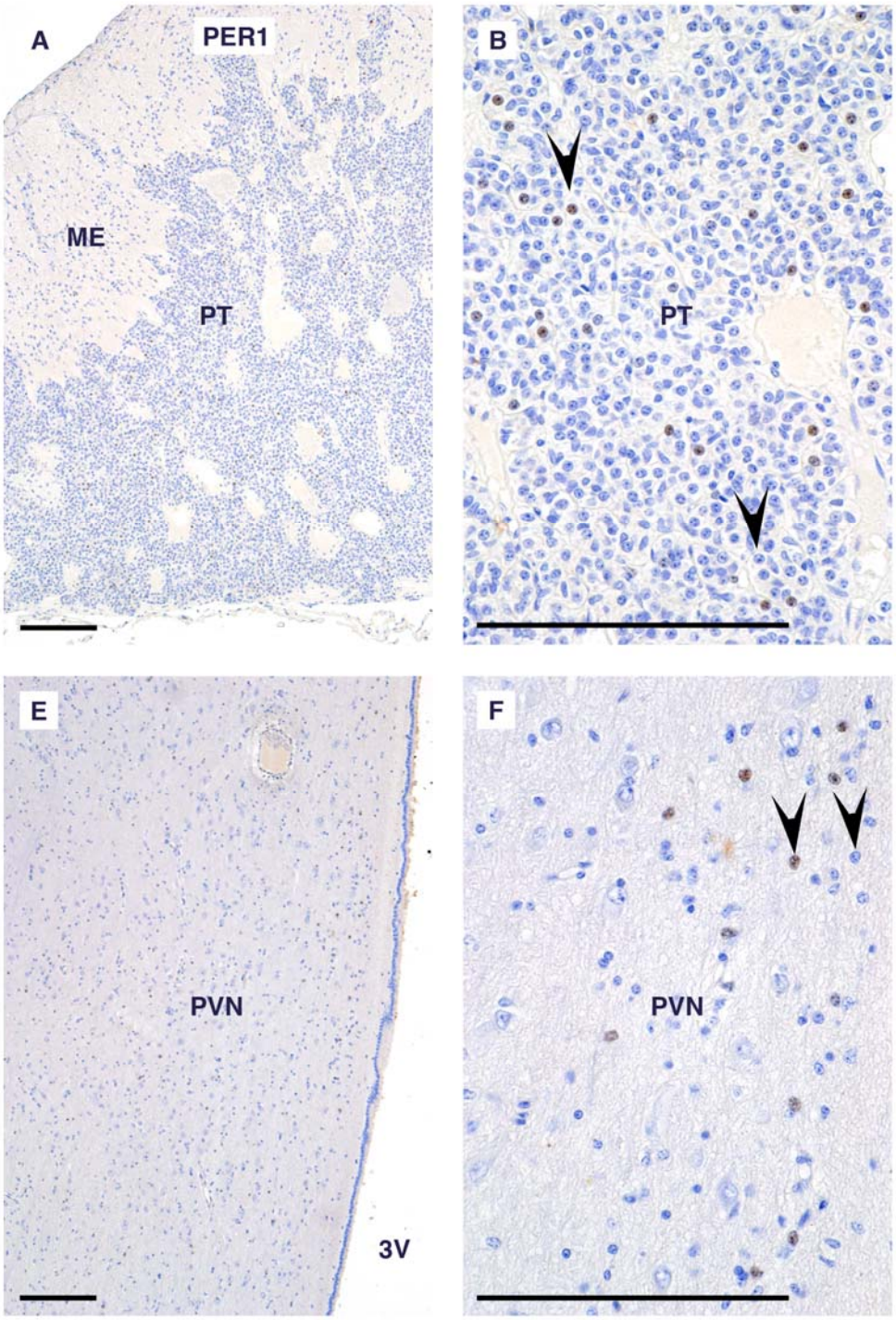
A
PER1
ME
PT
B
PT
E
PVN
3V
F
PVN

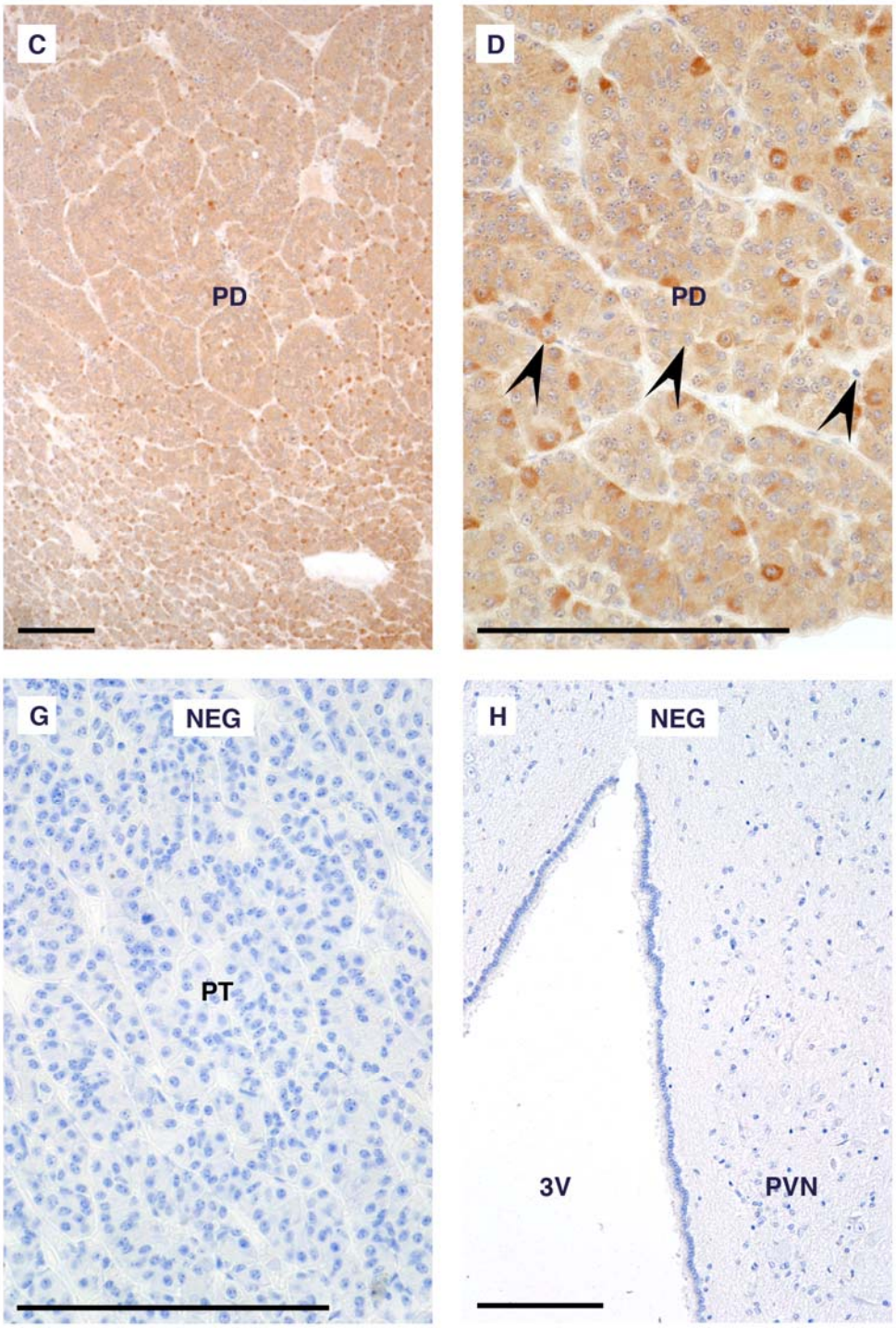

Figure 7.13 Photomicrographs showing ovine hypothalamopituitary sections containing the third ventricle (3V), PVN, PT and *pars distalis* (PD) with ovine PER1 staining (brown) with nuclear counterstain (blue). The arrowheads point to positively stained cells. G and H are negative controls omitting primary antibody. The scale bars represent 100 mm except in A, C and E, where it represents 1000 mm. G and H are negative controls omitting primary antibody.

7.3 RESULTS

7.3.1.1 CLOCK PROTEINS IN THE OVINE CORPUS LUTEUM

IHC was then performed on ovine sections that were obtained from corpora lutea that were sampled on Day 30 of the ovine ovarian cycle. These sections were obtained from an existing tissue bank of paraffin-embedded NBF-fixed normal ovine corpora lutea. These sections were used for initial optimisation of the IHC protocol. The ovine clock proteins: CRY1, PER1 and BMAL1 were all observed in the ovine corpora lutea (Figure 7.14). CRY1 localised mainly to the cytoplasm, without strong nuclear staining, in the LLCs and SLCs. The fibroblasts and vascular endothelial cells however, did not generally show CRY1 localisation. The oPER1 protein was also present in the cytoplasm of the LLCs, but with the nucleus also often strongly stained. The SLCs demonstrated considerably less cytoplasmic staining and virtually no nuclear staining. Fibroblasts and vascular endothelial cells showed only faint oPER1 staining. BMAL1 was also observed in the sheep CL, using commercial antibodies. It was present in all cell types, predominantly in the LLCs, where staining was both nuclear and cytoplasmic. SLCs were also positively stained but less notably in the nucleus. The fibroblasts and vascular endothelial cells were also BMAL1-positive.

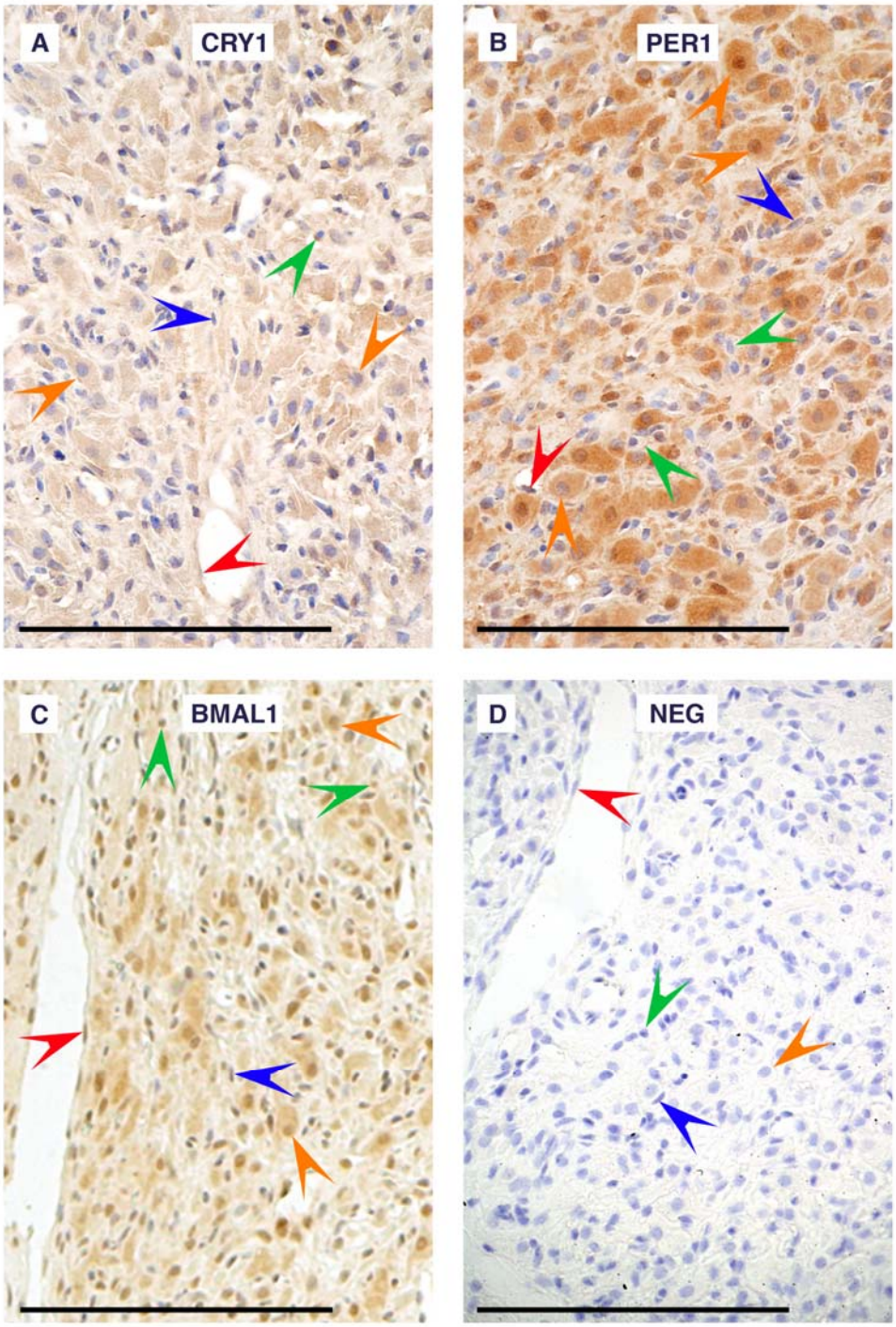

Figure 7.14 Photomicrographs showing ovine corpus luteum sections, containing an admixture of luteal cell types including LLCs, SLCs, fibroblasts and vascular endothelial cells, with staining (brown) for A: ovine CRY1, B: ovine PER1 and C: BMAL1. D is the negative control omitting primary antibody. The arrowheads point to putative: LLCs (orange), SLCs (green), fibroblasts (blue) and vascular endothelial cells (red). The scale bars represent 100 μm except in C, where it represents 1000 μm.

7.4 DISCUSSION

The general aim of this chapter was to raise antibodies against ovine CRY1 (oCRY1) and ovine PER1 (oPER1), with the purpose of using them to localise expression of the clock genes in the sheep CL. This was addressed by attempting to identify the specific ovine amino acid sequence of each of the two clock proteins, assessing the predicted tertiary structure using epitope mapping and hydropathy plotting to identify sites most likely to be antigenic, and that could then be used, in an immunisation protocol, to raise antibodies in rabbits, in sufficient quantities to be of practical value. To this aim, we used a commercial company (Diagnostic Scotland) to produce oCRY1 antibodies, while electing to raised the oPER1 antibodies in-house.

At the time of the study, only partial amino acid sequence was available for oCRY1 and oPER1. The alignment of these sequences with homolog sequences from other species (pig: *sus scrofa*, human: *homo sapiens*, rat: *rattus norvegicus*) as well as ovine CRY2 sequence, revealed a clear degree of homology. This is consistent with the concept that clock genes are highly conserved and that their function in generating a circadian clock evolved at an early stage of evolution. The degree of conservation in the ovine amino acid sequence meant that such sequence may not be recognised as antigenic in an immunisation protocol, as it may too closely resemble the native clock protein in the animal used for immunisation. It was important therefore, that time was spent optimising the design of the peptide-antigen, in order that it would be optimally antigenic.

To do this, potential epitopic sequences were identified in the ovine amino acid sequence, using epitope prediction and hydropathy analysis. The epitope-mapping recognised putative immunogenic amino acid sequences based on known epitopic sequences found in other proteins. The hydropathic characterisation was designed to identify the parts of the sequence which would most likely project from the native protein and therefore be recognised by the antibody when expressed in the tissue. The characterisation was made based on the hydrophilic or hydrophobic nature of each individual amino acid, which determine by the polarity of their side chains. As a result, a 16-amino acid sequence was selected to represent oCRY1 and a 16-amino

acid sequence was selected oPER1 for immunisation. The sequences had an additional amino acid: cysteine to allow coupling to the KLH and also to allow linkage to the ELISA plates. The KLH protein is added as it is highly immunogenic and increases the antigenic potential of the peptide when conjugated. The immunisation process involved the use of an adjuvant in a series of immunisations, used to initially inoculate then boost the production of antibodies in the rabbits.

The immunisation procedures were successful at raising antibodies to the oCRY1 and oPER1. This was assessed initially using an ELISA system, where the unconjugated peptide was used as a positive control ligand, to coat the wells of the ELISA plates. The immunised sera, at a range of dilutions, were applied to the plates and the presence of the antibody that subsequently bound to the plates was assessed using a secondary antibody in a colour-changing reaction. This revealed a clear dilution profile, indicating successful specific binding of the antibody to the positive control peptide, which allowed the selection of the sera from bleeds with the maximum titre. This highest titre antisera were collected from the immunised rabbits, collected from the exsanguinating Bleed 5 for oCRY1 and the exsanguinating Bleed 3 for oPER1. Aliquots of antisera were also purified using caprylic acid precipitation to remove the serum proteins, which left a resulting IgG antibody-rich solution. The neat and purified antisera were then stored in aliquots at -20^{o}C for future studies.

The antibodies were tested in IHC studies using ovine tissues that are known to express the clock genes; tissues that include the SCN, adjacent brain nuclei and the pituitary gland. The results for the oCRY1 antibodies revealed clearly defined immunoreactive cells. The oCRY1 studies were much more informative than the oPER1 antibodies. The oCRY1-positive cells were evident in the SCN; up to around 50 % of the cells were stained. This contrasts to the situation using commercial antibodies, raised against mouse CRY1, which failed to reveal CRY1-positive cells in the ovine SCN. The ovine antibodies also revealed clearly defined cells strongly staining in the PeVN and ME, where the immunostaining was evidently principally in the cytoplasm, but with some in the nuclei. Furthermore, in the PT, the staining was most strong, where the majority of cells were positive and the positive cells were formed into follicular bundles and stranded clusters, while in the PD, positive staining was seen with a pattern distinct from that of the PT.

The immunoreactivity was regarded as specific because there was no staining in the sections when the primary antibody was omitted. The pre-immune sera ELISAs were also devoid of any immunoreactivity. Also the staining was selective for different cells and showed a tissue-specific staining pattern. Results are consistent with the wide distribution of clock gene expression seen by looking at *cry1* mRNA in ovine brain using *in situ* hybridisation (Lincoln et al., 2002, Lincoln et al., 2003). They are also consistent with the view that circadian clocks are expressed in a range of different neurones in the basal hypothalamus and in the specific secretory cells of the pituitary gland. In particular, the very strong staining for oCRY1 in the PT fits with the idea that the PT is a melatonin-target tissue and that melatonin activates *cry1* expression in the PT to relay the effects of photoperiod on seasonal biology, through a circadian- or rather clock gene-based mechanism (Lincoln, 2006).

In contrast, the oPER1 antibodies failed to reveal immunoreactive cells in the SCN and produced very selective staining in other tissues. In the PT, relatively few cells (less than 10 %) were immuno-positive, and these did not reveal the basic follicular structure of the PT, indicating that they were distinct from the PT cells characterised by the oCRY1 antibodies. In the PD, there were clearly defined oPER1 immunoreactive cells, with strongly staining cytoplasm, that had a distribution that was again, very different from that of the oCRY1-positive cells. These oPER1-positive cells were tentatively identified as corticotrophs, due to their sparse location on the edge of the main clusters of pituitary (lactotroph) cells.

Overall, there was no consistency in the IHC patterns for the two clock proteins, which is contrary to the expectation that they would be co-localised in all cells expressing a circadian clock. The best explanation for the observed results is that the oPER1 antibodies recognised a specific epitope of the PER1 protein, that is expressed by a minority of cells and/or at a specific phase of synthesis and turnover in the circadian cycle. This fits with the observation that immunoreactivity for oPER1 was localised to the nucleus in the PT as well as the PVN, in a small proportion of cells, whereas the oCRY1 immunoreactivity was cytoplasmic in a wider range of cells than these two tissues. The more heterogeneous oPER1 staining patterns and sparser distribution of some of the staining suggests that the oCRY1 staining patterns are

more likely to reveal the true distribution of cells expressing the circadian clock than those of oPER1. The selection of the amino acid sequence used to raise the antibodies to PER1, based on putative epitope characteristics and hydropathy plots, may have generated highly specific antibodies, that are not useful in the general characterisation of oPER1 expression but may be specifically useful in characterising the cyclic changes in PER1 protein during the 24-h cycle. This will require further study in order to characterise the PER1 protein in order to confirm the specific PER1 protein (conformation) recognised. Also, there was evidence that the antibodies raised in different rabbits gave different patterns of distribution, although never the same as those for oCRY1.

The special focus of this thesis is on the role of clock genes in the CL. The ovine antibodies were used in preliminary studies to look at clock gene expression in the ovine CL. These studies revealed CRY1 and possibly PER1 immunoreactive cells. Notably, the large, LLCs showed staining for both oCRY1 and oPER1, as well as BMAL1. The staining was consistently cytoplasmic for all three clock proteins, with more clearly discernible nuclear staining of oPER1 and BMAL1 than of oCRY1. The greater nuclear localisation of BMAL1 than of CRY1 is consistent with the operation of a circadian clock where BMAL1 is the positive limb and CRY1 the negative limb of an oscillatory negative feedback loop. It is possible that while the nuclear localisation of PER1 occurs, CRY1 is left predominantly cytoplasmic. This has been observed for PER1 which heterodimerises with TIMELESS (TIM), a clock gene found in *Drosophila*, but then translocates into the nucleus in an undimerised form, as does TIM (Liu et al., 2007). It is also not inconsistent with the presence of a cell-based clock where the necessary time lags required are provided by protein behaviour. The staining of the cells was however, generally heterogeneous, which is comparable to that seen in the human CL. The largely random arrangement of the cell types in the ovine CL compared to the layered structure of the human CL meant that the cell types could only be identified using their homology. This was easier in the late luteal phase when the CL types were better differentiated than in the early luteal phase. A more definitive method of identifying the ovine cell types that the clock proteins localise to would require immunoflourescent co-localisation. The steroidogenic cells would be identified using 3βHSD, and the LLCs distinguished from the SLCs by morphology,

as ovine LLCs do not produce œstrogen and therefore do not contain aromatase. The fibroblasts would similarly be identified using cell morphology. The staining that was observed is considered to be specific as the negative control omitting the primary antibody was entirely clear of staining.

Unlike the situation with the neural and pituitary tissues, where expression of the oCRY1 and oPER1 immunoreactivity was very different for the two clock proteins, the patterns in the ovine CL were essentially the same or very similar. This may be accounted for by the proteins assuming different native conformations in the different tissues. These different conformations may indicate that the roles of these proteins are varied between the tissues, in which clock functions may be tissue-specific. The IHC was performed on brain and luteal sections as a preliminary study and so, multiple brains and corpora lutea, sampled across 24 hours were not used.

In conclusion, the ovine clock genes: oCRY1 and oPER1 as well as BMAl1 localised to all cell types in the ovine CL, though they were most consistent in the LLCs; which was very similar to that of the human granulosa-lutein cells.

In summary, this chapter has:-

1. successfully raised antibodies specifically against oCRY1 and oPER1;
2. detected oCRY1 in the ovine SCN, PeVN, ME, PT and CL;
3. detected oPER1 in the ovine PVN, PT, PD and CL;
4. detected BMAL1 in the ovine CL

8 GENERAL DISCUSSION

Reproduction is a timely process, requiring the temporal co-ordination and convergence of many critical events (Boden and Kennaway, 2006, Kennaway, 2005, de la Iglesia and Schwartz, 2006, Goldman, 1999). Several female reproductive structures are known to express clock genes, including the ovary, oviduct, oocyte, ovarian follicle, uterus and CL. The function of the clock genes in these structures is not yet known, but has been speculated to involve the regulation of reproduction and fertility. The expression of the canonical clock genes: *arntl* (*bmal1*), *clk*, *per1*, *per2* and *cry1* have been reported in the rat ovary, where *arntl* and *per2* were rhythmically expressed, in antiphase, suggesting that a functional circadian clock resides in the ovary (Karman and Tischkau, 2006). The expression of *per1* and *per2* has been observed throughout the œstrous cycle and has been localised using *in situ* hybridisation to the pre-antral, antral and pre-ovulatory follicles and interstitial glandular tissue (Fahrenkrug et al., 2006). The rhythmic expression of *arntl* and *per2* was also affected by LH (Karman and Tischkau, 2006). This suggests that clock genes function, potentially as endogenous clocks, throughout the maturation of the follicle.

The oviduct also expresses *bmal1* and *per2* rhythmically. The expression of the other canonical clock genes: *clk*, *per1*, *cry1* and *cry2* were also seen (Kennaway et al., 2003). It was proposed that the clock genes function to protect the developing embryo in the oviduct, for example, via the rhythmic expression of plasminogen activator inhibitor-1 (PAI-1) which can protect the early embryo from proteases and/or matrix remodelling before implantation in the uterus (Kennaway et al., 2003). The rhythmic expression of the clock and clock-controlled genes may provide a periodic environment to which the developing embryo exposed. The embryo spends somewhere between one to two weeks in this periodic oviductal environment, depending on the species, a time span of several

circadian periods, before implantation. This periodicity is likely to be necessary for the timed development of the embryo which also expresses its own intrinsic clock genes and for the timed passage through the oviduct, where the circadian clock provides a highly regulated control of the time before entry into the uterus. The uterus also expresses clock genes rhythmically, although their exact function remains unclear (Boden and Kennaway, 2006). P_4 production by the developing CL is known to act on the uterus to prime the development of the endometrium. It is probable that the clock gene expression in the uterus governs the circadian window of implantation, when the developing blastocyst is able to successfully implant; some five to ten days after ovulation. The importance of the circadian clock during gestation is indicated by the occurrence of increased fœtal resorption and full-term pregnancy failure in clock gene mutant mice (Miller et al., 2004).

Following ovulation, the cells of the dominant follicle that were exposed to the LH surge develop in a CL by the process of luteogenesis. The clock genes expressed in the ovarian follicle, particularly in the granulosa cells, appear to continue being expressed in the CL, particularly in the ovarian granulosa cell-derived granulosa-lutein cells (He et al., 2007a). During luteogenesis, the luteal cells proliferate and hypertrophy, recruit blood vessels, differentiate and rapidly develop into a large endocrine organ. The CL produces P_4 in progressively increasing quantities from the early through to the late luteal phase. P_4 is essential for implantation through the activation of endometrial development in the uterus and for feeding back on to the brain to stop gonadotrophin secretion and to block further ovulation. It thus determines the length of the œstrous or menstrual cycle. If pregnancy does not occur, the CL is destroyed by a luteolytic mechanism, which is regulated in a variety of ways in different mammals. This results in the withdrawal of P_4, with consequent effects on the uterus, including menstruation in women, as well as the removal of inhibition effects in the brain, that then triggers the onset of the next reproductive cycle. The lifespan of the CL, particularly in humans, is relatively stringently controlled, and is likely to feature clock gene regulation. Certainly, the clock genes: *bmal1*, *clk*, *per1*, *per2*, *cry1* and *cry2* were observed, in the studies

contained in this thesis, to be expressed in the human and the ovine CL throughout the luteal cycle. The clock proteins localised to all the cell types discernible in the human CL, and preliminary studies indicate that this is also true in the ovine CL. Although, at the start of these studies, no clock genes had been discovered in the CL, there are now other independent reports which corroborate the findings of clock gene transcription and translation in the mammalian CL (Boden and Kennaway, 2006, Fahrenkrug et al., 2006).

It is becoming increasingly evident that clock genes serve an important function in the regulation of reproduction. The characterisation of clock gene mutant phenotypes has revealed specific incidence of subfertility and impaired reproductive function (Boden and Kennaway, 2006, Kennaway et al., 2005). It has even been reported that colonies of *bmal1* null mutant mice should be maintained as heterozygotes as colonies of homozygotes have severe fertility impairment (Boden and Kennaway, 2006). It is already known that the pre-ovulatory LH surge is controlled by the circadian clock, gated to the night time in mammals including humans, by the SCN (Kennaway, 2005). Many other hormones involved in the reproductive axis are also known to be regulated by the circadian clock (Kennaway, 2005). What is not known, is the function of the clock genes and the circadian system in the regulation of reproduction as a whole, and particularly at the level of the gonads and reproductive tract, in the HPG axis. The female reproductive tract houses not only clock gene expression but many timely events, suggesting that the local expression of clock genes may be involved in regulating these events. Examples of these events, such as follicular development and ovulation, along with the reproductive tissues that house them, which express clock genes are summarised in Figure 8.1.

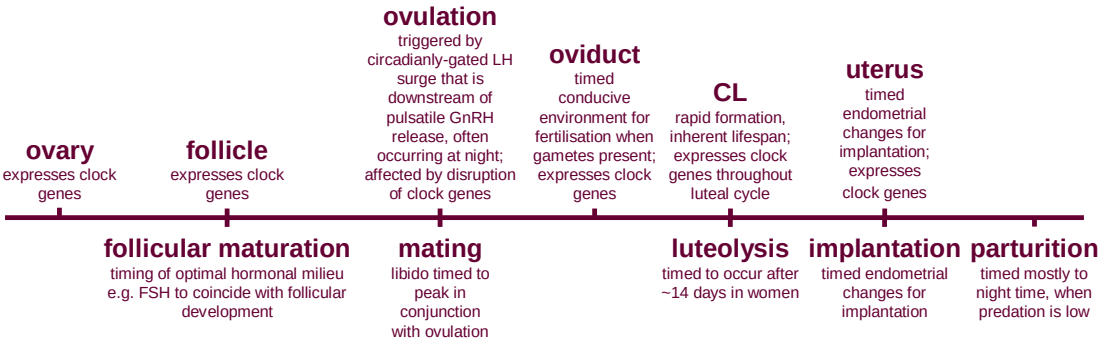

Figure 8.1 Timeline of temporally regulated tissues and events in reproduction.

The overall regulation of these processes is likely to occur at various levels of hierarchical organisation, both locally within the tissue and more systemically, controlled by the brain. The various levels at which clock genes and temporal processes may regulate the reproductive axis are illustrated in Figure 8.2. These processes are inter-related and feed back on each other to produce intercalated feedback loops. These looped processes occur in various tissues, which are also likely to possess endogenous clocks. Certainly, the hypothalamus, which governs many reproductive processes, contains the SCN – the master pacemaker of the circadian system, a nucleus composed mainly of cells with endogenous clocks. The reproductive tract too is likely to be composed of peripheral tissues clocks, which will also fall under the control of the SCN. The hypothalamus then is at the top of both the circadian and reproductive organisational hierarchies and as such, very likely enables the integration of these two systems spatially, in order to provide temporal co-ordination of both systems, with each other and with geophysical time. The function of clock genes in the hypothalamus however does not preclude a local function for the clock genes in the reproductive tract itself. It is likely that clock genes in the reproductive tract are of importance in the co-ordination of reproductive tract functions. This is best illustrated in the domestic chicken, where the pre-ovulatory follicles express clock gene rhythms that are linked to the regulation of steroidogenic synthesis and release, and these rhythms feed back to the

hypothalamus to govern the timing of gonadotrophin secretion and ovulation. Therefore, the SCN co-ordinates the reproductive axis with respect to the time of day, while the ovary co-ordinates the reproductive axis with respect to the maturation of the ovarian follicles, and combined together, these two systems ensure the optimal timing of the reproductive cycle.

This proposed two-system mechanism is illustrated in Figure 8.2. The circadian clock gene-expressing SCN pacemaker governs the pulsatile release of GnRH from the hypothalamus, which in turn effects the pulsatile release of LH and FSH from the pituitary gland, which also circadianly expresses clock genes. These gonadotrophins stimulate the maturation of the ovarian follicle, which is able to synthesis œstrogens from its clock gene-expressing steroidogenic granulosa cells. Œstrogens feed back to the hypothalamus, including the SCN, which is œstrogen-responsive - possessing both alpha (ERα) and beta (ERβ) œstrogen receptors, to direct the pre-ovulatory surge in LH release (Kruijver and Swaab, 2002, Vida et al., 2008, Shinohara et al., 2001). Ovulation, gated to the night time, releases the cumulus-oocyte complex, which expresses clock genes, from the pre-ovulatory follicle into the oviduct, which also expresses clock genes. The leftover follicular cells rapidly remodel into a clock gene-expressing CL, which also expresses StAR in a circadian fashion, and produces P_4. P_4 affects the clock gene expressing uterine endometrial cells, in preparation for implantation of the successfully fertilised embryo, as well as affecting the oviduct and embryo itself. It is able to feed back to the hypothalamus, where the SCN can respond via its P_4 receptors (PR) (Kruijver and Swaab, 2002, Shinohara et al., 2001). The embryo, which travels from the oviduct to implant as the feto-placental unit in the uterine endometrium, secretes hCG, which acts as a luteotrophic maternal recognition of pregnancy signal, that was found in the studies contained in this thesis to affect clock gene expression in the CL. The P_4 signalling back to the embryo as well as the hypothalamus and SCN – which possesses P_4 receptors, therefore closes two feedback loops. The CL, like the ovarian follicle, is also able to synthesise œstrogen, which may also signal back to the hypothalamus and SCN, where œstrogen is known to affect LH secretion.

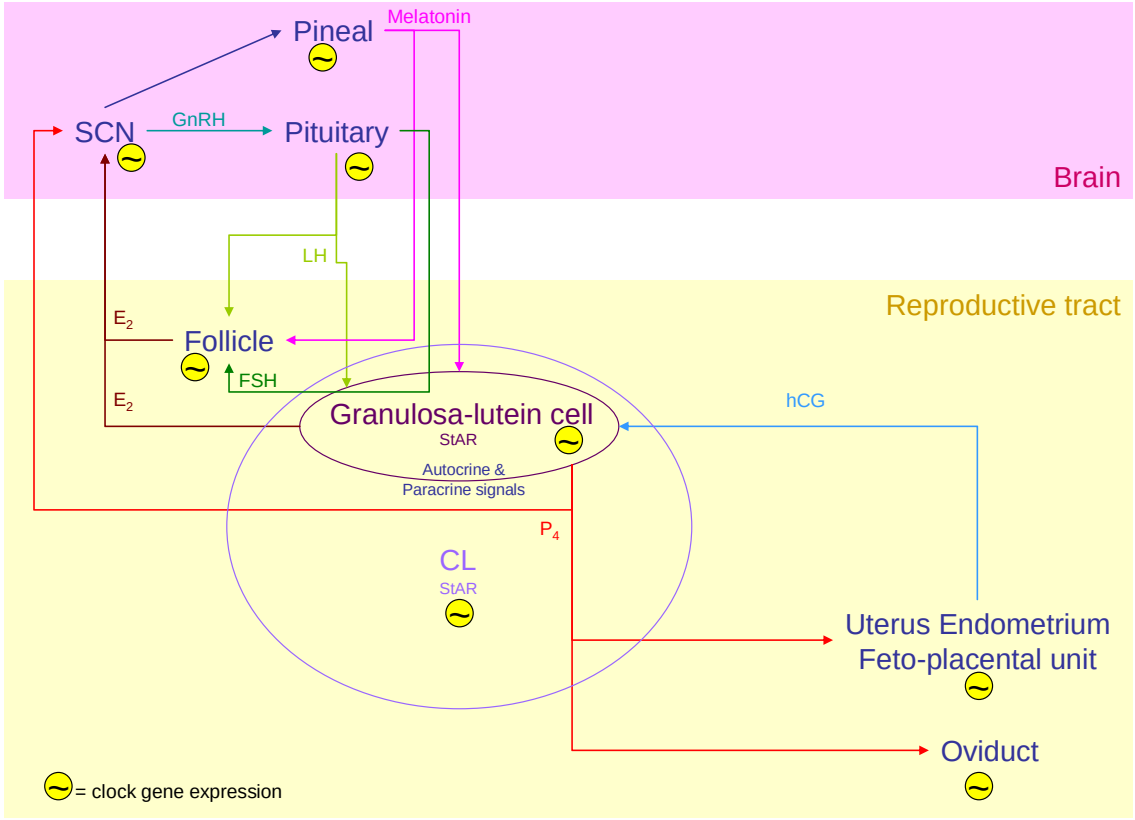

Figure 8.2 Hierarchical organisation of the intercalated feedback loops that regulate the function and timing of female reproductive processes.

The SCN also controls the nycthemeral secretion of melatonin, which acts as a measure of the photoperiod and which may thus impose another level of temporal regulation on the reproductive axis. This is likely to be how the circadian and reproductive systems are co-ordinated with seasonal geophysical time in seasonally reproductive species. Disruption of melatonin signals have been shown to affect the timing of implantation, demonstrating that melatonin does interact with the reproductive axis periods (Miller et al., 2004, Berria et al., 1988, Barbacka-Surowiak et al., 2003). Melatonin is also proposed to affect the CL, based on the reports of granulosa-lutein cells possessing both MT_1 and MT_2 melatonin receptors and on the observations of the studies reported in this thesis (Tamura et al., 2008).

In the ovine PT, which is a classical melatonin-target tissue, photoperiodism affects seasonal physiology through the phase control of clock gene: *cry1* and *per1* expression. With *cry1* expression linked to dusk and *per1* expression linked to dawn, the *per-cry* expression interval varies with the duration of the night and thus, it is proposed that with photoperiod, the relative coincidence between gene expression of the two genes is thought to determine the PER-CRY dimerisation and transcriptional control of downstream clock-controlled genes. The expression of these two clock genes therefore function as an internal coincidence timer (Lincoln et al., 2002). The expression of *cry1* in the ovine CL during the LL phase appears to be melatonin-inducible, much like it is in the ovine PT. In the mature ovine CL, all the clock genes: *bmal1*, *per1*, *cry1* and *cry2*, bar *per2*, were rhythmically expressed. However, the phase relationship between the peaks of expression of the positive limb gene: *bmal1* and the negative limb genes: *per1*, *cry1* and *cry2* of the circadian clock were not as expected for the classical endogenous circadian clock, epitomised by the clocks in the SCN. Moreover, *per2* was rhythmic in EL and not rhythmic in the mature late luteal CL.

This raises the question of whether there is true intrinsic circadian clockwork in these luteal cells. The phase relationships of clock gene expression from intact CL are not consistent with that of a classical circadian clock, but rhythmic clock gene expression was nevertheless, observed. These rhythms could be generated by rhythmic protein interaction, which is regulated via post-translational mechanisms, such as phosphorylation. Phosphorylation of the clock proteins already occurs in both the central and the peripheral clocks, where they are integral to the determination of the period of the clock. This is demonstrated clearly by the *tau* mutation in hamsters, which produces a shorter than 24 hour phenotype as a result of a mutation in the *CK1ε* gene, which encodes a kinase that phosphorylates clock proteins. Thus, the post-transcriptional and post-translational control of clock proteins may be a critical feature determining the clockwork. The question of whether there is true intrinsic circadian clockwork in luteal cells cannot therefore be answered until the temporal profile of the clock proteins have been characterised. These may well exist as it is already known that

post-translational mechanisms act to modulate the function of crucial proteins such as StAR, which is essential for the main function of the CL: steroidogenesis. The requirement for post-translational mechanisms for the provision of temporal clock gene function indicates that extrinsic factors may be required to drive the clock gene expression.

Melatonin may be such an extrinsic factor. Its secretion at night may regulate rhythmic clock gene transcription in the CL as does in the PT. This is possible since MT_1 and MT_2 melatonin receptors are expressed in the CL and melatonin is known to affect P_4 secretion from the CL (Woo et al., 2001). In the PT, where the role of melatonin in the control of clock gene transcription has been best studied, an increase in melatonin concentration at night activates *cry1* transcription, while the decrease in melatonin levels at dawn activates *per1* transcription; and this control provides phase control of these two gene rhythms. In the late luteal ovine CL, peak *cry1* expression occurred in the night time, consistent with the possibility of melatonin-induced activation, while *per1* expression peaked in the early morning, consistent with the possibility that it is regulated by melatonin withdrawal. This extrinsic regulation of *cry1* and *per1* by melatonin may be the mechanism by which luteal clock gene rhythms are functionally and seasonally co-ordinated. The involvement of extrinsic control from hormones, such as melatonin, is most probable since it provides a mechanism whereby the rhythmic function of the CL is linked to the peripheral physiology and ultimately linked to the day-night cycle. It is clear in humans that LH and hCG have a physiologically trophic effect on the CL. It was observed here that the acrophases and mean levels of putatively rhythmic clock gene expression were affected by time spent in culture and hCG-treatment, in the LGCs. The effect of hCG on rhythmic *arntl* and *bmal1* expression in the rat ovary has also now been reported (Karman and Tischkau, 2006). It is also likely that other multiple extrinsic factors impact on the clock gene driven temporal regulation of the CL.

If a melatonin-inducible clock gene expression mechanism operates in the CL as in the PT, this could affect clock gene driven outputs. In the current studies of the ovine CL,

the sheep were housed under short photoperiod because this is stimulatory to the reproductive axis, through the activation of gonadotrophin secretion via the melatonin-dependent system. However, we did not study the CL in animals exposed to long photoperiods, to measure clock gene expression in the CL. This could be achieved by holding the sheep under prolonged long photoperiod, which results in the development of photoperiodic refractoriness and the development of the reproductive axis. The current prediction is that, if the CL behaves like the PT, the development of the CL might be disrupted under long photoperiod and this might be reflected by decreased progesterone secretion. Thus, photoperiod may act through both the central control of gonadotrophin secretion in a classical fashion and also through a negative effect on the target tissues, such as the ovary.

The effect of melatonin on the induction of *cry1* in the CL may be specific to species whose reproductive axes are seasonally regulated, like the sheep and the hamster. Whether the same mechanism of melatonin-induced *cry1* activation is found in the human CL (and human PT) remains to be seen. There is evidence though that human fertility, certainly in males, is responsive to seasonal changes (Goldman, 1999, Kennaway, 2005). The expression of the clock genes in the testis, like that of the late luteal ovine CL, also appears to be unlike that of a classical circadian clock. Rather the clock gene expression appears to be involved in the regulation of spermatogenesis. The expression of the clock genes in both male and female gonads appear to recapitulate that which is involved in the regulation of embryonic development (Seron-Ferre et al., 2007, Sakamoto et al., 2002, Sladek et al., 2007). In this role, the clock genes do not appear to be functioning like a classical circadian clock, as they do during the development of the embryo as a whole. There is evidence that clock gene expression during luteogenesis recapitulates clock gene expression in the ontogenesis of organs such as the heart and the liver (Seron-Ferre et al., 2007, Sakamoto et al., 2002, Sladek et al., 2007).

The *per2* gene is of special interest and may be involved in the extra-circadian role of clock genes during ontogeny and development. It has already been shown to be unique

in several ways. Tissue-specific expression patterns and responses to stimuli such as food entrainment have been observed particularly in *per2* (Feillet et al., 2006). This particular clock gene was unusual in the ovine CL that it was expressed rhythmically during the early luteal phase but not during the late luteal phase, in direct contrast to the expression profile of the other clock genes measured. This was consistent with the observation that *per2* appears to function and respond in ways that are divergent from those of the other clock genes (Albrecht et al., 2007). It is a negative regulator of VEGF, which plays a major angiogenic role in the CL. VEGF is highly expressed during EL when it is essential for the development of rich capillary networks, after which, it continues to function to maintain and stabilise blood vessels, thus enhancing luteal function. VEGF withdrawal is also involved in the controlled regression of the microvascular tree during luteolysis (Fraser and Wulff, 2003, Kaczmarek et al., 2005). The rapid neovascularisation of the CL during luteogenesis in some ways recapitulate those seen in tumorigenisis. A role for *per2* has often been observed in the suppression, development, progression and treatment of cancer. Its expression is decreased along with that of *per1* and *cry2* in epithelial ovarian cancer (Tokunaga et al., 2008). Mutant *per2* mice have increased incidence of cancer and show abnormal expression of the oncogenes: *cyclin D* and *c-myc*. These genes are involved in controlling the proliferation of cells. The timing of cell division is in fact gated by the circadian clock, both within and among cells (Matsuo et al., 2003). Much evidence now supports the role of *per2* as a tumour suppressor gene, involved in regulating cell division as well as DNA repair, another factor which is involved in tumorigenesis (Albrecht et al., 2007). Another observation that was particular to *per2* was of its protein distribution in the human granulosa-lutein cells of the intact CL, which were observed to aggregate in discrete foci arranged around the edge of the cells, as if apposed to the cellular basement membrane. The PER2 protein has been found to oscillate circadianly in absence of rhythmic *per2* transcription. This is likely to be due to post-translational modifications such as phosphorylation, which has been reported to impact significantly on the amount of time that the protein is localised in the cytoplasm, either due to progress along the ubiquitin-proteosome degradation pathway or translocation into the nucleus (Albrecht et

al., 2007). The PER2 protein may also interact with progesterone receptors, perhaps modulating the autocrine progesterone signalling in the CL. PER2 possesses motifs that are similar to those of hormone co-activators and corepressors, such as the steroid hormone receptor co-activator-1 (SRC-1), which is known to interact with different nuclear receptors, including the progesterone and œstrogen receptors (Albrecht et al., 2007). It is therefore possible that PER2 may be able to act with nuclear receptors such as those of progesterone, though no interaction between PER2 and a nuclear receptor has yet been reported (Albrecht et al., 2007). PER2 may function as a scaffold protein, binding more than one protein partner in order to bring them into close proximity with each other to work as a complex to induce a specific cellular response.

The window during which the clock genes function in an extra-circadian role in luteogenesis may be small, as the rapid development of a fully functional tissues ensures the most efficient use of time during the finite luteal lifetime. Similarly, the window for luteolysis may also be small, meaning that the observation of clock gene function during this time must be specifically targeted to the very late luteal phase when the CL is actively initiating and undergoing luteolysis. Clock genes may well then be observed altering their different patterns of expression and/or protein localisation in the luteal cells, and have certainly already been shown to activate apoptotic pathway genes in other cells undergoing cell death (Gery et al., 2005, Chen-Goodspeed and Lee, 2007).

The role of clock genes in the timing of luteolysis is particularly pertinent in humans, where the CL has a relatively fixed lifespan, which is presumably determined by the onset of luteolysis. It was not possible however to determine whether the clock genes were rhythmically expressed over 24 hours in the intact human CL due to the inability to sample human corpora lutea over a 24-hour period. It was also difficult to determine *in vitro* whether clock gene expression was rhythmic in LGCs. The clock gene expression that was observed in the cells was highly variable over a 24-hour time course. This was unaltered between samples from cells after one day in culture and eight days in culture. Nor was hCG observed to have a statistically significant effect on rhythmicity. The

results of these LGC studies may not however be a true representation of clock gene expression in the intact CL. It is proposed that the dispersion of the LGCs in the culturing process disrupts the cell-to-cell communication which is required for the temporal synchrony of the cells, such that an overt rhythmic expression cannot be seen in the clock genes. It is likely that cell-to-cell communication between the luteal cells occurs. This is further supported by the evidence of more overtly rhythmic clock gene expression that was observed in the luteal fibroblast-like cells after serum shock. These cells, having grown to confluence, were able to preserve their channels of cell-to-cell communication, and thus synchronise their clock gene expression rhythms in order to evince detectable circadian rhythms (Balsalobre et al., 1998). The clock gene expression in the luteal fibroblast-like cells also suggests that these cells may be involved in the temporal regulation of the CL, perhaps in conjunction with the steroidogenic cells. The cell-to-cell communication channels in the intact CL may therefore exist both between cells of the same cell type and cells of different luteal cell types. The entrainment of the luteal fibroblast-like cells by serum shock indicates that these cells can be entrained and as such, are susceptible to extrinsic signals. These signals may originate from outside the ovary, for example hCG signalling to the steroidogenic cells, or from inside the ovary, where paracrine and autocrine signalling has already been demonstrated to be fundamental to the normal steroidogenic function of the CL (Johnson and Everitt, 2000, Duncan et al., 2009). The concept of cell-to-cell communication in the CL is not novel. Luteal œstradiol synthesis is known to involve the theca-lutein and granulosa-lutein cell types working together, using paracrine cell-to-cell signalling. Luteolysis also appears to involve paracrine signalling between the steroidogenic cells and the fibroblasts using activin (Myers et al., 2007a). The use of intercellular communication has also been shown to be crucial for the temporal function of cells in the SCN (Liu et al., 2007). The main features of this proposed cellular communication in the co-ordination of clock gene regulation of reproduction are illustrated in Figure 8.3.

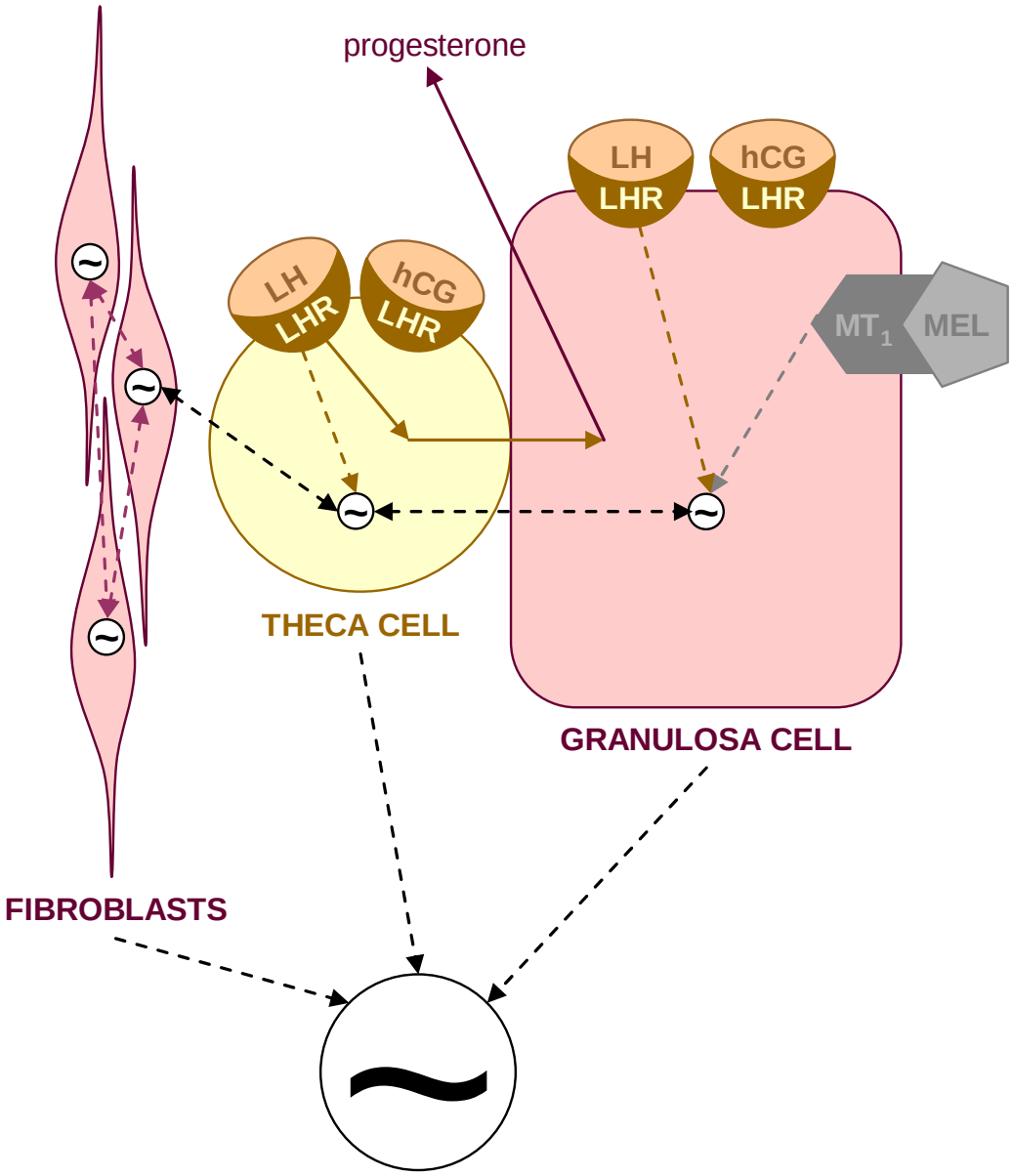

Figure 8.3 A schematic of the fully functional CL demonstrating the putative cell-to-cell communication pathways that mediate temporal regulation of luteal function and lifespan, including circadian gene expression, outlined by the dashed arrows. The undashed arrows indicate known cell-to-cell signalling pathways that mediate the synthesis of progesterone.

It is likely that the mechanisms controlling the luteal lifespan are different between sheep and humans. Sheep employ largely extrinsic control whereby $PGF_{2\alpha}$ production by the uterus provides the dominant control, while humans appear to be more dependent on intrinsic timing, which is likely to involve clock gene regulation. While the sheep utilises $PGF_{2\alpha}$ as its principal luteolytic signal, it is still possible that an intrinsic control mechanism exists. The regression of the CL could be induced artificially by $PGF_{2\alpha}$, which might alter the clock gene expression and dissociate the extrinsic and intrinsic regulation of the CL. Thus, it may be possible to develop a model where the uterine source of $PGF_{2\alpha}$ is removed and the subsequent fate of the CL is studied in a system where the intrinsic and extrinsic clocks have been dissociated. The intrinsic role of clock genes in the timing of the lifespan of the CL might be revealed, devoid of any other signalling from elsewhere in the reproductive axis.

The view of clock genes and clocks have been revised in several ways and there is now a better understanding of the different kinds of clocks working in cells and tissues, which interact with each other in a hierarchical organisation of homeostatic control, and which together provide the basis of co-ordinated time-keeping within an organism and in synchrony with geophysical time.

In summary, the main findings of this thesis were that clock genes are expressed in the human and ovine CL; that this expression is manifest at mRNA and protein level in all discernible cell types within the CL and that the pattern of expression differs between the early luteal phase compared to later luteal phases, in both sheep and humans. The circadian expression of the clock genes was established in the late luteal phase CL in sheep and could not be confidently ascertained in humans due to practical restrictions, although there was a trend towards circadian gene expression in the LGCs. With the exception of *per2*, the circadian pattern of clock gene expression emerged in the late luteal phase CL when the early luteal phase CL did not demonstrate circadian clock gene expression. This emergence later in the lifespan of the CL was akin to that observed in embryonic development, where the clock genes are initially non-rhythmic but then

acquire circadian rhythmicity with age. In this case, the clock genes have been proposed to perform a non-classical circadian timing role in the timing of embryonic development. The *per2* gene was also found to be special, in its pattern of rhythmic gene expression across the luteal lifespan (initially rhythmic, then becoming arrhythmic) and in its protein localisation in the granulosa-lutein cells (aggregating in cytoplasmic foci). The exceptional behaviour of *per2* is consistent with a growing body of evidence supporting its role as a unique clock gene in many respects, able to maintain circadian protein levels in the absence of circadian gene expression, integrating peripheral clock inputs and outputs and acting as a tumour suppressor gene (Feillet et al., 2006, Albrecht et al., 2007). The CL was also found to be a potential target of melatonin regulation, based on its possession of melatonin MT_1 receptors and the timing of circadian *cry1* gene expression in the late luteal phase. The expression of *cry1* is known to be directly melatonin-induced in the PT and may be similarly activated, downstream of a melatonin signal, in the CL. This supports the evolving view of a hierarchical organisation of the central and peripheral clocks, which are integrated in order to establish information feedback loops that maintain circadian homeostasis, and which can regulate seasonal physiology.

The better elucidation of the role of timing and temporal regulation of the female reproductive axis is particularly important as more and more women choose to have children later in life, with a corresponding increase in the financial investment in assisted reproductive technologies. The timing of the administration of fertility drugs and of surgical techniques may be revealed as important factors conducive to successful assisted reproduction. It is likely, for example, that the surgical implantation of the fertilised oocyte could be optimised to occur at a circadian time when the uterus and the endometrium are most prepared for successful implantation. The CL may also pose a useful paradigm for the study of clock gene expression in peripheral tissues where the expression of the clock genes may be multifunctional and may include non-classical circadian clock functions. It could also provide examples of how else clock gene-driven clockwork mechanisms can function. Reproduction, which is fundamental to life, may

represent a unique paradigm for unveiling primitive and highly conserved mechanisms, where circadian, seasonal and physiological rhythms are inherently linked and regulated co-ordinately.

9 BIBLIOGRAPHY

ABRAHAM, U., ALBRECHT, U. & BRANDSTATTER, R. (2003) Hypothalamic circadian organization in birds. II. Clock gene expression. *Chronobiol Int,* 20**,** 657-69.

ABRAHAMSON, E. E. & MOORE, R. Y. (2001) Suprachiasmatic nucleus in the mouse: retinal innervation, intrinsic organization and efferent projections. *Brain Res,* 916**,** 172-91.

ACEBO, C. & LEBOURGEOIS, M. K. (2006) Actigraphy. *Respir Care Clin N Am,* 12**,** 23-30, viii.

ALBRECHT, U., BORDON, A., SCHMUTZ, I. & RIPPERGER, J. (2007) The multiple facets of Per2. *Cold Spring Harb Symp Quant Biol,* 72**,** 95-104.

ALLADA, R., EMERY, P., TAKAHASHI, J. S. & ROSBASH, M. (2001) Stopping time: the genetics of fly and mouse circadian clocks. *Annu Rev Neurosci,* 24**,** 1091-119.

ALLEN, G., RAPPE, J., EARNEST, D. J. & CASSONE, V. M. (2001) Oscillating on borrowed time: diffusible signals from immortalized suprachiasmatic nucleus cells regulate circadian rhythmicity in cultured fibroblasts. *J Neurosci,* 21**,** 7937-43.

ALVAREZ, J. D., CHEN, D., STORER, E. & SEHGAL, A. (2003) Non-cyclic and developmental stage-specific expression of circadian clock proteins during murine spermatogenesis. *Biol Reprod,* 69**,** 81-91.

ANDERSSON, H., JOHNSTON, J. D., MESSAGER, S., HAZLERIGG, D. & LINCOLN, G. (2005) Photoperiod regulates clock gene rhythms in the ovine liver. *Gen Comp Endocrinol,* 142**,** 357-63.

ASCHOFF, J. (1960) Exogenous and endogenous components in circadian rhythms. *Cold Spring Harb Symp Quant Biol,* 25**,** 11-28.

ASCHOFF, J. (1998) Circadian parameters as individual characteristics. *J Biol Rhythms,* 13**,** 123-31.

ASCHOFF, J. (1999) Masking and parametric effects of high-frequency light-dark cycles. *Jpn J Physiol,* 49**,** 11-8.

ASCHOFF, J. & POHL, H. (1978) Phase relations between a circadian rhythm and its zeitgeber within the range of entrainment. *Naturwissenschaften,* 65**,** 80-4.

ATKINSON, L. E., HOTCHKISS, J., FRITZ, G. R., SURVE, A. H., NEILL, J. D. & KNOBIL, E. (1975) Circulating levels of steroids and chorionic gonadotropin during pregnancy in the rhesus monkey, with special attention to the rescue of the corpus luteum in early pregnancy. *Biol Reprod,* 12**,** 335-45.

AULETTA, F. J. & FLINT, A. P. (1988) Mechanisms controlling corpus luteum function in sheep, cows, nonhuman primates, and women especially in relation to the time of luteolysis. *Endocr Rev,* 9**,** 88-105.

AXMANN, I. M., LEGEWIE, S. & HERZEL, H. (2007) A minimal circadian clock model. *Genome Inform,* 18**,** 54-64.

BAERWALD, A. Y. (2009) Human antral folliculogenesis: what we have learned from the bovine and equine models. *Anim Reprod,* 6**,** 20-29.

BAKER, F. C. & DRIVER, H. S. (2007) Circadian rhythms, sleep, and the menstrual cycle. *Sleep Med,* 8**,** 613-22.

BALL, G. F. (2007) The ovary knows more than you think! New views on clock genes and the positive feedback control of luteinizing hormone. *Endocrinology,* 148**,** 3029-30.
BALSALOBRE, A. (2002) Clock genes in mammalian peripheral tissues. *Cell Tissue Res,* 309**,** 193-9.
BALSALOBRE, A., DAMIOLA, F. & SCHIBLER, U. (1998) A serum shock induces circadian gene expression in mammalian tissue culture cells. *Cell,* 93**,** 929-37.
BARBACKA-SUROWIAK, G., SUROWIAK, J. & STOKLOSOWA, S. (2003) The involvement of suprachiasmatic nuclei in the regulation of estrous cycles in rodents. *Reprod Biol,* 3**,** 99-129.
BARNEA, E. R. & KAPLAN, M. (1989) Spontaneous, gonadotropin-releasing hormone-induced, and progesterone-inhibited pulsatile secretion of human chorionic gonadotropin in the first trimester placenta in vitro. *J Clin Endocrinol Metab,* 69**,** 215-7.
BARNEA, E. R., SHURTZ-SWIRSKI, R. & KAPLAN, M. (1992) Factors controlling spontaneous human chorionic gonadotrophin in superfused first trimester placental explants. *Hum Reprod,* 7**,** 1022-6.
BEAVER, L. M., GVAKHARIA, B. O., VOLLINTINE, T. S., HEGE, D. M., STANEWSKY, R. & GIEBULTOWICZ, J. M. (2002) Loss of circadian clock function decreases reproductive fitness in males of Drosophila melanogaster. *Proc Natl Acad Sci U S A,* 99**,** 2134-9.
BEAVER, L. M., RUSH, B. L., GVAKHARIA, B. O. & GIEBULTOWICZ, J. M. (2003) Noncircadian regulation and function of clock genes period and timeless in oogenesis of Drosophila melanogaster. *J Biol Rhythms,* 18**,** 463-72.
BEHRMAN, H. R. (1993) Corpus luteum function and regression. *Reproductive Medicine Reviews,* 2**,** 153-80.
BERRIA, M., DESANTIS, M. & MEAD, R. A. (1988) Effects of suprachiasmatic nuclear ablation and melatonin on delayed implantation in the spotted skunk. *Neuroendocrinology,* 48**,** 371-5.
BODEN, M. J. & KENNAWAY, D. J. (2006) Circadian rhythms and reproduction. *Reproduction,* 132**,** 379-92.
BROWN, A., SMOLENSKY, M., D'ALONZO, G., REDMOND, D., CONRAD, E. & HSI, B. (1990a) Circadian rhythm in human activity objectively quantified by actigraphy. *Prog Clin Biol Res,* 341A**,** 77-83.
BROWN, A. C., SMOLENSKY, M. H., D'ALONZO, G. E. & REDMAN, D. P. (1990b) Actigraphy: a means of assessing circadian patterns in human activity. *Chronobiol Int,* 7**,** 125-33.
BROWN, S. A., ZUMBRUNN, G., FLEURY-OLELA, F., PREITNER, N. & SCHIBLER, U. (2002) Rhythms of mammalian body temperature can sustain peripheral circadian clocks. *Curr Biol,* 12**,** 1574-83.
BRUCE, V. G. & PITTENDRIGH, C. S. (1956) Temperature Independence in a Unicellular "Clock". *Proc Natl Acad Sci U S A,* 42**,** 676-82.
BUIJS, R. M. & KALSBEEK, A. (2001) Hypothalamic integration of central and peripheral clocks. *Nat Rev Neurosci,* 2**,** 521-6.
BUNNING, E. (1964) Circadian Leaf Movements in Bean Plants: Earlier Reports. *Science,* 146**,** 551.
BUNNING, E. & MOSER, I. (1969) Interference of Moonlight with the Photoperiodic Measurement of Time by Plants, and Their Adaptive Reaction. *Proc Natl Acad Sci U S A,* 62**,** 1018-1022.

CAMPBELL, B. K., SOUZA, C., GONG, J., WEBB, R., KENDALL, N., MARSTERS, P., ROBINSON, G., MITCHELL, A., TELFER, E. E. & BAIRD, D. T. (2003) Domestic ruminants as models for the elucidation of the mechanisms controlling ovarian follicle development in humans. *Reprod Suppl,* 61**,** 429-43.

CANO, P., JIMENEZ-ORTEGA, V., LARRAD, A., REYES TOSO, C. F., CARDINALI, D. P. & ESQUIFINO, A. I. (2008) Effect of a high-fat diet on 24-h pattern of circulating levels of prolactin, luteinizing hormone, testosterone, corticosterone, thyroid-stimulating hormone and glucose, and pineal melatonin content, in rats. *Endocrine,* 33**,** 118-25.

CARR, A. J., JOHNSTON, J. D., SEMIKHODSKII, A. G., NOLAN, T., CAGAMPANG, F. R., STIRLAND, J. A. & LOUDON, A. S. (2003) Photoperiod differentially regulates circadian oscillators in central and peripheral tissues of the Syrian hamster. *Curr Biol,* 13**,** 1543-8.

CHANDRASHEKARAN, M. K. (1998) Biological rhythms research: A personal account. *J. Biosci.,* 23**,** 545-5.

CHEN-GOODSPEED, M. & LEE, C. C. (2007) Tumor suppression and circadian function. *J Biol Rhythms,* 22**,** 291-8.

CHOMCZYNSKI, P. & SACCHI, N. (1987) Single-step method of RNA isolation by acid guanidinium thiocyanate-phenol-chloroform extraction. *Anal Biochem,* 162**,** 156-9.

CLOUDSLEY-THOMPSON, J. L. (1960) Adaptive functions of circadian rhythms. *Cold Spring Harb Symp Quant Biol,* 25**,** 345-55.

CZEISLER, C. A. & GOOLEY, J. J. (2007) Sleep and circadian rhythms in humans. *Cold Spring Harb Symp Quant Biol,* 72**,** 579-97.

DAAN, S. (1998) Colin Pittendrigh, Jurgen Ascoff, and the Natural Entrainment of Circadian Rhythms. *J Biol Rhythms,* 15**,** 195-207.

DACEY, D. M., LIAO, H. W., PETERSON, B. B., ROBINSON, F. R., SMITH, V. C., POKORNY, J., YAU, K. W. & GAMLIN, P. D. (2005) Melanopsin-expressing ganglion cells in primate retina signal colour and irradiance and project to the LGN. *Nature,* 433**,** 749-54.

DARDENTE, H. & CERMAKIAN, N. (2007) Molecular circadian rhythms in central and peripheral clocks in mammals. *Chronobiol Int,* 24**,** 195-213.

DARDENTE, H., FORTIER, E. E., MARTINEAU, V. & CERMAKIAN, N. (2007) Cryptochromes impair phosphorylation of transcriptional activators in the clock: a general mechanism for circadian repression. *Biochem J,* 402**,** 525-36.

DE HARO, L. & PANDA, S. (2006) Systems biology of circadian rhythms: an outlook. *J Biol Rhythms,* 21**,** 507-18.

DE LA IGLESIA, H. O., BLAUSTEIN, J. D. & BITTMAN, E. L. (1999) Oestrogen receptor-alpha-immunoreactive neurones project to the suprachiasmatic nucleus of the female Syrian hamster. *J Neuroendocrinol,* 11**,** 481-90.

DE LA IGLESIA, H. O. & SCHWARTZ, W. J. (2006) Minireview: timely ovulation: circadian regulation of the female hypothalamo-pituitary-gonadal axis. *Endocrinology,* 147**,** 1148-53.

DE REVIERS, M. M., TILLET, Y. & PELLETIER, J. (1991) Melatonin binding sites in the brain of sheep exposed to light or pinealectomized. *Neurosci Lett,* 121**,** 17-20.

DEVOTO, L., KOHEN, P., GONZALEZ, R. R., CASTRO, O., RETAMALES, I., VEGA, M., CARVALLO, P., CHRISTENSON, L. K. & STRAUSS, J. F., 3RD (2001) Expression of steroidogenic acute regulatory protein in the human

corpus luteum throughout the luteal phase. *J Clin Endocrinol Metab,* 86**,** 5633-9.

DEVOTO, L., VEGA, M., KOHEN, P., CASTRO, O., CARVALLO, P. & PALOMINO, A. (2002) Molecular regulation of progesterone secretion by the human corpus luteum throughout the menstrual cycle. *J Reprod Immunol,* 55**,** 11-20.

DEY, J., CARR, A. J., CAGAMPANG, F. R., SEMIKHODSKII, A. S., LOUDON, A. S., HASTINGS, M. H. & MAYWOOD, E. S. (2005) The tau mutation in the Syrian hamster differentially reprograms the circadian clock in the SCN and peripheral tissues. *J Biol Rhythms,* 20**,** 99-110.

DIAZ, F. J., ANDERSON, L. E., WU, Y. L., RABOT, A., TSAI, S. J. & WILTBANK, M. C. (2002) Regulation of progesterone and prostaglandin F2alpha production in the CL. *Mol Cell Endocrinol,* 191**,** 65-80.

DICKINSON, R. E., MYERS, M. & DUNCAN, W. C. (2008) Novel regulated expression of the SLIT/ROBO pathway in the ovary: possible role during luteolysis in women. *Endocrinology,* 149**,** 5024-5034.

DOI, M., HIRAYAMA, J. & SASSONE-CORSI, P. (2006) Circadian regulator CLOCK is a histone acetyltransferase. *Cell,* 125**,** 497-508.

DONG, G. & GOLDEN, S. S. (2008) How a cyanobacterium tells time. *Curr Opin Microbiol,* 11**,** 541-6.

DUNCAN, W. C. (2000) The human corpus luteum: remodelling during luteolysis and maternal recognition of pregnancy. *Rev Reprod,* 5**,** 12-7.

DUNCAN, W. C., GAY, E. & MAYBIN, J. A. (2005a) The effect of human chorionic gonadotrophin on the expression of progesterone receptors in human luteal cells in vivo and in vitro. *Reproduction,* 130**,** 83-93.

DUNCAN, W. C., HILLIER, S. G., GAY, E., BELL, J. & FRASER, H. M. (2005b) Connective tissue growth factor expression in the human corpus luteum: paracrine regulation by human chorionic gonadotropin. *J Clin Endocrinol Metab,* 90**,** 5366-76.

DUNCAN, W. C., MCNEILLY, A. S., FRASER, H. M. & ILLINGWORTH, P. J. (1996) Luteinizing hormone receptor in the human corpus luteum: lack of down-regulation during maternal recognition of pregnancy. *Hum Reprod,* 11**,** 2291-7.

DUNCAN, W. C., MCNEILLY, A. S. & ILLINGWORTH, P. J. (1998a) The effect of luteal "rescue" on the expression and localization of matrix metalloproteinases and their tissue inhibitors in the human corpus luteum. *J Clin Endocrinol Metab,* 83**,** 2470-8.

DUNCAN, W. C., MYERS, M., DICKINSON, R. E., VAN DEN DRIESCHE, S. & FRASER, H. M. (2009) Paracrine regulation of luteal development and luteolysis in the primate. *Anim Reprod,* 6**,** 34-46.

DUNCAN, W. C., RODGER, F. E. & ILLINGWORTH, P. J. (1998b) The human corpus luteum: reduction in macrophages during simulated maternal recognition of pregnancy. *Hum Reprod,* 13**,** 2435-42.

DUPRE, S. M., BURT, D. W., TALBOT, R., DOWNING, A., MOUZAKI, D., WADDINGTON, D., MALPAUX, B., DAVIS, J. R., LINCOLN, G. A. & LOUDON, A. S. (2008) Identification of melatonin-regulated genes in the ovine pituitary pars tuberalis, a target site for seasonal hormone control. *Endocrinology,* 149**,** 5527-5539.

EMERY, P. & REPPERT, S. M. (2004) A rhythmic Ror. *Neuron,* 43**,** 443-6.

EPPIG, J. J., WIGGLESWORTH, K. & PENDOLA, F. L. (2002) The mammalian oocyte orchestrates the rate of ovarian follicular development. *Proc Natl Acad Sci U S A,* 99**,** 2890-4.

ETCHEGARAY, J. P., LEE, C., WADE, P. A. & REPPERT, S. M. (2003) Rhythmic histone acetylation underlies transcription in the mammalian circadian clock. *Nature,* 421**,** 177-82.

EVANS, D. R. (1961) Biological Clocks. Volume XXV. Cold Spring Harbor Symposia on Quantitative Biology. *The Quarterly Review of Biology,* 36.

EVERETT, J. W. & SAWYER, C. H. (1950) A 24-hour periodicity in the "LH-release apparatus" of female rats, disclosed by barbiturate sedation. *Endocrinology,* 47**,** 198-218.

FAHRENKRUG, J., GEORG, B., HANNIBAL, J., HINDERSSON, P. & GRAS, S. (2006) Diurnal rhythmicity of the clock genes Per1 and Per2 in the rat ovary. *Endocrinology,* 147**,** 3769-76.

FEILLET, C. A., RIPPERGER, J. A., MAGNONE, M. C., DULLOO, A., ALBRECHT, U. & CHALLET, E. (2006) Lack of food anticipation in Per2 mutant mice. *Curr Biol,* 16**,** 2016-22.

FLECHON, J. E., PAVLOK, A. & KOPECNY, V. (1984) Dynamics of zona pellucida formation by the mouse oocyte. An autoradiographic study. *Biol Cell,* 51**,** 403-6.

FORGER, D., GONZE, D., VIRSHUP, D. & WELSH, D. K. (2007) Beyond intuitive modeling: combining biophysical models with innovative experiments to move the circadian clock field forward. *J Biol Rhythms,* 22**,** 200-10.

FORGER, D. B., DEAN, D. A., 2ND, GURDZIEL, K., LELOUP, J. C., LEE, C., VON GALL, C., ETCHEGARAY, J. P., KRONAUER, R. E., GOLDBETER, A., PESKIN, C. S., JEWETT, M. E. & WEAVER, D. R. (2003) Development and validation of computational models for mammalian circadian oscillators. *Omics,* 7**,** 387-400.

FOSTER, R. G. (2005) Neurobiology: bright blue times. *Nature,* 433**,** 698-9.

FOSTER, R. G. & HELFRICH-FORSTER, C. (2001) The regulation of circadian clocks by light in fruitflies and mice. *Philos Trans R Soc Lond B Biol Sci,* 356**,** 1779-89.

FRASER, H. M., LUNN, S. F., COWEN, G. M. & ILLINGWORTH, P. J. (1995) Induced luteal regression in the primate: evidence for apoptosis and changes in c-myc protein. *J Endocrinol,* 147**,** 131-7.

FRASER, H. M., LUNN, S. F., HARRISON, D. J. & KERR, J. B. (1999) Luteal regression in the primate: different forms of cell death during naturaland gonadotropin-releasing hormone antagonist or prostaglandin analogue-induced luteolysis. *Biol Reprod,* 61**,** 1468-79.

FRASER, H. M. & WULFF, C. (2003) Angiogenesis in the corpus luteum. *Reprod Biol Endocrinol,* 1**,** 88.

GALLEGO, M., EIDE, E. J., WOOLF, M. F., VIRSHUP, D. M. & FORGER, D. B. (2006) An opposite role for tau in circadian rhythms revealed by mathematical modeling. *Proc Natl Acad Sci U S A,* 103**,** 10618-23.

GAULT, P. M., MAUDSLEY, S. & LINCOLN, G. A. (2003) Evidence that gonadotropin-releasing hormone II is not a physiological regulator of gonadotropin secretion in mammals. *J Neuroendocrinol,* 15**,** 831-9.

GERY, S., GOMBART, A. F., YI, W. S., KOEFFLER, C., HOFMANN, W. K. & KOEFFLER, H. P. (2005) Transcription profiling of C/EBP targets identifies Per2 as a gene implicated in myeloid leukemia. *Blood,* 106**,** 2827-36.

GILCHRIST, R. B., LANE, M. & THOMPSON, J. G. (2008) Oocyte-secreted factors: regulators of cumulus cell function and oocyte quality. *Hum Reprod Update,* 14**,** 159-77.

GLOSSOP, N. R. & HARDIN, P. E. (2002) Central and peripheral circadian oscillator mechanisms in flies and mammals. *J Cell Sci,* 115**,** 3369-77.

GOLDMAN, B. D. (1999) The circadian timing system and reproduction in mammals. *Steroids,* 64**,** 679-85.

GOLDSTEIN, J. A. (2004) *Tuning the Brain: Principles and Practice of Neurosomatic Medicine* Routledge.

GONZALEZ, J. A. & DYBALL, R. E. (2006) Pinealectomy reduces optic nerve but not intergeniculate leaflet input to the suprachiasmatic nucleus at night. *J Neuroendocrinol,* 18**,** 146-53.

GOOLEY, J. J., LU, J., CHOU, T. C., SCAMMELL, T. E. & SAPER, C. B. (2001) Melanopsin in cells of origin of the retinohypothalamic tract. *Nat Neurosci,* 4**,** 1165.

GUILDING, C. & PIGGINS, H. D. (2007) Challenging the omnipotence of the suprachiasmatic timekeeper: are circadian oscillators present throughout the mammalian brain? *Eur J Neurosci,* 25**,** 3195-216.

GUILLAUMOND, F., DARDENTE, H., GIGUERE, V. & CERMAKIAN, N. (2005) Differential control of Bmal1 circadian transcription by REV-ERB and ROR nuclear receptors. *J Biol Rhythms,* 20**,** 391-403.

GUNDEL, A. & WEGMANN, H. M. (1989) Transition between advance and delay responses to eastbound transmeridian flights. *Chronobiol Int,* 6**,** 147-56.

GUO, H., BREWER, J. M., CHAMPHEKAR, A., HARRIS, R. B. & BITTMAN, E. L. (2005) Differential control of peripheral circadian rhythms by suprachiasmatic-dependent neural signals. *Proc Natl Acad Sci U S A,* 102**,** 3111-6.

HALBERG, F., CORNELISSEN, G., KATINAS, G., SYUTKINA, E. V., SOTHERN, R. B., ZASLAVSKAYA, R., HALBERG, F., WATANABE, Y., SCHWARTZKOPFF, O., OTSUKA, K., TARQUINI, R., FREDERICO, P. & SIGGELOVA, J. (2003) Transdisciplinary unifying implications of circadian findings in the 1950s. *J Circadian Rhythms,* 1**,** 2.

HANNIBAL, J., HINDERSSON, P., OSTERGAARD, J., GEORG, B., HEEGAARD, S., LARSEN, P. J. & FAHRENKRUG, J. (2004) Melanopsin is expressed in PACAP-containing retinal ganglion cells of the human retinohypothalamic tract. *Invest Ophthalmol Vis Sci,* 45**,** 4202-9.

HANNIBAL, J., MOLLER, M., OTTERSEN, O. P. & FAHRENKRUG, J. (2000) PACAP and glutamate are co-stored in the retinohypothalamic tract. *J Comp Neurol,* 418**,** 147-55.

HANON, E. A., LINCOLN, G. A., FUSTIN, J. M., DARDENTE, H., MASSON-PEVET, M., MORGAN, P. J. & HAZLERIGG, D. G. (2008) Ancestral TSH mechanism signals summer in a photoperiodic mammal. *Curr Biol,* 18**,** 1147-52.

HASTINGS, M. H., DUFFIELD, G. E., SMITH, E. J., MAYWOOD, E. S. & EBLING, F. J. (1998) Entrainment of the circadian system of mammals by nonphotic cues. *Chronobiol Int,* 15**,** 425-45.

HATTAR, S., LUCAS, R. J., MROSOVSKY, N., THOMPSON, S., DOUGLAS, R. H., HANKINS, M. W., LEM, J., BIEL, M., HOFMANN, F., FOSTER, R. G. & YAU, K. W. (2003) Melanopsin and rod-cone photoreceptive systems account for all major accessory visual functions in mice. *Nature,* 424**,** 76-81.

HE, P. J., HIRATA, M., YAMAUCHI, N., HASHIMOTO, S. & HATTORI, M. A. (2007a) Gonadotropic regulation of circadian clockwork in rat granulosa cells. *Mol Cell Biochem,* 302**,** 111-8.

HE, P. J., HIRATA, M., YAMAUCHI, N., HASHIMOTO, S., HATTORI, M. A., HE, P. J., HIRATA, M., YAMAUCHI, N., HASHIMOTO, S. & HATTORI, M. A. (2007b) The disruption of circadian clockwork in differentiating cells from rat reproductive tissues as identified by in vitro real-time monitoring system *J Endocrinol,* 193**,** 413-20.

HEFFNER, L. J. & SCHUST, D. J. (2006) *The reproductive system at a glance*.

HERZOG, E. D., GEUSZ, M. E., KHALSA, S. B., STRAUME, M. & BLOCK, G. D. (1997) Circadian rhythms in mouse suprachiasmatic nucleus explants on multimicroelectrode plates. *Brain Res,* 757**,** 285-90.

HIRATA, M., HE, P. J., SHIBUYA, N., UCHIKAWA, M., YAMAUCHI, N., HASHIMOTO, S. & HATTORI, M. A. (2008) Progesterone, but not estradiol, synchronizes circadian oscillator in the uterus endometrial stromal cells. *Mol Cell Biochem*.

HIROTA, T. & FUKADA, Y. (2004) Resetting mechanism of central and peripheral circadian clocks in mammals. *Zoolog Sci,* 21**,** 359-68.

IKONOMOV, O. C. & STOYNEV, A. G. (1994) Gene expression in suprachiasmatic nucleus and circadian rhythms. *Neurosci Biobehav Rev,* 18**,** 305-12.

ILLINGWORTH, P. J., REDDI, K., SMITH, K. & BAIRD, D. T. (1990) Pharmacological 'rescue' of the corpus luteum results in increased inhibin production. *Clin Endocrinol (Oxf),* 33**,** 323-32.

ILLNEROVA, H., VANECEK, J. & HOFFMANN, K. (1989) Different mechanisms of phase delays and phase advances of the circadian rhythm in rat pineal N-acetyltransferase activity. *J Biol Rhythms,* 4**,** 187-200.

INOUYE, S. T. & KAWAMURA, H. (1979) Persistence of circadian rhythmicity in a mammalian hypothalamic "island" containing the suprachiasmatic nucleus. *Proc Natl Acad Sci U S A,* 76**,** 5962-6.

ISHIKAWA, T., HIRAYAMA, J., KOBAYASHI, Y. & TODO, T. (2002) Zebrafish CRY represses transcription mediated by CLOCK-BMAL heterodimer without inhibiting its binding to DNA. *Genes Cells,* 7**,** 1073-86.

IVELL, R., BATHGATE, R. & WALTHER, N. (1999) Luteal peptides and their genes as important markers of ovarian differentiation. *J Reprod Fertil Suppl,* 54**,** 207-16.

JILG, A., MOEK, J., WEAVER, D. R., KORF, H. W., STEHLE, J. H. & VON GALL, C. (2005) Rhythms in clock proteins in the mouse pars tuberalis depend on MT1 melatonin receptor signalling. *Eur J Neurosci,* 22**,** 2845-54.

JIN, X., SHEARMAN, L. P., WEAVER, D. R., ZYLKA, M. J., DE VRIES, G. J. & REPPERT, S. M. (1999) A molecular mechanism regulating rhythmic output from the suprachiasmatic circadian clock. *Cell,* 96**,** 57-68.

JOHNSON, C. H. (2007) Bacterial circadian programs. *Cold Spring Harb Symp Quant Biol,* 72**,** 395-404.

JOHNSON, C. H., ELLIOTT, J. A. & FOSTER, R. (2003) Entrainment of circadian programs. *Chronobiol Int,* 20**,** 741-74.

JOHNSON, M. H. & EVERITT, B. J. (2000) *Essential Reproduction*, Blackwell Science Ltd.

JOHNSON, M. H., LIM, A., FERNANDO, D. & DAY, M. L. (2002) Circadian clockwork genes are expressed in the reproductive tract and conceptus of the early pregnant mouse. *Reprod Biomed Online,* 4**,** 140-5.

JOHNSTON, J. D., BASHFORTH, R., DIACK, A., ANDERSSON, H., LINCOLN, G. A. & HAZLERIGG, D. G. (2004) Rhythmic melatonin secretion does not correlate with the expression of arylalkylamine N-acetyltransferase, inducible cyclic amp early repressor, period1 or cryptochrome1 mRNA in the sheep pineal. *Neuroscience,* 124**,** 789-95.

JOHNSTON, J. D., TOURNIER, B. B., ANDERSSON, H., MASSON-PEVET, M., LINCOLN, G. A. & HAZLERIGG, D. G. (2006) Multiple effects of melatonin on rhythmic clock gene expression in the mammalian pars tuberalis. *Endocrinology,* 147**,** 959-65.

KACZMAREK, M. M., SCHAMS, D. & ZIECIK, A. J. (2005) Role of vascular endothelial growth factor in ovarian physiology - an overview. *Reprod Biol,* 5**,** 111-36.

KAEFFER, B. & PARDINI, L. (2005) Clock genes of Mammalian cells: practical implications in tissue culture. *In Vitro Cell Dev Biol Anim,* 41**,** 311-20.

KALRA, S. P. (1993) Mandatory neuropeptide-steroid signaling for the preovulatory luteinizing hormone-releasing hormone discharge. *Endocr Rev,* 14**,** 507-38.

KALSBEEK, A., CUTRERA, R. A., VAN HEERIKHUIZE, J. J., VAN DER VLIET, J. & BUIJS, R. M. (1999) GABA release from suprachiasmatic nucleus terminals is necessary for the light-induced inhibition of nocturnal melatonin release in the rat. *Neuroscience,* 91**,** 453-61.

KAPLAN, J. R. (2008) Origins and health consequences of stress-induced ovarian dysfunction. *Interdiscip Top Gerontol,* 36**,** 162-85.

KARMAN, B. N. & TISCHKAU, S. A. (2006) Circadian clock gene expression in the ovary: Effects of luteinizing hormone. *Biol Reprod,* 75**,** 624-32.

KARSCH, F. J., BATTAGLIA, D. F., BREEN, K. M., DEBUS, N. & HARRIS, T. G. (2002) Mechanisms for ovarian cycle disruption by immune/inflammatory stress. *Stress,* 5**,** 101-12.

KENNAWAY, D. J. (2004) Resetting the suprachiasmatic nucleus clock. *Front Biosci,* 9**,** 56-62.

KENNAWAY, D. J. (2005) The role of circadian rhythmicity in reproduction. *Hum Reprod Update,* 11**,** 91-101.

KENNAWAY, D. J., BODEN, M. J. & VOULTSIOS, A. (2005) Reproductive performance in female Clock(Delta19) mutant mice. *Reprod Fertil Dev,* 16**,** 801-10.

KENNAWAY, D. J., VARCOE, T. J. & MAU, V. J. (2003) Rhythmic expression of clock and clock-controlled genes in the rat oviduct. *Mol Hum Reprod,* 9**,** 503-7.

KING, D. P. & TAKAHASHI, J. S. (2000) Molecular genetics of circadian rhythms in mammals. *Annu Rev Neurosci,* 23**,** 713-42.

KING, V. M. & FOLLETT, B. K. (1997) c-fos expression in the putative avian suprachiasmatic nucleus. *J Comp Physiol [A],* 180**,** 541-51.

KO, C. H. & TAKAHASHI, J. S. (2006) Molecular components of the mammalian circadian clock. *Hum Mol Genet,* 15 Spec No 2**,** R271-7.

KONOPKA, R. J. & BENZER, S. (1971) Clock mutants of Drosophila melanogaster. *Proc Natl Acad Sci U S A,* 68**,** 2112-6.

KOW, L. M. & PFAFF, D. W. (1984) Suprachiasmatic neurons in tissue slices from ovariectomized rats: electrophysiological and neuropharmacological characterization and the effects of estrogen treatment. *Brain Res,* 297**,** 275-86.

KRAUCHI, K., CAJOCHEN, C., PACHE, M., FLAMMER, J. & WIRZ-JUSTICE, A. (2006) Thermoregulatory effects of melatonin in relation to sleepiness. *Chronobiol Int,* 23**,** 475-84.

KRUIJVER, F. P. & SWAAB, D. F. (2002) Sex hormone receptors are present in the human suprachiasmatic nucleus. *Neuroendocrinology,* 75**,** 296-305.

KUBISTA, M., ANDRADE, J. M., BENGTSSON, M., FOROOTAN, A., JONAK, J., LIND, K., SINDELKA, R., SJOBACK, R., SJOGREEN, B., STROMBOM, L., STAHLBERG, A. & ZORIC, N. (2006) The real-time polymerase chain reaction. *Mol Aspects Med,* 27**,** 95-125.

KUME, K., ZYLKA, M. J., SRIRAM, S., SHEARMAN, L. P., WEAVER, D. R., JIN, X., MAYWOOD, E. S., HASTINGS, M. H. & REPPERT, S. M. (1999) mCRY1 and mCRY2 are essential components of the negative limb of the circadian clock feedback loop. *Cell,* 98**,** 193-205.

LALL, G. S. & BIELLO, S. M. (2003) Neuropeptide Y, GABA and circadian phase shifts to photic stimuli. *Neuroscience,* 120**,** 915-21.

LAURIA, L., BALLARD, T. J., CALDORA, M., MAZZANTI, C. & VERDECCHIA, A. (2006) Reproductive disorders and pregnancy outcomes among female flight attendants. *Aviat Space Environ Med,* 77**,** 533-9.

LEE, C., ETCHEGARAY, J. P., CAGAMPANG, F. R., LOUDON, A. S. & REPPERT, S. M. (2001) Posttranslational mechanisms regulate the mammalian circadian clock. *Cell,* 107**,** 855-67.

LEHMAN, M. N., SILVER, R., GLADSTONE, W. R., KAHN, R. M., GIBSON, M. & BITTMAN, E. L. (1987) Circadian rhythmicity restored by neural transplant. Immunocytochemical characterization of the graft and its integration with the host brain. *J Neurosci,* 7**,** 1626-38.

LENTON, E. A. & WOODWARD, A. J. (1988) The endocrinology of conception cycles and implantation in women. *J Reprod Fertil Suppl,* 36**,** 1-15.

LESAUTER, J., LEHMAN, M. N. & SILVER, R. (1996) Restoration of circadian rhythmicity by transplants of SCN "micropunches". *J Biol Rhythms,* 11**,** 163-71.

LINCOLN, G., MESSAGER, S., ANDERSSON, H. & HAZLERIGG, D. (2002) Temporal expression of seven clock genes in the suprachiasmatic nucleus and the pars tuberalis of the sheep: evidence for an internal coincidence timer. *Proc Natl Acad Sci U S A,* 99**,** 13890-5.

LINCOLN, G. A. (2006) Decoding the nightly melatonin signal through circadian clockwork. *Mol Cell Endocrinol,* 252**,** 69-73.

LINCOLN, G. A., ANDERSSON, H. & HAZLERIGG, D. (2003) Clock genes and the long-term regulation of prolactin secretion: evidence for a photoperiod/circannual timer in the pars tuberalis. *J Neuroendocrinol,* 15**,** 390-7.

LINCOLN, G. A., JOHNSTON, J. D., ANDERSSON, H., WAGNER, G. & HAZLERIGG, D. G. (2005) Photorefractoriness in mammals: dissociating a seasonal timer from the circadian-based photoperiod response. *Endocrinology,* 146**,** 3782-90.

LIU, A. C., LEWIS, W. G. & KAY, S. A. (2007) Mammalian circadian signaling networks and therapeutic targets. *Nat Chem Biol,* 3**,** 630-9.

LOBBAN, M. C. (1960) The entrainment of circadian rhythms in man. *Cold Spring Harb Symp Quant Biol,* 25**,** 325-32.

LOUCOPOULOS, A. & FERIN, M. (1984) Gonadotropin-releasing hormone and its clinical applications. *Obstet Gynecol Annu,* 13**,** 275-88.

LOWREY, P. L. & TAKAHASHI, J. S. (2000) Genetics of the mammalian circadian system: Photic entrainment, circadian pacemaker mechanisms, and posttranslational regulation. *Annu Rev Genet,* 34**,** 533-562.
LUBOSHITZKY, R. (2000) Endocrine activity during sleep. *J Pediatr Endocrinol Metab,* 13**,** 13-20.
MACKLON, N. S. & FAUSER, B. C. (1999) Aspects of ovarian follicle development throughout life. *Horm Res,* 52**,** 161-70.
MADHRA, M., GAY, E., FRASER, H. M. & DUNCAN, W. C. (2004) Alternative splicing of the human luteal LH receptor during luteolysis and maternal recognition of pregnancy. *Mol Hum Reprod,* 10**,** 599-603.
MAHONEY, M. M. & SMALE, L. (2005) Arginine vasopressin and vasoactive intestinal polypeptide fibers make appositions with gonadotropin-releasing hormone and estrogen receptor cells in the diurnal rodent Arvicanthis niloticus. *Brain Res,* 1049**,** 156-64.
MALPAUX, B., THIERY, J. C. & CHEMINEAU, P. (1999) Melatonin and the seasonal control of reproduction. *Reprod Nutr Dev,* 39**,** 355-66.
MATSUO, T., YAMAGUCHI, S., MITSUI, S., EMI, A., SHIMODA, F. & OKAMURA, H. (2003) Control mechanism of the circadian clock for timing of cell division in vivo. *Science,* 302**,** 255-9.
MAYBIN, J. A. & DUNCAN, W. C. (2004) The human corpus luteum: which cells have progesterone receptors? *Reproduction,* 128**,** 423-31.
MCCLUNG, C. R. (2006) Plant circadian rhythms. *Plant Cell,* 18**,** 792-803.
MCKINNON, A. O. & VOSS, J. L. (1995) FSH and LH. *Equine Reproduction* WileyBlackwell.
MCLAUGHLIN, E. A. & MCIVER, S. C. (2009) Awakening the oocyte: controlling primordial follicle development. *Reproduction,* 137**,** 1-11.
MEGDAL, S. P., KROENKE, C. H., LADEN, F., PUKKALA, E. & SCHERNHAMMER, E. S. (2005) Night work and breast cancer risk: a systematic review and meta-analysis. *Eur J Cancer,* 41**,** 2023-32.
MESIANO, S. (2004) Myometrial progesterone responsiveness and the control of human parturition. *J Soc Gynecol Investig,* 11**,** 193-202.
MILLER, B. H., OLSON, S. L., TUREK, F. W., LEVINE, J. E., HORTON, T. H. & TAKAHASHI, J. S. (2004) Circadian clock mutation disrupts estrous cyclicity and maintenance of pregnancy. *Curr Biol,* 14**,** 1367-73.
MISTLBERGER, R. E. (2006) Circadian rhythms: perturbing a food-entrained clock. *Curr Biol,* 16**,** R968-9.
MOGA, M. M. & MOORE, R. Y. (1997) Organization of neural inputs to the suprachiasmatic nucleus in the rat. *J Comp Neurol,* 389**,** 508-34.
MOORE-EDE, M. C., SULZMAN, F. M. & FULLER, C. A. (1984) The Clocks That Time Us: Physiology of the Circadian Timing System Harvard University Press
MOORE, R. Y. & EICHLER, V. B. (1972) Loss of a circadian adrenal corticosterone rhythm following suprachiasmatic lesions in the rat. *Brain Res,* 42**,** 201-6.
MOORE, R. Y. & LENN, N. J. (1972) A retinohypothalamic projection in the rat. *J Comp Neurol,* 146**,** 1-14.
MOORE, R. Y., SPEH, J. C. & LEAK, R. K. (2002) Suprachiasmatic nucleus organization. *Cell Tissue Res,* 309**,** 89-98.
MORALES, C., GARCIA-PARDO, L., REYMUNDO, C., BELLIDO, C., SANCHEZ-CRIADO, J. E. & GAYTAN, F. (2000) Different patterns of

structural luteolysis in the human corpus luteum of menstruation. *Hum Reprod,* 15**,** 2119-28.

MORSE, D., CERMAKIAN, N., BRANCORSINI, S., PARVINEN, M. & SASSONE-CORSI, P. (2003) No circadian rhythms in testis: Period1 expression is clock independent and developmentally regulated in the mouse. *Mol Endocrinol,* 17**,** 141-51.

MOTLIK, J. & KUBELKA, M. (1990) Cell-cycle aspects of growth and maturation of mammalian oocytes. *Mol Reprod Dev,* 27**,** 366-75.

MURPHY, B. D. (2000) Models of luteinization. *Biol Reprod,* 63**,** 2-11.

MYERS, M., GAY, E., MCNEILLY, A. S., FRASER, H. M. & DUNCAN, W. C. (2007a) In vitro evidence suggests activin-A may promote tissue remodeling associated with human luteolysis. *Endocrinology,* 148**,** 3730-9.

MYERS, M., LAMONT, M. C., VAN DEN DRIESCHE, S., MARY, N., THONG, K. J., HILLIER, S. G. & DUNCAN, W. C. (2007b) Role of luteal glucocorticoid metabolism during maternal recognition of pregnancy in women. *Endocrinology,* 148**,** 5769-79.

MYERS, M., VAN DEN DRIESCHE, S., MCNEILLY, A. & DUNCAN, W. (2008) Activin A reduces luteinisation of human luteinised granulosa cells and has opposing effects to human chorionic gonadotropin (hCG) in vitro. *J Endocrinol,* 199**,** 201-212.

NAGOSHI, E., SAINI, C., BAUER, C., LAROCHE, T., NAEF, F. & SCHIBLER, U. (2004) Circadian gene expression in individual fibroblasts: cell-autonomous and self-sustained oscillators pass time to daughter cells. *Cell,* 119**,** 693-705.

NAKAHATA, Y., GRIMALDI, B., SAHAR, S., HIRAYAMA, J. & SASSONE-CORSI, P. (2007) Signaling to the circadian clock: plasticity by chromatin remodeling. *Curr Opin Cell Biol,* 19**,** 230-237.

NAKAMURA, T. J., MORIYA, T., INOUE, S., SHIMAZOE, T., WATANABE, S., EBIHARA, S. & SHINOHARA, K. (2005) Estrogen differentially regulates expression of Per1 and Per2 genes between central and peripheral clocks and between reproductive and nonreproductive tissues in female rats. *J Neurosci Res,* 82**,** 622-30.

NAKAMURA, T. J., SHINOHARA, K., FUNABASHI, T. & KIMURA, F. (2001) Effect of estrogen on the expression of Cry1 and Cry2 mRNAs in the suprachiasmatic nucleus of female rats. *Neurosci Res,* 41**,** 251-5.

NAKAO, N., YASUO, S., NISHIMURA, A., YAMAMURA, T., WATANABE, T., ANRAKU, T., OKANO, T., FUKADA, Y., SHARP, P. J., EBIHARA, S. & YOSHIMURA, T. (2007) Circadian clock gene regulation of steroidogenic acute regulatory protein gene expression in preovulatory ovarian follicles. *Endocrinology,* 148**,** 3031-8.

NARUSE, Y., OH-HASHI, K., IIJIMA, N., NARUSE, M., YOSHIOKA, H. & TANAKA, M. (2004) Circadian and light-induced transcription of clock gene Per1 depends on histone acetylation and deacetylation. *Mol Cell Biol,* 24**,** 6278-87.

NEILL, J. N. (2005) *Knobil and Neill's Physiology of Reproduction*.

NISWENDER, G. D., DAVIS, T. L., GRIFFITH, R. J., BOGAN, R. L., MONSER, K., BOTT, R. C., BRUEMMER, J. E. & NETT, T. M. (2007) Judge, jury and executioner: the auto-regulation of luteal function. *Soc Reprod Fertil Suppl,* 64**,** 191-206.

NISWENDER, G. D., JUENGEL, J. L., SILVA, P. J., ROLLYSON, M. K. & MCINTUSH, E. W. (2000) Mechanisms controlling the function and life span of the corpus luteum. *Physiol Rev,* 80**,** 1-29.

NUNEZ, A. A. & STEPHAN, F. K. (1977) The effects of hypothalamic knife cuts on drinking rhythms and the estrus cycle of the rat. *Behav Biol,* 20**,** 224-34.

OISHI, K., SAKAMOTO, K., OKADA, T., NAGASE, T. & ISHIDA, N. (1998) Antiphase circadian expression between BMAL1 and period homologue mRNA in the suprachiasmatic nucleus and peripheral tissues of rats. *Biochem Biophys Res Commun,* 253**,** 199-203.

OKAMURA, H. (2003) Integration of molecular rhythms in the mammalian circadian system. *Novartis Found Symp,* 253**,** 161-70, discussion 102-9, 281-4.

OKAMURA, H., TANAKA, M., KANEMASA, K., BAN, Y., INOUYE, S. T. & IBATA, Y. (1995) In situ hybridization histochemistry of vgf mRNA in the rat suprachiasmatic nucleus: co-localization with vasopressin/neurophysin and VIP/PHI. *Neurosci Lett,* 189**,** 181-4a.

PALM, I. F., VAN DER BEEK, E. M., WIEGANT, V. M., BUIJS, R. M. & KALSBEEK, A. (2001) The stimulatory effect of vasopressin on the luteinizing hormone surge in ovariectomized, estradiol-treated rats is time-dependent. *Brain Res,* 901**,** 109-16.

PANDO, M. P., MORSE, D., CERMAKIAN, N. & SASSONE-CORSI, P. (2002) Phenotypic rescue of a peripheral clock genetic defect via SCN hierarchical dominance. *Cell,* 110**,** 107-17.

PANG, S. F., LI, L., AYRE, E. A., PANG, C. S., LEE, P. P., XU, R. K., CHOW, P. H., YU, Z. H. & SHIU, S. Y. (1998) Neuroendocrinology of melatonin in reproduction: recent developments. *J Chem Neuroanat,* 14**,** 157-66.

PARANJPE, D. A. & SHARMA, V. K. (2005) Evolution of temporal order in living organisms. *J Circadian Rhythms,* 3**,** 7.

PEIRSON, S. N., BUTLER, J. N., DUFFIELD, G. E., TAKHER, S., SHARMA, P. & FOSTER, R. G. (2006) Comparison of clock gene expression in SCN, retina, heart, and liver of mice. *Biochem Biophys Res Commun,* 351**,** 800-7.

PEREDA, J., ZORN, T. & SOTO-SUAZO, M. (2006) Migration of human and mouse primordial germ cells and colonization of the developing ovary: an ultrastructural and cytochemical study. *Microsc Res Tech,* 69**,** 386-95.

PERREAU-LENZ, S., KALSBEEK, A., PEVET, P. & BUIJS, R. M. (2004a) Glutamatergic clock output stimulates melatonin synthesis at night. *Eur J Neurosci,* 19**,** 318-24.

PERREAU-LENZ, S., PEVET, P., BUIJS, R. M. & KALSBEEK, A. (2004b) The biological clock: the bodyguard of temporal homeostasis. *Chronobiol Int,* 21**,** 1-25.

PITTENDRIGH, C. S. (1960) Circadian rhythms and the circadian organization of living systems. *Cold Spring Harb Symp Quant Biol,* 25**,** 159-84.

PITTENDRIGH, C. S. & TAKAMURA, T. (1987) Temperature dependence and evolutionary adjustment of critical night length in insect photoperiodism. *Proc Natl Acad Sci U S A,* 84**,** 7169-7173.

PITTS, S., PERONE, E. & SILVER, R. (2003) Food-entrained circadian rhythms are sustained in arrhythmic Clk/Clk mutant mice. *Am J Physiol Regul Integr Comp Physiol,* 285**,** R57-67.

POHL, C. R., RICHARDSON, D. W., HUTCHISON, J. S., GERMAK, J. A. & KNOBIL, E. (1983) Hypophysiotropic signal frequency and the functioning of

the pituitary-ovarian system in the rhesus monkey. *Endocrinology,* 112**,** 2076-80.

PREITNER, N., DAMIOLA, F., LOPEZ-MOLINA, L., ZAKANY, J., DUBOULE, D., ALBRECHT, U. & SCHIBLER, U. (2002) The orphan nuclear receptor REV-ERBalpha controls circadian transcription within the positive limb of the mammalian circadian oscillator. *Cell,* 110**,** 251-60.

QIU, X., KUMBALASIRI, T., CARLSON, S. M., WONG, K. Y., KRISHNA, V., PROVENCIO, I. & BERSON, D. M. (2005) Induction of photosensitivity by heterologous expression of melanopsin. *Nature,* 433**,** 745-9.

RALPH, M. R. & LEHMAN, M. N. (1991) Transplantation: a new tool in the analysis of the mammalian hypothalamic circadian pacemaker. *Trends Neurosci,* 14**,** 362-6.

RALPH, M. R. & MENAKER, M. (1988) A mutation of the circadian system in golden hamsters. *Science,* 241**,** 1225-7.

RAND, D. A., SHULGIN, B. V., SALAZAR, J. D. & MILLAR, A. J. (2006) Uncovering the design principles of circadian clocks: mathematical analysis of flexibility and evolutionary goals. *J Theor Biol,* 238**,** 616-35.

RATAJCZAK, C. K., BOEHLE, K. L. & MUGLIA, L. J. (2008) Impaired Steroidogenesis and Implantation Failure in Bmal1-/- Mice. *Endocrinology*.

REA, M. A. (1998) Photic entrainment of circadian rhythms in rodents. *Chronobiol Int,* 15**,** 395-423.

REPPERT, S. M. (2000) Cellular and molecular basis of circadian timing in mammals. *Semin Perinatol,* 24**,** 243-6.

REPPERT, S. M. & WEAVER, D. R. (2001) Molecular analysis of mammalian circadian rhythms. *Annu Rev Physiol,* 63**,** 647-76.

RICHTER, C. P. (1978) "Dark-active" rat transformed into "light-active" rat by destruction of 24-hr clock: function of 24-hr clock and synchronizers. *Proc Natl Acad Sci U S A,* 75**,** 6276-80.

ROENNEBERG, T. & MERROW, M. (2007) Entrainment of the human circadian clock. *Cold Spring Harb Symp Quant Biol,* 72**,** 293-9.

ROIZEN, J., LUEDKE, C. E., HERZOG, E. D. & MUGLIA, L. J. (2007) Oxytocin in the circadian timing of birth. *PLoS ONE,* 2**,** e922.

ROSBASH, M. (1995) Molecular control of circadian rhythms. *Curr Opin Genet Dev,* 5**,** 662-8.

RUTTER, J., REICK, M. & MCKNIGHT, S. L. (2002) Metabolism and the control of circadian rhythms. *Annu Rev Biochem,* 71**,** 307-31.

RUTTER, J., REICK, M., WU, L. C. & MCKNIGHT, S. L. (2001) Regulation of clock and NPAS2 DNA binding by the redox state of NAD cofactors. *Science,* 293**,** 510-4.

SAKAMOTO, K., OISHI, K., NAGASE, T., MIYAZAKI, K. & ISHIDA, N. (2002) Circadian expression of clock genes during ontogeny in the rat heart. *Neuroreport,* 13**,** 1239-42.

SAPER, C. B. & FULLER, P. M. (2007) Inducible clocks: living in an unpredictable world. *Cold Spring Harb Symp Quant Biol,* 72**,** 543-50.

SATO, T. K., YAMADA, R. G., UKAI, H., BAGGS, J. E., MIRAGLIA, L. J., KOBAYASHI, T. J., WELSH, D. K., KAY, S. A., UEDA, H. R. & HOGENESCH, J. B. (2006) Feedback repression is required for mammalian circadian clock function. *Nat Genet,* 38**,** 312-9.

SAUNDERS, D. S. (2005) Erwin Bunning and Tony Lees, two giants of chronobiology, and the problem of time measurement in insect photoperiodism. *J Insect Physiol,* 51**,** 599-608.
SCHAMS, D. & BERISHA, B. (2004) Regulation of corpus luteum function in cattle--an overview. *Reprod Domest Anim,* 39**,** 241-51.
SCHIBLER, U., RIPPERGER, J. & BROWN, S. A. (2003) Peripheral circadian oscillators in mammals: time and food. *J Biol Rhythms,* 18**,** 250-60.
SCHIBLER, U. & SASSONE-CORSI, P. (2002) A web of circadian pacemakers. *Cell,* 111**,** 919-22.
SCHMIDT-KOENIG, K., GANZHORN, J. U. & RANVAUD, R. (1991) Orientation in birds. The sun compass. *Exs,* 60**,** 1-15.
SERON-FERRE, M., VALENZUELA, G. J. & TORRES-FARFAN, C. (2007) Circadian clocks during embryonic and fetal development. *Birth Defects Res C Embryo Today,* 81**,** 204-14.
SHEN, S., SPRATT, C., SHEWARD, W. J., KALLO, I., WEST, K., MORRISON, C. F., COEN, C. W., MARSTON, H. M. & HARMAR, A. J. (2000) Overexpression of the human VPAC2 receptor in the suprachiasmatic nucleus alters the circadian phenotype of mice. *Proc Natl Acad Sci U S A,* 97**,** 11575-80.
SHEWARD, W. J., MAYWOOD, E. S., FRENCH, K. L., HORN, J. M., HASTINGS, M. H., SECKL, J. R., HOLMES, M. C. & HARMAR, A. J. (2007) Entrainment to feeding but not to light: circadian phenotype of VPAC2 receptor-null mice. *J Neurosci,* 27**,** 4351-8.
SHINOHARA, K., FUNABASHI, T., NAKAMURA, T. J. & KIMURA, F. (2001) Effects of estrogen and progesterone on the expression of connexin-36 mRNA in the suprachiasmatic nucleus of female rats. *Neurosci Lett,* 309**,** 37-40.
SHINOHARA, K., HONMA, S., KATSUNO, Y., ABE, H. & HONMA, K. (1994) Circadian rhythms in the release of vasoactive intestinal polypeptide and arginine-vasopressin in organotypic slice culture of rat suprachiasmatic nucleus. *Neurosci Lett,* 170**,** 183-6.
SILVER, R., LESAUTER, J., TRESCO, P. A. & LEHMAN, M. N. (1996) A diffusible coupling signal from the transplanted suprachiasmatic nucleus controlling circadian locomotor rhythms. *Nature,* 382**,** 810-3.
SILVIA, W. J., LEWIS, G. S., MCCRACKEN, J. A., THATCHER, W. W. & WILSON, L., JR. (1991) Hormonal regulation of uterine secretion of prostaglandin F2 alpha during luteolysis in ruminants. *Biol Reprod,* 45**,** 655-63.
SKARZYNSKI, D. J., JAROSZEWSKI, J. J. & OKUDA, K. (2001) Luteotropic Mechanisms in the Bovine Corpus Luteum: Role of Oxytocin, Prostaglandin F2alpha, Progesterone and Noradrenaline. . *Journal of Reproduction and Development,* 47**,** 125-37
SLADEK, M., JINDRAKOVA, Z., BENDOVA, Z. & SUMOVA, A. (2007) Postnatal ontogenesis of the circadian clock within the rat liver. *Am J Physiol Regul Integr Comp Physiol,* 292**,** R1224-9.
SMITH, R. F., GHUMAN, S. P., EVANS, N. P., KARSCH, F. J. & DOBSON, H. (2003) Stress and the control of LH secretion in the ewe. *Reprod Suppl,* 61**,** 267-82.
SOARES, J. M., JR., MASANA, M. I., ERSAHIN, C. & DUBOCOVICH, M. L. (2003) Functional melatonin receptors in rat ovaries at various stages of the estrous cycle. *J Pharmacol Exp Ther,* 306**,** 694-702.

SOUSA-PINTO, A. & CASTRO-CORREIA, J. (1970) Light microscopic observations on the possible retinohypothalamic projection in the rat. *Exp Brain Res,* 11**,** 515-27.

SPENCER, T. E. & BAZER, F. W. (2002) Biology of progesterone action during pregnancy recognition and maintenance of pregnancy. *Front Biosci,* 7**,** d1879-98.

STAMOULI, A., O'SULLIVAN, M. J., FRANKEL, S., THOMAS, E. J. & RICHARDSON, M. C. (1996) Suppression of matrix metalloproteinase production by hCG in cultures of human luteinized granulosa cells as a model for gonadotrophin-induced luteal rescue. *J Reprod Fertil,* 107**,** 235-9.

STEPHAN, F. K. (2002) The "other" circadian system: food as a Zeitgeber. *J Biol Rhythms,* 17**,** 284-92.

STEPHAN, F. K. & ZUCKER, I. (1972) Circadian rhythms in drinking behavior and locomotor activity of rats are eliminated by hypothalamic lesions. *Proc Natl Acad Sci U S A,* 69**,** 1583-6.

STETLER, D., DAS, H., NUNBERG, J. H., SAIKI, R., SHENG-DONG, R., MULLIS, K. B., WEISSMAN, S. M. & ERLICH, H. A. (1982) Isolation of a cDNA clone for the human HLA-DR antigen alpha chain by using a synthetic oligonucleotide as a hybridization probe. *Proc Natl Acad Sci U S A,* 79**,** 5966-70.

STOCCO, C., TELLERIA, C. & GIBORI, G. (2007) The molecular control of corpus luteum formation, function, and regression. *Endocr Rev,* 28**,** 117-49.

STOUFFER, R. L. (2003) Progesterone as a mediator of gonadotrophin action in the corpus luteum: beyond steroidogenesis. *Hum Reprod Update,* 9**,** 99-117.

STOUFFER, R. L., OTTOBRE, J. S., MOLSKNESS, T. A. & ZELINSKI-WOOTEN, M. B. (1989) The function and regulation of the primate corpus luteum during the fertile menstrual cycle. *Prog Clin Biol Res,* 294**,** 129-42.

STRATMANN, M. & SCHIBLER, U. (2006) Properties, entrainment, and physiological functions of mammalian peripheral oscillators. *J Biol Rhythms,* 21**,** 494-506.

STURIALE, N. (1997) Time: Biology and Technology.

SUGINO, N. & OKUDA, K. (2007) Species-related differences in the mechanism of apoptosis during structural luteolysis. *J Reprod Dev,* 53**,** 977-86.

SUMOVA, A., JAC, M., SLADEK, M., SAUMAN, I. & ILLNEROVA, H. (2003) Clock gene daily profiles and their phase relationship in the rat suprachiasmatic nucleus are affected by photoperiod. *J Biol Rhythms,* 18**,** 134-44.

SZAFARCZYK, A., IXART, G., ALONSO, G., MALAVAL, F., NOUGUIER-SOULE, J. & ASSENMACHER, I. (1983) CNS control of the circadian adrenocortical rhythm. *J Steroid Biochem,* 19**,** 1009-15.

TAKAHASHI, J. S. (2004) Finding new clock components: past and future. *J Biol Rhythms,* 19**,** 339-47.

TAMURA, H., NAKAMURA, Y., KORKMAZ, A., MANCHESTER, L. C., TAN, D. X., SUGINO, N. & REITER, R. J. (2008) Melatonin and the ovary: physiological and pathophysiological implications. *Fertil Steril*.

THORNER, M. O., HARTMAN, M. L., VANCE, M. L., PEZZOLI, S. S. & AMPLEFORD, E. J. (1995) Neuroendocrine regulation of growth hormone secretion. *Neurosci Biobehav Rev,* 19**,** 465-8.

TOKUNAGA, H., TAKEBAYASHI, Y., UTSUNOMIYA, H., AKAHIRA, J., HIGASHIMOTO, M., MASHIKO, M., ITO, K., NIIKURA, H.,

TAKENOSHITA, S. & YAEGASHI, N. (2008) Clinicopathological significance of circadian rhythm-related gene expression levels in patients with epithelial ovarian cancer. *Acta Obstet Gynecol Scand,* 87**,** 1060-70.

TOSINI, G., POZDEYEV, N., SAKAMOTO, K. & IUVONE, P. M. (2008) The circadian clock system in the mammalian retina. *Bioessays,* 30**,** 624-33.

TREHERNE, J. E., FOSTER, W. A., EVANS, P. D. & RUSCOE, C. N. (1977) Free-running activity rhythm in the natural environment. *Nature,* 269**,** 796-7.

UEDA, H. R., HAYASHI, S., CHEN, W., SANO, M., MACHIDA, M., SHIGEYOSHI, Y., IINO, M. & HASHIMOTO, S. (2005) System-level identification of transcriptional circuits underlying mammalian circadian clocks. *Nat Genet,* 37**,** 187-92.

VAN DEN DRIESCHE, S., MYERS, M., GAY, E., THONG, K. J. & DUNCAN, W. C. (2008) HCG up-regulates hypoxia inducible factor-1 alpha in luteinized granulosa cells: implications for the hormonal regulation of vascular endothelial growth factor A in the human corpus luteum. *Mol Hum Reprod,* 14**,** 455-64.

VAN DER BEEK, E. M., HORVATH, T. L., WIEGANT, V. M., VAN DEN HURK, R. & BUIJS, R. M. (1997) Evidence for a direct neuronal pathway from the suprachiasmatic nucleus to the gonadotropin-releasing hormone system: combined tracing and light and electron microscopic immunocytochemical studies. *J Comp Neurol,* 384**,** 569-79.

VIDA, B., HRABOVSZKY, E., KALAMATIANOS, T., COEN, C. W., LIPOSITS, Z. & KALLO, I. (2008) Oestrogen receptor alpha and beta immunoreactive cells in the suprachiasmatic nucleus of mice: distribution, sex differences and regulation by gonadal hormones. *J Neuroendocrinol,* 20**,** 1270-7.

VIELHABER, E., EIDE, E., RIVERS, A., GAO, Z. H. & VIRSHUP, D. M. (2000) Nuclear entry of the circadian regulator mPER1 is controlled by mammalian casein kinase I epsilon. *Mol Cell Biol,* 20**,** 4888-99.

VITATERNA, M. H., TAKAHASHI, J. S. & TUREK, F. W. (2001) Overview of circadian rhythms. *Alcohol Res Health,* 25**,** 85-93.

VOKAC, Z., JEBENS, E. & VOKAC, M. (1984) Phase-shifts of apparent circadian rhythms due to west and east transmeridian flights or to corresponding night-shift sleep displacements. *Chronobiol Int,* 1**,** 139-44.

WATSON, J. D. & CRICK, F. H. (1953) Molecular structure of nucleic acids; a structure for deoxyribose nucleic acid. *Nature,* 171**,** 737-8.

WELSH, D. K., LOGOTHETIS, D. E., MEISTER, M. & REPPERT, S. M. (1995) Individual neurons dissociated from rat suprachiasmatic nucleus express independently phased circadian firing rhythms. *Neuron,* 14**,** 697-706.

WELSH, D. K., YOO, S. H., LIU, A. C., TAKAHASHI, J. S. & KAY, S. A. (2004) Bioluminescence imaging of individual fibroblasts reveals persistent, independently phased circadian rhythms of clock gene expression. *Curr Biol,* 14**,** 2289-95.

WELT, C. K., PAGAN, Y. L., SMITH, P. C., RADO, K. B. & HALL, J. E. (2003) Control of follicle-stimulating hormone by estradiol and the inhibins: critical role of estradiol at the hypothalamus during the luteal-follicular transition. *J Clin Endocrinol Metab,* 88**,** 1766-71.

WILLIAMS, L. M., HANNAH, L. T., HASTINGS, M. H. & MAYWOOD, E. S. (1995) Melatonin receptors in the rat brain and pituitary. *J Pineal Res,* 19**,** 173-7.

WOO, M. M., TAI, C. J., KANG, S. K., NATHWANI, P. S., PANG, S. F. & LEUNG, P. C. (2001) Direct action of melatonin in human granulosa-luteal cells. *J Clin Endocrinol Metab,* 86**,** 4789-97.

YAMAGUCHI, S., ISEJIMA, H., MATSUO, T., OKURA, R., YAGITA, K., KOBAYASHI, M. & OKAMURA, H. (2003) Synchronization of cellular clocks in the suprachiasmatic nucleus. *Science,* 302**,** 1408-12.

YAMAZAKI, S., NUMANO, R., ABE, M., HIDA, A., TAKAHASHI, R., UEDA, M., BLOCK, G. D., SAKAKI, Y., MENAKER, M. & TEI, H. (2000) Resetting central and peripheral circadian oscillators in transgenic rats. *Science,* 288**,** 682-5.

ZIMMERMAN, N. H. & MENAKER, M. (1979) The pineal gland: a pacemaker within the circadian system of the house sparrow. *Proc Natl Acad Sci U S A,* 76**,** 999-1003.

ZWIEBEL, L. J., HARDIN, P. E., LIU, X., HALL, J. C. & ROSBASH, M. (1991) A post-transcriptional mechanism contributes to circadian cycling of a per-beta-galactosidase fusion protein. *Proc Natl Acad Sci U S A,* 88**,** 3882-6.